Characterization of Polymicrobial Infections in Macaques with Chronic Cranial Implants and Evaluation of Alternative Antimicrobial Strategies

by

Mia Tova Rock Lieberman

B.S., University of California, Davis (2007)
D.V.M., University of California, Davis (2011)

Submitted to the Department of Biological Engineering
in partial fulfillment of the requirements for the degree of

Doctor of Philosophy

at the

MASSACHUSETTS INSTITUTE OF TECHNOLOGY

September 2018

Author ... Signature redacted .....
Department of Biological Engineering
August 8, 2018

Certified by ... Signature redacted .....
James G. Fox
Director, Division of Comparative Medicine, Professor,
Department of Biological Engineering
Thesis Supervisor

Accepted by ... Signature redacted .....
Forest M. White
Chairman, Department Committee on Graduate Theses

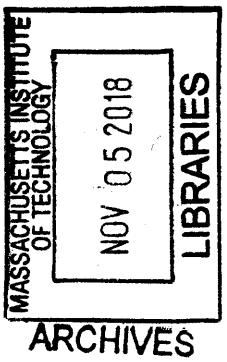

Characterization of Polymicrobial Infections in Macaques with Chronic Cranial Implants and Evaluation of Alternative Antimicrobial Strategies

by

Mia Tova Rock Lieberman

Submitted to the Department of Biological Engineering
on August 8, 2018, in partial fulfillment of the
requirements for the degree of
Doctor of Philosophy

Abstract

Macaques are the most commonly used non-human primate in cognitive neuroscience research due to similarities between the macaque and human brain. Cephalic recording chambers (CRCs) are often surgically implanted to obtain neuronal recordings. CRCs represent a persistent source of microbial contamination, which can occasionally progress to clinical sequelae of meningitis and brain abscesses. In this thesis, we first examined aerobic and anaerobic bacterial species colonizing CRCs using both traditional culture-dependent methods and 16S microbiota culture-independent methods. We evaluated the most prevalent species, and compared CRC bacterial communities to skin, oral and fecal bacterial communities. Our results indicated that CRC bacterial communities are predominantly composed of anaerobic flora and are relatively unique between individual macaques. Additionally CRC bacterial communities are more similar to skin and oral bacterial communities than fecal bacterial communities, indicating that fecal contamination of CRCs is a less likely source of contamination. Aerobic culture and sensitivity data from samples collected in 2011 identified *Staphylococcus aureus*, *Enterococcus faecalis* and *Proteus* spp. as the most prevalent species isolated, and that *E. faecalis* isolates displayed marked resistance to multiple antimicrobial classes. Routine CRC sanitization procedures were revised in September 2014 to prohibit antimicrobial use within CRCs, and we evaluated how *E. faecalis* lineages persisted and evolved between 2011 and 2017. We identified a shift in sequence type (ST) from ST4 and ST55, predominating in 2011, to ST48 predominating in macaques implanted after 2013. ST48 lineages were less resistant to antimicrobials and stronger biofilm producers as compared to ST4 and ST55 lineages. We concluded that loss of selective pressure from antimicrobial use within CRCs permitted ST48 to emerge as the predominant lineage due to its strong biofilm-forming abilities. Finally, we evaluated alternative *E. faecalis*

biofilm treatment strategies. We isolated lytic bacteriophages with activity against ST55 *E. faecalis* and evaluated the use of phages and antimicrobial peptides LL-37 and PR-39 against *E. faecalis* biofilm, alone, and in combination with antimicrobials. Our results identified that bacteriophages successfully decreased biofilm produced by ST55 and ST4 *E. faecalis* isolates and should be evaluated further for treatment of animal and human enterococcal-associated biofilm infections.

Thesis Supervisor: James G. Fox
Title: Director, Division of Comparative Medicine, Professor, Department of Biological Engineering

Acknowledgments

There are many individuals to thank during this journey to obtain my Ph.D. First, I would not be here today without the support and encouragement of Dr. James Fox. When I left clinical veterinary practice to join the post-doctoral comparative medicine program, I knew very little about laboratory animal medicine, but was excited about the opportunity to jump back into a research environment. Dr. Fox welcomed me warmly into the program, and his mentorship, guidance and support have been unwavering while honing my skills as a laboratory animal veterinarian, achieving DACLAM certification and navigating the complexities of obtaining a Ph.D. at MIT.

It has been a privilege to learn from and work with the amazing group of DCM veterinarians, staff researchers, veterinary technicians, animal care technicians and my fellow veterinary post-docs over the past 5 years. I would particularly like to thank Dr. Bob Marini for teaching me about primate medicine and for his songs, humor, advice, and additional support as part of my thesis committee. A big thanks to Dr. Jody Fox for her mentorship and assistance performing MICs, kill curves and anaerobic bacterial cultures. Dr. Alex Sheh and Dr. Anthony Mannion have been wonderful resources for collaborating on the nuts and bolts of analyzing genomes and microbiota samples. Emily Knebel did a fantastic job as a DCM summer veterinary student fellow and I am thankful for her assistance in performing and evaluating daptomycin kill curves and phage lysis curves.

Dr. Michael Gilmore, Dr. Daria Van Tyne, and Dr. François Lebroton have been fantastic colleagues and collaborators in guiding portions of this work examining the evolution of *E. faecalis* isolates collected from MIT macaques. Thanks to the McGovern Institute for Brain Research for financial support of this project. We appreciate the commitment from the Brain and Cognitive Science Department at MIT in supporting our work and prioritizing the health of macaques that are such valuable models for understanding the brain. I am greatly appreciative to Dr. Robert Desimone for his dedication to this project and the BCS researchers for their enthusiastic participation in facilitating sample collection from their hard-working macaques. The MIT veterinary and neuroscience communities are privileged to have such a collegiate relationship, and shared interest in promoting the highest standards of animal health and welfare.

I would also like to acknowledge Dr. Forest White who has been exceptionally supportive of my Ph.D. journey; from student to applicant, and now kindly serving as chair of my defense committee.

Dr. Robert Citorik and Dr. César de la Fuente-Núñez have been instrumental during this project and I am greatly appreciative of their assistance with the bacteriophage, biofilm and antimicrobial peptide portions of this work. Dr. Eric Ma has been a great colleague, co-author and friend, and is recognized for his willingness to teach me Bayesian statistics and rudimentary Python skills.

Many many thanks to Alyssa Pappa; her never wavering smile and assistance with figure preparation, journal article submission, poster-formatting and organizational skills for day to day life at DCM are unmatched.

My mentors at UC Davis deserve a shoutout - I first learned about phage therapy as an undergraduate from Dr. Rance LeFebvre; he and Dr. Barbara Byrne have encouraged my interest in veterinary microbiology and bacteriophage therapy throughout my career.

Finally, I would not be here at all without the support of my family. I am incredibly grateful to my husband, David Geisler, for his encouragement throughout this whole process. I could not have done this without you, and I promise I am finished collecting degrees! My parents nurtured my scientific curiosity from a young age, and provided a strong science background during my homeschooling years. Dad - I know you're a proud Caltech alum, but MIT isn't too shabby! I'd also like to acknowledge my in-laws for their support and encouragement during this journey, as well as for raising my husband to be the caring, amazing man he is!

Contents

List of Figures

List of Tables

Chapter 1

Use of Macaques (*Macaca* spp.) in Cognitive Neuroscience Research and Complications Associated with Cephalic Implants

Portions of this chapter have been previously published [1].

1.1 Introduction

Nonhuman primates (NHP) are an important animal model for cognitive neuroscience research, with the macaque (*Macaca mulatta*) being the most commonly utilized species (Figure 1-1) [5]. The anatomical and functional similarities between the human and macaque brain have been well characterized, and features such as a highly developed cerebral cortex (Figure 1-2), binocular color vision and front-facing eyes allow comparisons to humans that are impossible in rodent models [5]. At MIT, the Brain and Cognitive Science faculty are primarily studying visual pathways involved in object recognition, learning and memory, motivation-based decision making, and control of attention vs. distraction.

Figure 1-1: The rhesus macaque (*Macaca mulatta*) is the most commonly used non-human primate in research. Image reference: [2]

1.2 Description of typical cranial implants used in macaques involved in cognitive neuroscience research at MIT

Cognitive neuroscience researchers are often interested in elucidating specific pathways within the brain. These studies involve training macaques to sit in a chair and perform tasks on a computerized system, such as visual object recognition, or memory tasks [6]. Researchers are able to track eye movements and record electrical impulses of the neuronal pathway under study while macaques perform the tasks. The expertise of the investigator, and the region of the brain under study determine the style of cranial implant, its placement on the cranium, and the number and type of electrodes placed.

In preparation for neuronal recordings, macaques must undergo surgical procedures to facilitate access for placement of electrodes into the brain. Surgical implants typically involve two types of implanted devices.

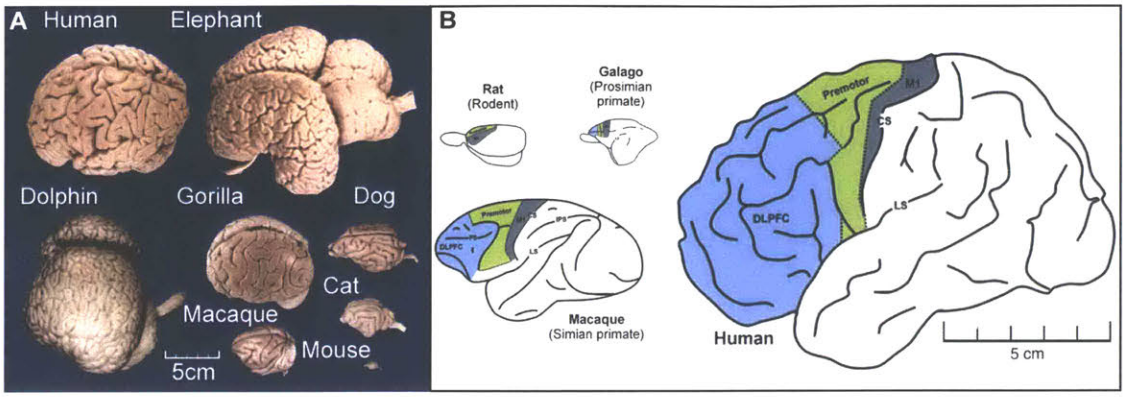

Figure 1-2: A. Relative brain sizes as compared to a human brain, including a macaque (monkey) and gorilla (ape). Image reference: [3]. B. Comparison of prefrontal cortex size between rat, galago, macaque and human brains. Originally published as Figure 3 in reference [4]; used with permission.

First, restraint pedestals are affixed to the cranium to permit head fixation while the chaired macaque performs tasks. Restraint pedestals minimize movement of the head during recordings and subsequent noise that might interfere with interpretation of electrical impulses [7]. The style of restraint pedestal used varies between investigators at MIT, but is most commonly a single titanium or plastic restraint post mounted in the occipital region Figure 1-3. Some investigators utilize a "pin-halo" style restraint involving a metal halo to interface with 3-4 small pins placed around the skull and attached using screws [8]. Traditionally, single restraint pedestal screws were anchored using polymethylmethacrylate (PMMA) dental acrylic, although updated designs are able to affix the restraint pedestal directly to the skull with screws [9]. Following placement of the restraint pedestals, a craniotomy is performed to perforate the bony skull and a cephalic recording chamber (CRC) is placed (Figure 1-3). The number and sizes of the craniotomies will depend on the area of the brain being studied and the types of electrodes (single vs. microarray) used.

Historically, commercially available CRCs were made of stainless steel, titanium, CILUX plastic, or thermoplastic polyetherimide Ultem plastic and affixed to the skull using a combination of screws and PMMA dental acrylic [10, 9, 11]. More recent innovations involve magnetic resonance imaging (MRI) and/or computed tomography (CT) to map the skull followed by computer aided design and 3D printing to customize the shape and size of the CRC to the individual macaque. [10, 9, 11]. These new designs can thus

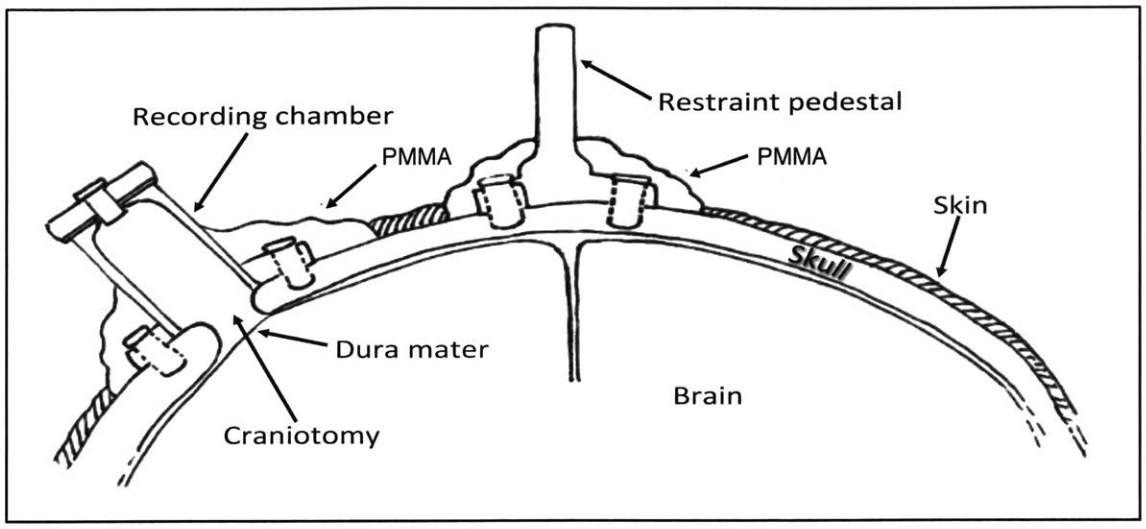

Figure 1-3: Illustration of a traditional cephalic recording chamber and single restraint pedestal with polymethylmethacrylate (PMMA) used to anchor screws

be lower-profile, PMMA-free and also feature lightweight, next-generation plastics such as carbon polyetheretherketone (PEEK) which are compatible with MRI studies due to their nonferrous nature [10, 9, 11].

Microelectrodes placed into the brain can be used for recording neuronal activity, stimulating neurons, or selective ablation of neuronal tissue in the desired brain region [6]. Microelectrodes are commonly made of tungsten or platinum and are a few microns in diameter [6]. In some cases, electrodes are placed prior to every recording session but some experimental paradigms involve chronic placement of microelectrode arrays . The latter array approach allows the ability to target neurons repeatedly between experiments. There are also described techniques for a hybrid of the two systems; Chronic Independently Movable Electrode systems permit repeated sampling of the same sites as well as sampling of multiple sites [12].

1.3 Complications of cephalic implantation

Complications of chronic cephalic implantation have been documented in macaques under study at MIT, as well as at other institutions. For the purposes of this dissertation, we will be focusing on infection-related complications with only brief discussions of other CRC implant complications.

1.3.1 Acute complications

Acute complications of cephalic implantation include issues arising during or in the early post-operative period, most commonly presenting within the first month following surgery. Complications occurring during surgery include hemorrhage, inadvertent damage to brain tissue or hematoma formation during electrode placement, and breaks in sterile surgical technique with introduction of bacteria into the brain, meninges or surrounding tissues.

Clinical signs are non-specific for space-occupying cranial lesions (i.e. brain abscess vs. hematoma) and deficits will depend on the location of the lesion. At MIT, macaques affected by cephalic hematomas and abscess have presented with hemi-inattention/visual deficits, hemiparesis, vomiting, lethargy, and anorexia. Complete blood counts may reveal leukocytosis, which can be a response etiher stress or infection. MRI imaging is the preferred method for distinguishing hematomas from abscess (Figure 1-4.) Treatment for small, subacute hematomas involves supportive care (analgesics +/- corticosteroids, fluid and nutritional support) and monitoring; euthanasia has been elected in cases of large hematomas resulting in more extensive neurologic deficits.

If euthanasia is not elected, treatment for brain abscess involves aspiration of abscess material for definitive aerobic and anaerobic culture, with selection of antimicrobial therapy based on sensitivity testing results. Periodic MRI imaging is essential during treatment to monitor abscess resolution and guide duration of antimicrobial therapy. Supportive care including analgesics, fluid and nutritional support is also an essential part of the treatment regimen. Brain abscess is most likely to arise from breaks in aseptic technique, either during surgery, or post-operatively, with the use of improperly sterilized electrodes or translocation of bacteria from the dura during electrode penetration.

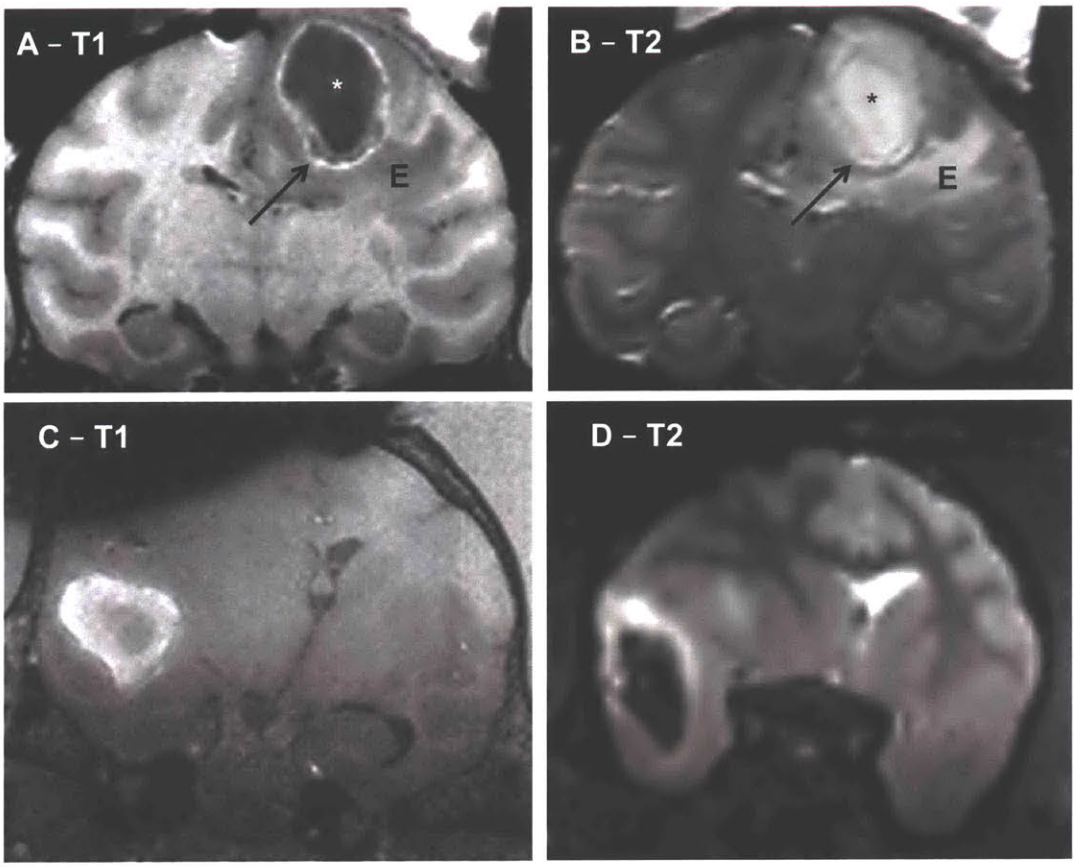

Figure 1-4: T1 and T2-weighted coronal-plane MRI images of space-occupying cranial lesions in research macaques. (A and B). Brain abscess 24 hours after clinical presentation; the asterisk designates the core while the arrow identifies a thin, distinct capsule. Note loss of brain architecture and edema (E) subadjacent to the abscess. (C and D). Hematoma 6 days after clinical presentation; note hyperintense appearance on T1-weighted image (C) and hypointense appearance on T2-weighted image due to the presence of paramagnetic intracellular methemoglobin. Interference from implant metallic components results in the image artifact obscuring the superior aspect of the brain in image C.

A case of acute post-surgical meningoencephalitis occurred in a macaque at MIT as the result of improper screw placement. Clinical signs of vomiting and stargazing presented 19 days following surgery; the macaque was euthanized after a rapid decline to unresponsiveness necessitating ventilatory support. During necropsy, hemorrhage and thick purulent material were visualized covering the frontal and occipital lobes and meninges. The tips of screws were observed to have penetrated through the skull. Histopathology confirmed expansion of the dura mater and leptomeninges

by hemorrhage, granulocytes and mononuclear cells, with infiltration into the brain and spinal cord parenchyma. Aerobic and anaerobic cultures identified *Staphylococcus aureus*, *Enterococcus faecalis*, *Lactobacillus* sp. and *Micromonas micros*. A break in sterile technique and inadvertent bacterial contamination of the screws was considered the most likely etiology.

1.3.2 Chronic complications

Chronic complications can occur months to years after surgical implantation and are often related to failure at the implant-tissue interface. Older-style implants utilizing PMMA to anchor implant hardware are more likely to be affected than PMMA-free implants. The curing of PMMA during surgery results in an exothermic reaction, with temperatures reaching up to 110°C and necessitating cooling techniques during application [13, 9]. As well as causing thermal damage to bone and soft tissue, PMMA is cytotoxic and does not bind well to bone [14, 11]. Over time, the natural healing physiologic response is formation of a robust granulation tissue bed. Growth of granulation tissue between the PMMA and bone can result in disruption of implant, bone and tissue integrity, causing weakening or loss of the implant hardware [10, 9]. PMMA-free implants featuring a radial leg design can also be affected by granulation tissue due to skin recession around the metal legs. Skin recession can result in increased bone exposure, bone infection, soft tissue infection and introduction of bacteria inside CRCs [10].

Within the CRC, formation of granulation tissue on the dura mater can result from repeated electrode introduction, bacterial colonization of CRCs, or a combination of these factors. Thickening of the dura will eventually interfere with placement of electrodes, necessitating periodic scar tissue removal, or alternate strategies to limit connective tissue growth [15, 16].

Meningitis results from bacterial infection of the meninges and has been more commonly observed in macaques with chronic, traditional-style implants utilizing PMMA. Over time, CRCs become colonized by bacteria when opened to introduce electrodes, breaks in aseptic technique during CRC sanitization, or from beneath PMMA associated with defects in the tissue-implant interface. Most animals tolerate bacterial colonization of CRCs without overt clinical signs; however, there is potential for bacteria to invade through the meninges and cause pathology. Clinical signs of meningitis are

non-specific, and can include lethargy, anorexia, vomiting, "star-gazing", head-pressing, and/or reluctance to move the head and neck [17, 18]. Definitive diagnosis of meningitis is made by sterile culture of cerebrospinal fluid, which is most commonly collected via cisternal puncture. Complete blood counts may reveal marked leukocytosis and can be sequentially monitored to evaluate treatment efficacy. Sterile collection and aerobic/anaerobic cultures of blood are recommended to evaluate for concurrent sepsis. Cultures of CRCs are often performed, but does not necessarily indicate the most likely causative bacterial species. Treatment of meningitis includes broad-spectrum antimicrobial therapy, analgesic, fluid and nutritional support and sometimes corticosteroids, depending on rapidity of diagnosis. Historically, treatment had been initiated for suspected cases without definitive diagnosis, and successful response to antimicrobial therapy was interpreted as a correct diagnosis.

1.4 Frequency of Meningitis and Evaluation of Implant Sanitization Practices

In 2011, the MIT Division of Comparative Medicine (DCM) surveyed investigators working with implanted macaques to characterize current CRC sanitization practices and frequency of meningitis episodes. Practices varied between investigators (and between macaques) regarding frequency of CRC sanitization, solutions used for sanitization, use of topical antimicrobials within CRCs, placement of packing materials within CRCs, and care of skin-implant wound margins. Detailed responses were available for 25 implanted macaques and it was determined that 4/25 macaques had been treated for suspected meningitis between 2009 and 2011, with one macaque treated on at least 5 separate occasions. Survey results from 2011 are available in Appendix A. To better understand potential etiologic agents of meningitis, the veterinary staff initiated a study to characterize aerobic bacterial species inhabiting CRCs and their antimicrobial resistance patterns. The results of these cultures and updates to CRC sanitization protocols will be described in Chapter 2.

1.5 Summary and Conclusions

In this chapter we have introduced the use of macaques as an essential model for cognitive neuroscience research and discussed complications associated with cephalic implants required for studying neural pathways. Bacterial meningitis and brain abscesses can be fatal, necessitating detailed understanding of best practices to prevent and treat these cases when they arise. Subsequent chapters will explore bacterial species commonly colonizing CRCs, examine how a particular bacterial species can persist over time, and finally, evaluate novel treatments for bacterial biofilms. Maintaining the highest standard of animal health and welfare is essential for both the veterinary and investigative staff privileged to work with macaques and other non-human primates. MIT Brain and Cognitive Science researchers are commended for their ongoing commitments to improvements to implant design and care, promotion of animal health, and eager cooperation in facilitating sample collection during this project.

Chapter 2

Characterization of Bacterial Communities within Cephalic Recording Chambers

Portions of this chapter have been previously published [1].

2.1 Introduction

As introduced in Chapter 1, macaques with chronic cephalic recording chamber implants can develop a robust granulation tissue response, as well as clinical sequelae of meningitis and brain abscesses secondary to bacterial colonization of CRCs. Prior to 2014, diagnosis of macaques with "suspect meningitis" was predominantly made based on clinical signs, a culture of the cephalic recording chamber, and prophylactic treatment with varying antimicrobial regimens (trimethoprim-sulfamethoxazole, enrofloxacin, ceftriaxone) and sometimes corticosteroids (dexamethasone sodium phosphate). This chapter focuses on techniques for identification of bacterial species commonly inhabiting CRCs to better understand which species are most common, and evaluate their pathogenic potential. First, we will introduce results obtained from aerobic bacterial culture and antimicrobial sensitivity testing performed in 2011. We will then discuss using culture-independent methods to identify both aerobic and anaerobic species, and compare communities between CRCs, the implant-skin margin, the oral cavity, and feces from samples collected in 2017. Finally, we will com-

pare results of culture-independent methods with aerobic and anaerobic cultures from 2018 to validate the use of culture-independent methods to characterize CRC bacterial communities.

2.2 Aerobic bacterial CRC cultures collected from macaques in 2011

2.2.1 Animals

Twenty-five macaques (19 male, 6 female) with chronic cephalic recording chambers were sampled in August, 2011. The population consisted of 25 rhesus macaques (*Macaca mulatta*) and 1 cynomolgus macaque (*Macaca fascicularis*), with a mean and standard deviation age of 10.7 $\pm$ 2.2 years (range 6-15 years). The macaques sampled in this study were under investigation by four different cognitive neuroscience research laboratories (A-D; Table 2.1). All macaques were housed in an AAALAC-International accredited facility under standards outlined by the 8th edition of the Guide [19]. Briefly, husbandry parameters included a 12:12 light-dark cycle, a diet of commercial primate biscuits (Purina 5038) supplemented with fruits, vegetables, nuts and cereal. Macaques were pair-housed, with exceptions for animals showing incompatibility with conspecifics. For this study, 44 CRCs with craniotomies, and 1 without a craniotomy, were sampled. The majority of macaques (11/25) had one CRC; 8/25 had two, and the remaining 6 macaques had three CRCs. Most (26) of the CRCs had been in place between one and three years, 12 had been implanted between three and five years, and 7 had been in place less than one year (Table 2.1). Antimicrobial agents were routinely used within CRCs for 14/25 macaques and included gentamicin sulfate 0.3%, oxytetracycline 5mg/g-polymyxin B 10,000U/g, bacitracin zinc 300U/g-neomycin sulfate 5mg/g-polymyxin B 10,000U/g and a 1:20 dilution of injectable enrofloxacin (2.27%). Packing materials were used in 12/25 macaques and included sterile petroleum jelly (N=6), non-woven sponge balls (n=5), and silicone elastomer (N=1). CRC sanitization solutions varied by investigator and included chlorhexidine (n=20), povidone-iodine (n=8), and hydrogen peroxide (N=3) (Appendix A). To minimize discomfort and stress, sampling of cephalic chambers was performed

under ketamine anesthesia (10mg/kg, intramuscular injection) during routine semi-annual physical examination. All animals remained on IACUC-approved protocols for cognitive neuroscience research at the conclusion of sampling and no animals were euthanized for reasons related to this study.

Animal ID	Sex	Age (years)	Lab ID	Study ID	# of CRCs	Duration of CRC implantation (years)	Antimicrobials used in CRC	Packing materials used in CRC
1	F	15	A	A1	1	1-3	G	None
2	F	14	A	A2	1	1-3	None	None
3	F	12	A	A3	1	1-3	E	None
4	M	11	B	B1	2	1-3	None	Sterile non-woven sponge balls
5	M	10	B	B2	3	3-5 (2), 1-3 (1)	T-PB	None
6	M	13	B	B3	2	3-5	T-PB	Sterile non-woven sponge balls
7	M	12	B	B4	3	3-5	None	None
8	M	13	B	B5	3	1-3	T-PB	Sterile non-woven sponge balls
9	M	13	B	B6	3	<1	T-PB	Sterile non-woven sponge balls
10	M	10	B	B7	1	<1	None	Sterile non-woven sponge balls, only post-operatively
11	M	10	B	B8	2	1-3	None	Silicone elastomer
12	M	12	C	C1	2	1-3	G	None
13	M	12	C	C2	3	1-3	BNP	None
14	M	11	C	C3	2	3-5	BNP or G	None
15	M	8	C	C4	1	1-3	BNP	Sterile petroleum jelly, occasionally with granulation tissue
16	F	10	C	C5	2	1-3	BNP or G	None
17	F	11	C	C6	3	1-3	BNP	None
18	M	10	C	C7	2	1-3	G	None
19	M	10	C	C8	2	<1	G	None
20	F	11	D	D1	1	3-5	None	Sterile petroleum jelly
21	M	8	D	D2	1	3-5	None	Sterile petroleum jelly
22	M	7	D	D3	1	1-3	None	None
23	M	7	D	D4	1	<1	None	Sterile petroleum jelly (when not on study)
24	M	11	D	D5	1	3-5	None	Sterile petroleum jelly
25	M	6	D	D6	1	1-3	None	Sterile petroleum jelly

Table 2.1: Population characteristics of 25 sampled research macaques in August, 2011. At the time of sampling, macaque #10 had a CRC without a craniotomy. Macaque #18 was a cynomolgus macaque; all other macaques were rhesus macaques. Antimicrobial use within CRCs and CRC packing material are listed for each animal as designated. Antimicrobial key: G, gentamicin sulfate 0.3%; E, enrofloxacin 2.27% diluted 1:20, T-PB, oxytetracycline 5mg/g-polymyxin B 10,000U/g; BNP, bacitracin zinc 400U/g-neomycin sulfate 5mg/g-polymyxin B 10,000U/g

2.2.2 Bacterial culture and Kirby-Bauer antimicrobial susceptibility testing

Sterile culture swabs (CultureSwab MaxV(+), BD, Franklin Lakes, NJ) were used to sample the interior of cephalic recording chambers, including any discharge present. The swabs were plated onto chocolate agar, trypticase soy agar with 5% sheep blood and MacConkey agar plates and incubated at 37°C in 5% CO_2 for 24h. The swabs, themselves, were then incubated in thioglycollate broth at 37°C for 24h and re-plated onto the media listed above. Microbial growth was streaked onto blood agar to obtain isolated colonies, which were then identified using the Analytical Profile Index identification system (API 20 E and API 20 Strep, bioMérieux, Durham, NC). Antibiotic susceptibility profiles were determined by disk diffusion using the Clinical and Laboratory Standards Institute break points (M2-A10) [20]. Antimicrobial agents tested included ampicillin, amoxicillin/clavulanic acid, bacitracin, cephalothin, erythromycin, gentamicin, oxacillin, trimethoprim-sulfamethoxazole, enrofloxacin, tetracycline, oxy-tetracycline, ceftriaxone, doxycycline, neomycin, cefazolin, polymyxin B and vancomycin. Gentamicin, chloramphenicol, streptomycin, and vancomycin disks were purchased from BD (BBL Sensi-Disc, Franklin Lakes, New Jersey); the remainder of the antimicrobial disks were obtained from Oxoid (Basingstoke, United Kingdom).

2.2.3 Aerobic bacterial culture results

From aerobic cultures of the 45 cephalic recording chambers sampled, 72 bacterial isolates were examined, with the most common species being *Staphylococcus aureus* (N=20), *Enterococcus faecalis* (N=15), *Proteus mirabilis* (N=6) and *Streptococcus dysgalactiae* (N=5) (Table 2.2). The vast majority of cephalic recording chambers grew polymicrobial cultures with a mean and standard deviation of 2.8 ± 1.5 different species (Table 2.3). Kirby-Bauer testing revealed that *S. aureus* and *S. dysgalactiae* isolates were susceptible to the majority of antimicrobials tested, while *E. faecalis* and *Proteus* spp. isolates displayed resistance to multiple classes of antimicrobial agents. Parenteral antimicrobial agents commonly used therapeutically and in the perioperative period included trimethoprim-sulfamethoxazole

(TMS), enrofloxacin and ceftriaxone. Antimicrobial sensitivity results revealed that 56% (40/72) of isolates tested were resistant to trimethoprim-sulfamethoxazole, 69% (49/71) were resistant to enrofloxacin and 35% (25/72) were resistant to ceftriaxone (Table 2.4). For topical antimicrobial agents used within CRCs, 40% (23/58) were resistant to bacitracin, 53% (38/72) were resistant to neomycin, 56% (35/62) were resistant to polymyxin B and 32% (23/72) were resistant to gentamicin (Table 2.4). A full list of bacterial isolates and their antimicrobial sensitivities is included in Tables 2.5, 2.6, and 2.7. Due to the marked antimicrobial resistance to multiple antimicrobial classes present in *E. faecalis* strains, further characterization of 15 isolates was performed. These results will be presented in Chapter 3.

Bacterial Isolate	Number (%) of Isolates
Staphylococcus aureus	20 (27.8)
Enterococcus faecalis	15 (20.8)
Proteus mirabilis	6 (8.3)
Group C β-*Streptococcus dysgalactiae*	5 (6.9)
Proteus vulgaris	4 (5.6)
Staphylococcus intermedius	4 (5.6)
Enterococcus avium	3 (4.2)
Escherichia coli	2 (2.8)
Group A β-*Streptococcus pyogenes*	2 (2.8)
Leuconostoc spp.	2 (2.8)
Streptococcus uberis	2 (2.8)
Aerococcus viridans 2	1 (1.4)
Enterococcus durans	1 (1.4)
Group F β-*Streptococcus constellatus*	1 (1.4)
Proteus penneri	1 (1.4)
Proteus sp.	1 (1.4)
Staphylococcus epidermidis	1 (1.4)
Staphylococcus xylosus	1 (1.4)
Total	**72 (100)**

Table 2.2: Aerobic bacterial culture results from 45 CRCs of research macaques (N=25). Cultures were pooled for animals with multiple CRCs.

Number of Isolates	# (Percentage) of Macaques
0	1 (4%)
1	4 (16%)
2	7 (28%)
3	5 (20%)
4	4 (16%)
5	3 (12%)
6	1 (4%)

Table 2.3: The majority of macaque CRCs display polymicrobial colonization

Antimicrobial Phenotype - All Aerobic Isolates	AMP	AMC	B	CR	E	GM	OX	SXT	ENO	TE	T	CRO	D	N	CZ	PB	VA
# Resistant	26	6	23	24	20	23	24	40	49	38	40	25	3	38	28	35	11
# Sensitive	44	62	28	40	22	46	34	31	11	31	31	45	24	29	39	8	4
# Intermediate	1	4	7	8	16	3	0	1	11	2	1	2	3	5	5	19	6
# Isolates Tested	71	72	58	72	58	72	58	72	71	71	72	72	30	72	72	62	21
% Resistant	36.62	8.333	39.66	33.33	34.48	31.94	41.38	55.56	69.01	53.52	55.56	34.72	10	52.78	38.89	56.45	52.38
# Sensitive	61.97	86.11	48.28	55.56	37.93	63.89	58.62	43.06	15.49	43.66	43.06	62.5	80	40.28	54.17	12.9	19.05

Table 2.4: Percent of resistant and sensitive aerobic bacterial isolates as tested by Kirby-Bauer disk diffusion testing. Antimicrobial key: AMP- Ampicillin, AMC- Amoxicillin/Clavulanic Acid, B- Bacitracin, CR- Cephalothin, E- Erythromycin, GM- Gentamicin, OX- Oxacillin, SXT- Trimethoprim-Sulfamethoxazole, ENO- Enrofloxacin, TE- Tetracycline, T- Oxytetracycline, CRO- Ceftriaxone, D- Doxycycline, N- Neomycin, CZ- Cefazolin, PB- Polymixin B, VA- Vancomycin

Animal ID	Study ID	Antimicrobial Used	Culture Results	AMP	AMC	B	CR	E	GM	OX	SXT	ENO	TE	T	CRO	D	N	CZ	PB	VA
20	D1		*Aerococcus viridans 2*	S	S	15	S	S	S	S	S	S	31	30	S		S	S	S	
7	B4		*Enterococcus avium*	18	25	16	15	0	13	0	0	24	0	0	20		28	23	13	18
7	B4		*Enterococcus avium*	24	27	8	19	0	10	0	0	14	0	0	19		13	16	0	20
13	C2	N, PB, B	*Enterococcus avium*	S	S	21	32	15	28	0	21	0	0	0	0	17	0	13	10	17
5	B2	T-PB	*Enterococcus durans*	25	25	9	20	19	0	0	0	15	15	8	19		0	23	0	16
1	A1	GM	*Enterococcus faecalis*	17	25	13	11	0	0	0	0	0	0	0	0		12	9	0	15
4	B1		*Enterococcus faecalis*	16	13	0	13	0	12	0	0	14	0	0	13		0	13	0	9
5	B2	T-PB	*Enterococcus faecalis*	24	27	0	14	0	19	0	0	18	7	7	15	14	0	12	0	
5	B2	T-PB	*Enterococcus faecalis*	25	35	0	16	0	16	0	0	0	0	0	22		0	16	0	20
5	B2	T-PB	*Enterococcus faecalis*	16	22	11	13	0	14	0	0	0	0	0	18		0	13	0	15
6	B3	T-PB	*Enterococcus faecalis*	0	19	0	11	0	12	0	0	14	0	0	10		0	12	0	13
8	B5		*Enterococcus faecalis*	18	19	0	12	0	10	0	19	13	0	0	0		0	12	0	13
9	B6	T-PB	*Enterococcus faecalis*	16	22	11	11	14	12	0	0	0	0	0	0		0	12	0	15
11	B8		*Enterococcus faecalis*	19	19	11	9	0	12	0	0	0	0	0	0		10	11	0	13
11	B8		*Enterococcus faecalis*	21	24	11	11	10	13	0	0	0	0	0	0		10	12	0	13
15	C4	N, PB, B	*Enterococcus faecalis*	23	25	0	13	0	18	0	0	18	0	0	11	16	0	11	0	12
16	C5	N, PB, B, GM	*Enterococcus faecalis*	20	21	0	13	0	18	0	0	17	0	0	10	14	0	11	0	
16	C5	N, PB, B, GM	*Enterococcus faecalis*	21	22	0	12	0	18	0	0	17	0	0	10	14	0	11	0	12
18	C7	GM	*Enterococcus faecalis*	19	24	11	11	10	0	0	0	0	0	0	0		8	11	0	15
19	C8	GM	*Enterococcus faecalis*	25	27	15	10	0	0	0	0	0	0	0	0	11	14	12	0	15

Table 2.5: Aerobic culture and Kirby-Bauer antimicrobial sensitivity results by isolate cultured, Part 1. Numbers represent the zone of inhibition measured around each antimicrobial disk. Color coding indicates resistant (red), sensitive (green) or intermediate (yellow) antimicrobial phenotype. Antimicrobial key: AMP- Ampicillin, AMC- Amoxicillin/Clavulanic Acid, B- Bacitracin, CR- Cephalothin, E- Erythromycin, GM- Gentamicin, OX- Oxacillin, SXT- Trimethoprim-Sulfamethoxazole, ENO- Enrofloxacin, TE- Tetracycline, T- Oxytetracycline, CRO- Ceftriaxone, D- Doxycycline, N- Neomycin, CZ- Cefazolin, PB- Polymixin B, VA- Vancomycin

Animal ID	Study ID	Antimicrobial Used	Culture Results	AMP	AMC	B	CR	E	GM	OX	SXT	ENO	TE	T	CRO	D	N	CZ	PB	VA
7	B4		*Escherichia coli*	16	23		12		20		28	9	21	20	31		20	0		
21	D2		*Escherichia coli*	17	20		14		19		24	9	18	19	26		11	0		
13	C2	N, PB, B	*Group A β-Streptococcus pyogenes*	35	36	24	35	28	23	24	0	20	25	24	35	24	18	38	9	
15	C4	N, PB, B	*Group A β-Streptococcus pyogenes*	32	35	25	33	26	21	22	0	20	25	23	30	25	18	35	10	
12	C1	GM	*Group C β-Streptococcus dysgalactiae*	38	40	26	37	30	21	25	0	15	25	26	36	24	0	26	11	
13	C2	N, PB, B	*Group C β-Streptococcus dysgalactiae*	37	41	27	40	31	24	28	0	21	25	24	35	27	18	39	10	
16	C5	N, PB, B, GM	*Group C β-Streptococcus dysgalactiae*	37	39	27	38	28	22	27	0	20	27	26	35	28	18	35	10	
19	C8	GM	*Group C β-Streptococcus dysgalactiae*	36	36	25	35	26	21	20	0	15	21	23	36	26	0	36	12	
20	D1		*Group C β-Streptococcus dysgalactiae*	43	43	29	41	32	25	29	0	30	31	30	42	31	18	42	8	
5	B2	T-PB	*Group F β-Streptococcus constellatus*	37	39	25	37	29	24	25	0	24	0	8	36	12	19	42	10	
11	B8		*Leuconostoc spp.*		20	23	23	32	29	0	0	14		7	21		28	15	15	0
25	D6		*Leuconostoc spp.*	20	27	20	17	27	17	0	16	15	16	17	16		16	24	9	0
9	B6	T-PB	*Proteus mirabilis*	0	19		15		18		0	12	8	0	33		17	9	0	
14	C3	N, PB, B, GM	*Proteus mirabilis*	0	20		18		0		0		0	0	29		0	15		
15	C4	N, PB, B	*Proteus mirabilis*	0	20		18		0		0	0	0	0	29		0	0		
16	C5	N, PB, B, GM	*Proteus mirabilis*	0	18		17		0		0	0	0	0	29		0	0		
17	C6	N, PB, B	*Proteus mirabilis*	0	20		17		0		0	12	0	0	23		0	0		
24	D5		*Proteus mirabilis*	0	18		16		20		0	10	0	0	22		18	11		
12	C1	GM	*Proteus penneri*	0	16		0		9		0	9	8	0	25		14	0	12	
20	D1		*Proteus sp. (unknown)*	19	23		16		10		17	28	0	0	21		19	17	0	
6	B3	T-PB	*Proteus vulgaris*	0	15		0		9		0	31	0	0	0		17	21		
6	B3	T-PB	*Proteus vulgaris*	0	14		0		0		0	0	0	0	0		0	0		
7	B4		*Proteus vulgaris*	0	20		0		0		0	9	9	0	0		20	0		
12	C1	GM	*Proteus vulgaris*	0	16		0		11		0	10	8	0	24		15	0	0	

Table 2.6: Aerobic culture and Kirby-Bauer antimicrobial sensitivity results by isolate cultured, Part 2. Numbers represent the zone of inhibition measured around each antimicrobial disk. Color coding indicates resistant (red), sensitive (green) or intermediate (yellow) antimicrobial phenotype. Antimicrobial key: AMP- Ampicillin, AMC- Amoxicillin/Clavulanic Acid, B- Bacitracin, CR- Cephalothin, E- Erythromycin, GM- Gentamicin, OX- Oxacillin, SXT- Trimethoprim-Sulfamethoxazole, ENO- Enrofloxacin, TE- Tetracycline, T- Oxytetracycline, CRO- Ceftriaxone, D- Doxycycline, N- Neomycin, CZ- Cefazolin, PB- Polymixin B, VA- Vancomycin

Animal ID	Study ID	Antimicrobial Used	Culture Results	AMP	AMC	B	CR	E	GM	OX	SXT	ENO	TE	T	CRO	D	N	CZ	PB	VA
1	A1	GM	*Staphylococcus aureus*	32	37	18	38	25	24	22	27	14	29	28	25	28	20	36	10	
3	A3	ENO	*Staphylococcus aureus*	37	38	15	37	0	29	23	22	10	29	27	26	30	25	35	11	
4	B1		*Staphylococcus aureus*	31	35	18	38	28	23	20	29	14	29	28	27	29	18	34	0	
5	B2	T-PB	*Staphylococcus aureus*	38	37	19	39	28	22	21	28	14	27	27	26	29	21	33	14	
6	B3	T-PB	*Staphylococcus aureus*	39	37	18	37	25	18	21	26	12	23	23	24		19	35	8	
7	B4		*Staphylococcus aureus*	38	37	17	38	25	21	20	27	20	25	23	24		19	33	8	
12	C1	GM	*Staphylococcus aureus*	36	37	0	37	14	19	21	29	9	30	24	27	27	0	32	10	
13	C2	N, PB, B	*Staphylococcus aureus*	30	37	0	37	15	21	21	33	8	27	23	27	30	0	35	9	
14	C3	N, PB, B, GM	*Staphylococcus aureus*	36	34	0	34	19	21	21	28	8	26	25	25	28	0	33	9	
15	C4	N, PB, B	*Staphylococcus aureus*	30	33	0	35	14	21	20	28	0	25	24	24	27	0	34	10	
16	C5	N, PB, B, GM	*Staphylococcus aureus*	35	34	0	35	14	22	20	30	7	28	26	25	27	0	33	0	
17	C6	N, PB, B	*Staphylococcus aureus*	38	36	0	39	15	20	21	33	20	30	29	29	31	0	37	0	
18	C7	GM	*Staphylococcus aureus*	36	35	18	36	26	21	23	26	24	24	26	24	29	20	33	10	
19	C8	GM	*Staphylococcus aureus*	36	35	0	36	15	21	21	30	8	29	28	25	30	0	35	0	
20	D1		*Staphylococcus aureus*	37	35	19	36	26	21	19	28	19	28	24	25	28	19	32	0	
21	D2		*Staphylococcus aureus*	14	25	25	26	26	20	20	27	27	25	25	25		20	31	10	
22	D3		*Staphylococcus aureus*	15	20	14	21	23	19	17	25	12	11	0	13		19	19	0	
23	D4		*Staphylococcus aureus*	38	39	0	40	13	20	21	31	0	24	24	26		0	35	0	
23	D4		*Staphylococcus aureus*	15	15	14	20	19	18	18	25	11	9	0	12		18	19	0	
24	D5		*Staphylococcus aureus*	26	30	16	29	24	28	20	27	24	24	23	19		25	31	12	
24	D5		*Staphylococcus epidermidis*	45	45	14	46	27	28	27	29	29	26	26	35		23	40	12	
5	B2	T-PB	*Staphylococcus intermedius*	14	25	0	35	29	24	21	28	13	8	0	26	12	10	32	10	
12	C1	GM	*Staphylococcus intermedius*	32	39	0	40	16	21	22	31	0	28	28	29	29	0	34	10	
14	C3	N, PB, B, GM	*Staphylococcus intermedius*	30	34	0	35	14	22	20	29	8	24	23	24	24	0	33	10	
24	D4		*Staphylococcus intermedius*	34	36	0	39	14	18	23	31	10	22	19	24		0	34	0	
6	B3	T-PB	*Staphylococcus xylosus*	0	14	0	0	0	0	0	0	9	0	0	25		19	35	8	
8	B5	T-PB	*Streptococcus uberis*	18	20	0	13	0	0	0	0	12	0	0	17		0	12	0	13
10	B7		*Streptococcus uberis*	17	23	12	11	17	8	0	0	0	0	0	0		0	12	0	14

Table 2.7: Aerobic culture and Kirby-Bauer antimicrobial sensitivity results by isolate cultured, Part 3. Numbers represent the zone of inhibition measured around each antimicrobial disk. Color coding indicates resistant (red), sensitive (green) or intermediate (yellow) antimicrobial phenotype. Antimicrobial key: AMP- Ampicillin, AMC- Amoxicillin/Clavulanic Acid, B- Bacitracin, CR- Cephalothin, E- Erythromycin, GM- Gentamicin, OX- Oxacillin, SXT- Trimethoprim-Sulfamethoxazole, ENO- Enrofloxacin, TE- Tetracycline, T- Oxytetracycline, CRO- Ceftriaxone, D- Doxycycline, N- Neomycin, CZ- Cefazolin, PB- Polymixin B, VA- Vancomycin

2.2.4 Updates to CRC sanitization protocols implemented in September, 2014

Based on confirmed antimicrobial resistant phenotypes of bacterial species present in chambers, in September, 2014, the MIT veterinary staff finalized updated recommendations for routine CRC sanitization procedures to decrease indiscriminate antimicrobial use. Specific changes outlined techniques to maintain asepsis when opening CRCs, including use of sterile, single use instrument packs. Recommended solutions for sanitization inside CRCs were limited to 1-2% diluted povidone-iodine and sterile saline due to the concern for neurotoxicity with hydrogen peroxide and chlorhexidine. Recommendations for CRC sanitization frequency were based on the amount and type of discharge present and determined by the veterinary staff. Use of packing material other than silicone elastomer was discouraged, and use of topical antimicrobial agents within CRCs was strictly prohibited without explicit veterinary approval. Perioperative systemic trimethoprim-sulfamethoxazole and enrofloxacin have been replaced by cefazolin, and post-operative ceftriaxone use is restricted to surgical procedures involving a craniotomy. Animals with suspected meningitis now undergo thorough diagnostic work-up, including culture and sensitivity testing of isolates in cerebrospinal fluid to guide choices in antimicrobial therapy and minimize further spread of bacterial resistance genes within the macaque colony. Finally, Updated implant design utilizing MRI and computer-aided design was recommended to customize implants to individual macaque skull morphology and minimize the amount of PMMA required to stabilize hardware.

2.3 Evaluation of bacterial species inhabiting CRCs using next-generation sequencing methods for 2017 samples

While culture-dependent methods can provide valuable insight into bacterial species colonizing CRCs, there are several limitations of these techniques. First, species identification from 2011 was performed only from aerobic cultures. We were interested in assessing anaerobic species, since

they have been previously isolated from macaques with brain abscesses and meningitis. Standard culture techniques are challenging to perform on polymicrobial samples, as overgrowth of more prevalent, less-fastidious, or rapidly-growing species may complicate isolation of less-prevalent, more-fastidious and/or slower-growing species, and are dependent on the use of selective media. Selection of unique, individual colonies for isolation in mixed-culture samples is dependent on the skill of the microbiologist, and colonies of closely-related species can look very similar on agar plates. Finally, use of biochemical testing based on commercially available API strips is not 100% accurate in discriminating between closely related species [21, 22, 23].

To overcome these limitations, we wished to explore culture-independent methods for characterizing bacterial species living within CRCs. Advances in next-generation sequencing technology have allowed multiple scientific disciplines to characterize bacterial communities, from those colonizing the human body, to those living beneath the ocean floor [24, 25]. The microbiome is defined as the collective genomes of microbial symbionts, while the microbiota is defined as the collective microbes, themselves [24]. Culture-independent methods of bacterial identification rely on using the 16S ribosomal RNA (rRNA) gene as a phylogenetic marker and comparison of sequences to a reference database [26]. The 16S rRNA gene features nine hypervariable regions, which display wide diversity between bacterial species (Figure 2-1). The hypervariable regions are adjacent to highly conserved sequences, which can be utilized for design of polymerase chain reaction (PCR) primers [27].

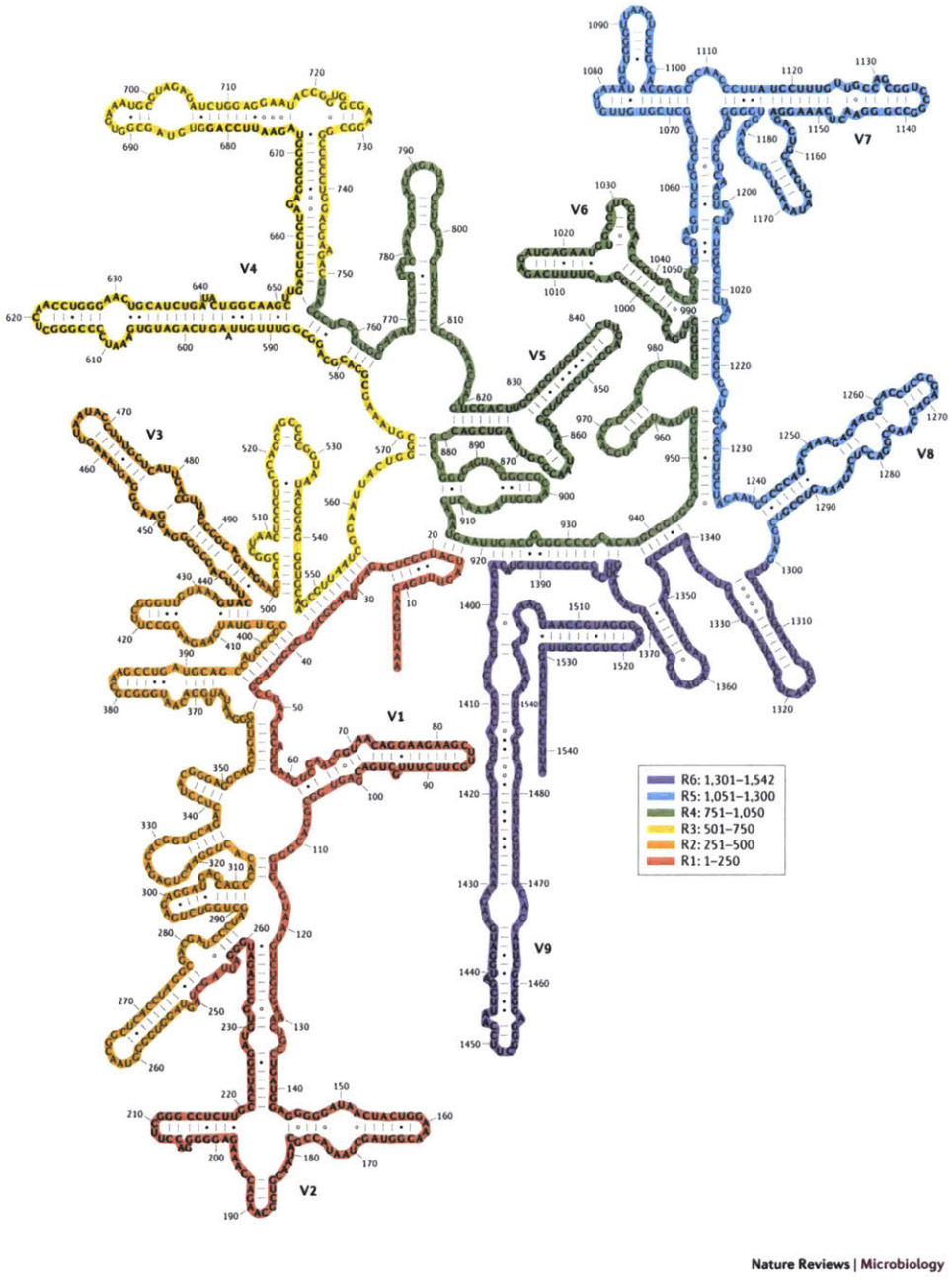

Figure 2-1: Secondary structure of the 16S rRNA of *Escherichia coli* to illustrate locations of variable regions 1-9. Figure reused with permission [28]

Currently, the most common methodology for microbiota sequencing utilizes Illumina sequencing-by-synthesis techniques following PCR amplification of varying hypervariable regions (V1-V3, V3-V4, V4-V5, etc.) [29, 30]. Sequences are compared to reference databases and typically matched at a threshold of 95-97% sequence identity for assignment to an

operational taxonomic unit (OTU); the microbiota equivalent of a "species" [26]. Ecological techniques used for macro-communities have been adapted and widely used for microbiota diversity analysis. Alpha diversity metrics, such as the Shannon diversity index, are used to estimate both the richness (number) and evenness (relative abundance) of OTUs within a single community. Rarefaction curves are commonly displayed to illustrate the relationship between the number of sequences per sample (i.e. richness) as a function of the number of samples (sequencing depth) [26].

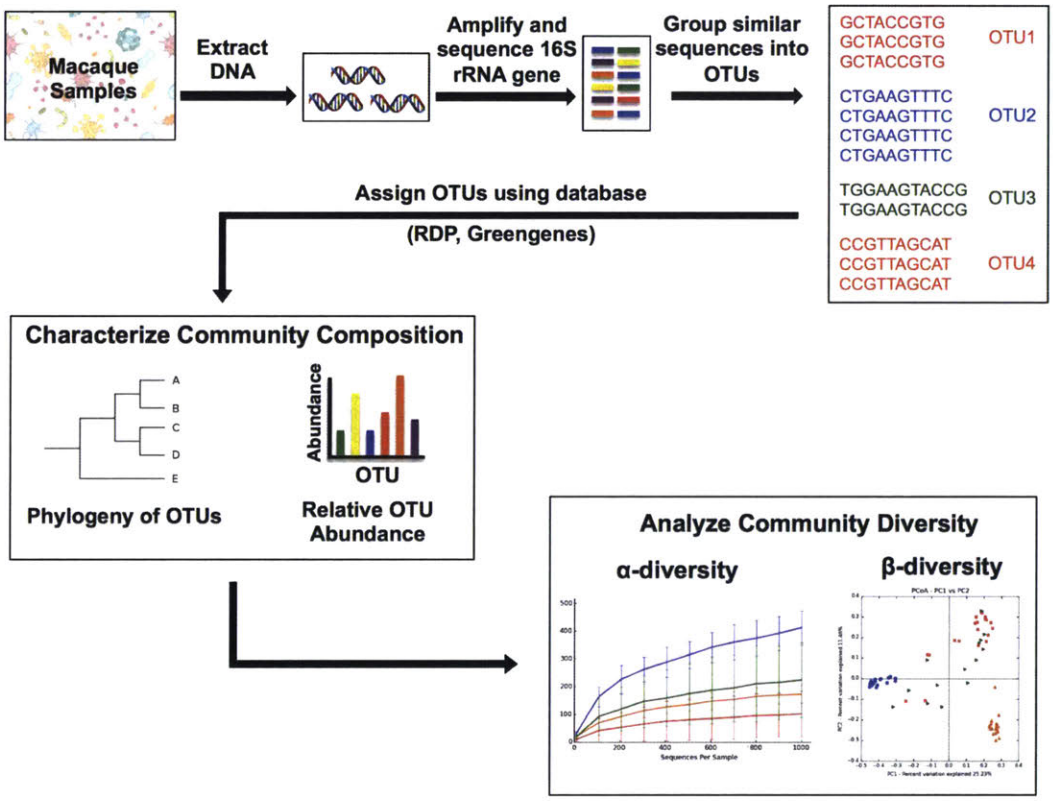

Figure 2-2: Overview of steps from DNA extraction to community analysis for microbiota studies.

Beta diversity measurements are used to compare overlap between populations and can be evaluated using a distance or dissimilarity matrix such as UniFrac [31]. Unweighted UniFrac uses both the presence and absence of OTUs, as well as the branch length in a phylogenetic tree for population comparisons, while weighted UniFrac also accounts for relative abundance of OTUs [32]. Distances between populations can be visualized using principal coordinate analysis (PCoA), where samples located closer together are more closely related than samples located farther apart [31, 32]. The work-

flow of microbiome analysis is illustrated in Figure 2-2.

To evaluate whether purulent exudate from macaque CRCs could be analyzed using microbiota techniques, we performed a pilot study on seven implanted macaques using samples collected in March-April 2017. The goals of this study were to assess the anaerobic bacterial population of CRC bacterial communities and compare bacterial communities between macaques. Additionally, we were interested in comparing OTUs to previously identified and culture results.

2.4 Pilot study methods

2.4.1 Animals

Seven rhesus macaques (4 males and 3 females) under investigation by three different laboratories were selected for sampling. Three macaques had two CRCs, and four macaques had a single CRC. Samples from one macaque with two CRCs were pooled, and samples for the other two macaques with 2 CRCs were analyzed separately. Most CRCs had been in place between 1-3 years (5 CRCs), 2 CRCs were implanted <1 year, and 2 CRCs in the same individual (macaque #9) had been implanted 6 years previously (Table 2.8). Sampling was performed in chair-restrained macaques just prior to routine CRC sanitization procedures. All macaques had a minimum washout period of 3 weeks with cessation of systemic antimicrobial administration. A sterile syringe was used to collect 0.1-1 ml of exudate from the CRC. Samples were collected into an empty sterile plastic vial, and extra samples for culture, when available, were saved in freeze media consisting of brucella broth with 20% glycerol and stored at -80°C until processing.

Animal ID	Sex	Age (years)	Lab ID	Study ID	Implant date (month/year)	# of CRCs Sampled	CRC materials	Culture Sample Available?
26	F	7	A	A4	10/16	1	Ultem, ceramic screws, PMMA	Yes
27	M	8	E	E1	10/16	1	PEEK, titanium screws, PMMA	No
28	M	17	B	B9	3/15	2	PEEK, titanium screws, PMMA-free	No
29	F	7	A	A5	11/15	1	Ultem, ceramic screws, PMMA with gentamicin	Yes
30	M	8	A	A6	12/14	2 - pooled	Delrin ceramic screws, PMMA with gentamicin	Yes
9	M	18	B	B6	4/11	2	Ultem, titanium screws, PMMA	Yes
31	F	16	A	A7	2/15	1	Delrin, ceramic screws, PMMA with gentamicin	Yes

Table 2.8: Population characteristics of 7 research macaques sampled in March-April 2017.

2.4.2 DNA extraction, sequencing and analysis

Genomic DNA was extracted from samples on the same day as collection using the DNA Microbiome kit according to manufacturer instructions (Qiagen, USA). This kit was chosen due to inclusion of a benzonase pretreatment step. Benzonase degrades host DNA and was considered a beneficial step, since most samples were visually purulent, containing a high percentage of leukocytes. A maximum of 0.5 ml CRC exudate was used for DNA extraction. Samples were submitted to the MIT BioMicro Center Core facility for PCR amplification of the 16S rRNA V4 region, library preparation and sequencing. Individual samples were barcoded and pooled to construct the sequencing library using previously published protocols [33]. F515 and R806 sequencing primers used are listed in Appendix B. Sequencing was performed using an Illumina MiSeq to generate pair-ended 250x250 reads. Overlapping pair-end reads were aligned using QIIME 1.9.1 within the MicrobiomeHelper v. 2.0.0 virtual box [34, 33]. Quality filtering of paired samples was performed using a Phred quality threshold of 20. After quality filtering, the mean read length was approximately 295 bp. The mean number of reads/sample was 270,886 (range 160,785-373,366 reads). Open reference OTU picking was performed on a total of 2,437,974 reads at 97% sequence similarity using the uclust method. Taxonomic assignments were determined using the Ribosomal Database Project classifier against the GreenGenes database. Alpha diversity was determined using Observed OTUs and Shannon Index metrics and displayed using rarefaction curves. Beta-diversity was determined using unweighted and weighted UniFrac and results displayed as PCoA plots [31]. Alpha and beta diversity analyses were rarefied to the lowest sequencing depth of 160,785 reads. OTUs were summarized at different taxonomic levels and displayed as bar graphs.

2.4.3 Aerobic and anaerobic cultures of CRC samples from pilot study animals

Samples from macaques #9, #26, #29, #30 and #31 were plated on 3% Brucella agar plates in an anaerobic chamber (10% CO_2, 10% H_2, 80% N_2 and incubated at 37°C for 48 hours. Morphologically different individ-

ual colonies were selected for isolation, and replated onto 1.5% Brucella agar (Remel). After 36-48 hours of incubation, colonies were examined, Gram-stained and tested for aerotolerance. Aerotolerance was determined by colony transfer to TSA with 5% sheep blood (Remel) and incubated aerobically at 37°C, 5% CO_2. For species identification, pure cultures of anaerobic and aerobic species were collected into 1ml of PBS, and spun for 3 minutes at 10,000 $\times$ *g*. Pellets were resuspended in 200μl of PBS, 25μl was added to 75μl PBS and incubated for 10 minutes at 95°C. After heating, samples were centrifuged for 3 minutes at 10,000 $\times$ *g*. After measurement of DNA concentrations using a NanoDrop spectrophotometer (Thermo Fisher Scientific, Waltham, MA), samples were stored at -20°C. For samples with low DNA yield ($<$ 10ng/μl), 50μl of the resuspended pellet was added to 200μl of a mixture containing 5% Chelex-100 resin and 0.02% proteinase K and incubated at 56°C for 60 minutes. Samples were then vortexed, incubated for 10 minutes at 95°C and centrifuged for 3 minutes at 10,000 $\times$ *g*. PCR amplification of the 16S rRNA gene using the F9 and R1541 primers was performed according to previously published protocols [35] using a commercially-available bead-based PCR kit (illustra PuReTaq Ready-To-Go PCR Beads, GE Healthcare Bio-Sciences, Pittsburgh, PA). PCR bands were separated by electrophoresis on a 1% gel at 100-120V for 30-40 minutes and visualized with UV light following ethidium bromide staining. PCR products (5μl) were purified by adding 2μl of a mixture containing 0.4 U/μl exonuclease I and 0.4 U/μl shrimp alkaline phosphatase and incubated for 20 min at 37°C followed by 20 min at 80-85°C. PCR products were submitted for sequencing at a commercial laboratory (Quintara Biosciences, Cambridge, MA) and sequences identified using the Basic Local Alignment Search Tool (`https://blast.ncbi.nlm.nih.gov/Blast.cgi`). For seven samples, multiple bands were visualized in the 1.5 Kb range and overnight cultures plated on TSA with 5% sheep blood were identified using API Coryne strips according to manufacturer instructions (bioMérieux, Durham, NC).

2.4.4 Pilot results

Alpha diversity

Rarefaction curves, Shannon index and observed OTUs are displayed in Figure 2-3. Rarefaction curves leveled off around 20,000 sequences sug-

gesting that sampling depth was sufficient to characterize bacterial communities. The average Shannon diversity index was 4.76 and the average number of observed OTUs was 989 per sample. Macaque #28 had a higher number of observed OTUs (1883, 1953) and thus a higher Shannon index (7.33 and 6.81) in CRCs 1 and 2, respectively as compared to the other sampled macaques. Due to the small sample size and restriction of sample type to CRCs only, no statistics were performed.

Beta diversity

PCoA plots of unweighted (top) and weighted (bottom) UniFrac distances are displayed in Figure 2-4. On unweighted UniFrac plots, three predominant clusters were present. The 2 CRC samples from macaque#9 clustered together, the 2 CRC samples from macaque #28 clustered together and 4 CRC samples from macaques #26, #27, #30 and #31 clustered together. The CRC sample from macaque #29 was distinct from macaques #9 and #28, and closer, but still slightly separated from the 4-sample CRC cluster. On weighted UniFrac plots, the only discernable cluster were the two samples from macaque #28.

Taxonomy Bar charts

Phylum and genus level bar charts are displayed in Figures 2-5 and 2-6. At both the phylum and genus level, all macaques displayed a unique CRC community composition. In macaques #26, #28 and #29, the Firmicutes phylum was predominant, while in macaques #30, #9 and #31, the Fusobacteria phylum was predominant. Macaque #27 had approximately equal ratios of Firmicutes, Fusobacteria and Bacteroidetes phyla. At the genus level, *Fusobacterium* spp. were detected in all macaques except macaque #28. *Fusobacterium* spp. contributed to more than a quarter of sample reads in CRC samples from macaques #9 (81% and 48%), #27 (27%), #29 (27%), #30 (58%) and #31 (58%). The *Clostridiales* order accounted for >70% and >54% of reads in the two CRCs from macaque #28. Other selected OTUs representing >1% of sample reads in multiple CRCs included *Parvimonas*, *Bacteroides*, *Streptococcus*, *Peptinophilus*, *Peptrostreptococcus*, and *Porphyromonas*, and *Corynebacterium*. Full pilot taxonomy results are archived at `https://figshare.com/s/32fedb5a71d548d52df2`.

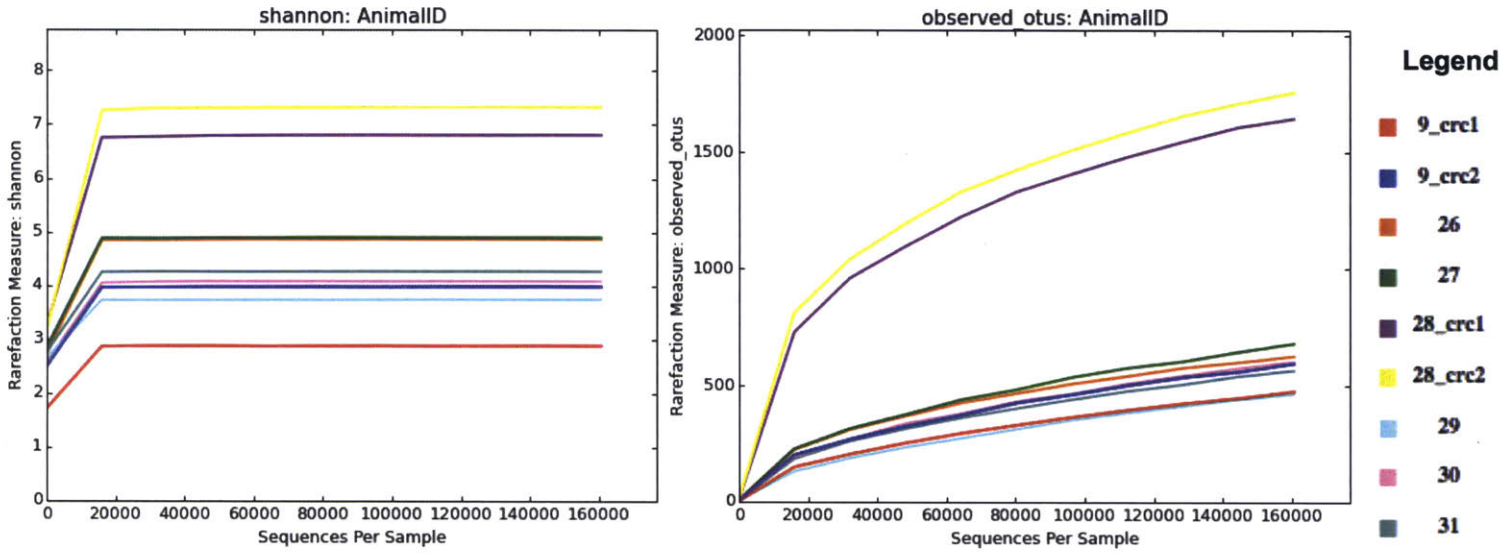

Animal ID	Study ID	Sample	Shannon Diversity Index	Observed OTUs
9	B6	CRC 1	2.88363691	579
		CRC 2	3.982357703	662
26	A4	CRC 1	4.867520919	625
27	E1	CRC 1	4.904092494	933
28	B9	CRC 1	7.334302024	1953
		CRC 2	6.811891531	1883
29	A5	CRC 1	3.74263841	614
30	A6	CRCs pooled	4.085426431	899
31	A7	CRC 1	4.270526037	751

Figure 2-3: Rarefaction curves and alpha diversity results as calculated using the Shannon diversity index and observed OTUs metrics for each CRC sample. Samples were rarefied to 160,785 reads

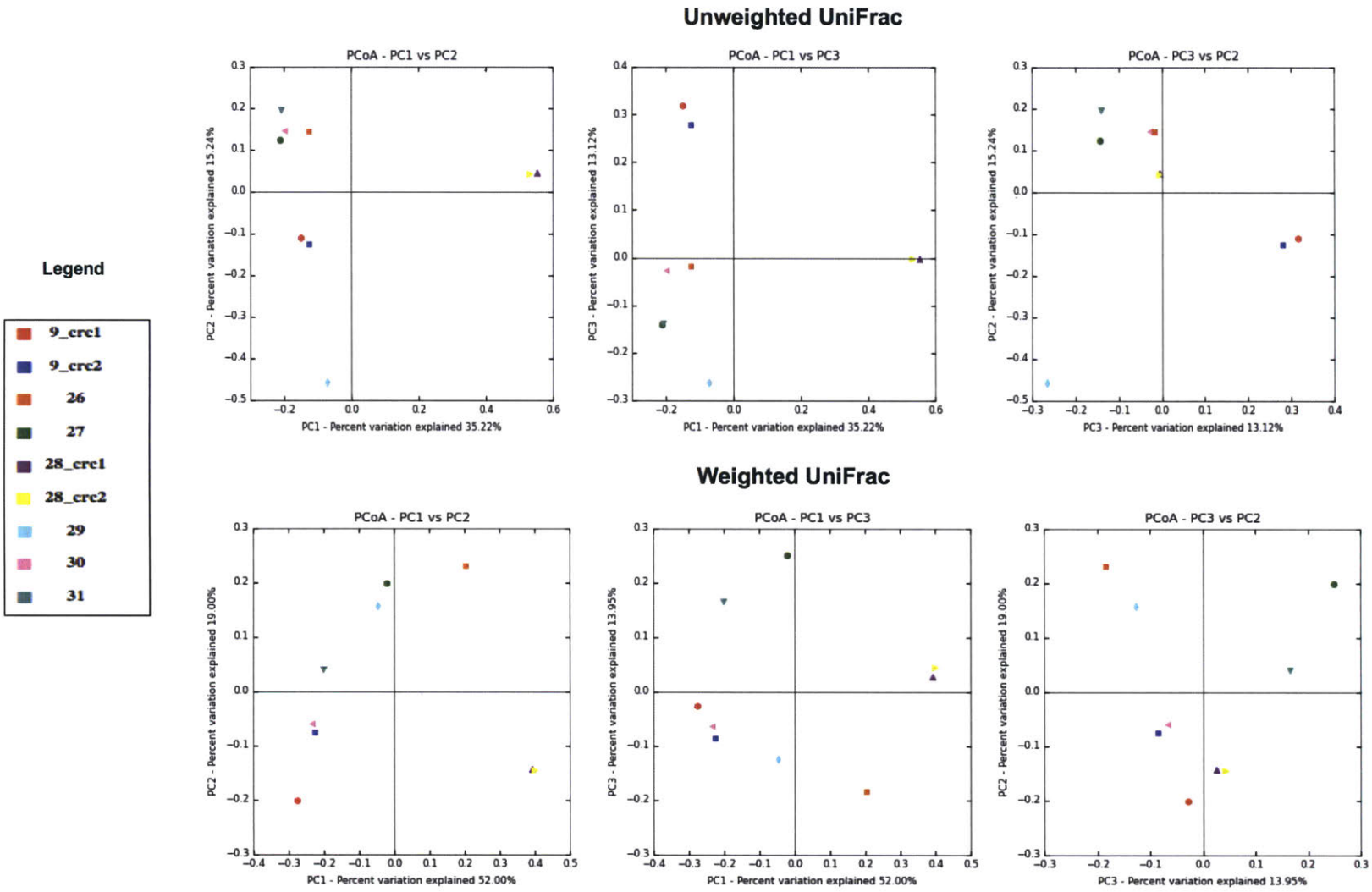

Figure 2-4: Principal coordinate analysis of unweighted and weighted UniFrac plots. Samples were rarefied to 160,785 reads

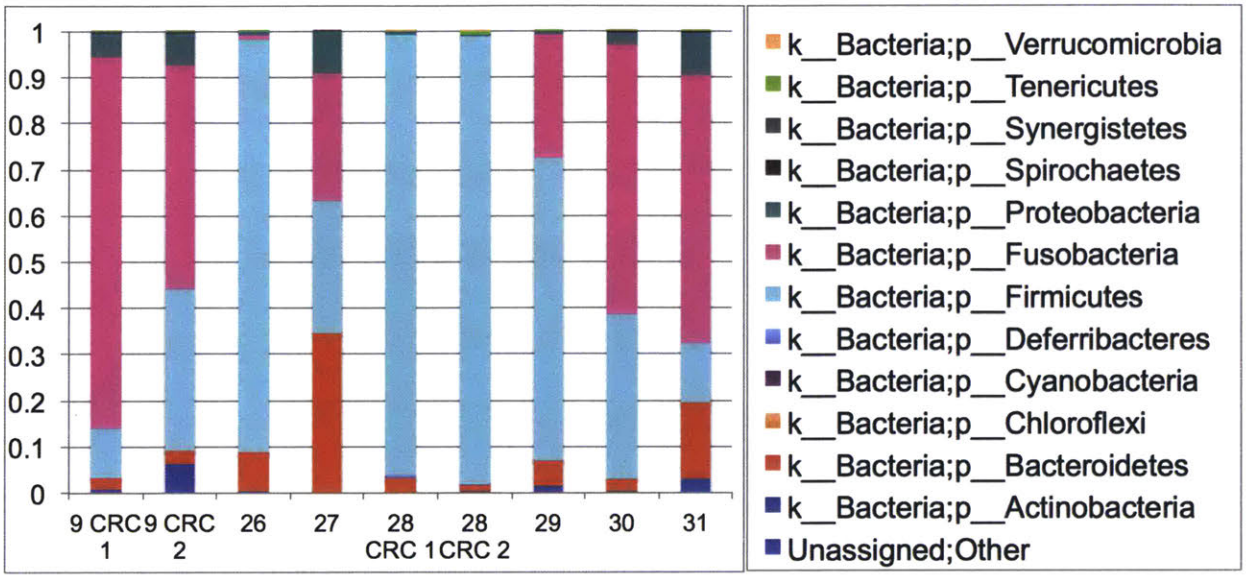

Figure 2-5: Phylum-level taxonomic assignments for 9 CRCs from 7 macaques. Samples were rarefied to 160,785 reads

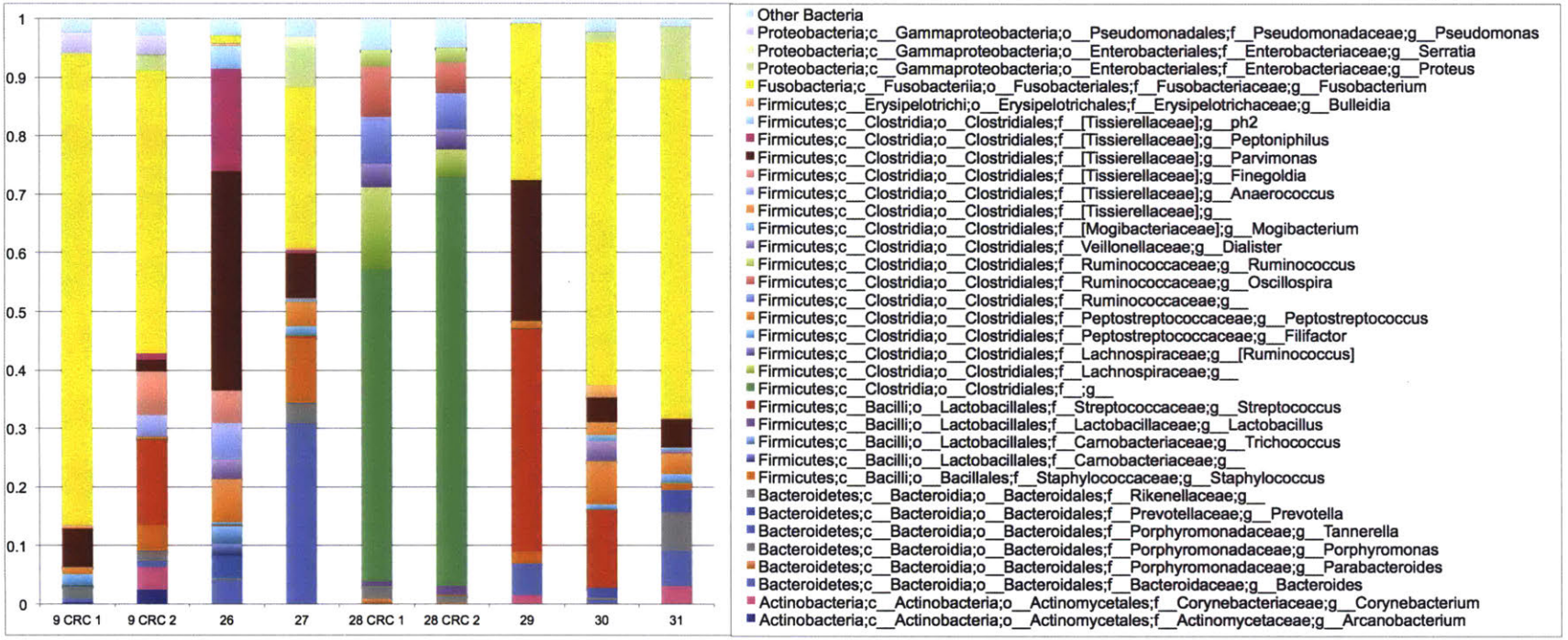

Figure 2-6: Genus-level taxonomic assignments for 9 CRCs from 7 macaques. Note that genera representing <1% of sample reads are represented as Other Bacteria. Samples were rarefied to 160,785 reads

Pilot aerobic and anaerobic culture results

Aerobic and anaerobic culture results are displayed in Table 2.9. Overall, despite the limited number of species cultured per sample, the majority of culture results corresponded with identified OTUs representing more than 0.5% of sample reads (Figure 2.9). *Fusobacterium* species were cultured from 5/6 CRC samples with three CRCs culturing *F. necrophorum* and two CRCs culturing *F. nucleatum*. *Bacteroides* was cultured from 4 CRCs, and *Parvimonas micra* and *Corynebacterium ulcerans* were cultured from 3 CRCs each.

Animal ID	Isolate	O_2 tolerance	16S Sequencing Result	Identity	Coverage	OTU Called	OTU Percentage of Reads	# Duplicate isolates
9 CRC 1	1	Anaerobic	*Fusobacterium necrophorum*	99%	70%	*Fusobacterium*	80.57%	
	2	Anaerobic	*Bacteroides fragilis*	100%	98%	*Bacteroides*	0.56%	2
9 CRC 2	1	Anaerobic	*Finegoldia magna*	99%	69%	*Finegoldia*	7.42%	2
	2	Anaerobic	*Fusobacterium necrophorum*	99%	98%	*Fusobacterium*	48.30%	2
	3	Anaerobic	*Parvimonas micra*	98%	69%	*Parvimonas*	2.03%	
	4	Aerobic	*Corynebacterium ulcerans*	API Coryne Strip		*Corynebacterium*	3.87%	4
	5	Aerobic	*Streptococcus dysgalactiae* subsp *equisimilis*	99%	86%	*Streptococcus*	14.58%	
	6	Aerobic	*Enterococcus durans*	99%	84%	*Enterococcus*	0.93%	
	7	Aerobic	*Actinomyces* sp. *Marseille-P3257*	90%	92%	*Actinomyces*	0.09%	
26	1	Anaerobic	*Parvimonas micra*	99%	97%	*Parvimonas*	37.40%	
	2	Aerobic	*Atopobacter phocae*	98%	69%	*Carnobacteriaceae* (family)	2.01%	
	3	Anaerobic	*Bacteroides fragilis*	100%	86%	*Bacteroides*	3.98%	
29	1	Aerobic	*Staphylococcus aureus*	99%	87%	*Staphylococcus*	2.00%	3
	2	Aerobic	*Streptococcus dysgalactiae* subsp *equisimilis*	99%	70%	*Streptococcus*	38.17%	
	3	Aerobic	*Corynebacterium ulcerans*	API Coryne Strip		*Corynebacterium*	1.62%	2
	4	Anaerobic	*Bacteroides fragilis*	99%	98%	*Bacteroides*	5.34%	3
	5	Aerobic	*Neisseria baciliformis*	99%	70%	*Neisseriaceae* (family)	0.06%	
	6	Anaerobic	*Fusobacterium nucleatum*	99%	70%	*Fusobacterium*	26.67%	
30	1	Anaerobic	*Fusobacterium necrophorum*	99%	98%	*Fusobacterium*	58.46%	3
	2	Aerobic	*Streptococcus gordonii*	99%	71%	*Streptococcus*	13.24%	
31	1	Anaerobic	*Bacteroides fragilis*	99%	70%	*Bacteroides*	5.99%	2
	2	Aerobic	*Staphylococcus aureus*	99%	70%	*Staphylococcus*	1.02%	
	3	Anaerobic	*Fusobacterium nucleatum*	99%	99%	*Fusobacterium*	57.95%	2
	4	Anaerobic	*Negativicoccus massiliensis*	96%	74%	*Dialister*	0.45%	
	5	Aerobic	*Corynebacterium ulcerans*	97%	98%	*Corynebacterium*	3.10%	5
	6	Anaerobic	*Parvimonas micra*	98%	96%	*Parvimonas*	4.86%	

Table 2.9: Aerobic and anaerobic culture results from 6 CRC samples from 5 macaques. Species identification was performed by PCR amplification and sequencing of the 1.5Kb 16S rRNA gene with identity and coverage referring to results from NCBI BLAST. Two *Corynebacterium ulcerans* isolates were identified using the API Coryne strip. Culture results are compared to the OTU called and OTU percentage of reads from microbiota sequencing results for each macaque.

Discussion

The amount of variation in CRC communities was surprising, as was the extent of the anaerobic component. We hypothesized that macaques with multiple CRCs would have similar communities within their CRCs. While this was the case for macaque #28, the bacterial communities in macaque #9's two CRCs differed in OTU abundance, as visualized on both weighted UniFrac plots (Figure 2-4) and taxonomy bar charts (Figures 2-5, 2-6). The genus-level taxonomy bar chart identified larger percentages of reads assigned to *Fusobacterium* spp. and *Parvimonas* spp. in macaque #9's CRC 1, versus larger number of reads assigned to *Streptococcus* spp., *Finegoldia* spp. and *Staphylococcus* spp. in CRC 2. The four CRC samples that clustered together on unweighted UniFrac (from macaques #26, #27, #30 and #31) represented animals under study by two different laboratories, without obvious commonalities in age of CRC, CRC style, or implant materials used. It should be noted that macaque #28 had PMMA-free CRCs, and this is one possible factor contributing to the marked differences in observed bacterial communities. Unfortunately, the small numbers of CRCs sampled in this study complicates the ability to draw robust conclusions on how CRC materials affect bacterial community composition.

When comparing culture-dependent and culture-independent bacterial identification, two genera differed in results from sequencing the whole 1.5Kb 16S rRNA gene as compared to the OTU taxonomic assignment. *Atopobacter phocae*, a member of the Lactobacillus order and *Carnobacteriaceae* family was identified from macaque #26, and *Negativicoccus massiliensis*, a member of the Veillonellales order and *Vellionellaceae* family from macaque #31 [36, 37]. OTU taxonomic assignment most likely classified *Negativicoccus massiliensis* as the *Dialister* genus; these species are closely related, phylogenetically [37]. While, there were some OTUs identified as representing >1% of sample reads that were not identified on culture, (i.e. *Porphyromonas* spp. and *Peptostreptococcus* spp.) our culture results did validate the use of the microbiota pipeline as a tool to correctly identify many prominent species from grossly purulent samples.

2.5 Expanded microbiota study

With pilot study results confirming that culture-independent methods were able to successfully characterize CRC bacterial communities, we expanded our investigation to include more macaques, and sample CRCs in parallel with other body sites to identify primary sources of CRC colonization. 18 macaques were selected for sampling to compare CRC communities with skin, oral and fecal communities.

2.5.1 Animals

Samples from 18 implanted macaques were used for the expanded microbiota study. The population consisted of 3 females and 15 males ranging in age from 4 years to 19 years, and under investigation by four different laboratories (Tables 2.10, 2.11). Four macaques had two CRCs sampled separately, two macaques had three CRCs sampled separately and the remaining 13 macaques had a single CRC. Macaques #37 and #39 had PMMA-free implants. Oral swabs and fresh fecal samples were collected from all 18 macaques, and swabs of the skin-CRC implant margin were collected for 17/18 macaques for a total of 79 samples (Tables 2.10, 2.11). 3/18 macaques sampled for the expanded study were also sampled during the pilot study (macaques #9, #29 and #30).

Animal ID	Sex	Age (years)	History of Pair Housing	Lab ID	Study ID	Samples	CRC implant date	Implant materials	Counts per Sample
9	M	19	No	B	B6	CRC 1	4/2011	Ultem, titanium screws, PMMA	15625
						CRC 2			6954
						oral swab			24824
						skin margin			8661
						feces			6761
29	F	8	Yes	A	A5	CRC 1	11/2015	Ultem, ceramic screws, PMMA	3115
						oral swab			32872
						skin margin			3324
						feces			5160
30	M	9	Yes	A	A6	CRC 1	12/14	Delrin, ceramic screws, PMMA w/gentamicin	3660
						CRC 2			1729
						CRC 3			987
						oral swab			13481
						feces			15100
32	F	13	Yes	A	A8	CRC	9/2015	Ultem, ceramic screws, PMMA w/gentamicin	5245
						oral swab			23604
						skin margin			2139
						feces			12361
33	M	5	Yes	E	E2	CRC	7/2017	PEEK, titanium brackets/screws, PMMA	24457
						oral swab			33487
						skin margin			19359
						feces			8169
34	M	8	Yes	E	E3	CRC	8/2017	PEEK, titanium brackets/screws, PMMA	7308
						oral swab			22533
						skin margin			14318
						feces			10392
35	M	19	No	B	B10	CRC 1	4/2017	PEEK, ceramic screws, PMMA	10388
						CRC 2			212
						oral swab			24795
						skin margin			4835
						feces			6734
36	M	5	Yes	E	E4	CRC	4/2017	PEEK, titanium brackets/screws, PMMA	6392
						oral swab			25590
						skin margin			497
						feces			7534
37	M	unknown; mature adult	Yes	B	B11	CRC 1 R2	8/2012	PEEK, titanium screws, PMMA-free	248
						CRC 2 C2			3155
						oral swab			24997
						skin margin			19514
						feces			2756

Table 2.10: Demographs of 18 implanted macaques, part 1

Animal ID	Sex	Age (years)	History of Pair Housing	Lab ID	Study ID	Samples	CRC implant date	Implant materials	Counts per Sample
38	F	7	Yes	A	A9	CRC	6/2017	Ultem, ceramic + titanium screws, PMMA	1379
						oral swab			24108
						skin margin			6962
						feces			11311
39	M	9	Yes	B	B11	CRC 1	9/2017	PEEK, ceramic screws, PMMA-free	2192
						CRC 2			35
						CRC 3			255
						oral swab			27066
						skin margin			10244
						feces			2507
40	M	10	No	B	B12	CRC 1	10/2014	Ultem, titanium screws, PMMA	7960
						CRC 2	6/2013		6010
						oral swab			22912
						skin margin			4287
						feces			10185
41	M	5	Yes	D	D7	CRC 1	5/2017	Cilux, ceramic screws, PMMA	309
						oral swab			28807
						skin margin			598
						feces			15617
42	M	9	Yes	D	D8	CRC 1	7/2014	Stainless steel, titanium, PMMA	3946
						oral swab			22390
						skin margin			3799
						feces			2033
43	M	4	Yes	D	D9	CRC 1	9/2017	Cilux, ceramic screws, PMMA	214
						oral swab			22685
						skin margin			473
						feces			8226
44	M	5	Yes	D	D10	CRC 1	2/2017	Stainless steel, titanium, PMMA	9617
						oral swab			26205
						skin margin			2088
						feces			11506
45	M	8	Yes	E	E5	CRC 1	5/2016	PEEK, titanium + stainless steel screws, PMMA	5221
						oral swab			29422
						skin margin			3839
						feces			32103
46	M	5	Yes	E	E6	CRC 1	3/2017	PEEK, titanium screws, PMMA	7516
						oral swab			22175
						skin margin			23310
						feces			6192

Table 2.11: Demographs of 18 implanted macaques, part 2

2.5.2 DNA extraction, sequencing and analysis

Genomic DNA was extracted from samples using the DNeasy PowerLyzer PowerSoil kit according to manufacturer instructions (Qiagen, USA). This kit was chosen due to its versatility in handling a wide range of sample types, after consultation with the manufacturer for recommendations. Samples were stored at -80°C if same-day processing could not be performed. A maximum of 0.2 ml CRC exudate and 0.2g of feces was used for DNA extraction; oral and skin swabs were added directly to the glass bead tubes with solution C1. Bead beating was performed for 8 minutes (Bullet Blender, Next Advance, Troy, NY). Genomic DNA from individual samples were barcoded and pooled to construct the sequencing library using previously published protocols [33] and submitted to the MIT BioMicro Center core facility for PCR amplification of the 16S rRNA V4-V5 region. Sequencing was performed using an Illumina MiSeq to generate pair-ended 300x300 reads. F515 and R926 sequencing primers used are listed in Appendix B. Overlapping pair-end reads were aligned using PEAR and paired reads shorter than 200 bp were filtered out [38]. Subsequent analysis and normalization were performed using QIIME 1.9.1 within the MicrobiomeHelper v. 2.0.0 virtual box [34, 33]. Chimeric sequences were removed by comparison to the database Bacteria_RDP_trainset15_092015.fa. OTUs were assigned using open reference picking, as previously described for the pilot study, and OTUs present at less than 0.1% of reads were removed. The average number of reads/sample for all sites was 11,252 sequences. The average number of reads for CRC, skin, oral and fecal samples were 5,158, 7,543, 25,108 and 9,702, respectively. Taxonomic assignments were determined using the Ribosomal Database Project classifier against the GreenGenes database. To control for differences in sequencing depth, OTU tables were rarified at a single sequencing depth. Alpha diversity was determined using Observed OTUs and Shannon Index metrics and displayed using rarefaction curves. Differences in alpha diversity between sampling sites were calculated using a non-parametric two-sample t-test using 999 Monte Carlo permutations in QIIME with $P < 0.05$ considered significant. Beta-diversity was determined using unweighted and weighted UniFrac and results displayed as PCoA plots [31]. Statistical analysis of beta diversity between communities within samples from each macaque was evaluated using an

unweighted Unifrac Monte Carlo significance test with 100 permutations, with Boferroni-corrected $P<0.05$ considered significant. OTUs were summarized at the phylum and genus level, and displayed as bar graphs. Taxonomy data rarefied to 200 sequences and 1000 sequences are archived at `https://figshare.com/s/75b71eee0d0e2084a1dc`. For display purposes, genera representing <1% of reads were classified as "Other Bacteria".

2.5.3 May-June 2018 Diagnostic lab aerobic and anaerobic cultures and Kirby-Bauer sensitivities

Sterile culture swabs (CultureSwab MaxV(+), BD, Franklin Lakes, NJ) were used to sample the interior of cephalic recording chambers, including any discharge present. The swabs were plated onto chocolate agar, trypticase soy agar with 5% sheep blood, MacConkey agar and CDC anaerobic agar with 5% sheep blood, and incubated at 37°C in 5% CO_2 for 24 h (aerobic) or within anaerobic containers. The swabs, themselves, were then incubated in thioglycollate broth at 37°C for 24 h and re-plated onto the media listed above. Microbial growth was streaked onto blood agar to obtain isolated colonies, which were then identified using the Analytical Profile Index identification system (API 20 E, API 20 Staph and API 20 Strep, bioMerieux, Durham, NC). Antibiotic susceptibility profiles were determined by disk diffusion using the Clinical and Laboratory Standards Institute break points (M2-A10) [20]. Antimicrobial agents tested on non-*Corynebacterium* aerobic isolates included ampicillin, amoxicillin/clavulanic acid, bacitracin (Gram positive bacteria only), ceftriaxone, cefazolin, cephalothin, chloramphenicol, enrofloxacin, erythromycin (Gram positive bacteria only), gentamicin, linezolid, meropenem, neomycin, oxacillin (Gram positive bacteria only), streptomycin, trimethoprim/sulfa-methoxazole, tetracycline, and vancomycin. Gentamicin, chloramphenicol, streptomycin, and vancomycin disks were purchased from BD (BBL Sensi-Disc, Franklin Lakes, New Jersey); the remainder of the antimicrobial disks were obtained from Oxoid (Basingstoke, United Kingdom).

2.6 Results

2.6.1 Sequence counts

Ten samples had sequence counts <1000, including macaque #30 CRC 3, macaque #35 CRC 2, macaque #36 skin margin, macaque #37 CRC 1, macaque #39 CRC 2 and 3, macaque #41 CRC 1 and skin margin, and macaque #43 CRC 1 and skin margin (Tables 2.10, 2.11). To account for discrepancies in sequence counts, and minimize sample loss, diversity analysis was performed with rarefaction to both 200 sequences and 1000 sequences. Unless otherwise stated, results from samples rarefied to 1000 sequences will be presented.

2.6.2 Alpha diversity

Rarefaction curves and alpha diversity were analyzed from samples rarefied to 1000 sequences. Shannon diversity, observed OTUs and boxplots comparing sampling sites are displayed in Figure 2-7. Non-parametric Monte Carlo permutations identified that fecal samples have a significantly higher alpha diversity as measured by both the Shannon index and observed OTU metrics compared to CRC samples, oral samples and skin margin samples (** P=0.006, *P=0.012). Oral samples displayed a higher alpha diversity than CRC samples for both the Shannon index and observed OTU metrics (**P=0.006, *P=0.018). Skin samples displayed a higher alpha diversity than CRC samples as measured by the Shannon diversity index (*P=0.018), but not from the observed OTU metric. Differences between these methods are because the Shannon diversity index accounts for both richness and evenness, while the observed OTU metric only accounts for richness. Average alpha diversity measurements are displayed in Table 2.12. Overall, the mean CRC alpha diversity was decreased for the expanded study as compared to the pilot study (Shannon 3.4 vs. 4.8; observed OTUs 61 vs. 989). These differences may be related to low numbers of reads for some CRC samples, and differences in extraction kits (smaller sample volumes used in the PowerLyzer kit and decreased efficiency for extracting bacterial from host DNA without the benzonase pre-treatment step).

Site	Average Shannon Diversity Index	Average Observed OTUs
CRC (N=19)	3.427863696	61
Feces (N=18)	6.1937195	230
Oral (N=18)	4.987944393	109
Skin (N=14)	4.715879701	126

Table 2.12: Average Shannon diversity index and observed OTUs for each sampling site.

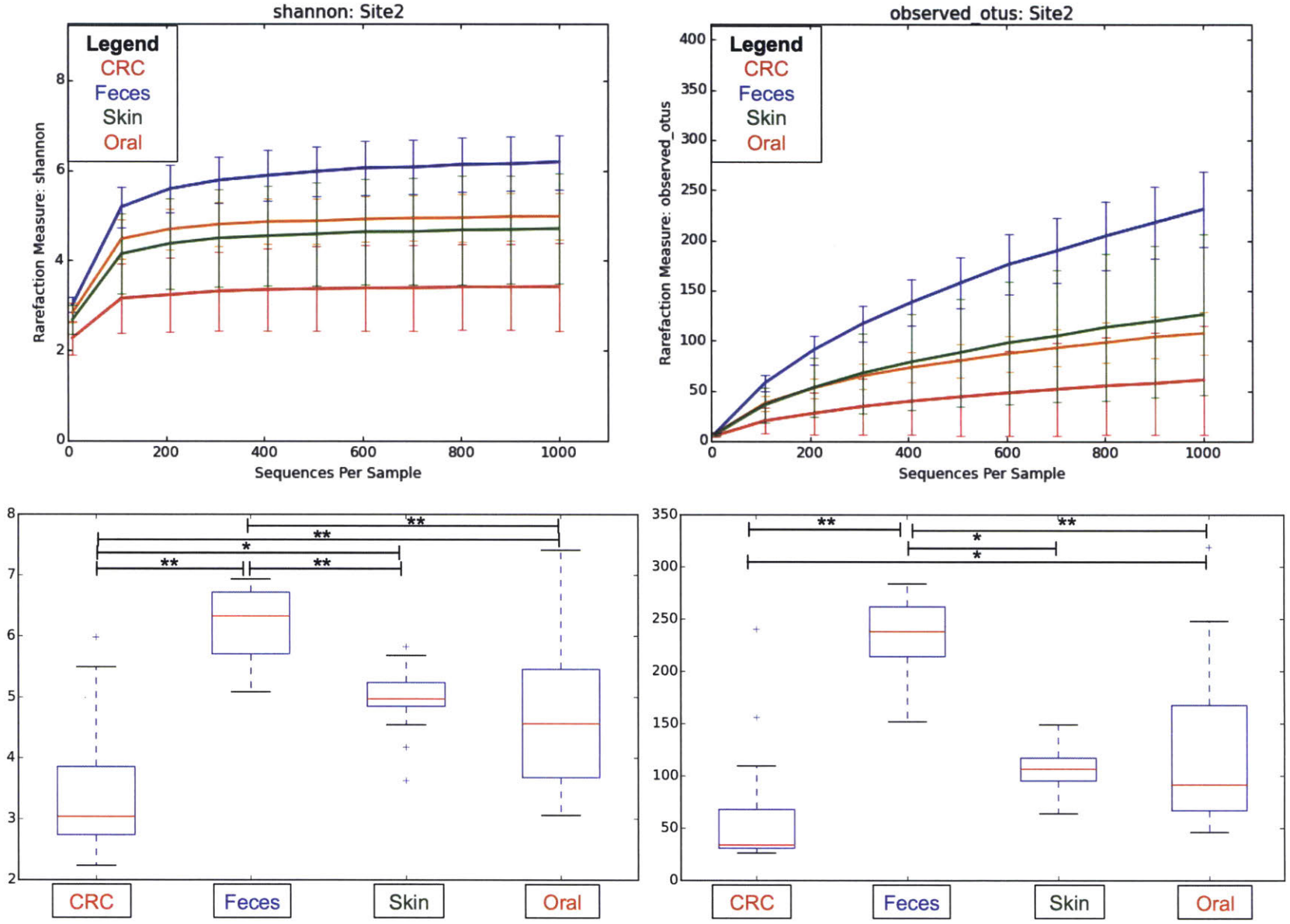

Figure 2-7: Rarefaction curves and boxplots comparing alpha diversity results as calculated using the Shannon diversity index and observed OTUs metrics between sampling sites. Differences between alpha diversity calculated using a non-parametric, two-sample t-test using 999 Monte Carlo permutations. ** P=0.006, *P<0.02.

2.6.3 Beta Diversity

PCoA plots of unweighted and weighted UniFrac distances of samples by site, rarefied to 1000 sequences, are displayed in Figure 2-8. On both unweighted and weighted UniFrac plots, fecal samples and oral samples clustered together, while CRC and skin margin samples were more intermixed. To better understand the source of bacteria colonizing CRCs, we compared unweighted Unifrac beta-diversity within all samples from each macaque, individually. Unweighted UniFrac was chosen for this comparison to focus on OTUs only, rather than their abundance. Non-parametric Monte Carlo simulations identified that CRC communities were significantly different from fecal, skin, oral, and other CRC communities in 85% (22/26), 26% (6/23), 27% (7/26), and 20% (2/10) of macaques, respectively (Table 2.13).

Within-Macaque Comparison	N	Bonferroni-Corrected P ≤ 0.01 (significant)	Bonferroni-Corrected P = 1 (non-significant)
CRC vs. Feces	26	22 (85%)	4 (15%)
CRC vs. Skin	23	6 (26%)	17 (74%)
CRC vs. Oral	26	7 (27%)	19 (73%)
CRC vs. CRC	10	2 (20%)	8 (80%)

Table 2.13: Number (%) of macaques with significant and non-significant differences in beta diversity between CRCs and other body sites, as measured by unweighted UniFrac.

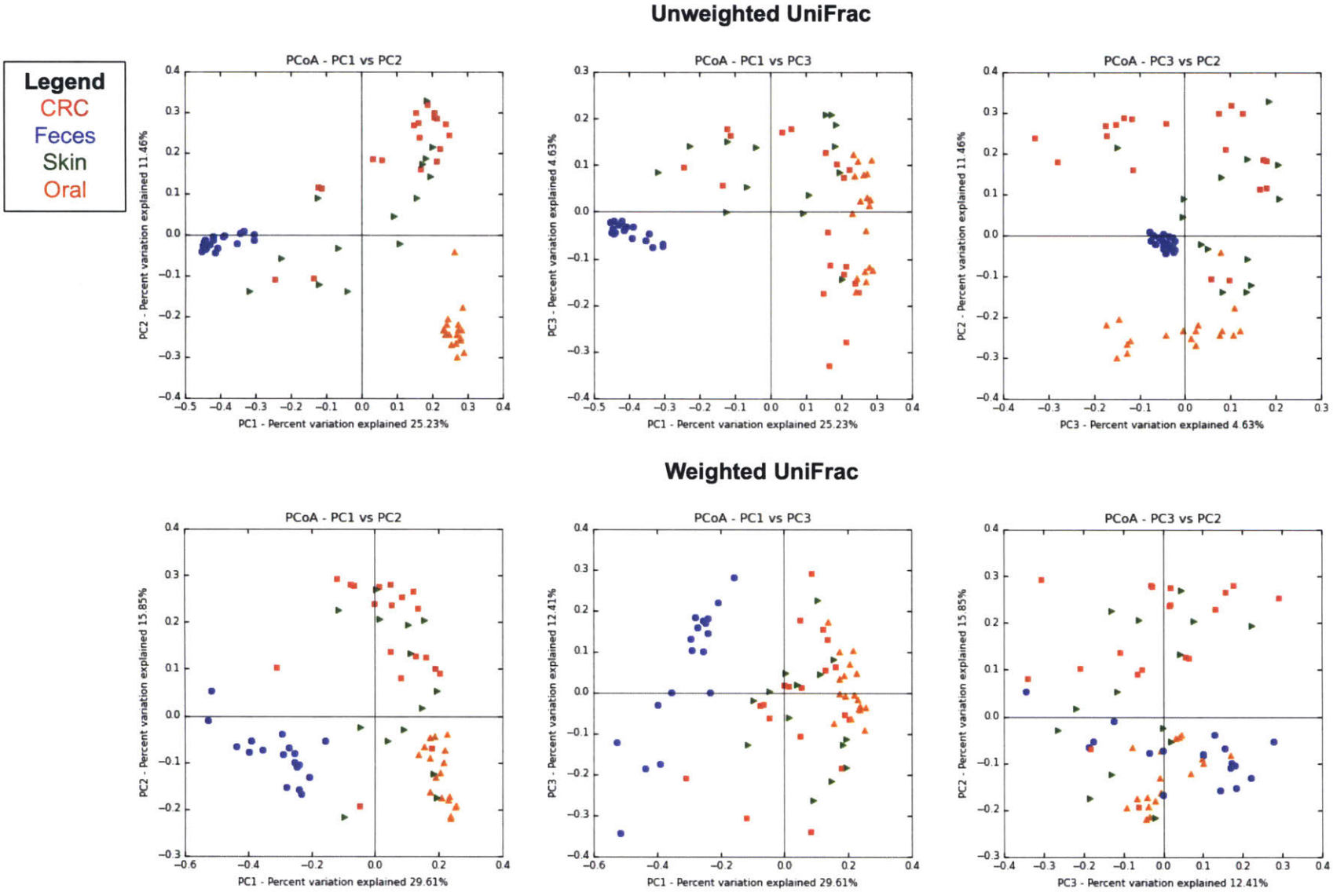

Figure 2-8: Principal coordinate analysis plots of unweighted (top) and weighted (bottom) UniFrac distances for each CRC sample rarefied at 1000 sequences.

2.6.4 Taxonomy Bar Charts

Comparison of sampling sites

At the phylum level, fecal samples were predominated by Bacteroidetes and Firmicutes, whereas oral, CRC, and skin samples had contributions from Fusobacteria. CRC and skin samples had larger contributions from Actinobacteria, and oral samples had larger contributions from Proteobacteria (Figure 2-9).

At the genus level, fecal samples had a larger contribution of samples from the Bacteriodales order (18%) and *Prevotella* spp. (24%) compared to oral, CRC, and skin samples (Figure 2-10). Oral, CRC, and skin samples had larger contributions of samples reads from *Porphyromonas* spp., which was present at <1% of reads in fecal samples. *Streptococcus* spp. were present in higher percentages in oral and skin samples (14-15%) as compared to CRC and fecal samples (2-3%). *Parvimonas* spp. were present in both CRC and skin samples around 6% and present at <1% in fecal and oral samples.

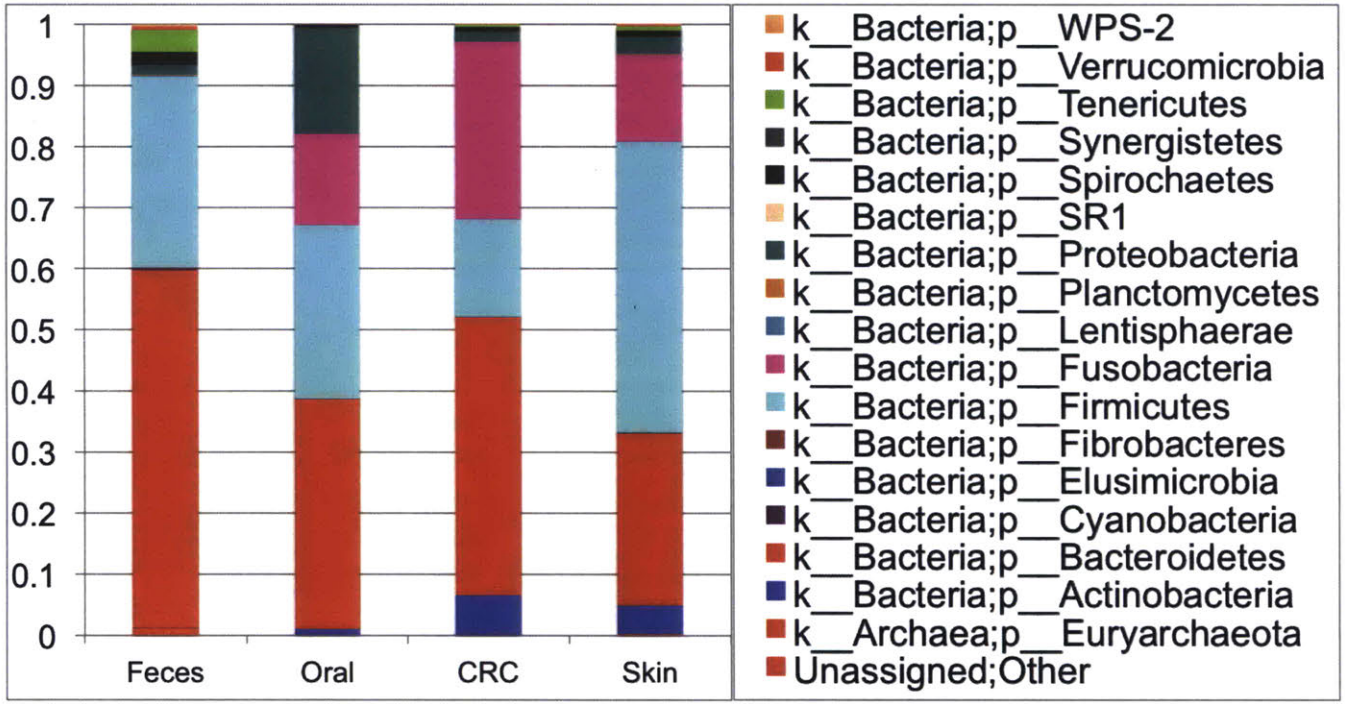

Figure 2-9: Phylum-level taxonomy bar chart from samples rarefied to 1000 sequences. Feces (N=18), Oral (N=18), CRC (N=19), Skin (N=14) samples.

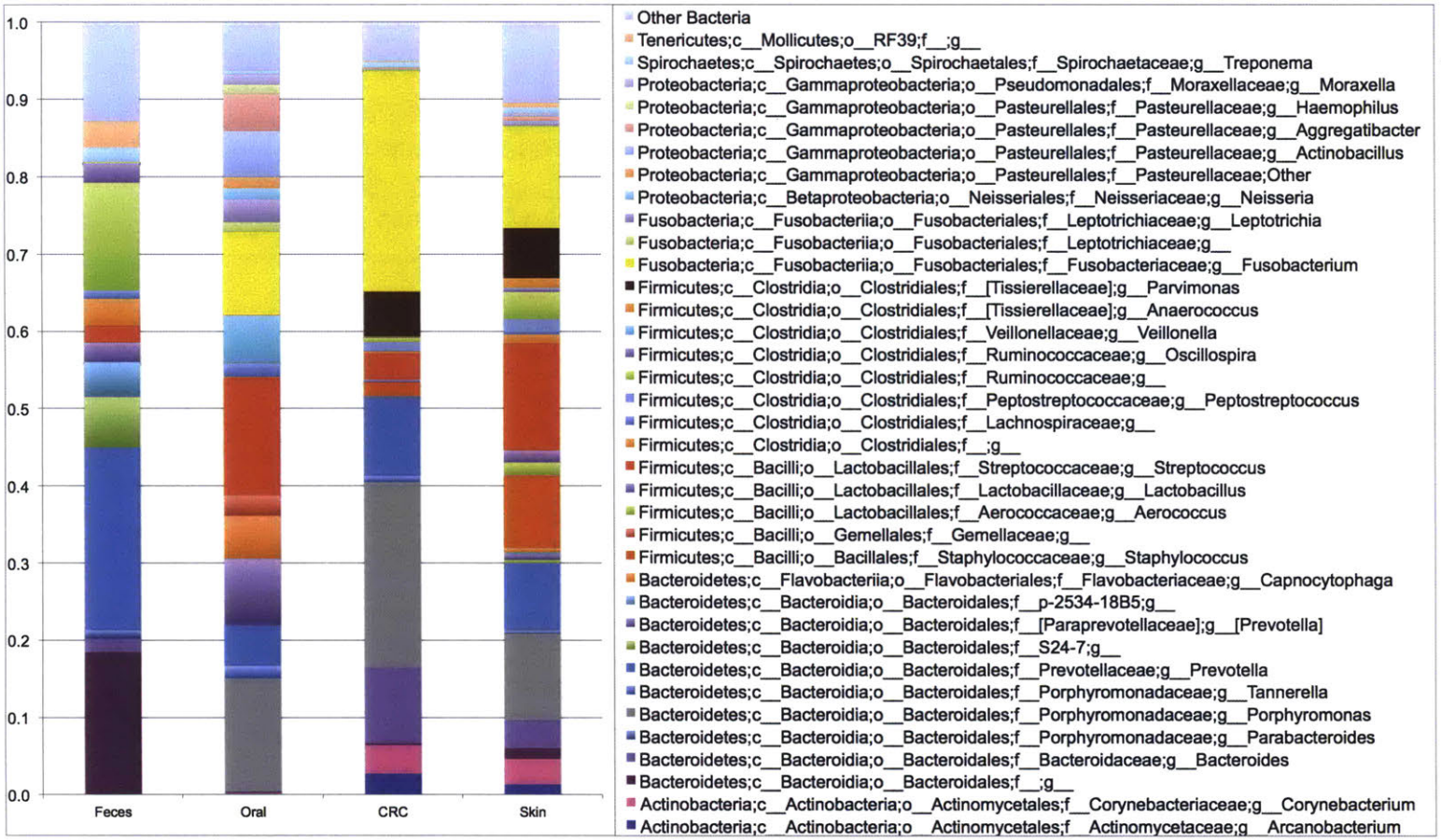

Figure 2-10: Genus-level taxonomy bar chart from samples rarefied to 1000 sequences. Feces (N=18), Oral (N=18), CRC (N=19), Skin (N=14) samples.

Individual sites

CRCs

As in the pilot study, all macaques displayed a unique CRC community composition at both the phylum and genus level (Figures 2-11, 2-12). At the phylum level, 15/19 CRCs were comprised of >40% Bacteroidetes phyla with varying contributions from the Firmicutes and Fusobacteria phyla. CRC 1 from Macaque #39 displayed a markedly different distribution of phyla compared to the other macaques, with Firmicutes contributing as 69.7% of phyla. The CRC from macaque #38 was also different, with Fusobacteria contributing 55% of phyla with Bacteroidetes and Firmicutes only contributing 7-8% each. Macaque #44 was mostly split between Bacteroidetes (49%) and Fusobacteria (45%) phyla.

At the genus level, OTUs identified in high prevalence were similar to those identified in the pilot study, including *Fusobacterium* spp., *Bacteroides* spp., *Corynebacterium* spp., *Porphyromonas* spp., *Prevotella* spp., *Parvimonas* spp., *Streptococcus* spp., and *Staphylococcus* spp.. *Staphlyococcus* spp. was identified to contribute 35% of reads for CRC 1 from Macaque #39, explaining the source of the high percentage of Firmicutes identified at the phylum level. Macaque #39 had a PMMA-free implant and the two other CRCs of this animal had low sample reads (35 and 255; Table 2.11). We did not appreciate any effects of the age of CRC implant duration on the taxonomy distribution.

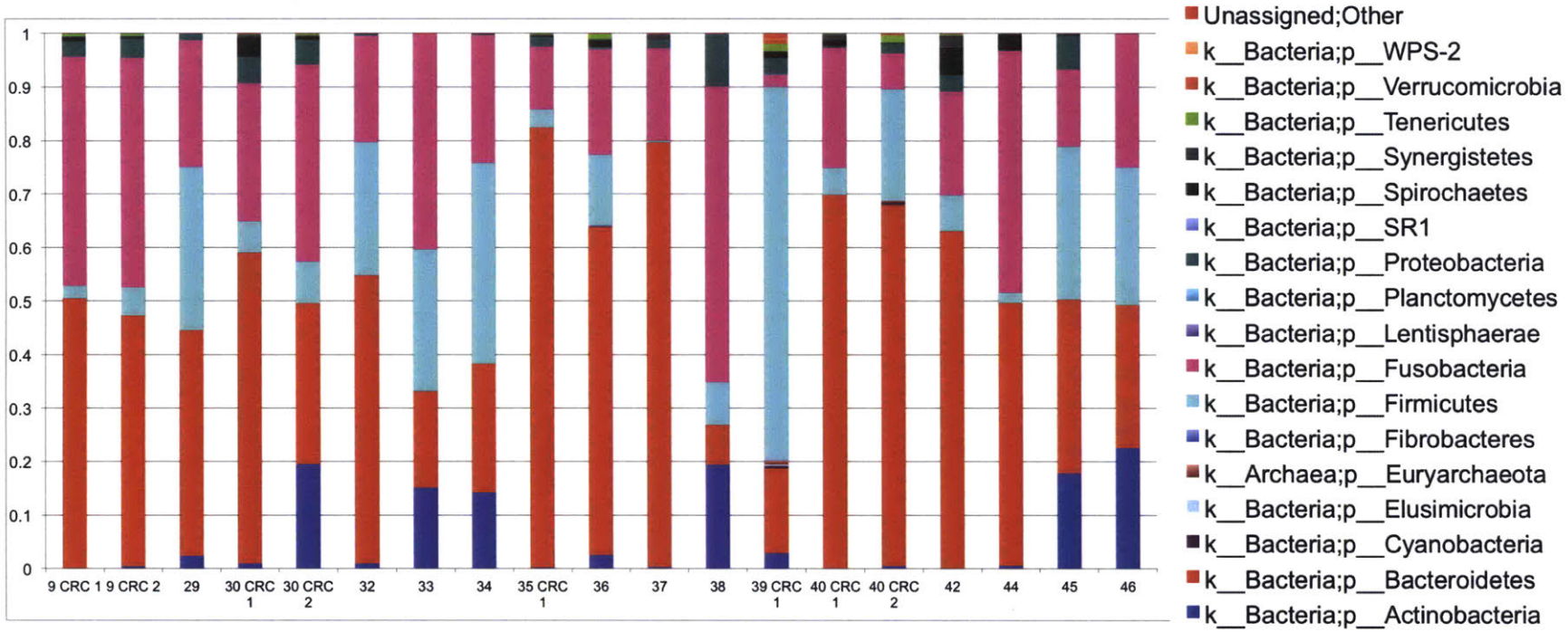

Figure 2-11: Phylum-level taxonomy bar chart from CRC samples rarefied to 1000 sequences.

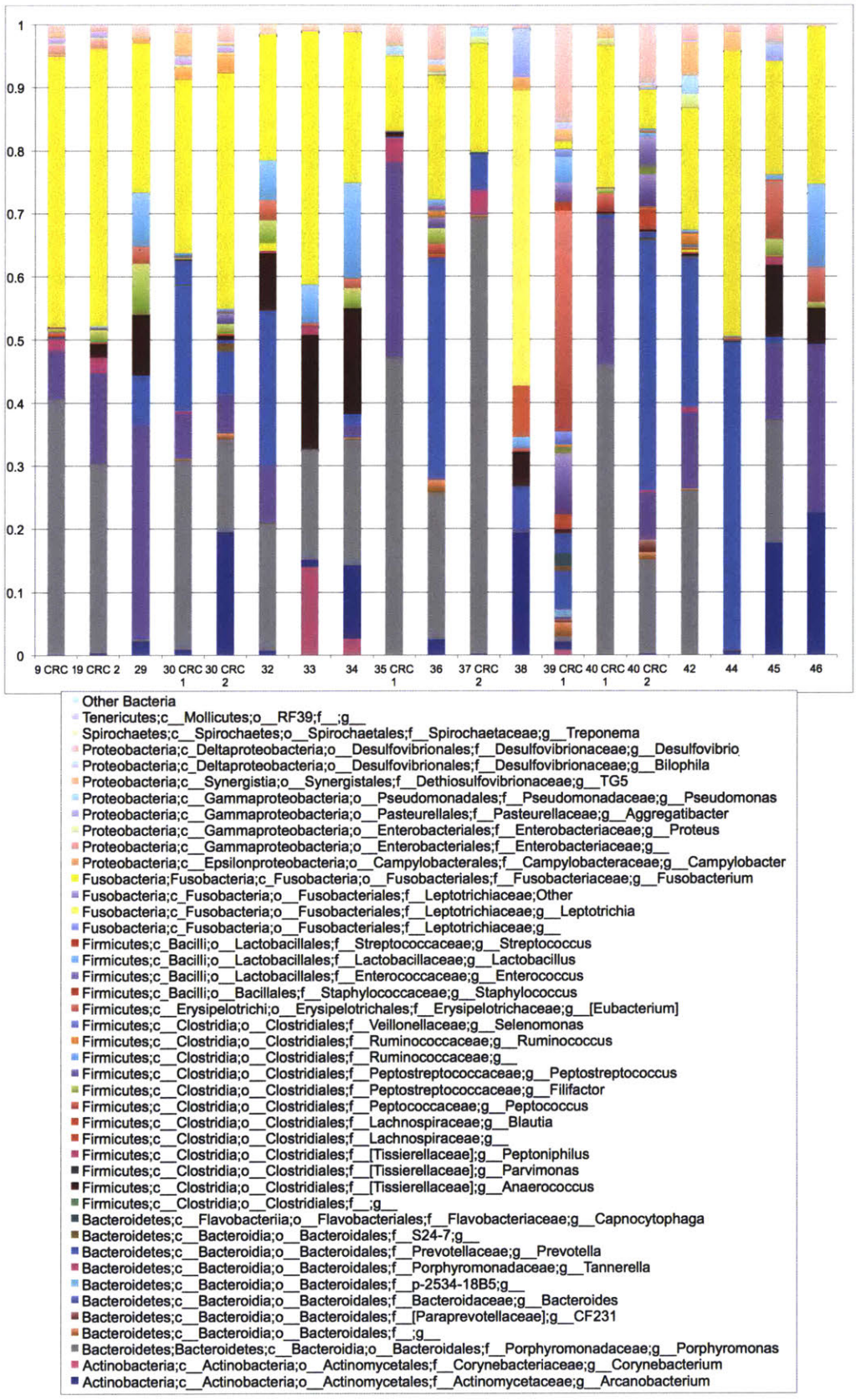

Figure 2-12: Genus-level taxonomy bar chart from CRC samples rarefied to 1000 sequences.

Macaques with multiple CRCs

To better compare communities in macaques with multiple CRCs we examined phylum-level and genus-level taxonomy bar charts for samples rarefied to 200 sequences for macaques #9 (2 CRCs), #30 (3 CRCs), #35 (2 CRCs), #37 (2 CRCs), #39 (2 CRCs) and #40 (2 CRCs) (Figure 2-13). Even with rarefaction to a sequence count of 200, CRC 2 from macaque #39 did not have enough reads for inclusion in the analysis. At the phylum level, similar community compositions were noted for macaques #9, #30 (CRCs 1 and 3) and #40. Macaque #30 CRC 2 had higher levels of the Actinobacteria phyla compared to CRCs 1 and 3. Macaque #37 CRC 1 had more Firmicutes in CRC 1 and more Bacteroidetes and Fusobacteria in CRC 2. Macaque #39 had more Tenericutes and Actinobacteria and less Firmicutes and Bacteroidetes in CRC 3 vs. CRC 1.

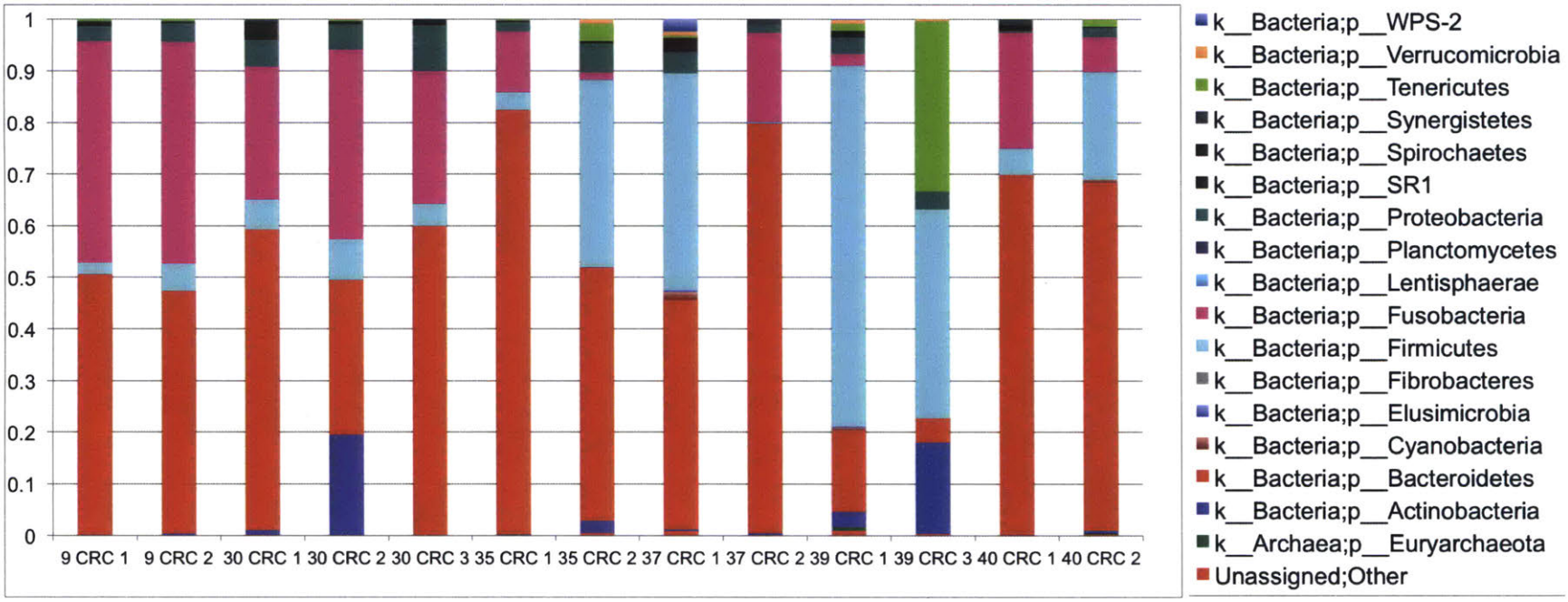

Figure 2-13: Phylum-level taxonomy bar chart from macaques with multiple CRC samples, rarefied to 200 sequences.

At the genus level (Figure 2-14), differences in community composition between CRCs from the same macaque were more readily apparent. Macaque #9 (CRC 1 and 2) and macaque # 30 (CRC 1 and 3) had the most visually similar bar charts of all paired CRC samples. The two macaques with significant differences between CRCs, as identified by unweighted UniFrac Monte Carlo simulations, were macaques #30 (CRC 1 vs. 2) and macaque #37. Macaque #30 CRC 2 had a larger contribution from *Corynebacterium* spp. as compared to CRCs 1 and 3. Macaque #37 also displayed marked differences in taxonomic contributions, as CRC 2 had 69% of sample reads from *Porphyromonas* spp. and 17% of sample reads from *Fusobacterium* spp. while CRC 1 had more diverse contributions from the *Ruminococceacaea* family, *BS11* family from the *Bacteriodales* order and *Staphylococcus* genus. For macaque #35, CRC 1 had large contributions of sample reads from *Porphyromonas* spp. (47%) and *Bacteroides* spp. (31%), whereas CRC 2 had more OTUs contributing to diversity and only 4% of reads from *Porphyromonas* spp..

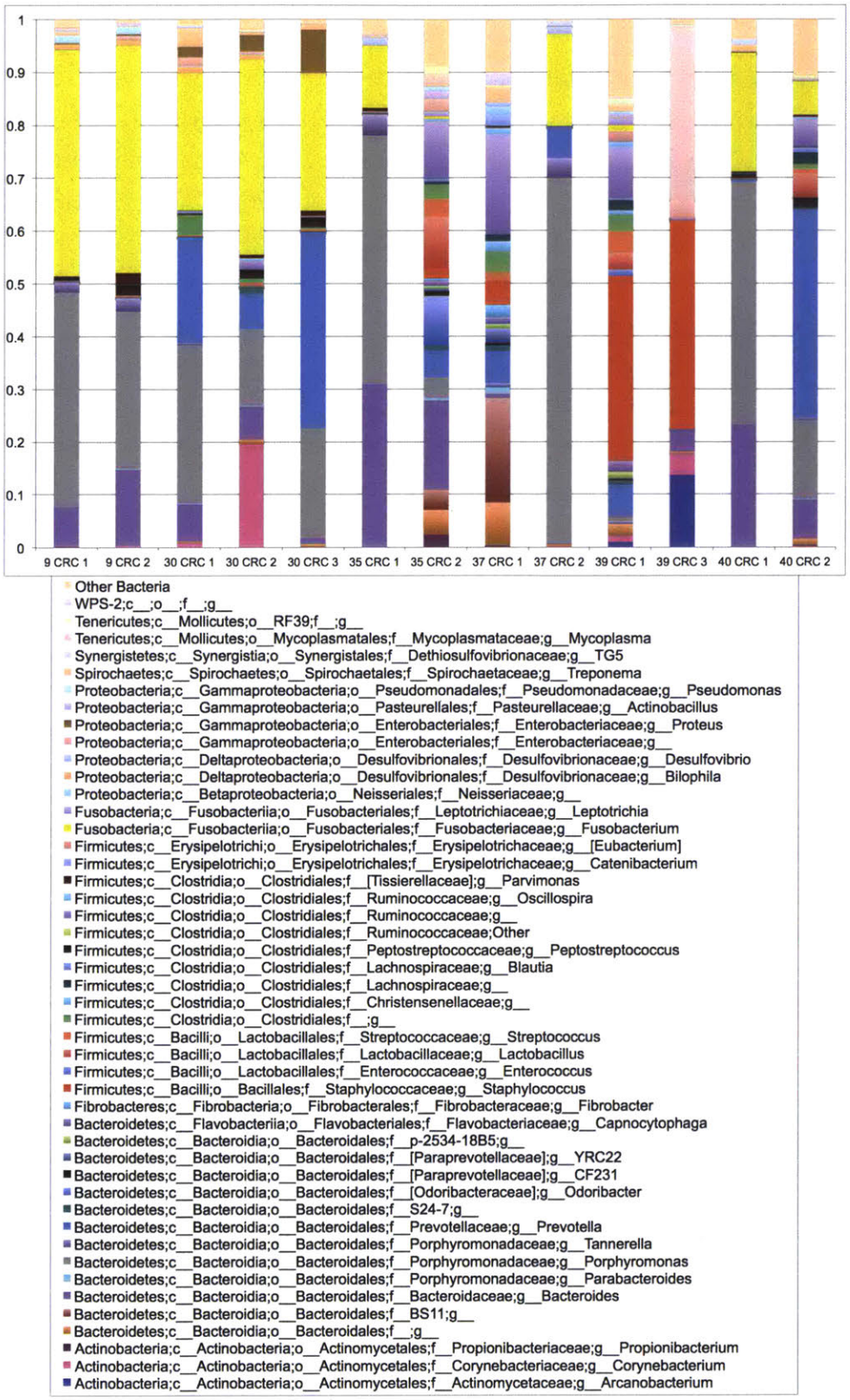

Figure 2-14: Genus-level taxonomy bar chart from macaques with multiple CRC samples, rarefied to 200 sequences. Note that genera representing <1% of sample reads are represented as Other Bacteria.

Skin swabs

At the phylum level, bacterial community composition of skin-implant margin swabs were very similar with minor differences (Figure 2-15). The Bacteriodetes phylum contributed approximately 33% of sample reads on average, with smaller contributions for macaques #29, #33 and #38 (9-10%) and larger contributions for macaques #32, #35 and #40 (60-70%). The Firmicutes phylum contributed 40% of sample reads on average, with smaller contributions in the three macaques with more Bacteriodetes. Fusobacterium contributed approximately 18% of samples reads on average, with macaques #9 and #29 having larger contributions (38-46%).

At the genus level, genera contributing to a higher prevalence of reads for skin sample communities included *Staphylococcus*, *Streptococcus*, *Fusobacterium*, *Porphyromonas*, *Parvimonas*, *Corynebacterium* and *Prevotella* (Figure 2-16).

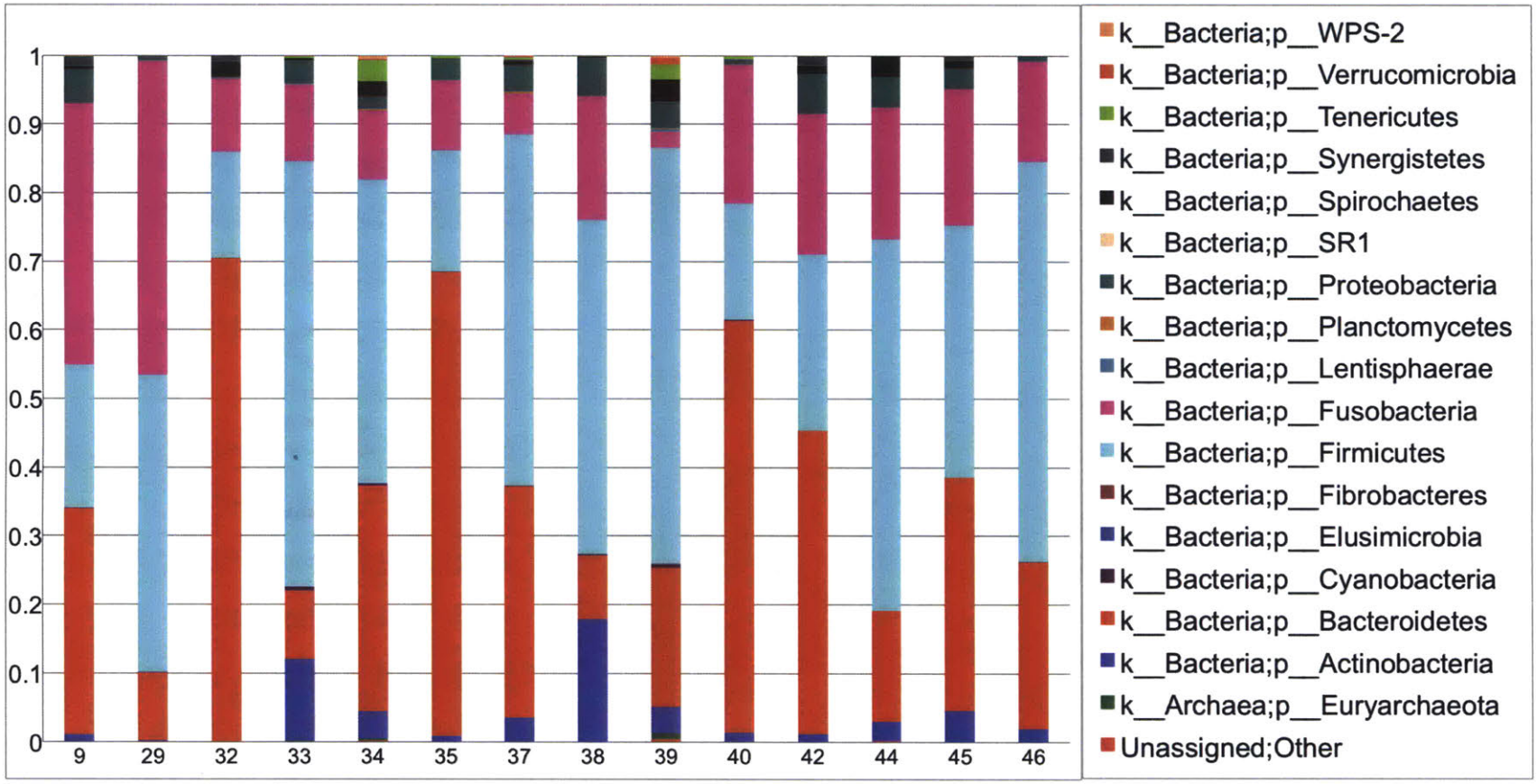

Figure 2-15: Phylum-level taxonomy bar chart for skin-implant swab samples rarefied to 1000 sequences.

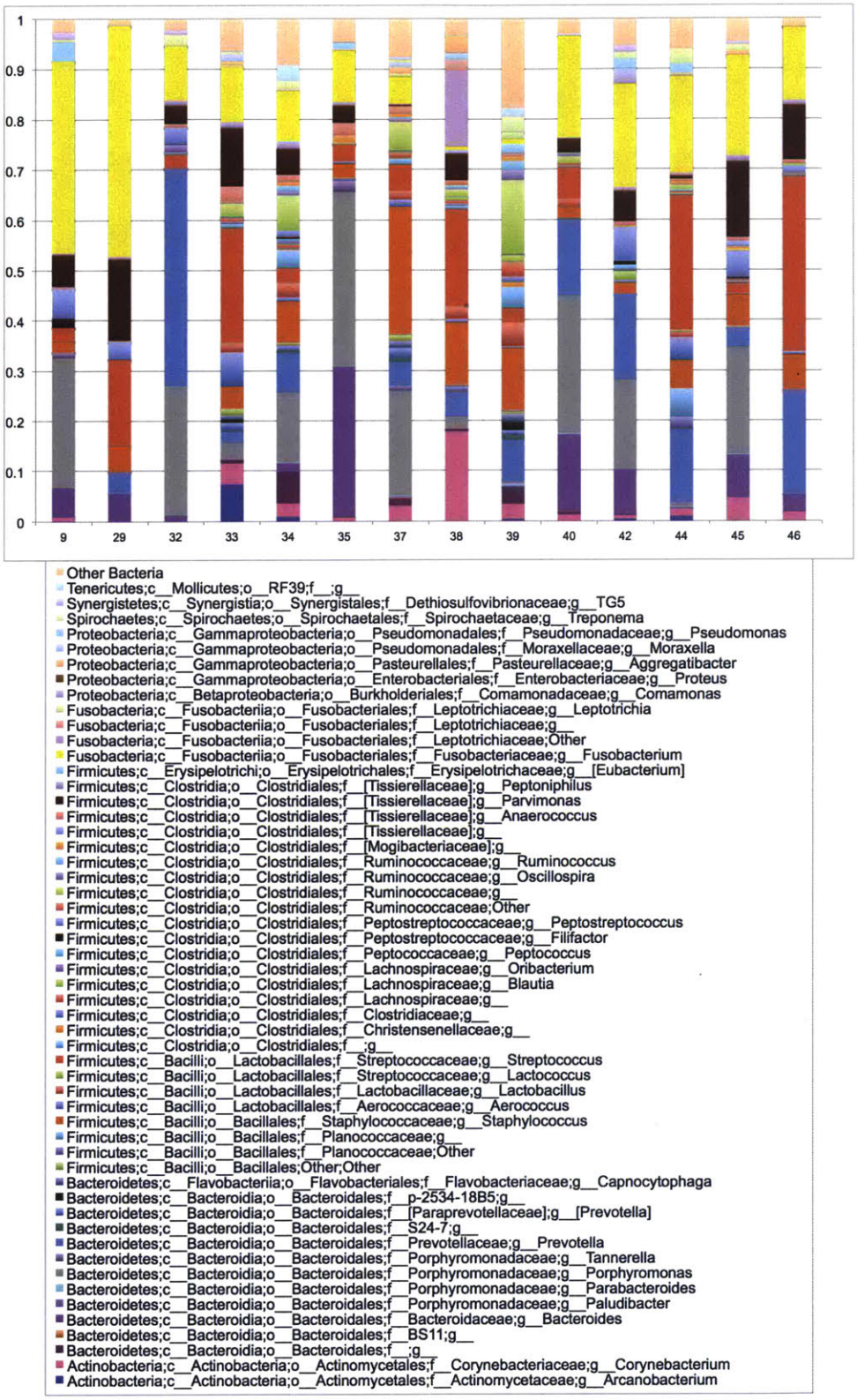

Figure 2-16: Genus-level taxonomy bar chart for skin-implant swab samples rarefied to 1000 sequences. Note that genera representing <1% of sample reads are represented as Other Bacteria..

Oral

At the phylum level, community composition was very consistent between macaques. The main phyla contributing to reads included Bacteroidetes (37% average of reads), Firmicutes (29% average of reads), Proteobacteria (17%) of reads and Fusobacteria (15%) of reads (Figure 2-17).

At the genus level, OTUs contributing a high prevalence of sample reads included *Porphyromonas* spp. (14% average of reads), *Streptococcus* spp. (16% average of reads), *Fusobacterium* spp. (11% average of reads), and *Prevotella* spp. (13% average of reads) (Figure 2-18).

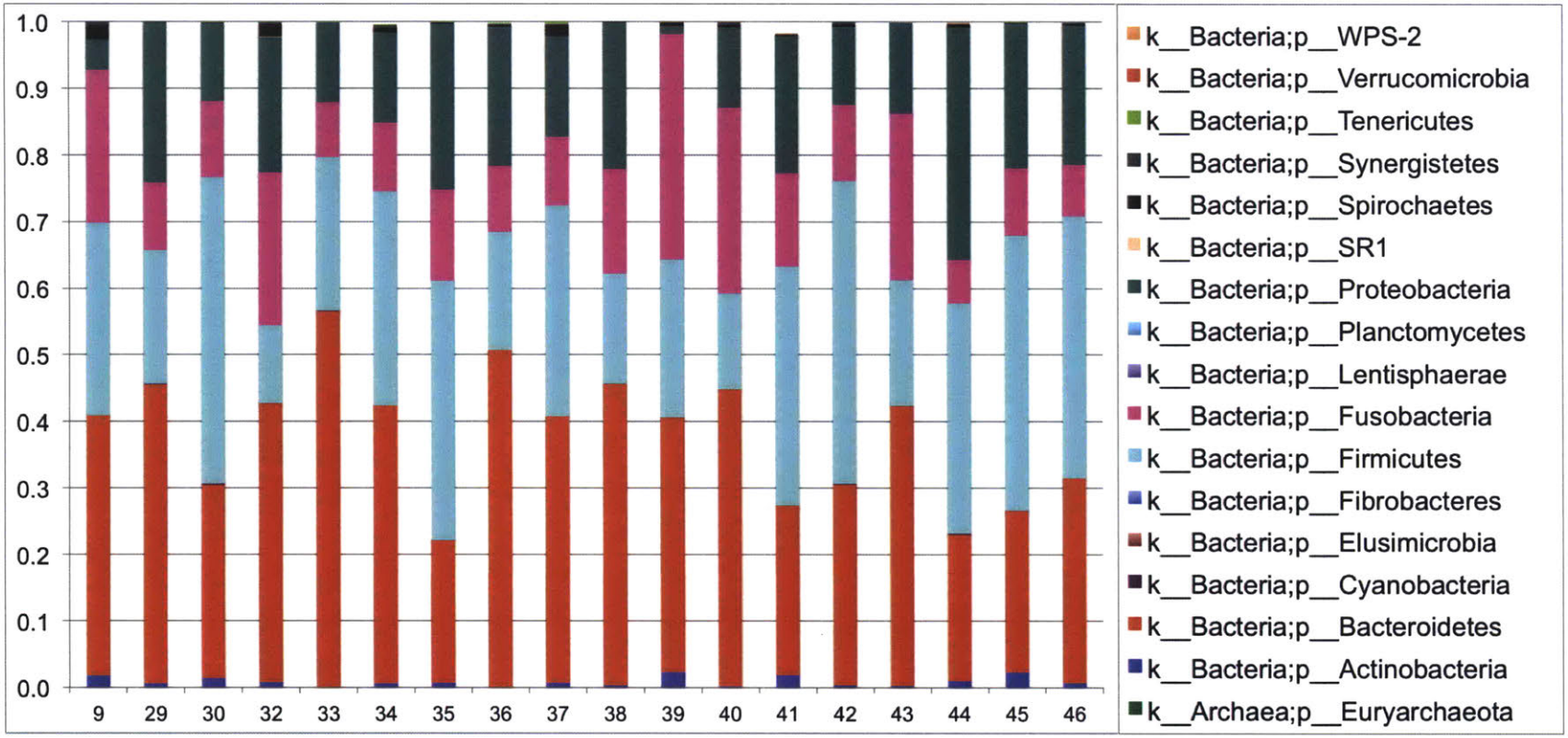

Figure 2-17: Phylum-level taxonomy bar chart for oral swab samples rarefied to 1000 sequences.

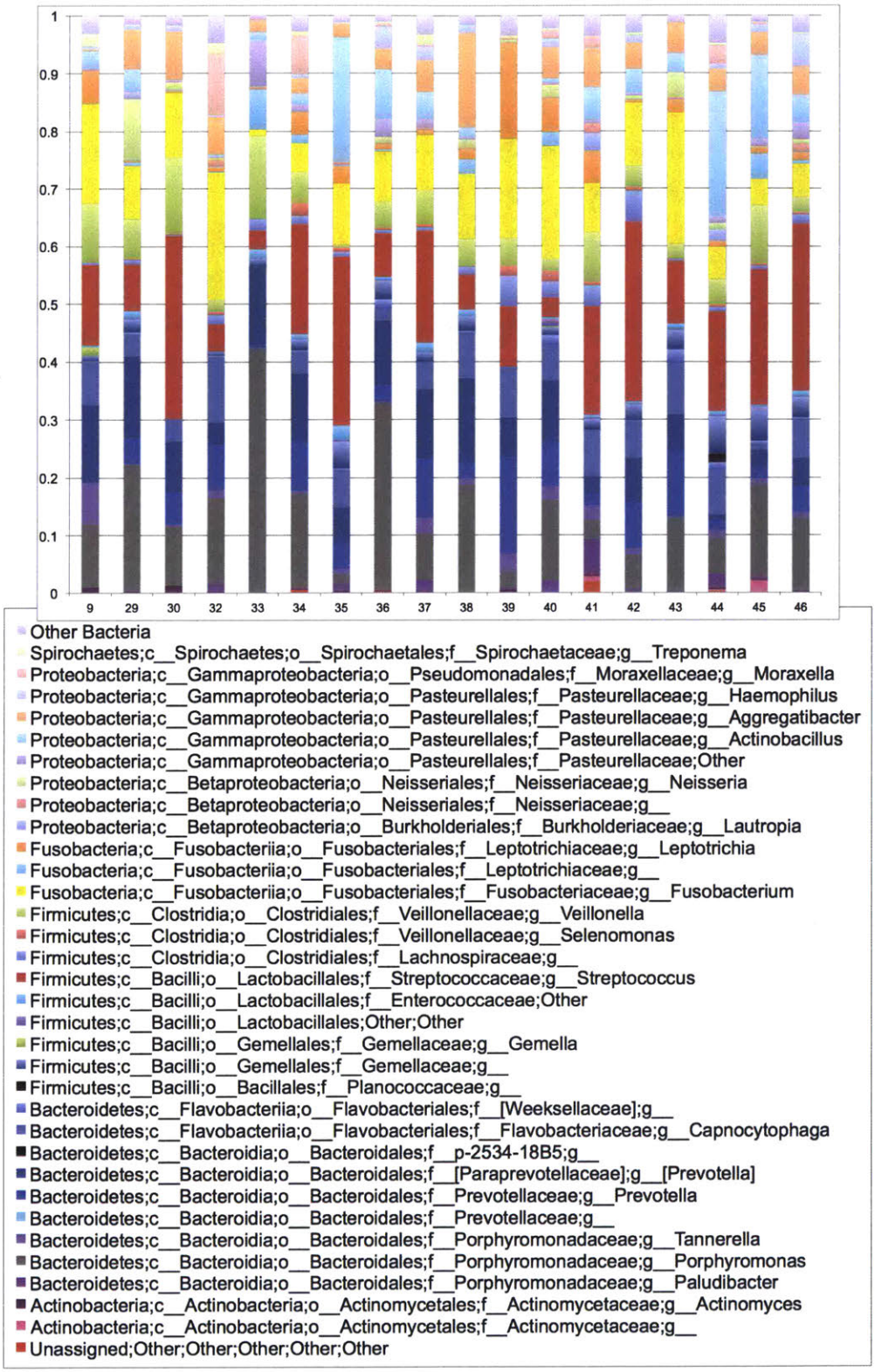

Figure 2-18: Genus-level taxonomy bar chart for oral swab samples rarefied to 1000 sequences. Note that genera representing <1% of sample reads are represented as Other Bacteria.

Feces

At the phylum level, community composition was very consistent between macaques (Figure 2-19). Bacteroidetes phyla accounted for 56% of sample reads on average (range 39-80%) and Firmicutes phyla accounted for 33% of sample reads on average (range 16-44%).

At the genus level, community composition was consistent between most macaques, although most OTUs could only be identified down to the order or family level (Figure 2-20). Predominant OTUs contributing to the population included the *Prevotella* genus (19% average of reads), Bacteroidales order (20% average of reads), and the *Ruminococcaecaea* family (15% average of reads. *Helicobacter* spp. were identified in only 7/18 samples, all at a prevalence of <0.05%.

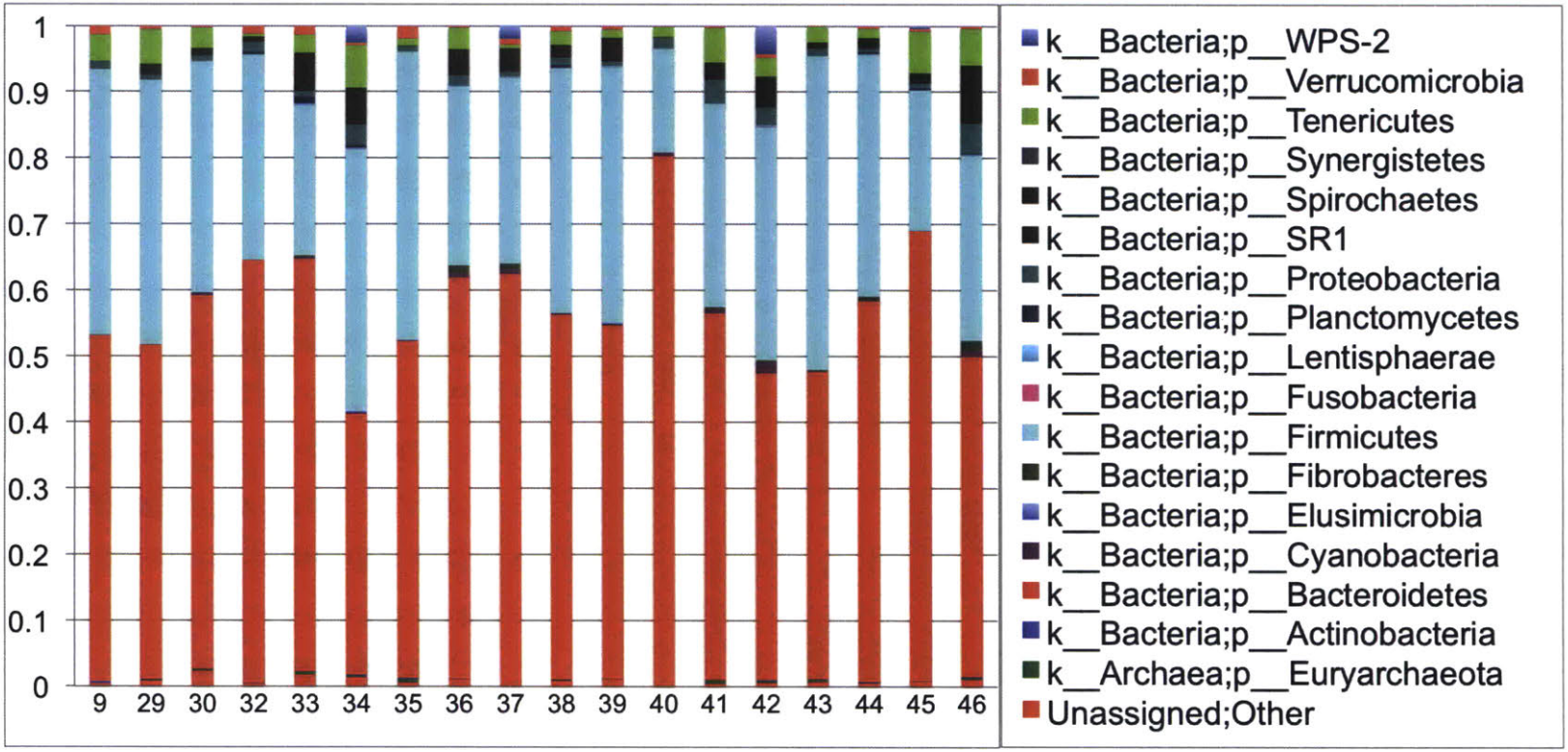

Figure 2-19: Phylum-level taxonomy bar chart for fecal samples rarefied to 1000 sequences.

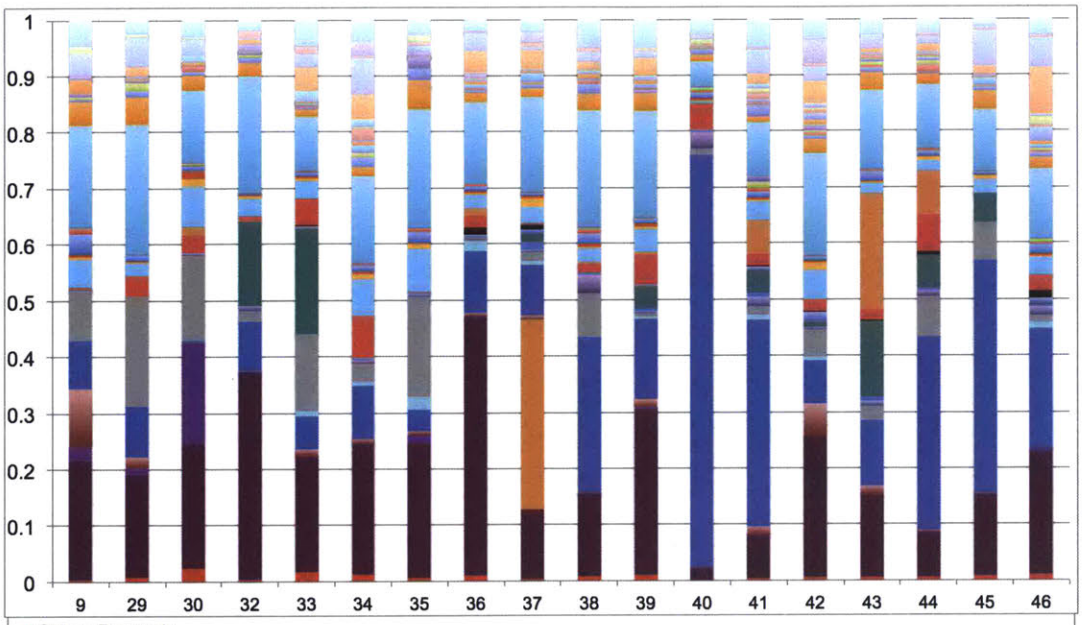

Other Bacteria
WPS-2;c__;o__;f__;g__
Verrucomicrobia;c__Verrucomicrobiae;o__Verrucomicrobiales;f__Verrucomicrobiaceae;g__Akkermansia
Verrucomicrobia;c__Verruco-5;o__WCHB1-41;f__RFP12;g__
Tenericutes;c__Mollicutes;o__RF39;f__;g__
Spirochaetes;c__Spirochaetes;o__Spirochaetales;f__Spirochaetaceae;g__Treponema
Spirochaetes;c__Spirochaetes;o__Sphaerochaetales;f__Sphaerochaetaceae;g__Sphaerochaeta
Proteobacteria;c__Deltaproteobacteria;o__Desulfovibrionales;f__Desulfovibrionaceae;g__Desulfovibrio
Proteobacteria;c__Betaproteobacteria;o__Burkholderiales;f__Alcaligenaceae;g__Sutterella
Proteobacteria;c__Alphaproteobacteria;o__RF32;f__;g__
Proteobacteria;c__Alphaproteobacteria;o__;f__;g__
Firmicutes;c__Erysipelotrichi;o__Erysipelotrichales;f__Erysipelotrichaceae;g__[Eubacterium]
Firmicutes;c__Erysipelotrichi;o__Erysipelotrichales;f__Erysipelotrichaceae;g__Catenibacterium
Firmicutes;c__Clostridia;o__Clostridiales;f__[Mogibacteriaceae];g__
Firmicutes;c__Clostridia;o__Clostridiales;f__Veillonellaceae;g__Phascolarctobacterium
Firmicutes;c__Clostridia;o__Clostridiales;f__Veillonellaceae;g__Dialister
Firmicutes;c__Clostridia;o__Clostridiales;f__Ruminococcaceae;g__Ruminococcus
Firmicutes;c__Clostridia;o__Clostridiales;f__Ruminococcaceae;g__Oscillospira
Firmicutes;c__Clostridia;o__Clostridiales;f__Ruminococcaceae;g__
Firmicutes;c__Clostridia;o__Clostridiales;f__Lachnospiraceae;g__Roseburia
Firmicutes;c__Clostridia;o__Clostridiales;f__Lachnospiraceae;g__Lachnospira
Firmicutes;c__Clostridia;o__Clostridiales;f__Lachnospiraceae;g__Coprococcus
Firmicutes;c__Clostridia;o__Clostridiales;f__Lachnospiraceae;g__
Firmicutes;c__Clostridia;o__Clostridiales;f__Clostridiaceae;g__Clostridium
Firmicutes;c__Clostridia;o__Clostridiales;f__Christensenellaceae;g__
Firmicutes;c__Clostridia;o__Clostridiales;f__;g__
Firmicutes;c__Bacilli;o__Lactobacillales;f__Streptococcaceae;g__Streptococcus
Firmicutes;c__Bacilli;o__Lactobacillales;f__Lactobacillaceae;g__Lactobacillus
Fibrobacteres;c__Fibrobacteria;o__Fibrobacterales;f__Fibrobacteraceae;g__Fibrobacter
Cyanobacteria;c__4C0d-2;o__YS2;f__;g__
Bacteroidetes;c__Bacteroidia;o__Bacteroidales;f__p-2534-18B5;g__
Bacteroidetes;c__Bacteroidia;o__Bacteroidales;f__[Paraprevotellaceae];g__YRC22
Bacteroidetes;c__Bacteroidia;o__Bacteroidales;f__[Paraprevotellaceae];g__CF231
Bacteroidetes;c__Bacteroidia;o__Bacteroidales;f__S24-7;g__
Bacteroidetes;c__Bacteroidia;o__Bacteroidales;f__RF16;g__
Bacteroidetes;c__Bacteroidia;o__Bacteroidales;f__Prevotellaceae;g__Prevotella
Bacteroidetes;c__Bacteroidia;o__Bacteroidales;f__Porphyromonadaceae;g__Parabacteroides
Bacteroidetes;c__Bacteroidia;o__Bacteroidales;f__Bacteroidaceae;g__Bacteroides
Bacteroidetes;c__Bacteroidia;o__Bacteroidales;f__BS11;g__
Bacteroidetes;c__Bacteroidia;o__Bacteroidales;f__;g__
Unassigned;Other;Other;Other;Other;Other

Figure 2-20: Genus-level taxonomy bar chart for fecal samples rarefied to 1000 sequences. Note that genera representing <1% of sample reads are represented as Other Bacteria.

2.7 May-June 2018 Aerobic and Anaerobic CRC cultures

Aerobic and anaerobic cultures and Kirby-Bauer sensitivities on aerobic species were performed from cultures of 23 CRCs from 15 macaques by the Division of Comparative Medicine diagnostic lab in May-June 2018. Similarly to 2011 results, the majority of cultures were polymicrobial (Table 2.14. Only 1 CRC cultured was negative for aerobic and anaerobic growth (macaque #39 CRC 2, and this CRC had a extremely low sample read count of 35 for the microbiota study). 13 out of the 15 macaques cultured had also been sampled as part of the microbiota study, although macaque #28 had been explanted and re-implanted in between the pilot microbiota sampling and collection of cultures. Data is presented in Tables 2.15, 2.16 and 2.17. Similar to data collected in 2011, The most common bacterial species identified was *S. aureus* with 23 isolates identified from 14/15 macaques. Similarly to results from 2011 (Table 2.7), *S. aureus* isolates remained largely susceptible to the tested antimicrobials, with the exception of enrofloxacin. One difference between 2011 and 2018 *S. aureus* isolates was the presence of gentamicin resistance in 3 isolates. We noted an increase in the prevalence of both *S. pyogenes* and *E. coli* cultured from CRCs, including 6 *E. coli* isolates with a beta-hemolytic phenotype. The *E. coli* isolates cultured in 2018 displayed increased resistance to amoxicillin/clavulanic acid and ceftriaxone as compared to the two *E. coli* isolates cultured in 2011. *Proteus* spp. displayed similar resistance patterns to 2011; however, the three 2018 *P. mirabilis* were sensitive to cefazolin whereas 2011 isolates displayed resistance or intermediate resistance (Figure 2.6).

Number of Isolates	# (Percentage) of CRCs (N=23)
0	1 (4%)
2	5 (22%)
3	5 (22%)
4	7 (30%)
5	2 (9%)
6	2 (9%)
9	1 (4%)

Table 2.14: Number and percentage of isolates per CRC cultured in 2018 (N=23 CRCs), includes both aerobes and anaerobes

Animal ID	Study ID	Site	Date	Isolate	AMP	AMC	B	CRO	CZ	CR	CHLOR	ENO	E	GM	LZ	MERO	N	OX	STR	TE	SXT	VA
28	B9	CRC 2	5/8/18	*Enterococcus faecalis*	20	20	14	0	7	12	16	15	19	9	20	13	0	0	0	0	0	15
38	A9	CRC 1	5/9/18	*Enterococcus faecalis*	20	20	14	0	7	12	16	15	19	9	20	13	0	0	0	0	0	15
39	B12	CRC 1	5/15/18	*Enterococcus faecalis*	20	20	14	0	7	12	16	15	18	9	20	13	0	0	0	0	0	15
39	B12	CRC 2	5/15/18	*Enterococcus faecalis*	24	24	18	0	8	9	10	20	0	0	25	15	0	0	0	0	0	17
34	E3	CRC 1	5/16/18	*Enterococcus faecium*	0	0	19	0	0	0	20	0	17	14	26	0	17	0	8	20	0	22
9	B6	CRC 2	5/10/18	*Staphylococcus aureus*	35	40	19	25	41	37	19	10	23	20	25	38	20	22	15	23	26	16
9	B6	CRC 2	5/10/18	*Staphylococcus aureus*	38	38	18	24	37	38	19	19	22	19	25	36	19	22	14	23	27	16
16	C5	CRC 1	6/12/18	*Staphylococcus aureus*	35	37	21	21	34	36	21	26	24	22	26	33	20	22	15	24	29	18
16	C5	CRC 2	6/12/18	*Staphylococcus aureus*	40	37	21	21	34	36	21	26	24	22	26	33	20	22	15	24	29	18
28	B9	CRC 1A	5/8/18	*Staphylococcus aureus*	36	37	17	24	34	38	19	0	0	21	25	37	19	18	14	22	28	15
28	B9	CRC 2A	5/8/18	*Staphylococcus aureus*	38	38	19	25	35	38	20	0	24	20	25	33	21	19	14	24	27	16
29	A5	CRC 1	5/9/18	*Staphylococcus aureus*	40	38	18	22	34	40	21	12	23	9	25	30	20	23	15	24	28	16
32	A8	CRC 1	5/18/18	*Staphylococcus aureus*	40	40	17	20	37	35	18	25	22	20	26	35	20	17	13	23	27	16
33	E2	CRC 1	5/15/18	*Staphylococcus aureus*	38	38	19	24	37	39	20	11	23	20	25	35	21	21	15	24	28	16
35	B10	CRC 1	5/15/18	*Staphylococcus aureus*	38	40	20	25	35	39	21	10	25	21	25	36	20	24	15	8	28	16
35	B10	CRC 2	5/15/18	*Staphylococcus aureus*	35	39	17	22	30	32	17	25	22	19	23	37	19	20	14	23	25	16
36	E4	CRC 1	5/23/18	*Staphylococcus aureus*	44	40	18	24	38	40	19	11	23	20	26	38	19	19	14	24	18	16
37	B11	CRC 1	5/3/18	*Staphylococcus aureus*	35	34	22	22	32	34	19	24	23	20	25	30	20	20	14	22	26	15
37	B11	CRC 1	5/3/18	*Staphylococcus aureus*	38	36	18	21	34	40	20	24	23	19	24	31	20	20	14	23	27	15
37	B11	CRC 2	5/3/18	*Staphylococcus aureus*	34	35	22	24	32	34	22	27	25	22	25	32	22	22	14	25	28	16
37	B11	CRC 2	5/3/18	*Staphylococcus aureus*	36	40	20	22	34	38	20	27	24	22	24	34	21	22	16	26	24	16
38	A9	CRC 1	5/9/18	*Staphylococcus aureus*	40	40	18	23	40	40	19	11	24	9	25	33	21	22	14	24	38	16
39	B12	CRC 1	5/15/18	*Staphylococcus aureus*	38	39	18	24	35	38	20	11	24	20	25	36	21	21	14	10	27	16
39	B12	CRC 2	5/15/18	*Staphylococcus aureus*	40	40	19	24	38	37	20	11	23	21	25	36	19	21	15	9	28	17
42	D8	CRC 1	5/9/18	*Staphylococcus aureus*	43	44	18	22	40	42	18	25	25	19	23	33	21	24	15	22	25	15
42	D8	CRC 1	5/9/18	*Staphylococcus aureus*	36	38	16	24	35	37	18	18	24	19	24	34	20	21	14	24	27	15
46	E6	CRC 1	5/17/18	*Staphylococcus aureus*	40	30	20	24	35	35	20	11	25	0	27	37	21	23	13	25	27	16
51	B18	CRC 1	5/11/18	*Staphylococcus aureus*	38	38	16	20	32	32	19	24	24	21	24	32	20	19	14	24	28	17
32	A8	CRC 1	5/18/18	*Staphylococcus chromogenes*	23	24	18	30	33	32	22	31	28	30	29	38	27	21	18	23	21	18
33	E2	CRC 1	5/15/18	*Streptococcus pyogenes*	31	38	27	31	30	30	24	21	28	19	28	32	20	27	16	25	0	21
35	B10	CRC 1	5/15/18	*Streptococcus pyogenes*	40	42	32	40	40	42	27	28	29	19	30	44	17	33	10	27	13	22
35	B10	CRC 2	5/15/18	*Streptococcus pyogenes*	39	40	29	37	38	40	27	28	28	18	29	41	17	29	10	26	0	21
36	E4	CRC 1	5/23/18	*Streptococcus pyogenes*	44	44	23	40	40	44	27	33	31	23	29	40	16	35	16	28	22	24
38	A9	CRC 1	5/9/18	*Streptococcus pyogenes*	27	24	23	22	24	27	25	18	26	19	27	25	20	27	12	23	0	20
46	E6	CRC 1	5/17/18	*Streptococcus pyogenes*	40	40	28	36	30	30	26	22	31	18	30	35	19	27	10	30	0	23
51	B18	CRC 1	5/11/18	*Streptococcus pyogenes*	31	38	27	31	30	30	24	21	28	19	28	32	20	27	16	25	0	21

Table 2.15: Gram-positive aerobic bacterial isolates and Kirby-Bauer sensitivities from 2018 CRC cultures. Color coding indicates resistant (red), sensitive (green) or intermediate (yellow) antimicrobial phenotype. Macaque #28 has CRCs designated as 1A and 2A because this animal was explanted and reimplanted between the original microbiota study and when cultures were obtained. Antimicrobial key: AMP- Ampicillin, AMC- Amoxicillin/Clavulanic Acid, B- Bacitracin, CRO- Ceftriaxone, CZ- Cefazolin, CR- Cephalothin, CHLOR - Chloramphenicol, ENO- Enrofloxacin, E- Erythromycin, GM- Gentamicin, LZ - Linezolid, MERO- Meropenem, OX- Oxacillin, STR- Streptomycin, TE- Tetracycline, SXT- Trimethoprim-Sulfamethoxazole, VA- Vancomycin

Animal ID	Study ID	Site	Date	Isolate	AMP	AMC	CRO	CZ	CR	CHLOR	ENO	GM	LZ	MERO	N	STR	TE	SXT	VA
29	A5	CRC 1	5/9/18	*Escherichia coli*	0	14	0	0	0	24	0	0	0	26	18	15	22	0	0
38	A9	CRC 1	5/9/18	*Escherichia coli*	0	14	0	0	0	23	0	0	0	25	17	14	19	0	0
35	B10	CRC 2	5/15/18	*Escherichia coli* -beta	0	8	0	0	0	23	0	19	0	27	17	14	21	14	0
39	B12	CRC 2	5/15/18	*Escherichia coli* -beta	0	11	0	0	0	23	0	20	0	28	17	14	0	24	0
42	D8	CRC 1	5/9/18	*Escherichia coli* -beta	0	0	0	0	0	24	0	18	0	24	17	14	21	23	0
16	C5	CRC 1	6/12/18	*Escherichia coli* -beta	0	11	0	0	0	24	0	22	0	30	20	16	0	26	0
16	C5	CRC 2	6/12/18	*Escherichia coli* -beta	0	11	0	0	0	23	0	22	0	29	20	16	0	26	0
28	B9	CRC 2A	5/8/18	*Escherichia coli* -beta	0	0	0	0	0	24	0	18	0	24	17	13	18	23	0
35	B10	CRC 1	5/15/18	*Escherichia coli* -beta	0	0	0	0	0	24	0	21	0	27	18	16	0	26	0
28	B9	CRC 1A	5/8/18	*Proteus mirabilis*	0	20	31	19	20	0	0	0	0	27	11	0	7	0	0
28	B9	CRC 2A	5/8/18	*Proteus mirabilis*	0	20	29	18	17	0	0	0	0	22	11	0	0	0	0
37	B11	CRC 2	5/3/18	*Proteus mirabilis*	0	22	30	20	24	0	0	0	0	25	0	0	0	0	0
29	A5	CRC 1	5/9/18	*Proteus penneri*	0	7	0	0	0	8	0	9	0	24	13	7	8	0	0
38	A9	CRC 1	5/9/18	*Proteus vulgaris*	0	7	0	0	0	7	0	9	0	24	13	0	8	0	0
9	B6	CRC 2	5/10/18	*Pseudomonas aeruginosa*	0	0	15	0	0	0	17	18	0	26	15	0	8	0	0
9	B6	CRC 1	5/10/18	*Pseudomonas aeruginosa*	0	0	16	0	0	0	19	17	0	30	15	8	9	0	0
35	B10	CRC 1	5/15/18	*Pseudomonas aeruginosa*	0	0	18	0	0	0	19	19	0	33	16	8	9	0	0
35	B10	CRC 2	5/15/18	*Pseudomonas aeruginosa*	0	0	0	17	0	0	18	18	0	33	16	9	8	0	0
34	E3	CRC 1	5/16/18	*Enterobacter cloacae*	0	0	0	0	0	23	26	21	0	26	19	0	0	0	0

Table 2.16: Gram-negative aerobic bacterial isolates and Kirby-Bauer sensitivities from 2018 CRC cultures. Color coding indicates resistant (red), sensitive (green) or intermediate (yellow) antimicrobial phenotype. Macaque #28 has CRCs designated as 1A and 2A because this animal was explanted and reimplanted between the original microbiota study and when cultures were obtained. Antimicrobial key: AMP- Ampicillin, AMC- Amoxicillin/Clavulanic Acid, B- Bacitracin, CRO- Ceftriaxone, CZ- Cefazolin, CR- Cephalothin, CHLOR - Chloramphenicol, ENO- Enrofloxacin, E- Erythromycin, GM- Gentamicin, LZ - Linezolid, MERO- Meropenem, OX- Oxacillin, STR- Streptomycin, TE- Tetracycline, SXT- Trimethoprim-Sulfamethoxazole, VA- Vancomycin

Bacterial Isolate	Number (%) of Isolates	Aerotolerance
Staphylococcus aureus	23 (27.3)	
Escherichia coli	9 (10.7)	
Corynebacterium ulcerans	8 (9.5)	
Group A β-*Streptococcus pyogenes*	7 (8.3)	
Proteus spp.	5 (5.9)	
Enterococcus faecalis	4 (4.8)	**Aerobic**
Pseudomonas aeruginosa	4 (4.8)	
Enterococcus faecium	1 (1.2)	
Enterobacter cloacae	1 (1.2)	
Staphlyococcus chromogenes	1 (1.2)	
Streptococcus milleri group	1 (1.2)	
Prevotella spp.	6 (7.1)	
Fusobacterium spp.	4 (4.8)	
Bacteroides spp.	3 (3.6)	
Anaerococcus prevotii	2 (2.3)	
Group F β-*Streptococcus constellatus*	1 (1.2)	**Anaerobic**
Collinsella aerofaciens	1 (1.2)	
Micromonas micros	1 (1.2)	
Peptinophilis assachrolyticus	1 (1.2)	
Propionibacterium propionicum	1 (1.2)	
Total	**84 (100)**	

Table 2.17: Summary of aerobic and anaerobic bacterial species cultured from CRCs in 2018. Data from 22 CRCs from 15 macaques

2.8 Discussion

The Human Microbiome Project and numerous other studies have utilized 16S sequencing techniques to characterize the microbiota of various body sites in both healthy and diseased states [24, 39]. Published use of these techniques on macaques have predominantly been focused around studies examining microbiota changes in the context of various infective states, including simian immunodeficiency virus (SIV) infection, *Shigella* infection and *Helicobacter pylori* infection [40, 41, 42, 43].

One previous report characterized the gut microbiota from healthy macaques and compared stool samples, luminal samples and mucosal samples at various intestinal sites [43]. Our fecal microbiota results are consistent with these previous findings; with the Bacteroidetes phylum (and specifically the *Prevotellaceae family*), and Firmicutes phylum demonstrating higher prevalence than the Proteobacteria phylum and *Spirochaetaceae* families [43]. One difference between our results and those previously published is that the prevalence of *Helicobacteriaceae* was much lower in our study (on average 0.005% of sample reads) [43]. While Yasuda et al. identified that the *Helicobacteriaceae* were more prevalent in mucosal samples vs. stool samples, they found that stool samples were highly predictive of *Helicobacter* abundance elsewhere in other gut sites [43]. We have previously cultured, identified and characterized intestinal helicobacters from macaques; our low prevalence of idiopathic colitis may be related to the low prevalence of *Helicobacter* in the macaques sampled as part of this study [44, 45, 46, 47].

Two previous publications have analyzed the microbiota of the oral cavity and dental plaque in rhesus macaques; one report characterized dysbiosis in SIV-infected macaques and one study compared the microbiota between mild and moderate-severe cases of naturally-occuring periodontitis [48, 49]. Macaques at MIT do not receive regular dental scaling and polishing procedures, and most have varying levels of periodontitis with severity typically correlating with increasing age. The periodontitis study identified taxa with differential abundance in diseased vs. healthy sites [49]. For our study, oral swabs were passed around the cheek pouches, dorsal tongue, and the gingiva superior to the teeth, to minimize sampling of dental plaque. Overall, our oral microbiota results featured a combi-

nation of OTUs identified to be more abundant in the diseased category (including *Prevotella* spp., *Streptococcus* spp. and *Treponema* spp.) and the healthy category (*Capnocytophaga* spp., *Gemella* spp., *Fusobacterium* spp., *Actinomyces* spp. and *Leptotrichia* spp.). *Porphyromonas gingivalis* is known to be a key human periodontal pathogen; however, there were no identified differences in relative proportions between diseased and healthy states in macaques [49]. The SIV-oral microbiota study compared samples from the dorsal tongue to dental plaque in healthy macaques [48]. Identified dental plaque taxa were similar to those listed above, however this study only identified *Porphyromonas* spp. from the dorsal tongue, and not from dental plaque samples. These results are in agreement with our identification of *Porphyromonas* spp. from non-dental plaque samples.

One previous report compared the skin microbiota between zoo-housed primates (chimpanzee, gorilla, baboons), two rhesus macaques living in Cayo Santiago, Puerto Rico and human volunteers [50]. Samples from this study were collected by swabbing the axillary region (for all species). At the phylum level, the authors identified predominant contributions from Firmicutes (45%), Bacteroidetes (35%), Actinobacteria and Fusobacteria (8-10% each) in the two macaques sampled. Our skin swab phylum-level results are fairly similar, although our population had decreased Actinobacteria (4% on average) and increased Fusobacteria (17% on average). At the genus-level, more differences were noted between our results and previously published findings; specifically, our macaque population had increased contributions from *Streptococcus* spp., *Staphylococcus* spp. and *Fusobacterium* spp. and decreased contributions from *Prevotella* spp. and the *Ruminococcaceae* family. These differences are likely related to sampling site (skin-implant margin vs. axillary region), our larger sample size (14 macaques after rarefaction vs. 2 macaques in the published study) and husbandry (indoor vs. outdoor-housing). We also noted *Corynebacterium* spp. identified at >0.1% in all analyzed skin swabs with the exception of macaque #32. *C. ulcerans* has previously been reported as a common isolate from macaque CRCs [51]. The presence of the phosopholipase D toxin virulence factor in *C. ulcerans* can promote infiltration and dissemination into tissues and further promote skin inflammation [51, 52].

Previous reports utilizing 16S microbiota techniques to analyze purulent exudate are limited to a single recent publication evaluating intra-

abdominal abscesses [53]. Abdominal abscesses differ from CRCs because patients are typically clinically ill, and they are not necessarily associated with implanted materials. Abdominal abscesses typically arise secondary to Crohn's disease, appendicitis, hepatobiliary disease or penetrating abdominal trauma [54, 55, 56, 57]. Despite etiological differences, abdominal abscess culture results are comparable to CRCs, in that many are polymicrobial (2-6 species), with similarities in species commonly identified (*Bacteroides fragilis*, *Prevotella*, *Porphyromonas* spp., and *Peptostreptococcus* spp., enterococci, streptococci, and *Staphylococcus aureus* [53]. In this report, the authors successfully sequenced and analyzed 26/43 abscess samples. Although samples were divided into polymicrobial and monomicrobial categories based on Gram stain and culture results, there was no significant difference in the mean number of OTUs identified between them (15.2 and 17 OTUs for polymicrobial and monomicrobial samples, respectively). While the dominant OTUs identified were consistent with the culture results for "monomicrobial" samples, this was not true for the majority of polymicrobial samples. The dominant OTUs identified from microbiota analysis in polymicrobial samples included *Lactobacillus* spp., *Prevotella* spp., *Fusobacterium* spp., and *Bacteroides* spp. with "cultureable" *Staphylococcus* spp., *Streptococcus* spp., *Enterococcus* spp. representing a small minority of sample reads, or not being detected at all [53]. This comparison has similarities to our results comparing culture-dependent and culture-independent methods from CRC samples; anaerobes predominate in OTU analysis, whereas cultured organisms such as *S. aureus*, *E. faecalis*, *Proteus* spp. and *Streptococcus* spp. contribute to a smaller percentage of sample reads.

While culture-independent methods can identify many more OTUs than species easily cultured, these techniques are best utilized in a complimentary fashion. Traditional culture methods allow more definitive identification to the species level, as well the ability to perform additional antimicrobial susceptibility testing; both of these factors are important when treating a clinically ill macaque. However, like previous publications, [53] cultures performed in parallel with culture-independent techniques were only able to identify a small fraction of OTUs and are not necessarily representative of the predominant flora colonizing CRCs. We did observe some changes in species prevalence between cultures obtained in 2018 as compared to 2011.

While *S. aureus* remained the most prevalent species, we saw increases in *S. pyogenes*, *E. coli*, *C. ulcerans* and *P. aeruginosa* and decreases in *E. faecalis* and *S. dysgalactiae* from samples. Kirby-Bauer antimicrobial sensitivities between 2011 and 2018 species remained relatively stable overall.

Culture-independent techniques can be a useful tool to monitor bacterial populations sequentially and potentially assess how updates to implant materials, or sanitization practices can affect bacterial communities over time. Additionally, our parallel analysis of the microbiota diversity at different sampling sites within individual macaques has provided a unique insight on the source of bacterial communities commonly colonizing CRCs. We had initially hypothesized that fecal contamination was the likely source of bacterial colonization of CRCs. Analysis of PCoA plots and taxonomy bar charts suggested that the majority of CRC bacterial communities were different than fecal communities. This was confirmed by comparison of unweighted UniFrac beta diversity, where 22/26 macaques had significant differences between their CRC and fecal bacterial communities. We identified that CRC bacterial communities were most similar to skin-implant margin and oral communities, and confirmed that these communities were not significantly different on unweighted UniFrac beta diversity in 17/23 and 19/26 macaques, respectively. The majority of our macaques are pair-housed and we hypothesize that grooming behavior between macaques can contribute to the spread of oral flora to the skin margin. Because macaques periodically move between housing rooms within the MIT vivarium, we were unable to evaluate whether housing room location affects the microbiota, but acknowledge that this could be another potential factor. Our results also suggest that strict peri-implant skin sanitization and introduction of regular dental cleanings could be potential targets for limiting bacterial colonization of CRCs.

2.9 Conclusions

In this chapter we have discussed how traditional culture methods and culture-independent methods can be used to characterize bacterial species colonizing cephalic recording chambers of implanted macaques. We have identified *Staphylococcus aureus*, *E. coli*, *C. ulcerans*, *Proteus* spp., *E. faecalis* and *Streptococcus* spp. as highly prevalent aerobic species using tradi-

tional culture methods, but microbiota analysis suggests that the predominant species colonizing CRCs are strict anaerobes. Our results confirm that CRCs are extremely diverse in the composition of bacterial communities between macaques, and even between CRCs implanted within the same macaque. Paired analysis of different body sites indicates that there are more similarities between CRC, skin margin and oral communities than with fecal communities. Future studies should evaluate how different skin margin sanitization protocols and introduction of regular dental prophylaxis might impact CRC bacterial communities over time.

Chapter 3

Colonization dynamics of *Enterococcus faecalis* in CRCs from 2011-2017

Portions of this chapter have been previously published [1] or are currently in press [58].

3.1 Introduction

In Chapter 2, we introduced characterization of bacterial species colonizing CRCs from a community perspective, as determined by both culture-dependent and culture-independent methods. This chapter and the remainder of this dissertation will now focus on how one species, *Enterococcus faecalis*, persists and evolves within CRCs, both within individual macaques, and within the macaque colony at MIT over a seven-year period. *E. faecalis* was the second most prevalent bacterial species isolated from CRC cultures collected from 25 macaques in 2011. Initial Kirby-Bauer antimicrobial sensitivity testing identified that >50% isolates were resistant to multiple antimicrobial classes, including bacitracin, macrolides (erythromycin), aminoglycosides (gentamicin, neomycin), penicillins/cephalosporins (oxacillin, cephalothin, ceftriaxone, cefazolin), fluoroquinolones (enrofloxacin), trimethoprim-sulfamethoxazole, tetracycline and polymyxin B (Table 3.1). Because of this marked resistance, we extensively characterized isolates to improve understanding of their potential pathogenicity.

Animal ID	Study ID	Antimicrobial Used	Culture Results	AMP	AMC	B	CR	E	GM	OX	SXT	ENO	TE	T	CRO	D	N	CZ	PB	VA
1	A1	GM	*Enterococcus faecalis* #1	17	25	13	11	0	0	0	0	0	0	0	0		12	9	0	15
4	B1	None	*Enterococcus faecalis* #2	16	13	0	13	0	12	0	0	14	0	0	13		0	13	0	9
5	B2	T-PB	*Enterococcus faecalis* #3	24	27	0	14	0	19	0	0	18	7	7	15	14	0	12	0	
5	B2	T-PB	*Enterococcus faecalis* #4	25	35	0	16	0	16	0	0	0	0	0	22		0	16	0	20
5	B2	T-PB	*Enterococcus faecalis* #5	16	22	11	13	0	14	0	0	0	0	0	18		0	13	0	15
6	B3	T-PB	*Enterococcus faecalis* #11	0	19	0	11	0	12	0	0	14	0	0	10		0	12	0	13
8	B5	None	*Enterococcus faecalis* #12	18	19	0	12	0	10	0	19	13	0	0	0		0	12	0	13
9	B6	T-PB	*Enterococcus faecalis* #13	16	22	11	11	14	12	0	0	0	0	0	0		0	12	0	15
11	B8	None	*Enterococcus faecalis* #14	19	19	11	9	0	12	0	0	0	0	0	0		10	11	0	13
11	B8	None	*Enterococcus faecalis* #15	21	24	11	11	10	13	0	0	0	0	0	0		10	12	0	13
15	C4	N, PB, B	*Enterococcus faecalis* #6	23	25	0	13	0	18	0	0	18	0	0	11	16	0	11	0	12
16	C5	N, PB, B, GM	*Enterococcus faecalis* #7	21	22	0	12	0	18	0	0	17	0	0	10	14	0	11	0	12
16	C5	N, PB, B, GM	*Enterococcus faecalis* #8	20	21	0	13	0	18	0	0	17	0	0	10	14	0	11	0	
18	C7	GM	*Enterococcus faecalis* #9	19	24	11	11	10	0	0	0	0	0	0	0		8	11	0	15
19	C8	GM	*Enterococcus faecalis* #10	25	27	15	10	0	0	0	0	0	0	0	0	11	14	12	0	15

Table 3.1: Aerobic culture and Kirby-Bauer antimicrobial sensitivity results for 15 *E. faecalis isolates*. Numbers represent the zone of inhibition measured around each antimicrobial disk. Color coding indicates resistant (red), sensitive (green) or intermediate (yellow) antimicrobial phenotype. Antimicrobial key: AMP- Ampicillin, AMC- Amoxicillin/Clavulanic Acid, B- Bacitracin, CR- Cephalothin, E- Erythromycin, GM- Gentamicin, OX- Oxacillin, SXT- Trimethoprim-Sulfamethoxazole, ENO- Enrofloxacin, TE- Tetracycline, T- Oxytetracycline, CRO- Ceftriaxone, D- Doxycycline, N- Neomycin, CZ- Cefazolin, PB- Polymixin B, VA- Vancomycin

3.2 Relevance of *Enterococcus faecalis* as a human pathogen

Enterococcus faecalis is an important cause of healthcare-associated infections, and is the third most common cause of central line-associated bloodstream infections, the fifth most common cause of catheter-associated urinary tract infections, and the sixth most common cause of healthcare-associated infections, overall [59]. The enterococci possess mechanisms of both acquired and intrinsic resistance to multiple antimicrobial agents, making nosocomial infections especially difficult to treat successfully. Additionally, the ability to form biofilm contributes to enterococcal catheter-associated blood and urinary tract infections [60, 61]. CRCs offer an interface for biofilm formation in cranially-implanted macaques, and we hypothesized that *E. faecalis* isolated from recording chambers would have similar sequence types, virulence factors, and biofilm genes as human isolates.

3.3 Characterization of 15 *E. faecalis* CRC isolates from 2011 sampling

3.3.1 Animals, CRC maintenance and bacterial culture

Sampling of implanted macaques, CRC sanitization procedures and bacterial culture techniques were previously described in Section 2.2.1. Of the 25 macaques sampled, *E. faecalis* was isolated from 11 animals; two macaques had two separate isolates and one macaque had 3 separate isolates (Table 3.2)

Animal ID	Sex	Age (years)	Lab ID	Study ID	# of CRCs	Duration of CRC implantation (years)	Antimicrobials used in CRC	Packing materials used in CRC	*E. faecalis* Isolate(s)
1	F	15	A	A1	1	1-3	G	None	#1
4	M	11	B	B1	2	1-3	None	Sterile non-woven sponge balls	#2
5	M	10	B	B2	3	3-5 (2), 1-3 (1)	T-PB	None	#3, #4, #5
6	M	13	B	B3	2	3-5	T-PB	Sterile non-woven sponge balls	#11
8	M	13	B	B5	3	1-3	T-PB	Sterile non-woven sponge balls	#12
9	M	13	B	B6	3	<1	T-PB	Sterile non-woven sponge balls	#13
11	M	10	B	B8	2	1-3	None	Silicone elastomer	#14, #15
15	M	8	C	C4	1	1-3	BNP	Sterile petroleum jelly, occasionally with	#6
16	F	10	C	C5	2	1-3	BNP or G	None	#7, #8
18	M	10	C	C7	2	1-3	G	None	#9
19	M	10	C	C8	2	<1	G	None	#10

Table 3.2: Population characteristics of 11 macaques with *E. faecalis* isolated from CRCs in August, 2011. Macaque #18 was a cynomolgus macaque; all other macaques were rhesus macaques. Antimicrobial use within CRCs and CRC packing material are listed for each animal as designated. Antimicrobial key: G, gentamicin sulfate 0.3%; E, enrofloxacin 2.27% diluted 1:20, T-PB, oxytetracycline 5mg/g-polymyxin B 10,000U/g; BNP, bacitracin zinc 400U/g-neomycin sulfate 5mg/g-polymyxin B 10,000U/g

3.3.2 Minimum inhibitory concentration testing

Minimum inhibitory concentrations for key antibiotics were determined by broth microdilution in CAMHB (Cation-Adjusted Mueller Hinton Broth) as recommended by the Clinical Laboratories and Standards Institute (CLSI) [62]. For daptomycin MIC determination, the CAMHB was supplemented with calcium to a final concentration of 50 μg/ml. Amoxi-cillin-clavulanic acid and trimethoprim-sulfamethoxazole combinations were tested for MIC using Etest strips according to the manufacturer's instructions (Etest, bioMérieux, Durham, NC). The MIC was read at the lowest concentration where the ellipse of inhibited growth intersected the testing strip. All antibiotics used for broth microdilution were purchased from Sigma-Aldrich Chemical Company (St Louis, MO). Control strains included vancomycin-susceptible ATCC *E. faecalis* 29212 and vancomycin-resistant ATCC *E. faecalis* 51299.

3.3.3 DNA extraction, PCR and multi-locus sequence typing (MLST)

DNA was extracted from overnight broth cultures of *E. faecalis* using a commercially available kit (Qiagen DNeasy Blood and Tissue Kit, USA). Manufacturer instructions were modified by the addition of 50μl of lysozyme (50 mg/ml) and 10μl mutanolysin (2500 U/ml, Sigma-Aldrich) during a 30 minute incubation at 37°C before the addition of proteinase K and buffer.

Polymerase chain reaction (PCR) amplification of the D-alanine:D-alanine ligase gene (ddl), 16S rRNA gene, and MLST genes were performed using the listed primers (Appendix B), with amplification conditions based on previously published protocols [63, 64]. PCR products were separated by electrophoresis through a 1% agarose gel at 100-120V for 30-40 minutes, prior to ethidium bromide staining and visualization with UV light. Prior to sequencing, PCR products were purified using a commercial kit according to manufacturer instructions (Qiagen, USA), or purified prior to sequencing by a commercial laboratory (QuintaraBio, Cambridge, MA). Purified PCR products underwent Sanger sequencing at the DNA Core Facility at the Massachusetts General Hospital Center for Computational and Integrative Biology, or at a commercial laboratory (QuintaraBio, Cambridge, MA). Sequence types were identified using the *E. faecalis* MLST website

(http://pubmlst.org/efaecalis) at the University of Oxford [65].

3.3.4 Whole genome sequencing, antimicrobial resistance genes and virulence factor identification

E. faecalis isolates #1, #12, and #13, from macaques #1, #8, and #9, respectively, were each sequenced on a single SMRT cell on a Pacific Biosciences RS2 at the University of Massachusetts Deep Sequencing Core Facility. DNA libraries were prepared for sequencing with the SMRTbell Template Prep Kit 1.0 and the DNA/Polymerase Binding Kit P6 v2, according to manufacturer instructions (Pacific Biosciences, Menlo Park, CA). A total of 87,196, 93,299 and 85,195 reads were obtained for genomes from isolates 1, 12 and 13, respectively; resulting in 3 polished contigs for isolates 1 and 12, and 2 polished contigs for isolate 13. N50 read lengths were 24,838, 24,224 and 23,305 bases, and average reference coverage was 327.48, 338.83 and 293.2 for isolates 1, 12, and 13, respectively. Filtered subreads were assembled *de novo* using the Hierarchical Genome Assembly Process (HGAP 3.0) workflow, with the Celera assembler and assembly polishing by Quiver [66]. Quality trimming was performed during the preassembly stage of HGAP. This whole genome sequencing project has been deposited at DDBJ/ENA/GenBank under the accession numbers MCFU00000000, MCFV00000000 and MCFW00000000 for *E. faecalis* isolates #1, #12 and #13, respectively. The genome assemblies described in this paper are versions MCFU01000000, MCFV01000000, and MCFW01000000. Assembled genomes were annotated using the Pathosystems Resource Integration Center (PATRIC) annotation service, and the proteomes were compared with vancomycin-susceptible ATCC *E. faecalis* 29212 [67]. Assembled genomes were analyzed using the PubMLST, ResFinder, VirulenceFinder and PATRIC databases to confirm sequence type and identify genes of interest [65, 67, 68, 69]. The ATCC 29212 genome used for comparison was retrieved from GenBank under the accession number CP00816 [70]. Identification thresholds were set at 98% identity over a minimum length of 60% for ResFinder, and 95% identity over a length of 60% for VirulenceFinder. Because fluoroquinolone resistance often results from point mutations in DNA supercoiling enzymes, DNA gy-

rase (*gyrA*) and topoisomerase IV subunits A and B (*parC* and *parE*) FASTA protein sequences were compared between macaque isolates and *E. faecalis* reference strain ATCC 29212 using the multiple sequence alignment tool on PATRIC to identify amino acid polymorphisms.

3.3.5 Static biofilm assay

Biofilm formation was assayed by measuring crystal violet binding, according to previously published protocols with slight modification [71, 72]. Macaque *E. faecalis* isolates, and positive control ATCC *E. faecalis* 29212, were plated on tryptic soy agar containing 5% sheep blood, and incubated at 37°C in 5% CO_2 for 24 h. Sterile 1μl disposable loops were used to inoculate isolates into 5 ml of tryptic soy broth supplemented with 1% glucose (w/v). Following overnight incubation at 37°C, the optical density at 600 nm was recorded using a microtiter plate spectrophotometer (Epoch, Biotek Instruments, Inc., Winooski, VT). For each isolate, 2μl of overnight culture was diluted into 198μl of tryptic soy broth supplemented with 1% glucose, in triplicate, in 96 well polystyrene plates. For comparison, 4 negative controls containing glucose-supplemented tryptic soy broth without bacterial inoculum were included. Microtiter plates were incubated at 37°C, shaking at 100 rpm and biofilm formation was evaluated at 24 h. Following aspiration of medium and planktonic cells, wells were washed three times with 200μl of phosphate-buffered saline, inverted, and dried for 45 min. The remaining biofilm was fixed with 200μl of methanol for 20 min, and plates were inverted and air-dried for an additional 45 min. Biofilm was stained with 150μl of 1% crystal violet for 20 min. Excess stain was removed via aspiration, followed by rinsing under running tap water. After again air-drying, biofilm-bound crystal violet was solubilized via the addition of 150μl ethanol for 25 min. The absorbance of the extracted dye was measured at 570 nm using a microtiter plate spectrophotometer, and adjusted for the absorbance of the negative control. Biofilm optical density was normalized to the initial bacterial cell mass by dividing the absorbance of the extracted dye by the OD_{600} of the initial inoculum. Each biofilm test was run in triplicate, and biological replicates were repeated in triplicate on a separate day, independently, to confirm results. Beeswarm plots for each isolate did not qualitatively show systematic bias due to batch ef-

fects between experiments, thus data was pooled for analysis (Figure 3-1). Beeswarm plots were generated using the Python programming language (Python 3.5.2, matplotlib 1.5.1, seaborn 0.8.0), and Bayesian analysis was done using PyMC3 (ver 3.0 rc2) (Figure 3-1). Data was analyzed using a Kruskal-Wallis test with Dunn's multiple correction in GraphPad Prism (GraphPad Software, Inc., La Jolla, CA) with $P < 0.05$ considered significant.

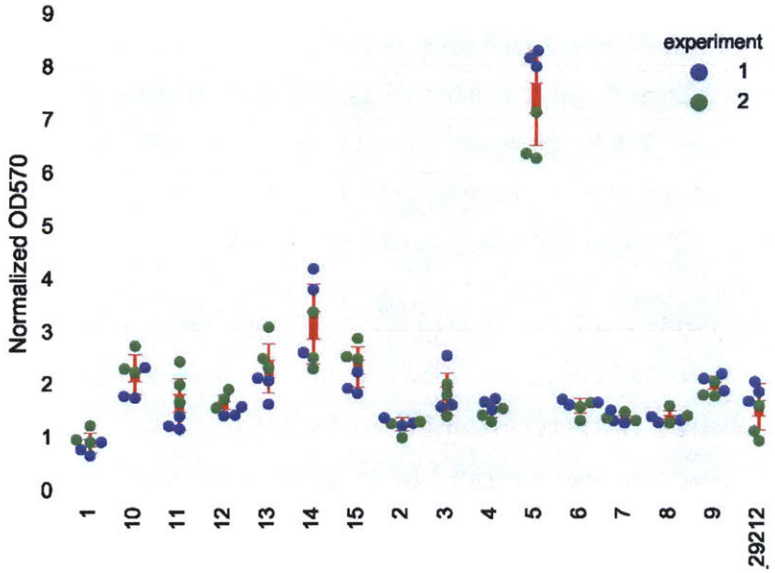

Figure 3-1: Beeswarm Plot of Crystal Violet Biofilm Experimental Data

3.3.6 Biofilm assessment under flow

In collaboration with Dr. César de la Fuente-Núñez in the Lu laboratory at MIT, a flow cell system was assembled and sterilized as previously described [73, 74], and biofilm formation was assessed using BM2 medium [62 mM potassium phosphate buffer (pH 7), 7 mM $(NH_4)_2SO_4$, 2 mM $MgSO_4$, 10 μM $FeSO_4$, 0.4% (wt/vol) glucose]. The chambers were inoculated with overnight cultures of *E. faecalis* isolates #1, #5, #12 and #13, and bacteria were allowed to attach to the surface of the flow cell chambers for 7 h 40 min. Bacteria were then grown for 43 h under a flow of 2.4 ml/min, after which viable bacteria were stained with SYTO-9 and subsequently visualized using a confocal laser scanning microscope (Zeiss LSM 700).

Three-dimensional reconstructions were generated using the Imaris software package (Bitplane AG).

3.4 Results from 2011 *E. faecalis* isolate characterization

3.4.1 Minimum inhibitory concentration testing

Minimum inhibitory concentration testing for the 15 *E. faecalis* isolates confirmed high-level resistance to aminoglycosides, as well as resistance to bacitracin, chloramphenicol, fluoroquinolones, erythromycin, tetracycline, and trimethoprim-sulfamethoxazole (Table 3.3). Aminoglycoside resistance was especially common, with 14/15 isolates displaying high-level resistance to streptomycin, 7/15 isolates resistant to neomycin, and 4/15 isolates with high-level resistance to gentamicin. No resistance to vancomycin, linezolid or daptomycin was identified among isolates. Five isolates (#1, #2 #4, #9 and #11) displayed an elevated meropenem MIC (8 μg/ml) compared to ATCC 29212 (4 μg/ml). No CSLI susceptibility breakpoint for meropenem has been established for *E. faecalis* ; however, 8 μg/ml is within the previously reported MIC_{90} [75, 76]. Isolates #6, #7, #11, and ATCC 29212, possessed MICs to linezolid (4 μg/ml) above the CLSI breakpoint of $\leq$2 μg/ml. Previous literature suggests these isolates fall within the MIC_{90} range for the enterococci, and should be classified as intermediate resistant [77, 78].

Antimicrobial (µg/ml)	*E. faecalis* Isolate ID[d]															ATCC 29212	CLSI[f] Susceptible Breakpoints
	1	4	9	10	13	14	15	2	3	6	7	8	11	12	5		
Ampicillin	2	2	2	2	2	2	2	4	2	4	2	2	4	2	1	2	≤8
Bacitracin	8	16	16	16	16	16	16	**>128**	**>128**	**>128**	**>128**	**>128**	**>128**	**>128**	8	16	NA
Ceftriaxone[a]	>128	>128	>128	>128	>128	>128	>128	128	64	>128	>128	>128	>128	>128	128	>128	IR
Chloramphenicol	**64**	**64**	**>128**	**64**	**64**	**64**	**64**	**32**	**32**	**32**	**64**	**32**	**32**	**32**	**64**	4	≤8
Ciprofloxacin	**>16**	**>16**	**>16**	**>16**	**>16**	**>16**	**>16**	0.5	1	1	1	1	1	1	**16**	0.5	≤1
Daptomycin	2	1	2	1	1	1	1	1	0.5	1	1	1	2	1	0.5	1	≤4
Enrofloxacin	**>16**	**>16**	**>16**	**>16**	**>16**	**>16**	**>16**	**0.5**	**1**	**0.5**	**1**	**0.5**	**1**	**1**	**16**	0	NA
Erythromycin	**>64**	**>64**	**>64**	**>64**	0.25	**>64**	**>64**	**64**	**64**	**>64**	**64**	**>64**	**>64**	**>64**	**>64**	**1**	≤0.5
Gentamicin[a,b]	**>2048**	**>2048**	**>2048**	**>2048**	16	**32**	16	**32**	16	**32**	**32**	**32**	**64**	**32**	16	16	**Low-Level IR**; HLAR: >500
Linezolid	2	2	2	2	2	2	2	2	2	**4**	**4**	2	**4**	2	2	**4**	≤2
Meropenem	**8**	**8**	**8**	4	4	4	4	**8**	2	4	4	4	**8**	4	1	4	NA
Neomycin[a,b]	**128**	64	**256**	**256**	**128**	**256**	**128**	**>2048**	**>2048**	**>2048**	**>2048**	**>2048**	**>2048**	**>2048**	64	64	**Low-Level IR**; HLAR: NA
Streptomycin[a,b]	**>2048**	**2048**	**2048**	**2048**	**>2048**	**>2048**	**>2048**	**>2048**	**>2048**	**>2048**	**>2048**	**>2048**	**>2048**	**>2048**	64	64	**Low-Level IR**; HLAR: >1000
Tetracycline	**128**	**>128**	**>128**	**>128**	**128**	**>128**	**>128**	**64**	**64**	**64**	**64**	**64**	**64**	**64**	**>128**	**32**	≤4
Vancomycin	1	2	2	2	2	2	2	2	1	2	2	2	2	2	0.5	2	≤4
Trimethoprim-sulfamethoxazole[a]	>32	>32	>32	0.125	0.064	0.25	0.25	0.064	0.094	0.125	0.064	0.064	0.125	0.094	0.012	0.047	**IR**
Amoxicillin-clavulanic acid[c]	1.5	1.5	1	1	1	1	1	1.5	1.5	1.5	1.5	1	1.5	1.5	0.5	1	NA
Sequence Type	4							55							330	30	
CRC antimicrobial use[e]	G	T-PB	G	G	T-PB	None	None	None	T-PB	BNP	BNP; G	BNP; G	T-PB	T-PB	T-PB		

[a] Intrinsic resistance is known for these antimicrobials
[b] High-level aminoglycoside resistance (HLAR) is indicated by boxes
[c] MIC determined via Etest
[d] Isolate resistance, aside from known intrinsic resistance (IR) and HLAR is indicated by red shading with bold text; isolate MIC values exceeding ATCC 29212 are indicated in blue shading with bold text.
[e] G = gentamicin sulfate 0.3%; T-PB = oxytetracycline 5mg/g-polymyxin B 10,000U/g; BNP = bacitracin zinc 400U/g-neomycin sulfate 5mg/g-polymyxin B 10,000U/g
[f] Clinical and Laboratory Standards Institute Antimicrobial Susceptibility Testing Standards; NA = not available

Table 3.3: Minimum Inhibitory Concentration (MIC) via Broth Microdilution and Etest Results for Macaque Chamber *E. faecalis* Isolates as Compared to ATCC *E. faecalis* 29212. Sequence types and historical recording chamber antimicrobial exposure are indicated for each macaque isolate.

3.4.2 Sequencing and annotation

Multi-locus sequencing typing (MLST) identified three sequence types present among the 15 isolates (Table 3.3). Most were either ST4 (N=7) or ST55 (N=7), and a single isolate (isolate #5) was identified as ST330. Proteome predictions identified 260, 221 and 208 unique proteins encoded by isolates #1 (ST4), #12 (ST55) and #13 (ST4), respectively, not included in those encoded by vancomycin-sensitive *E. faecalis* ATCC 29212 (ST30). The complete dataset may be found at `https://doi.org/10.1371/journal.pone.0169293.s004`.

The vast majority (359/691) of these genes were annotated as hypothetical and most likely reside on mobile elements. Mobile element related genes identified included transposases, type III restriction-modification system proteins, phage proteins, transcriptional regulator proteins, and others, which were more abundant in the ST4 isolates than ST55. An additional distinguishing feature between the ST4 isolates and ST55 isolate is the presence in the latter of the CRISPR (clustered regularly interspaced short palindromic repeats)-*cas* (CRISPR-associated genes) system. While both ST4 isolates lacked CRISPR-*cas* genes, a type II-A CRISPR-*cas* system was identified in ST55 isolate 12, based on the presence of *cas1*, *cas2*, *csn1* and *csn2* [79].

3.4.3 Antimicrobial resistance genes

A variety of acquired antimicrobial resistance genes were identified in the genomes of isolates #1, #12 and #13 using ResFinder and PATRIC (Table 3.4). Four genes encoding resistance to aminoglycosides were identified, including *str* in ST4, *aph(3')-III* and *ant(6')-Ia* in ST55, and the bifunctional aminoglycoside-modifying enzyme *aac(6')-aph(2")* in ST4 isolate #1. Other genes noted among the three isolates included macrolide resistance genes *lsa(A)* and *erm(B)*, tetracycline resistance genes, *tet(M)*, *tet(S)*, and *tet(L)*, and the chloramphenicol resistance gene *cat*. Increased trimethoprim-sulfamethoxazole resistance was identified in ST4 isolate #1 encoded by *dfrG*. The bacitracin resistance genes *bcrA* (ATP binding domain of ATP transporter), *bcrB* (membrane-bound permease of ABC transporter) and *bcrR* (regulatory protein of the *bcrABD* operon) were identified in ST55 isolate #12 using the specialty gene finder in PATRIC [67]. Multiple sequence

alignment of the genes encoding topoisomerase IV subunit A *(parC)* and DNA gyrase subunit A *(gyrA)* revealed single amino acid polymorphisms in *parC* codon 80 (Ser to Ile) in *gyrA* codon 83 (Ser to Ile) in both ST4 fluoroquinolone-resistant isolates as compared to the less fluoroquinolone-resistant ST55 isolate #12 and ATCC 29212. No single amino acid polymorphisms were detected in topoisomerase IV subunit B *(parE)*.

Antimicrobial (µg/ml)	Isolate Id [c]				Relevant Resistance Genes Identified[d]
	1	13	12	ATCC 29212	
Bacitracin	8	16	**>128**	16	*bcrA*, *bcrB*, *bcrR* (isolate 12)
Chloramphenicol	**64**	**64**	**32**	4	*cat* (all isolates)
Ciprofloxacin	**>16**	**>16**	1	0.5	*parC* (S80I) and *gyrA* (S83I) mutations (isolates 1 and 13)
Enrofloxacin	**>16**	**>16**	1	0.25	*parC* (S80I) and *gyrA* (S83I) mutations (isolates 1 and 13)
Erythromycin	**>64**	0.25	**>64**	**1**	*ermB* (isolates 1 and 12), *lsa(A)* (all isolates and 29212)
Gentamicin[a]	**>2048**	16	**32**	16	*aac(6')-aph(2")* (isolate 1)
Neomycin[a]	**128**	**128**	**>2048**	64	*aph(3')-III* (isolate 12)
Streptomycin[a]	**>2048**	**>2048**	**>2048**	64	*str* (isolates 1 and 13), *aph(3')-III* and *ant(6)-Ia* (isolate 12)
Tetracycline	**128**	**128**	**64**	**32**	*tetM* (all isolates and 29212), *tetL* (isolates 1 and 13), *tetS* (isolate 12)
Trimethoprim-sulfamethoxazole[b]	**>32**	0.064	0.094	0.047	*dfrG* (isolate 1)
Sequence Type	4	4	55	30	

[a] High-level aminoglycoside resistance (HLAR) is indicated by boxes

[b] MIC determined by Etest

[c] Isolate resistance, aside from known intrinsic resistance and HLAR, is indicated by red shading with bold text; isolate MIC values exceeding ATCC 29212 are indicated in blue shading with bold text.

[d] Assembled genomes were uploaded to ResFinder with a 98% threshold for gene identification and a minimum length of 60%. The PATRIC specialty gene finder tool was used to identify *bcrABR* genes. Multiple sequence alignment was performed in PATRIC to identify amino acid polymorphisms conferring fluoroquinolone resistance.

Table 3.4: Selected Antimicrobial Resistance MIC Results, and Resistance Genes Identified from Whole Genome Sequence Data

3.4.4 Virulence factor and biofilm formation-associated genes

Genes encoding virulence factors from isolates #1 (ST4), #12 (ST55) and #13 (ST4) were identified using VirulenceFinder and the specialty feature tool in PATRIC (Table 3.5). Genes associated with the cytolysin toxin (*cylA, cylB, cylL* and *cylM*) were identified in both ST4 isolates. Many genes associated with biofilm formation were identified, including aggregation substance (*agg*), enterococcal surface protein (*espfs*), endocarditis and biofilm-associated pili genes (*ebpA, ebpB, ebpC*), collagen adhesion precursor (*ace*), gelatinase toxin (*gelE*) and sortase (*srtA*). The ST4 isolates possessed more biofilm-associated factors compared to ST55 isolate #12, which lacked aggregation substance and gelatinase. Because of this finding, we further hypothesized that ST4 isolates would produce more biofilm than ST55 isolates and performed biofilm assays to evaluate this hypothesis. Other virulence factors identified included sex pheromone-associated genes (*cad, cCF10, camE, cOB1*), the cell wall adhesion expressed in serum gene (*efaAfs*), the enterococcal Rgg-like regulator gene associated with macrophage persistence (*ElrA*), hyaluronidases (*hylA, hylB*), and the thiol peroxidase gene to protect against oxidative stress (*tpx*) (Table 3.5) [80, 81, 82, 83, 84, 85, 86, 87].

		ST4		ST55	ST30
Virulence Factor Function[c]	**Gene**	**Isolate 1**	**Isolate 13**	**Isolate 12**	**ATCC 29212[d]**
Collagen adhesin precursor	*ace*	+	+	+	+
Aggregation substance	*agg*	+	+	-	+
Endocarditis and biofilm-associated pili genes	*ebpA*	+	+	+	+
	ebpB	+	+	+	+
	ebpC	+	+	+	+
Cell wall adhesin expressed in serum	*efaAfs*	+	+	+	+
Enterococcal surface protein	*esp*	+	+	+	-
Gelatinase toxin (metalloendoprotease)	*gelE*	+	+	-	+
Sortase A	*SrtA*	+	+	+	+
Cytolysin (hemolysin-bacteriocin)	*cylL*	+	+	-	+
Post-translational cytolysin modification	*cylM*	+	+	-	+
Transport of cytolysin	*cylB*	+	+	-	+
Activation of cytolysin	*cylA*	+	+	-	+
Sex pheromone	*cad*	+	+	+	+
Sex pheromone cAM373 precursor	*camE*	+	+	+	+
Sex pheromone	*cCF10*	+	+	+	+
Sex pheromone	*cOB1*	+	+	+	+
Enterococcal Rgg-like regulator	*ElrA*	+	+	+	+
Hyaluronidase	*hylA*	+	+	+	+
	hylB	-	-	+	-
Thiol peroxidase (oxidative stress resistance)	*tpx*	+	+	+	+

[a] Assembled genomes were uploaded to ResFinder with a 95% threshold for gene identification and a minimum length of 60%. https://cge.cbs.dtu.dk/services/VirulenceFinder/

[b] The PATRIC Specialty Gene Finder tool was used to confirm virulence factors following annotation.

[c] Genes associated with biofilm production are designated with blue shading and bolded text and genes associated with cytolysin toxin production are designated with red shading and bolded text.

[d] Genome was obtained from GenBank accession CP008816.

Table 3.5: Acquired Virulence Factor Genes Identified Using VirulenceFinder[a] and PATRIC[b]. Blue shading indicates genes associated with biofilm-formation; red shading indicates the cytolysin-hemolysin operon

3.4.5 Biofilm production

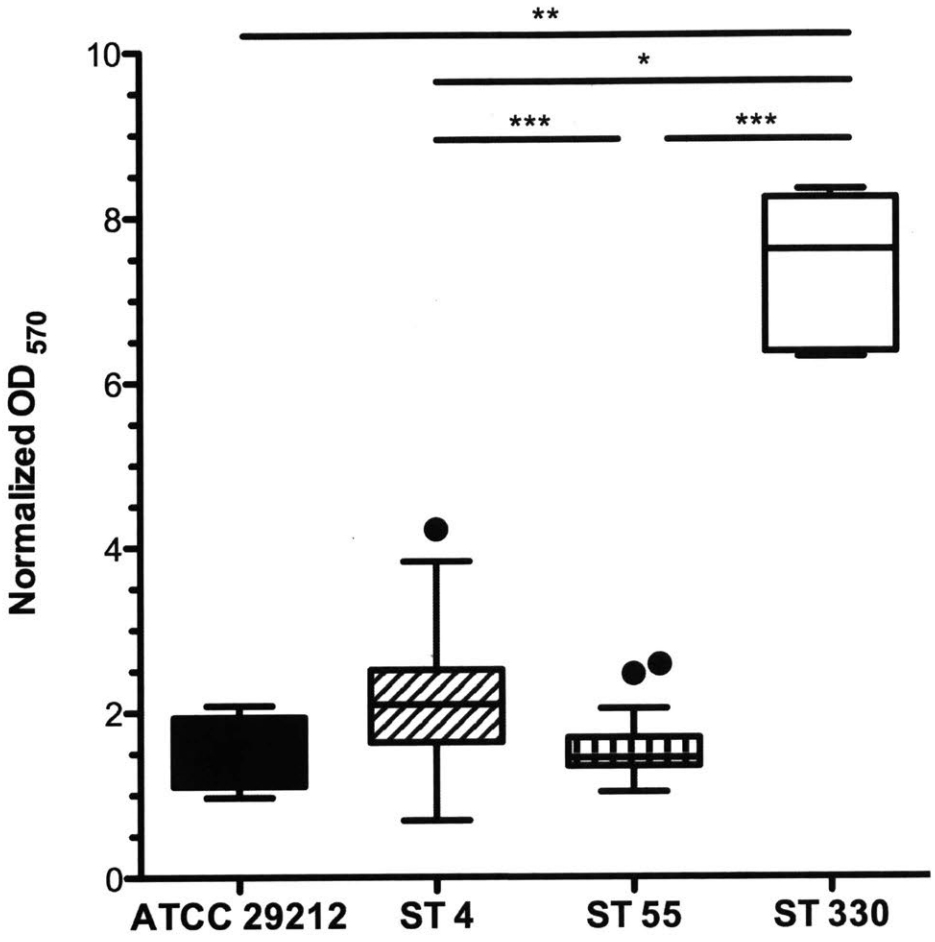

Figure 3-2: 24 hour Biofilm Production for 15 *E. faecalis* Isolates Assessed by Crystal Violet Staining. ST4 and ST330 isolates produce significantly more biofilm than ST55 isolates. Mean normalized OD_{570} for pooled data were 2.016 $\pm$ 0.016 for ST 4 isolates, 1.500 $\pm$ 0.2942 for ST55 isolates, 8.191 $\pm$ 0.1489 for the ST330 isolate and 1.894 $\pm$ 0.1833 for the ATCC 29212 control strain.

Significant differences in biofilm production, as measured by crystal violet binding, were noted among the *E. faecalis* isolates (Figure 3-2), $P < 0.0001$, Kruskal-Wallis with Dunn's Multiple Comparison). The ST330 isolate was a robust biofilm former, producing more biofilm than the ST4, ST55 isolates, or control ATCC *E. faecalis* 29212 (Figure 3-2). Flow cell assays also revealed that ST55 isolate #12 exhibited a biofilm-deficient phenotype when

compared to ST4 isolates #1, and #13, and ST330 isolate #5 (Figure 3-3). Interestingly, ST 4 isolate #13 showed a hyper-biofilm phenotype compared to all other isolates tested (Figure 3-3).

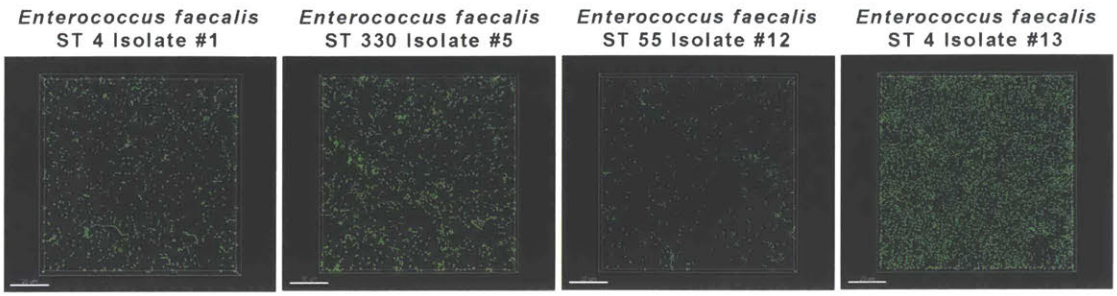

Figure 3-3: Biofilm Growth of *E. faecalis* in Flow Cell Chambers. Attached cells grown in flow cell chambers for 43 h were stained green with SYTO-9, and visualized at 63X magnification. Images are representative for each isolate.

3.5 Discussion

As previously mentioned, human enterococcal infections are often associated with implanted materials, including central venous catheters, urinary catheters, biliary stents, and endodontic implants [88, 89, 90, 91]. In this study, our *E. faecalis* isolates were isolated from chronic CRCs, and are also likely associated with biofilm. Most isolates belonged to two multi-drug resistant sequence types and we identified a variety of resistance genes and virulence genes from representative sequenced whole genomes.

3.5.1 Antimicrobial resistance

Minimum inhibitory concentration testing via broth dilution was elected to both confirm initial Kirby-Bauer disk diffusion results and quantify the magnitude of resistance. There were some discrepancies between disk diffusion and MIC results; specifically, disk diffusion suggested some isolates displayed resistance to ampicillin, amoxicillin-clavulanic acid and vancomycin. MIC testing found all isolates to be below the resistant breakpoint for ampicillin (8 μg/ml) and vancomycin (4 μg/ml). While no CLSI resistance breakpoint is noted for amoxicillin-clavulanic acid, all isolates and

the ATCC control strain 29212 had an MIC between 0.5-1.5 μg/ml. Discrepancies between disk diffusion classification and MIC susceptibilities may be attributed to failure to record disk diffusion results at exactly 24 hours, or error in agar inhibitory zone measurement.

Antimicrobial resistance profiles obtained by MIC and Etest related well to antimicrobial resistance genes identified from representative whole genome sequence data (Table 3.4). Gentamicin MIC profiles also matched well, but not perfectly, with a history of gentamicin exposure. Specifically, *E. faecalis* isolates #1, #7, #8, #9 and #10 (5/15 isolates; 33%) were isolated from macaques #1, #16, #18 and #19 with a history of gentamicin sulfate administration into their recording chambers. While ST4 isolates #1, #9 and #10 display high-level gentamicin resistance (HLGR), ST55 isolates #7 and #8 from macaque #16 lacked HLGR. The *aac(6')-aph(2")* gene has previously been established to confer HLGR, which is supported by the differences in MIC between HLGR ST4 isolate #1 (>2048 μg/ml) and non-HLGR isolate #13 (16 μg/ml) [92]. The presence of the *aac(6')-aph(2")* gene was confirmed to be in close proximity to genes encoding plasmid recombination enzymes in ST4 isolate #1. The acquisition of such mobile-element-derived genes may be inhibited by an intact CRISPR-*cas* system, which was identified in ST55 isolate #12 [93]. Additionally, both ST4 and ST55 isolates display high-level streptomycin resistance, and ST55 isolates also demonstrate increased resistance to neomycin. The presence of high-level aminoglycoside resistance is significant because it abolishes synergistic treatment with the combination of an aminoglycoside and cell-wall inhibitor [92, 94].

The plasmid-derived *bcrABD* operon with an upstream regulator *bcrR* has previously been identified to confer bacitracin resistance in *E. faecalis* [95]. We identified *bcrA*, *bcrB* and *bcrR* in ST55 isolate #12 with 89%, 89% and 94% homology, respectively, to previously reported bacitracin resistance genes [95]. Previous mutagenesis experiments have established that the *bcrD* gene encoding undecaprenol kinase is not required for high-level bacitracin resistance [95]. While macaque #8 (ST55 isolate #12) did not have a history of bacitracin exposure, triple-antibiotic ointment containing bacitracin was used within chambers for macaques #15 and #16 (isolates #6, #7 and #8). Use of triple-antibiotic ointment is the hypothesized source of selective antibiotic pressure in our macaque colony.

Multiple genes conferring resistance to tetracyclines were identified, in-

cluding both ribosomal protection genes and genes encoding efflux pumps [96]. Macaques #5, #6, #8 and #9, from which *E. faecalis* isolates #3, #4, #5, #11, #12 and #13 were identified, had a history of exposure to combination oxytetracycline-polymyxin B ointment inside recording chambers (Figure 3.3). Isolates #4, #5 and #13 displayed a higher MIC ($\geq$128 μg/ml) than isolates #3, #11 and #12, suggesting that the *tetL* gene may be responsible for conferring increased tetracycline resistance as compared to tetS and tetM. Two single amino acid polymorphisms previously identified to confer fluoroquinolone resistance were observed in genes encoding DNA gyrase subunit A (*gyrA*) and topoisomerase IV subunit A (*parC*) in both ST 4 isolates sequenced [97, 98]. Enrofloxacin is the most commonly used fluoroquinolone in our colony and has been administered systemically both perioperatively, and therapeutically for clinical cases of wounds or suspected meningitis. Macaque #3 had chamber exposure to dilute enrofloxacin but *E. faecalis* was not isolated from the chamber of this individual.

3.5.2 Biofilm formation and virulence factors

The ability of the enterococci to form biofilms contributes to the pathogenicity of implant-associated infections, as mature biofilms allow *E. faecalis* to withstand antimicrobial agents at 10-1000-fold greater concentrations than those required to control planktonic bacteria (cells living free-floating in liquid culture) [99]. We identified virulence factor genes associated with biofilm formation including aggregation substance (*agg*), enterococcal surface protein (*esp*), adhesion of collagen from *E. faecalis* (*ace*), gelatinase (*gelE*), endocarditis and biofilm-associated pili genes (*Ebp*) and sortase A (*SrtA*) [86, 100, 101, 102, 103]. ST4 isolates produced significantly more biofilm than ST55 isolates. Interestingly, one ST330 isolate formed a robust static biofilm, and additional genetic analysis will be needed to relate this phenotype to genotype (Figure 3-2). Whole genome sequencing of representative strains showed that ST55 isolate #12 lacked both *agg* and *gelE*, which were present in ST4 isolates. Nevertheless, we cannot attribute increased biofilm production by ST4 to the presence of *agg* and *gelE*, as the *agg*- and *gelE*-positive ATCC 29212 *E. faecalis* strain showed no significant differences in biofilm-forming ability compared to either ST4 or ST55 isolates. It is probable that increased biofilm production by ST4 and ST330

isolates, compared to ST55 isolates, is polygenic in nature, as multiple genes including *esp*, *agg*, *gelE*, and *srtA* have been individually shown to contribute to biofilm formation [104, 105, 106, 107].

As well as genes associated with biofilm formation, we identified the presence of genes encoding the cytolysin toxin in both ST4 isolates sequenced. The cytolysin toxin has been shown to increase the lethality of infection in multiple species, including mice, rabbits and humans, and can act synergistically with aggregation substance to increase lethality of infection in a rabbit endocarditis model [108, 109]. Due to the rarity of confirmed *Enterococcus*-associated implant complications we cannot definitively assess how ST4 isolates bearing the cytolysin toxin contribute to pathogenicity in macaques with chronic implants.

3.5.3 Translation to the human hospital environment

Our macaque colony models an environment with many similarities to humans possessing indwelling devices in a long-term care facility. Macaques are housed in a high-density environment, with approximately 12 animals per housing room. Human intensive care units (ICUs) vary in size, but recent reports have suggested a median ICU bed density in the range of 12-30 beds [110, 111]. Similar to a mixed-population ICU, macaques are housed in a mixed population, and surgically naïve individuals and individuals with cephalic implants of varying duration can be pair-housed or housed in close proximity within the same room. Besides topical antimicrobial exposure inside recording chambers, macaques in our vivarium are exposed to systemic antimicrobial therapy during the perioperative period and when clinically indicated, such as prophylactic treatment for wounds resulting from an altercation with a conspecific. This chronic intermittent antimicrobial exposure provides a selective pressure for antimicrobial-resistant isolates to emerge, as well as provide a niche for intestinal overgrowth and permit breakdown of colonization resistance [112]. MIC testing suggests that our *E. faecalis* isolates remained susceptible to ampicillin, amoxicillin-clavulanic acid, vancomycin, daptomycin and meropenem. Vancomycin, daptomycin and meropenem are not used in our facility, and will continue to be excluded, as these are last-resort antimicrobials to be used for treating human infections. Finally, chronic cephalic implants serve as a nidus for

biofilm formation and persistent infection. A variety of bacterial species, including *Staphylococcus*, *Enterococcus*, and *Corynebacterium* spp. have been previously cultured from the skin margins of macaque cephalic implants [51, 113]. As discussed in Section 2.6.4, bacterial colonization most likely arises from the translocation of skin flora or oral flora. Examination of taxonomy bar charts from Chapter 2 identified that *Enterococcus* was present in low abundance at all sampling sites, but contributed to a higher percent of sample reads in oral and skin samples vs. feces (Table 3.6).

Site	Mean	Std. Dev	Minimum	Maximum
CRC	0.0787045	0.2915644	0	1.2773723
Skin	0.0916014	0.1762231	0	0.57471264
Oral	0.01001632	0.0243759	0	0.10303377
Feces	5.4992E-05	0.0190803	0	0.00079777

Table 3.6: Percentage contribution of *Enterococcus* spp. to sample reads of microbiota samples from Chapter 2. Samples were rarefied to 1000 sequences.

Because of the parallels between the macaque colony under study and a human hospital environment, it is not surprising to see similarities in identified pathogens. Specifically, the main two *E. faecalis* sequence types, ST4 and ST55, detected in the macaque population have been previously identified as agents of human infection [114, 115, 116, 117]. These finding support the use of using implanted macaques to model the epidemiology of *E. faecalis* over time.

3.6 Long-term colonization dynamics of *E. faecalis* in CRCs over time

Analysis of 2011 antimicrobial resistance data highlighted the importance of refining CRC sanitization procedures and improving antimicrobial stewardship. As previously mentioned in Section 2.2.4, major updates were introduced to routine CRC sanitization protocols in September, 2014. For our next study, our goals were to identify the impact of these changes on the dominant *E. faecalis* lineages colonizing implanted macaques, and to examine how *E. faecalis* persists in CRCs of implanted research macaques

over time spans as long as seven years. Specifically, for macaques with persistent CRC colonization, we wanted to determine if there were changes in sequence types, antimicrobial resistance profiles, biofilm production, or other genetic changes conferring increased growth or survival after updated implementation of CRC sanitization protocols. This next section will examine how *E. faecalis* sequence types changed over time in the macaque colony and evaluate hypotheses for our findings.

3.6.1 Animals

Ten rhesus macaques (*Macaca mulatta*; 8 males, 2 females) with cephalic implants were sampled. Macaque cohort and implant parameters are listed in Table (3.7). All macaques were housed in an AAALAC-International accredited facility under standards outlined by the 8th edition of the *Guide* [19]. Briefly, husbandry parameters included a 12:12 light-dark cycle, a diet of commercial primate biscuits (Purina 5038) supplemented with fruits, vegetables, nuts and cereal. Macaques were pair-housed, with exceptions for animals showing incompatibility with conspecifics. Macaque CRC and implant margin samples were obtained from chair-restrained macaques during routine implant sanitization procedures. Briefly, the chamber was opened and a sterile polyester-tipped applicator swab (Puritan Medical Products, Guilford, ME) was used to gently sample the chamber and exudate present. Implant margin swabs were obtained by application of the swab around the base of the CRC acrylic and/or the restraint pedestal. The MIT Committee on Animal Care (CAC) approved all study procedures. Macaques remained on study for the purpose of their CAC-approved cognitive neuroscience research protocol. No macaques were euthanized for the purposes of this study, but three macaques were euthanized for medical reasons with intravenous sodium pentobarbital (86 mg/kg, Fatal Plus, Vortech Pharmaceuticals, Dearborn, MI). Macaque #6 was euthanized for seizures, macaque #25 for meningitis and retro-orbital abscessation (culturing *S. aureus*, *E. faecalis*, *Fusobacterium nucleatum*, and *Prevotella* spp.), and macaque #46 as a result of surgical complications. Macaques #1, #8, #26, and #50 were euthanized at their research endpoint. We also compared genomic data between macaques #9 and the 2011 isolate from macaque #1. To our knowledge, CRC sanitization procedures after Septem-

ber, 2014 followed updated guidelines and no antimicrobials were used inside CRCs post-2014 for macaques included in this study. Animals and isolates are listed in Figure 3-4

Animal ID	Study ID	Isolate Source	Sex	Year of Birth	Year of Arrival	Year Implanted	Number of CRCs	Implant materials[a]	CRC Antimicrobials, Packing Materials, Sanitization Solutions Prior to 2014[b]	Euthanasia Date
1	A1	CRC	F	1996	2000	06/2006	1	Delrin, PMMA, ceramic screws	G, no packing material, PI, saline	01/2015
6	B3	CRC	M	1998	2006	4/2008	3	Ultem, PMMA, titanium screws	T-PB, non-woven sponge balls, HP, PI, CHX, saline	03/2015
8	B5	CRC	M	1998	2006	11/2008	2	Ultem, PMMA, titanium screws	T-PB, non-woven sponge balls, HP, PI, CHX, saline	08/2016
9	B6	CRC	M	1998	2007	4/2011	3	Ultem, PMMA, titanium screws	T-PB, non-woven sponge balls, HP, PI, CHX, saline	NA
25	D6	abscess	M	2005	2006	06/2013	1	CILUX, PMMA, ceramic screws	No antimicrobials, petroleum jelly, CHX, saline	11/2013
26	A4	CRC	F	2009	2016	10/2016	1	Ultem, PMMA, ceramic screws	NA	06/2017
27	E1	CRC	M	2008	2011	6/2016	1	PEEK, PMMA, titanium straps and screws	NA	NA
47	B16	CRC	M	2007	2010	3/2016	1	Ultem, PMMA, titanium screws	NA	3/2016
48	E7	restraint pedestal	M	2007	2012	9/2014	NA	Titanium	NA	NA
49	E8	restraint pedestal	F	2009	2013	12/2015	NA	Titanium	NA	NA
50	B17	restraint pedestal	M	1997	2006	06/2007	NA	Titanium	NA	06/2016

[a]PMMA = polymethylmethacrylate bone cement

[b]G = gentamicin sulfate 0.3%; T-PB = oxytetracycline 5mg/g-polymyxin B 10,000U/g; HP = hydrogen peroxide, PI = povodone iodine, CHX = chlorhexidine solution

Table 3.7: Demographics of macaques for long-term *E. faecalis* colonization study

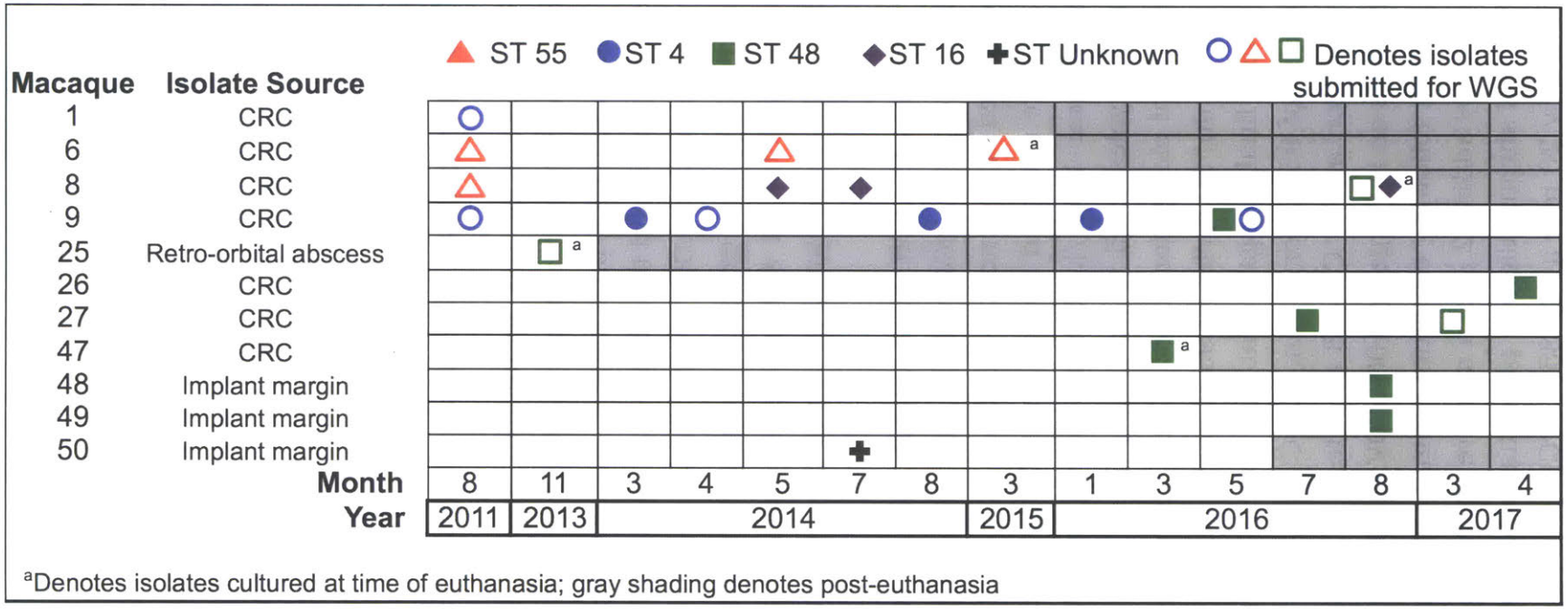

Figure 3-4: Sequence types of E. faecalis isolates collected from research macaques between 2011 and 2017. ST is designated by colored symbol with each row representing an individual macaque. Gray shading indicates timepoints after euthanasia date.

3.6.2 Bacterial isolation

Swabs were plated on tryptic soy agar (TSA) with 5% sheep blood and incubated overnight at 37°C in 5% CO_2. When necessary, subcultures onto phenylethyl alcohol blood agar and/or bile esculin azide agar were used to facilitate isolation of colonies from Gram-negative species. Colonies that grew on bile esculin azide and/or with a visual appearance consistent with *Enterococcus* (light gray, alpha-hemolytic, catalase-negative) were selected for further isolation.

3.6.3 DNA extraction, PCR and MLST

Crude DNA extraction for 16S sequencing was performed by collecting colonies with a 1μl disposable loop into 200μl of a solution containing 5% chelex-100 resin and 0.02% proteinase K. Samples were heated at 56°C for 1 hour, briefly vortexed, and then heated at 95°C for 10 minutes. Samples were then centrifuged at 10,000 $\times$ g for 3 minutes and stored at -20°C until use. Genomic DNA was extracted from overnight broth cultures using a commercially available kit with enzymatic lysis, as previously described in section 3.3.3. DNA was eluted in 10mM Tris-HCl, 0.5mM EDTA and pH 9.5 buffer.

Polymerase chain reaction (PCR) amplification of 16S rRNA gene, MLST housekeeping genes, *tetS*, *tetM*, *aph-IIIa*, and *aac-6'-aph-2"* were performed using primers listed in Appendix B [63, 64, 118, 119, 120]. PCR primers for *mutL* and *str* were designed using Primer-BLAST (`https://www.ncbi.nlm.nih.gov/tools/primer-blast/`). Thermocycler parameters used: *mutL*: 95 °C for 4 min, 35 cycles of 95 °C for 1 min, 58 °C for 45 seconds, 72 °C for 1 minute and final elongation at 72 °C for 8 minutes; *tetS*, *str*, and *aph-IIIa*: 95 °C for 5 min, 30 cycles of 95 °C for 1 min, 57 °C for 1 min, 72 °C for 1 minute and final elongation at 72 °C for 8 minutes; *tetM*: 95 °C for 5 min, 30 cycles of 95 °C for 1 min, 52 °C for 1 min, 72 °C for 1 minute and final elongation at 72 °C for 8 minutes. PCR bands were separated by electrophoresis on a 1% gel at 100-120V for 30-40 minutes and visualized with UV light following ethidium bromide staining. PCR products (5 μl) were purified by adding 2 μl of a mixture containing 0.4 U/μl exonuclease I and 0.4 U/μl shrimp alkaline phosphatase and incubated for 20 min at 37°C followed by 20 min at 80-85°C. PCR products were submitted for

sequencing at a commercial laboratory (Quintara Biosciences, Cambridge, MA). Enterococcal sequence types were identified by using the *E. faecalis* MLST website (`http://pubmlst.org/efaecalis`) [65].

3.6.4 Whole genome sequencing, assembly and annotation

E. faecalis genomic DNA from macaques #6, #9, #25 and #27 were sequenced on a single SMRT cell per isolate using a Pacific Biosciences RS2 sequencer at the University of Massachusetts Deep Sequencing Core Facility (Worcester, MA). *E. faecalis* genomic DNA from macaque #8 was sequenced using an Illumina MiSeq at the MIT Biomicro Center. PacBio DNA libraries were prepared for sequencing with the SMRTbell Template Prep Kit 1.0 and the DNA/Polymerase Binding Kit P6 v2, according to manufacturer instructions (Pacific Biosciences, Menlo Park, CA). *E. faecalis* genomic DNA from macaque #8 was concentrated using Agencourt AMPure XP beads at a 1.8x ratio, and eluted in 10 mM Tris-HCl, pH 8.5 buffer to remove EDTA from the DNA sample. The bacterial DNA library was prepared using the Qiaseq FX DNA library kit (Qiagen) with 1μg of DNA per manufacturer's instructions. Fragmentation of DNA was performed at 32°C for 4 min. AMPure XP beads were used to perform library purification as indicated in the Qiaseq FX DNA library kit manual. Barcoded and adapter-ligated DNA libraries were pooled with other DNA libraries. Quality control prior to sample loading included both sizing Illumina libraries with the Advanced Analytical Fragment Analyzer and quantifying libraries with qPCR performed using KAPA SYBR FAST qPCR Master Mix (KM4114) on a Roche LightCycler 480 II. 2x300 base paired end reads were generated on an Illumina MiSeq using a MiSeq Reagent Kit v3 (Illumina). PacBio Genomes were assembled using the Hierarchical Genome Assembly Process (version 3.0) workflow hosted on the SMRT Portal 2.3. Reads, coverage and annotation are found in Table 3.8. Illumina genome assembly was performed using the spades tool on the Pathosystems Resource Integration Center (PATRIC) website, version 3.5.2 [67]. Annotation on assembled genomes was performed using the RAST tool kit on the PATRIC website, version 3.5.2 [67]. Genes encoding antimicrobial resistance and virulence factors were identified using ResFinder, VirulenceFinder and the PATRIC database specialty

genes features [67, 68, 69]. Identification threshold parameters were set at 98% identity over a minimum length of 60% for ResFinder, and 95% identity over a minimum length of 60% for VirulenceFinder.

Macaque	#1	#6			#9		#8		#25	#27
ST	4	55			4		55		48	
WGS Technology	Pacbio	PacBio			PacBio		PacBio	Illumina	Pacbio	
Isolate Date	Aug 2011	Aug 2011	May 2014	Mar 2015	Aug 2011	May 2016	Aug 2011	Aug 2016	Nov 2013	Mar 2017
Genome size	3044487	3011796	3024067	3037432	2983064	2986755	3015699	2806131	2919427	2920131
Total Reads	87196	83861	92116	81501	88233	65930	86533	1807478	95407	86807
Contigs	3	2	2	3	2	5	3	19	2	2
N50	24838	17828	13530	16398	15312	7003	24224	364769	15106	16627
Average Reference Coverage	327.48	257.05	211.55	226.35	239.31	74.75	338.83	142.19	269.22	260.61
Number of Genes Annotated	2962	2941	2946	2995	2881	2907	2939	2670	2786	2775
NCBI Accession Number	MCFU00000000	QFYO00000000	QFYN00000000	QFYM00000000	MCFW00000000	QFYL00000000	MCFV00000000	QFYJ00000000	QFYK00000000	QFYI00000000

Table 3.8: Whole genome sequencing metadata

3.6.5 Antimicrobial susceptibility testing

Minimum inhibitory concentrations (MICs) for selected antimicrobial agents were determined by the broth microdilution method in Cation-adjusted Mueller Hinton Broth as recommended by the CLSI breakpoints (M07-A9, M100-2D) [121, 122]. All antibiotics used for broth microdilution were purchased from Sigma-Aldrich Chemical Company (St Louis, MO). *E. faecalis* strain ATCC 29212 and 51299 were used as standard reference strains. MICs were performed at least three times on separate experimental days. For the purposes of this study, intrinsic aminoglycoside resistance was defined for MICs <500 μg/ml for gentamicin, <1000 μg/ml for streptomycin and <1000 μg/ml for neomycin. For povidone-iodine, a 10% solution (Triadine, Triad Group Inc, Hartland, WI) was diluted with cation-adjusted Mueller Hinton broth to test concentrations of 2.5% to 0.0098%. MICs were recorded 24 hours following incubation. To determine the minimum bactericidal concentration for povidone-iodine, 5μl from selected wells spanning the MIC were spotted onto 5% sheep blood TSA. Following overnight incubation at 37°C in 5% CO_2, spots were examined for positive or negative growth.

3.6.6 Variant analysis

The variant analysis service on the PATRIC website was used for variant identification using the BWA-mem aligner and FreeBayes SNP caller. For macaque #6, filtered subreads from *E. faecalis* strains isolated in May 2014 and March 2015 were individually compared to the 2011 isolate. For macaque #9, filtered subreads from strains isolated in April 2014 and May 2016 were individually compared to the 2011 isolate. To examine inter-macaque variation, filtered subreads from the 2011 ST55 isolate from macaque #8 were compared to the 2011 ST55 isolate from macaque #6, the 2011 ST4 isolate from macaque #9 were compared to the 2011 ST4 isolate from macaque #1, and the 2017 ST48 isolate from macaque #27 was compared to the 2013 ST48 isolate from macaque #25. During genome analysis, it was determined that the genome of the April 2014 ST4 isolate from macaque #9 was likely mixed, thus it was excluded from subsequent genome sequence-based analyses. Variant filtering was performed to exclude variants with <50% frequency, covered by fewer than 10 reads, or

those found in genes with three or more variants called, due to the possibility of mapping errors or recombination events. Putative *de novo* variants are archived at `https://figshare.com/s/a7dc6538f8c0ff2ae216`.

3.6.7 Biofilm analysis

Biofilm production was assayed using the crystal violet method as previously described in Section 3.3.5, with minor modifications [72]. Briefly, 5μl of overnight *E. faecalis* culture were inoculated into 195μl of tryptic soy broth supplemented with 1% glucose, in replicates of 6-12 in a 96-well plate. Following 22-24 hours of static incubation at 37°C, the OD_{600} was measured to determine overnight colony growth using a microtiter plate spectrophotometer (Epoch, Biotek Instruments, Inc., Winooski, VT). Biofilm staining was performed as previously described in Section 3.3.5. Biofilm production was normalized to bacterial growth by dividing OD_{570} by the OD_{600}, and the normalized OD_{570} values were used for statistical analysis.

3.6.8 Daptomycin kill cuve

Time-kill curves with daptomycin were performed according to previously published protocols [123]. Briefly, 10ml aliquots of cation-adjusted Mueller Hinton Broth with 50 μg/ml $CaCl_2$ were inoculated with 5 colonies of macaque #6 ST55 isolates from 2011, 2014 and 2015, Macaque #9 ST 4 isolates from 2011, 2014 and 2016 and the ATCC control strain 29212. After isolates reached a McFarland standard of 0.5, 0.1ml were added to flasks containing 10ml fresh Mueller Hinton broth with 0, 1, 2, 4, and 8 μg/ml daptomycin. Samples for OD_{600} and spot dilutions were collected at 0, 2, 4, 6, 8 and 24 hours after inoculation. Following overnight incubation at 37°C, colonies were enumerated and kill curves plotted.

3.6.9 Protein alignments

Mutant diacylglycerol kinase amino acid sequences were submitted to Phyre2 [124] to generate predicted structures and aligned to DgkB from *S. aureus* in PyMol version 2.0.7 [125].

3.6.10 Mutagenicity assay

Mutagenicity was determined with slight modifications to previous protocols [126]. 50-125μl of overnight *E. faecalis* culture in brain heart infusion broth was plated onto BHI agar impregnated with 50 μg/ml of rifampicin in replicates of 3-5 plates. To determine the concentration of the overnight inoculum, serial dilutions of the overnight culture inoculum were spotted onto TSA with 5% sheep blood (Remel). Colonies were enumerated following overnight incubation at 37°C in 5% CO_2 and the concentration of the plated inoculum was determined. The mutation frequency was calculated as follows:

μ = # of rifampicin-resistant colonies/inoculum plated

3.6.11 Phage induction

Overnight cultures of ST48 isolates from macaques #8, #25, the 2017 isolate from macaque #27, and #47 and were adjusted to an OD_{600} of approximately 0.15 in duplicate, in 3ml of fresh brain heart infusion broth (BHI) and incubated at 37°C shaking at 150 rpm for 90 minutes. Norfloxacin (3μg/ml) was added to one set of tubes and cultures were incubated for another 2.5 hours at 37°C with continued shaking. The second set of tubes was centrifuged to pellet cells and resuspended in 2ml 10mM-1mM Tris-EDTA buffer; then re-spun and resuspended in 2ml TE buffer with 1mM $CaCl_2$. The resuspended cultures were transferred to a 6-well plate and exposed to 254-nm UV light (8W bulb) for 45 seconds. 1ml of UV-exposed cultures was added to 4ml of fresh BHI with 100 mM $CaCl_2$ and incubated 37°C shaking at 150 rpm for two hours. After incubation, tubes were centrifuged and the supernatant was passed through a 0.2μ PES filter. 50μl of supernatant was mixed with 50μl of overnight donor cultures (2011 isolates from macaques 1 and 2) and incubated for 5 minutes at 25°C. 5ml of 0.25% molten BHI agar with 100mM $MgCl_2$ and 100mM $CaCl_2$ was added and 1ml was added onto 1.5% bottom BHI agar with 100mM $MgCl_2$ and 100mM $CaCl_2$ in duplicate in 6-well plates. After top agar solidification, plates were incubated at 37°C overnight and examined for plaques the following day.

3.6.12 Dessication resistance

Cultures of ST55 (2011 isolate from macaque #6), ST4 (2011 and 2016 isolates from macaque #9) and ST48 (2016 isolate from macaque #9, 2013 isolate from macaque #25 and 2017 isolate from macaque #27) were cultivated in 5 ml BHI, shaking at 37°C overnight. The overnight inoculum was serially diluted in PBS and dilutions spotted onto blood agar, as previously described, for enumeration of colonies the following day. Additionally, 2 μl aliquots were spotted on the bottom of an empty petri dish and allowed to dry under the blower of a class II biosafety cabinet for 4 days. After incubation, each spot was resuspended in 100 μl of PBS and serial dilutions were spotted onto blood agar prior to overnight incubation at 37°C. Colonies were enumerated the following day and percent recovery was calculated as follows:

$$\% \text{ recovery} = 100\% \times \frac{2\mu\text{l} \times \text{CFU/ml recovered}}{2\mu\text{l} \times \text{CFU/ml overnight inoculum}}$$

3.6.13 Growth curves

200μl of overnight cultures of 2011 and 2016 ST4 isolates from macaque #9, and ST48 isolates from macaques #6 (2017 isolate), #9, and #25 were inoculated into 10ml of fresh BHI broth and incubated at 37°C shaking at 150 rpm. At times 0, 0.5, 1, 1.5, 2, 3, 4, 5 and 6 hours post-inoculation, an aliquot of culture was removed to measure the OD_{600}. 10μl of serial dilutions of aliquots removed at times 0.5, 1, 1.5, 2, 4 and 5 hours post-inoculation, were spotted onto TSA with 5% sheep blood, incubated overnight at 37°C in 5% CO_2. Colonies were enumerated the following day and graphs of colony count and OD_{600} over time were made for each isolate.

3.6.14 ST4-ST48 co-culture experiment

Overnight cultures of ST4 (2011 and 2016 from macaque #9) and ST48 isolates (2016 from macaque #9 and 2017 isolate from macaque #27) were diluted to an OD_{600} of approximately 0.2 in fresh BHI broth. Diluted cultures were mixed together as follows: 10 ml ST 4 2011 + 10 ml ST 48 2016, 10 ml ST 4 2011 + 10 ml ST 48 2017, 10 ml ST 4 2016 + 10 ml ST 48 2016 and 10 ml ST 4 2016 + 10 ml ST 48 2017. 4 ml of mixtures and 2 ml

of individual isolates were added in duplicate to 12 well flat-bottom tissue culture plates and incubated at 37°C overnight, shaking at 150rpm. Cells were passaged daily for 5 days as follows: 40 μl was transferred to 4ml fresh BHI in an adjacent well and 1.5 ml collected for pelleting by centrifugation. DNA was extracted from pellets collected on days 1 and 5 using the DNeasy blood and tissue kit as previously described in Section 3.3.3. Quantitative PCR was performed to evaluate changes from days 1 to 5 in ST 4 and ST 48 isolates via rhamulokinase (*rhamK*) and *fsr* quorum-sensing system (*fsrB*), respectively, using primers listed in Appendix B. qPCR experiments were run using the Fast SYBR Green master mix (ThermoFisher) on an Applied Biosystems 7500 Fast Real-Time PCR system using the following thermocycler settings: 95 °C for 20 seconds, 40 cycles of 95 °C for 1 second (melt), 60 °C for 30 seconds (anneal/extend). Threshold cycles (C_t) differences between co-cultured isolates were graphed and compared to mono-cultures at days 1 and 5.

3.6.15 Statistics

Biofilm measurement data was analyzed using Bayesian estimation, implemented in the Python programming language, using PyMC3. All code and data for making the violin plots are archived online on GitHub (`https://github.com/ericmjl/mia-stats/releases/tag/mia-mbio`) and Zenodo (`https://zenodo.org/account/settings/github/repository/ericmjl/mia-stats`; DOI 10.5281/zenodo.1248852). Mutagenicity data, and dessication resistance data were analyzed using GraphPad Prism (GraphPad Software, Inc., La Jolla, CA) with $P < 0.05$ considered significant.

3.7 Results of long-term *E. faecalis* colonization study

3.7.1 *E. faecalis* isolates and sequence types

To identify the genetic lineages of *E. faecalis* colonizing research macaques, we compared the MLST of 20 strains isolated from 10 macaques over a seven-year period, to 4 strains isolated in 2011 (Figure 3-4). From the 10 more recently sampled macaques, we identified four dominant *E. faecalis*

sequence types: ST4, ST16, ST48, and ST55. Macaques #6 and #9 remained colonized by ST55 and ST4 strains, respectively, over the 4-5 year course of sampling. The May 2016 sample from macaque #9 was colonized by both ST4 and ST48 strains. Macaque #8, initially colonized with a ST55 strain in 2011, yielded only an ST16 strain in May and July 2014. Samples collected at the time of euthanasia of macaque #8 in August 2016 yielded both ST16 and ST48 strains.*E. faecalis* strains belonging to ST48 were first identified in our macaque colony in a sample collected from macaque #25 in November 2013. Subsequent samples from macaques #26, #27, #47, #48, and #49, show that ST48 became the predominant lineage identified in 2016 and 2017. We also identified one unknown sequence type from macaque #50. This isolate is a single locus *pstS* variant of ST594, containing the *pstS* 21 allele rather than *pstS* 12 found in ST594. Isolates from macaques #48, #49, and #50 were collected from swabs of the skin margin surrounding the CRC implant.

3.7.2 Antimicrobial susceptibility

To determine changes in antimicrobial resistance over time for ST55 and ST4 strains, and to evaluate the resistance profiles of the more recent ST16 and ST48 strains, we determined MICs for a diverse panel of antimicrobials (Tables 3.9, 3.10). ST55 isolates were susceptible to ampicillin and enrofloxacin, intrinsically resistant to gentamicin, and resistant to bacitracin, erythromycin, and tetracycline, and high-levels of streptomycin and neomycin. There were no remarkable changes in MICs in ST55 isolates from macaque #6 over a four-year period. ST4 isolates showed susceptibility to ampicillin, bacitracin, and erythromycin, intrinsic gentamicin resistance, and resistance to enrofloxacin and tetracycline, and high-level resistance to streptomycin. The only change in MICs noted for ST4 isolates over the five year sampling period was an increase in neomycin resistance, from 128 μg/ml in the 2011 isolate to 256 μg/ml in the April 2014 isolate, and a further increase to 2048 μg/ml in the 2016 isolate. ST16 isolates displayed susceptibility to ampicillin and bacitracin, resistance to enrofloxacin and erythromycin, and high-level aminoglycoside resistance, including high-level gentamicin resistance. ST48 isolates expressed fewer resistances, showing susceptibility to ampicillin, bacitracin, enrofloxacin, erythromycin

and tetracycline, and only intrinsic aminoglycoside resistance (Table 3.10). We also examined the effectiveness of povidone-iodine and evaluated both minimum inhibitory concentrations and minimum bactericidal concentrations. The MIC for povidone-iodine for all ST4, ST48 and ST55 isolates was 0.3125%, and the minimum bactericidal concentration was 0.625%.

	Macaque ID						
	6			9			CLSI Resistance Breakpoint (µg/ml)
Isolate Date	Aug 2011	May 2014	March 2015	Aug 2011	April 2014	May 2016	
Sequence Type	55			4			
Antimicrobial	(µg/ml)						
Ampicillin	1-2	1	1	1-2	1	1	≤16
Bacitracin	>128	>128	>128	8-16	4	8	NA
Enrofloxacin	1	1	1	64	64	64	NA
Erythromycin	>64	>64	>64	0.25	0.25	0.5	≥8
Gentamicin	16-64	32	32	8-16	16	16-32	Low level IR; HLAR >500
Neomycin	>2048	>2048	>2048	128	256	2048	Low level IR; HLAR NA
Streptomycin	>2048	>2048	>2048	>2048	>2048	>2048	Low level IR; HLAR >1000
Tetracycline	64	64	64	128-256	256	256	≥16
Povodone-Iodine	0.3125%	0.3125%	0.3125%	0.3125%	0.3125%	0.3125%	NA

Table 3.9: Minimum inhibitory concentration testing in ST55 and ST4 *E. faecalis* strains over time isolated from macaques #6 and #9

	Macaque ID												
	25	47	9	27	8	48	49	27	26	8			CLSI Resistance Breakpoint (µg/ml)
Isolate Date	Nov. 2013	March 2016	May 2016	July 2016	Aug. 2016	Aug. 2016	Aug. 2016	March 2017	April 2017	May 2014	July 2014	Aug. 2016	
Sequence Type	48									16			
Antimicrobial	(µg/ml)												
Ampicillin	1	2	1	1	2	1	2	1	1	0.5	1	1	≤16
Bacitracin	16	16	8	16	16	16	8	16	16	4	8	8	NA
Enrofloxacin	1	1	1	1	2	1	2	0.5	1	32	32	64-128	NA
Erythromycin	0.25	0.25	0.25	0.25	0.25	0.25	0.25	0.125	0.125	>64	>64	>64	≥8
Gentamicin	8	16	16	16	128	32	8	16	16	>2048	>2048	>2048	Low level IR; HLAR >500
Neomycin	256	128	64	128	512	128	64	128	64	>2048	>2048	>2048	Low level IR; HLAR NA
Streptomycin	128	128	64	64	128	64	64	128	64	>2048	>2048	>2048	Low level IR; HLAR >1000
Tetracycline	2	2	2	2	2	2	1	1	0.5	256	128	256	≥16
Povodone-Iodine	0.3125%	0.3125%	0.3125%	0.3125%	0.3125%	0.3125%	0.3125%	0.3125%	0.3125%	0.3125%	0.3125%	0.3125%	NA

Table 3.10: Minimum inhibitory concentration testing in ST48 and ST16 *E. faecalis* strains

3.7.3 Antimicrobial resistance genes

Genome sequences were examined to identify antimicrobial resistance genes present in ST4, ST55, and ST48 strains, and to determine if there were changes in antimicrobial resistance genotypes over time in sequential isolates from the same macaque. Known antibiotic resistance genes were identified employing ResFinder and the specialty gene tool on the Pathosystems Resource Integration Center (PATRIC) [68, 67]. Antimicrobial resistance genes identified in the genome sequences are displayed in Table 3.11. All sequenced ST55, ST4 and ST48 isolates possessed the *lsa(A)* gene encoding an ABC-efflux pump; however, only ST55 isolates displayed phenotypic resistance to erythromycin [127]. Erythromycin resistance in ST55 isolates therefore is most likely attributable to the uniquely occurring plasmid-encoded *ermB* identified in ST55, but not in ST4 or ST48 isolates. The tetracycline resistance of ST55 and ST4 isolates could be attributed to chromosomal *tetM* and *tetS* genes found in the ST55 strains, and plasmid-encoded *tetL* and *tetM* genes detected in the ST4 strains. Selected PCR on the May 2014 ST16 isolate confirmed the presence of *tetM* and *tetS* as the likely origin for tetracycline resistance in this strain. Both ST4 and ST55 isolates possessed the chloramphenicol acetyltransferase gene *cat* on a plasmid; while we did not assess chloramphenicol MICs on new isolates, we previously confirmed chloramphenicol resistance in the 2011 ST4 and ST55 isolates (Figure 3.3). Plasmid-encoded aminoglycoside resistance genes identified included *ant(6)-Ia* and *aph(3')-III* in ST55 isolates, *str* in ST4 isolates, and *ant(6)-Ia* in ST48 isolates. Marked neomycin resistance in ST55 isolates was most likely due to the *aph(3')-III* gene, while high-level streptomycin resistance likely resulted from *str* and *ant(6)-Ia genes* [128]. PCR was used to confirm the presence of *str*, *aph-IIIa*, and *aac-6'-aph-2"* in the May 2014 ST16 isolate from macaque #8, with high-level gentamicin resistance most likely conferred by the aac-6'-aph-2" gene [128]. Fluoroquinolone resistance, (i.e. enrofloxacin), typically arises from mutations in DNA supercoiling enzymes. We confirmed the stable persistence of previously identified mutations in topoisomerase IV (*parC*) and DNA gyrase subunit A (*gyrA*) 3.4. Additionally, deletion of 16bp upstream of a MATE family efflux pump was identified in the 2016 ST4 strain, which might explain the increased neomycin resistance observed in this lineage over time.

Macaque ID		6			9		8		25	27
ST		ST 55			ST 4		ST 16[a]	ST 48	ST 48	
Antimicrobial Resistance	**Gene**	**Aug 2011**	**May 2014**	**Mar 2015**	**Aug 2011**	**May 2016**	**May 2014**	**Aug 2016**	**Nov 2013**	**Mar 2017**
Macrolides/ Lincosamides	*lsa(A)*	+	+	+	+	+	NA	+	+	+
	erm(B)	+	+	+	-	-	NA	-	-	-
Tetracycline	*tet(L)*	-	-	-	+	+	NA	-	-	-
	tet(M)	+	+	+	+	+	+	-	-	-
	tet(S)	+	+	+	-	-	+	-	-	-
Bacitracin	*bcrABR*	+	+	+	-	-	NA	***bcrA* only**	***bcrA* only**	***bcrA* only**
Chloramphenicol	*cat*	+	+	+	+	+	NA	-	-	-
Aminoglycoside	*str*	-	-	-	+	+	+	-	-	-
	ant(6)-Ia	+	+	+	-	-	NA	+	+	+
	aph(3')-III	+	+	+	-	-	+	-	-	-
	aac-6'-aph-2"	-	-	-	-	-	+	-	-	-
Fluoroquinolone	*parC*	-	-	-	**S82I**	**S82I**	NA	-	-	-
	gyrA	-	-	-	**S84I**	**S84I**	NA	-	-	-

[a]Determined by PCR
NA = not assessed

Table 3.11: Antimicrobial resistance genes identified by whole genome sequencing and PCR from selected *E. faecalis* strains

3.7.4 Virulence factor genes and biofilm production

We examined previously identified (Table 3.5) virulence factors in the strains that were sequenced (Table 3.12). Profiles were largely similar across strains, with variability noted in the presence of aggregation substance *agg*, gelatinase *gelE*, serine protease *sprE*, the quorum-sensing locus *fsr*, the cytolysin operon, and the hyaluronidase *hylB*. All sequenced ST55 and ST4 strains contained the *E. faecalis* pathogenicity island, which harbored the cytolysin operon in the ST4 strains [129]. The pathogenicity island was not present in the ST48 strains that were sequenced. Phenotypically, all ST4 strains displayed beta hemolysis on sheep blood agar plates. This is presumably due to the cytolysin operon, but cannot be stated with certainty since hemolysis of ovine erythrocytes by the cytolysin is difficult to detect [130]. A plasmid-encoded bacteriocin was identified in the ST4 strains, possibly contributing to the hemolytic activity observed in this strain. Finally, no changes in virulence factor genes over time within isolates from the same macaque were observed.

Next, we examined if the ability of *E. faecalis* to persistently colonize the CRCs was associated with the ability to form biofilms, by measuring the biofilm-forming capacity of 15 strains (Figure 3-5). Posterior credible intervals from Bayesian estimation modeling identified a subtle increase over time in biofilm formation among ST55 strains from the same animal, and a more substantial increase in the 2016 ST4 isolate compared to prior isolates from the same macaque. ST48 isolates showed variable biofilm forming capabilities; however, nearly all isolates formed more biofilm than the ST55 and ST4 strains from 2011 and 2014 (Figure 3-5). This finding suggests that increased biofilm formation may have contributed to the strain succession leading to ST48 predominance following the change in maintenance sanitization protocol.

Macaque ID		6			9		25	8	27
ST		ST 55			ST 4		ST 48		
Virulence Factor Function	Gene	Aug 2011	May 2014	Mar 2015	Aug 2011	May 2016	Nov 2013	Aug 2016	Mar 2017
Collagen adhesin precursor	*ace*	+	+	+	+	+	+	+	+
Aggregation substance	*agg*	-	-	-	+	+	++	+	++
Endocarditis & biofilm-associated pili genes	*ebpA*	+	+	+	+	+	+	+	+
	ebpB	+	+	+	+	+	+	+	+
	ebpC	+	+	+	+	+	+	+	+
Cell wall adhesin expressed in serum	*efaAfs*	+	+	+	+	+	+	+	+
Enterococcal surface protein	*esp*	+	+	+	+	+	+	+	+
Gelatinase toxin	*gelE*	-	-	-	+	+	+	+	+
Serine protease	*SprE*	-	-	-	+	+	+	+	+
Sortase A	*SrtA*	+	+	+	+	+	+	+	+
Quorum-sensing locus	*fsrABDC*	-	-	-	-	-	+	+	+
Cytolysin (hemolysin-bacteriocin)	*cylL*	-	-	-	+	+	-	-	-
Post-translational cytolysin modification	*cylM*	-	-	-	+	+	-	-	-
Transport of cytolysin	*cylB*	-	-	-	+	+	-	-	-
Activation of cytolysin	*cylA*	-	-	-	+	+	-	-	-
Sex pheromone	*cad*	+	+	+	+	+	+	+	+
Sex pheremone cAM373 precursor	*camE*	+	+	+	+	+	+	+	+
Sex pheromone	*cCF10*	+	+	+	+	+	+	+	+
Sex pheromone	*cOB1*	+	+	+	+	+	+	+	+
Enterococcal Rgg-like regulator	*ElrA*	+	+	+	+	+	+	+	+
Hyaluronidase	*hylA*	+	+	+	+	+	+	+	+
	hylB	+	+	+	-	-	+	+	+
Thiol peroxidase	*tpx*	+	+	+	+	+	+	+	+

Table 3.12: Virulence factor genes identified by whole genome sequencing from selected *E. faecalis* strains

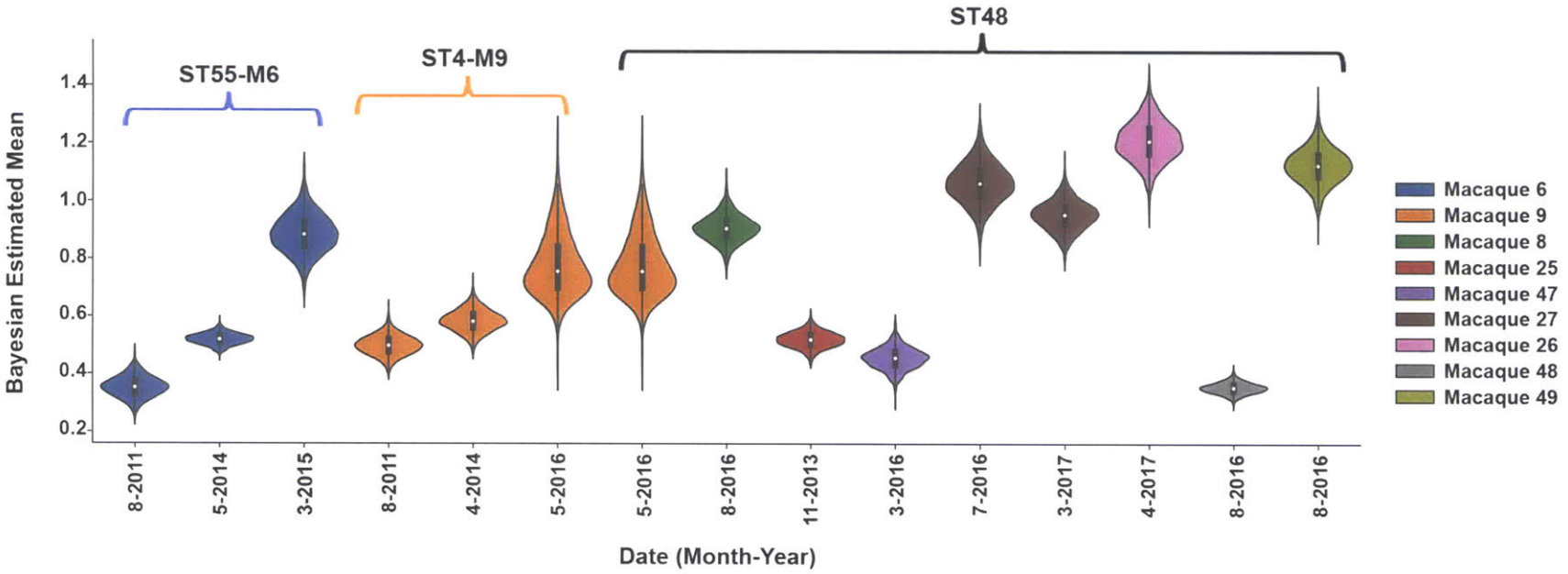

Figure 3-5: Posterior credible intervals of biofilm production from 15 *E. faecalis* strains. Biofilm was measured using a crystal violet assay [72]. Each macaque is represented in a different color with ST labeled as indicated. Experiments were performed a minimum of three times on different days using 6-12 replicates per strain. Violin plots show the Bayesian estimated posterior of mean OD_{570} readings; interquartile range is indicated by the thicker black bars inside each violin, and median is indicated by the white circle.

3.7.5 Gene and mobile element differences between strains

To identify if *E. faecalis* strains of the same ST were isogenic, we compared annotated gene lists from PATRIC. Comparison of ST55 annotated gene lists from macaque #6 between the 2011 and 2014 strains identified only one difference for a gene not annotated as hypothetical proteins (a terminase small subunit in the 2014 strain), thus these two strains could be considered isogenic. The 2015 ST55 strain from macaque #6 had multiple differences in annotated genes as compared to 2011/2014 isolates and was not considered isogenic. For ST4 strains, multiple differences in annotated genes were identified between 2011 and 2016 strains from macaque #9; thus these isolates were not isogenic. Comparison of the ST48 annotated gene lists between the 2013 isolate from macaque #25 and the 2017 isolate from macaque #27 did not reveal differences in genes annotated, therefore these two isolates could be considered isogenic. Comparison of the ST48 annotated gene lists between the 2016 isolate from macaque #8 and the 2013/2017 isolates from macaques #25 and #27 revealed multiple differences in annotated genes, thus these strains are not considered isogenic.

To understand how *E. faecalis* strains differed from one another in their mobile genetic element content both within and between macaques, we analyzed the plasmid and prophage content of all sequenced strains. All sequenced ST55 strains harbored a plasmid similar to pB of *E. faecalis* strain CLB21560 (99% identity over 74% coverage; GenBank accession CP019514.1). All sequenced ST4 strains harbored a plasmid that was similar to pEF123 of *E. faecalis* strain EF123 (99% identity over 85% coverage; GenBank accession KX579977.1). ST48 strains isolated in 2013 and 2017 both contain a presumed plasmid most closely related (97% identity over 59% coverage) to pBEE99 of *E. faecalis* strain E99 [131]; however, no known *rep* genes were identified. Sequential isolates from the same macaque displayed only minor changes in their plasmid gene contents over time, and the same plasmids from ST55, ST4, and ST48 strains were all found in more than one animal, suggesting that they were stably maintained.

In contrast to relatively stable plasmid maintenance in strains from the same ST, prophage content was found to be more dynamic between strains (Figure 3-6). The two ST55 strains isolated from different macaques in

2011 contain an identical prophage region; however, this region appeared to be duplicated in the 2014 strain and further shuffled in the 2015 strain from macaque #6 (Figure 3-6A). Separately, a prophage region detected in the ST4 strain isolated from macaque #1 in 2011 was absent from the sequenced ST4 strains of macaque #9 (Figure 3-6B). The ST48 strains contained multiple small, phage-like elements, one of which is found in all *E. faecalis* strains [132]. We evaluated the possibility that one of these elements might have contributed to the sequence type shift within the colony. This was attempted by trying to induce release of lysogenic bacteriophages from ST48 isolates and examining for their activity against ST55 and ST4 isolates. Unfortunately, neither exposure to UV light nor addition of norfloxacin succeeded at inducing a phage that would plaque on the 2011 isolates of ST55 and ST4 from macaques #6 and #9, respectively.

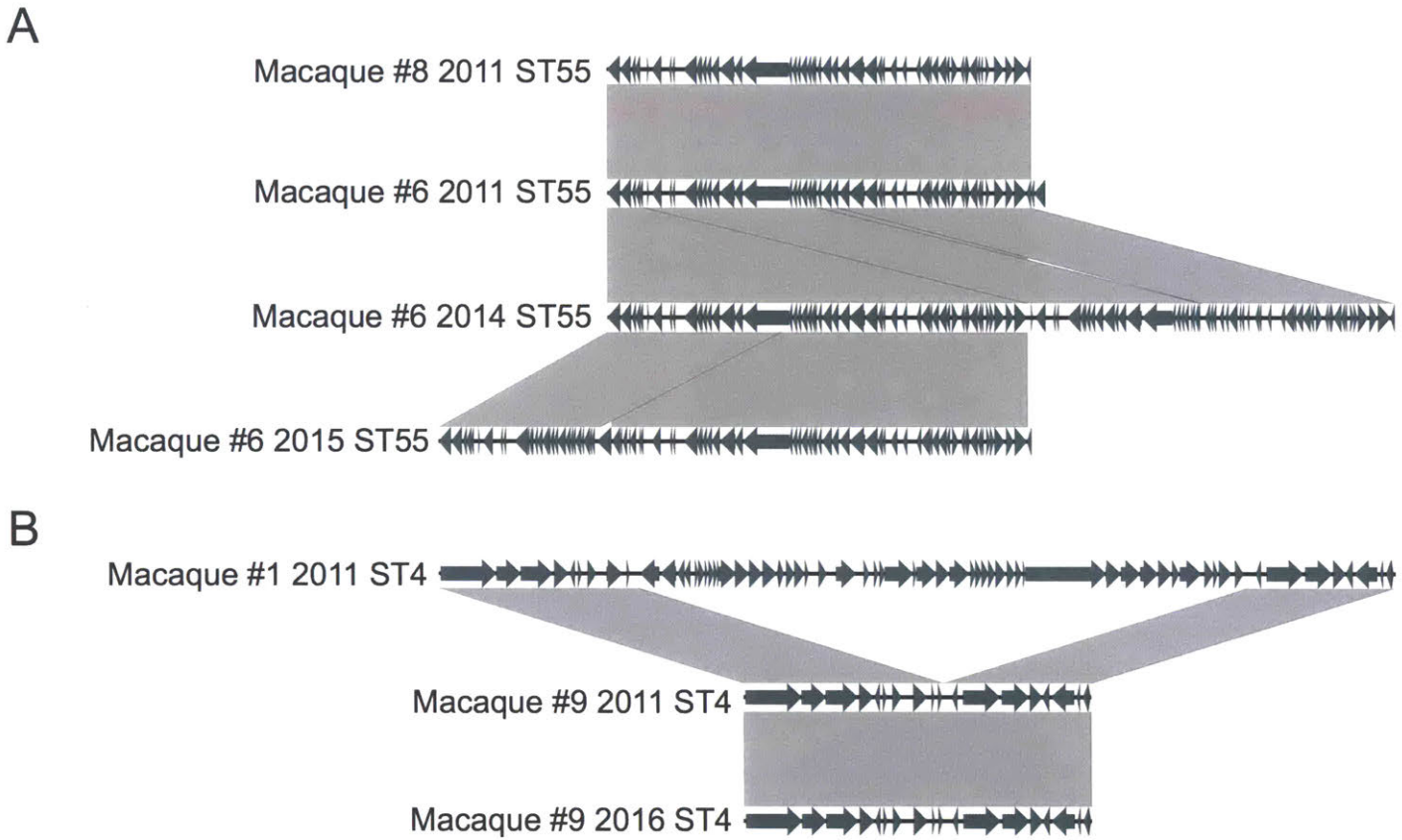

Figure 3-6: Differences in prophage content between ST55 (A) and ST4 (B) strains. Phages were compared to one another using BLAST, and plots were generated using EasyFig [133]. Grey shading indicates regions with >95% nucleotide identity)

3.7.6 Variant analysis

We next identified variants between strains of the same ST. Specifically, we evaluated for variants in genes in common between ST, or variants in genes that might affect growth, antimicrobial resistance, or survival. Classification and numbers of variants are listed in Table 3.13, and putative identified variants are archived at `https://figshare.com/s/a7dc6538f8c0ff2ae216`. Overall, ST4 isolates had a higher average number of variants detected (both within and between macaques; 44) than ST55 and ST48 isolates (23 and 28, respectively). In all cases, approximately half of all variants detected were nonsynonymous changes, with the remaining variants divided between synonymous mutations, intergenic variants, and insertion/deletion variants. Both ST4 and ST55 isolates had nonsynonymous variants identified within a transcription regulator containing a diacylglycerol (DAG) kinase domain (Figure 3-8), the phosphate transport ATP-binding protein *pstB*, and DNA mismatch repair genes (*mutL* for 2016 ST4 isolate (Figure 3-9) and *mut*S for the 2011 ST55 isolate (Figure 3-10). Mutant ST4 and ST55 DAG kinase sequences were submitted to Phyre2 to generate a structural model of each protein [124]. The top match was the DAG kinase DgkB from *S. aureus* [134]. Comparison of the ST4 mutant to the wild type *S. aureus* DgkB protein revealed that the A168S mutation was on a loop sequence and was not predicted to be located in proximity to the adenosine-diphosphate (ADP)-binding site (Figure 3-7A). Comparison of the ST55 mutant to the wild type *S. aureus* DgkB protein revealed that the T40I mutation was predicted to be approximately 4 angstroms from ADP (Figure 3-7B).

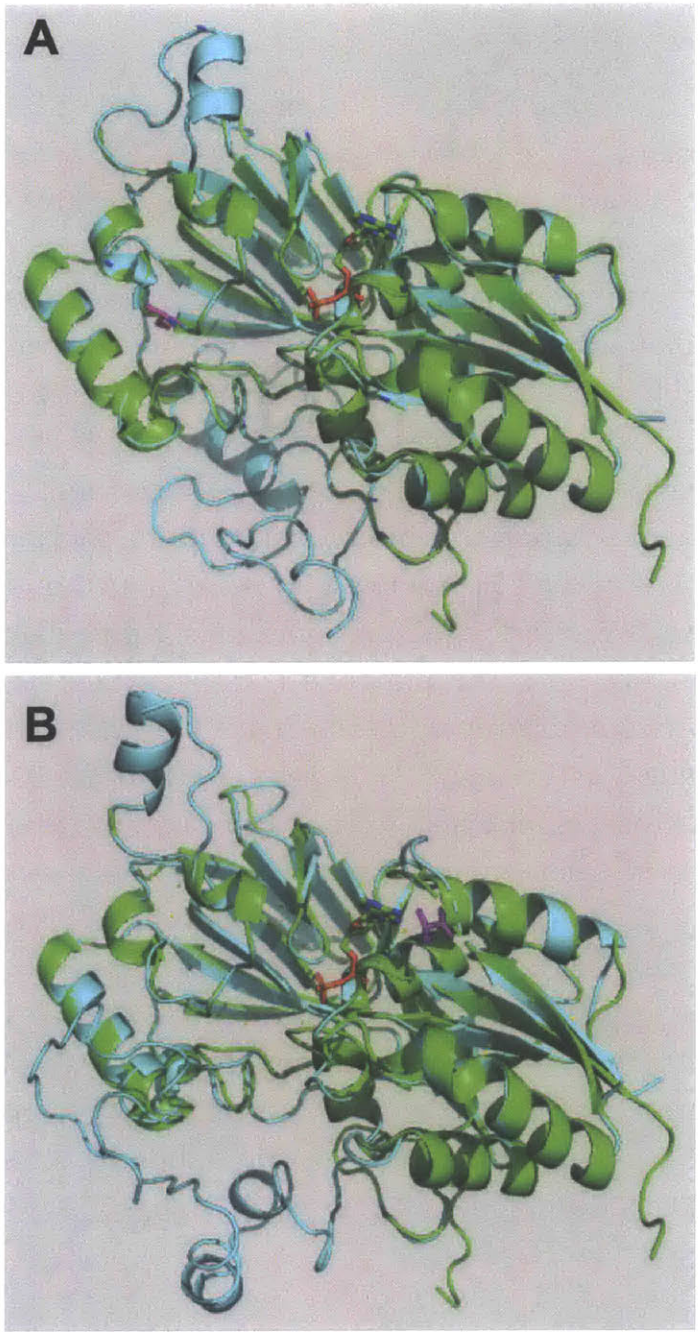

Figure 3-7: Mutant *E. faecalis* DAG kinase predicted protein structures (cyan) were aligned to the *S. aureus* DgkB predicted protein structure (green). ADP is shown as a stick figure in the binding pocket. A. ST4 mutant with A168S (magenta) is distant to the binding pocket. B. ST55 mutant with T40I (magenta) located approximately 4 angstroms from ADP.

Reference Genome	Variants	Comparison Genome		
		Macaque 6		Macaque 8
	Isolate Year	2014	2015	2011
Macaque 6 2011	**Total**	21	19	28
	Non-synonymous	12	10	13
	Synonymous	4	4	6
	Intergenic	5	5	5
	Insertions/Deletions	0	0	4

		Macaque 9	Macaque 1
	Isolate Year	2016	2011
Macaque 9 2011	**Total**	44	43
	Non-synonymous	31	26
	Synonymous	8	10
	Intergenic	5	4
	Insertions/Deletions	0	3

		Macaque 27
	Isolate Year	2017
Macaque 25 2013	**Total**	28
	Non-synonymous	16
	Synonymous	7
	Intergenic	3
	Insertions/Deletions	2

Table 3.13: Numbers and types of variants identified within and between *E. faecalis* strains

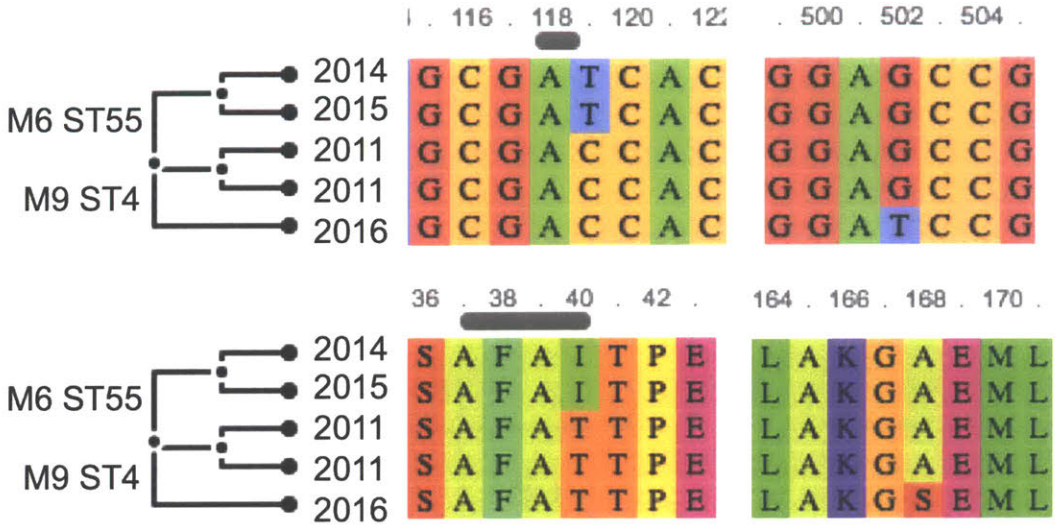

Figure 3-8: Multiple sequence alignment for nucleotide and amino acid DAG kinase sequences showing C119T/T40I in ST55 2014 and 2015 isolates and G502T/A168S in the 2016 ST4 isolate.

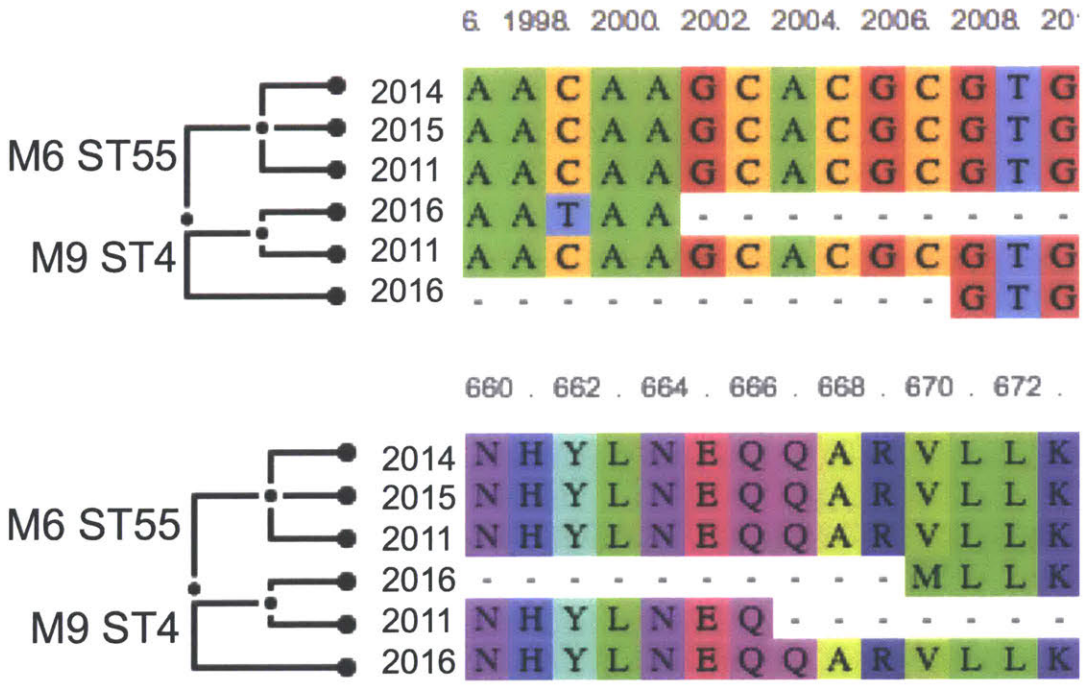

Figure 3-9: Multiple sequence alignment for nucleotide and amino acid *mutL* sequences showing C1999T/Q666* in the 2016 ST4 isolate.

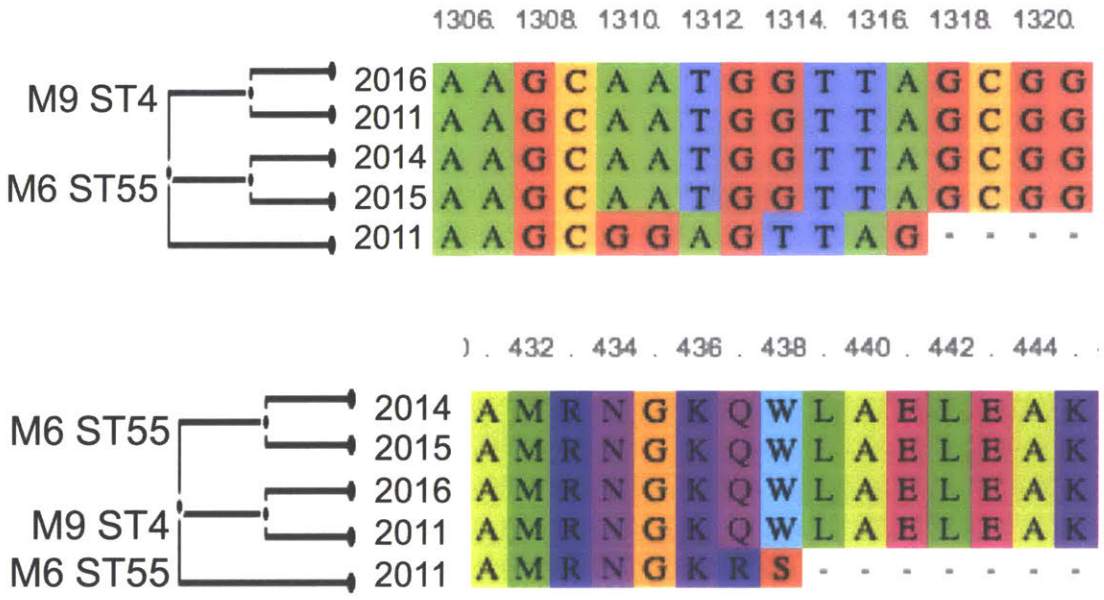

Figure 3-10: Multiple sequence alignments for nucleotide and amino acid *mutS* sequences showing a deletion leading to a framshift and nonsense mutation resulting in QWL to RS* in the 2011 ST 55 isolate.

3.7.7 Evaluation of daptomycin time-kill curves

To evaluate possible effects of the identified mutations in the DAG kinase gene we performed daptomycin time-kill curves using daptomycin at 1x, 2x, 4x and 8x the MIC (1, 2, 4 and 8 μg/ml) (as previously determined using the methods listed in section 3.3.2. We hypothesized that *E. faecalis* strains with functional mutations in DAG kinase would have impaired bacterial membrane integrity and thus, altered time-kill curves upon exposure to daptomycin. No changes in sensitivity to daptomycin at 1, 2 or 4 μg/ml were noted; isolates with DagK mutations did display delayed killing with exposure to 8 μg/ml as compared to wild-type and ATCC 29212 strains (Figure 3-11).

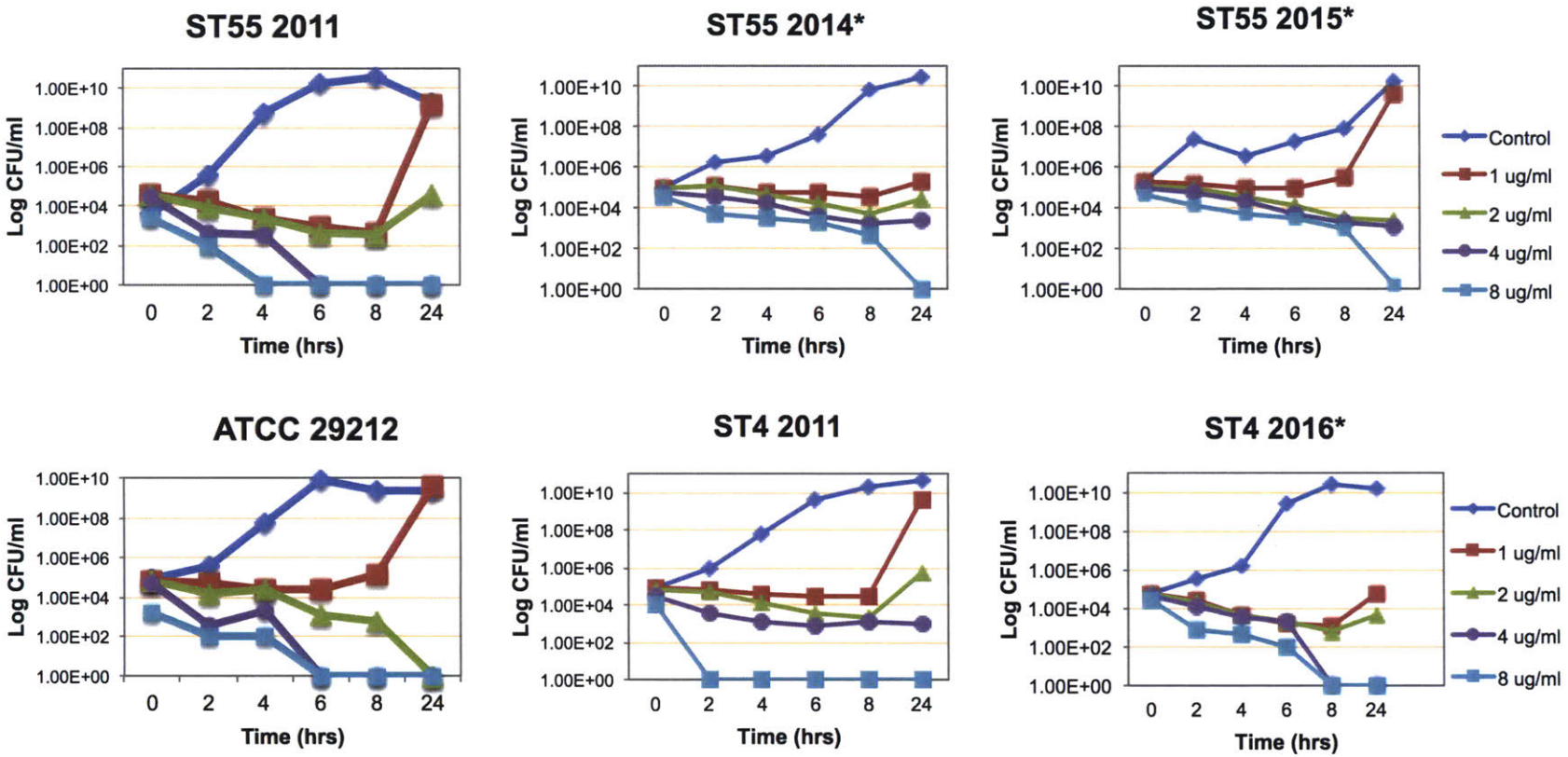

Figure 3-11: Time-kill curves for ST55 and ST4 macaque *E. faecalis* isolates and ATCC 29212. Isolates with DagK mutations are indicated with an asterisk.

3.7.8 Identification of transient hypermutator phenotype

To evaluate the effects of the identified *mutL* and *mutS* we measured mutagenicity in ST55 and ST4 strains with a standard rifampicin mutagenicity assay [126]. We hypothesized that strains with mutations in DNA mismatch repair genes might have higher spontaneous mutation rates, and confirmed a hypermutator phenotype in the 2011 ST55 isolate and the 2016 ST4 isolate (Figure 3-12). The median mutation frequencies for the 2011 ST55 isolate and 2016 ST 4 isolate were approximately 30-fold and 40-fold higher, respectively, than isolates with wild-type versions of *mutL* and *mutS* from the same macaque. Representative mutagenicity data are shown in Figure 3-12.

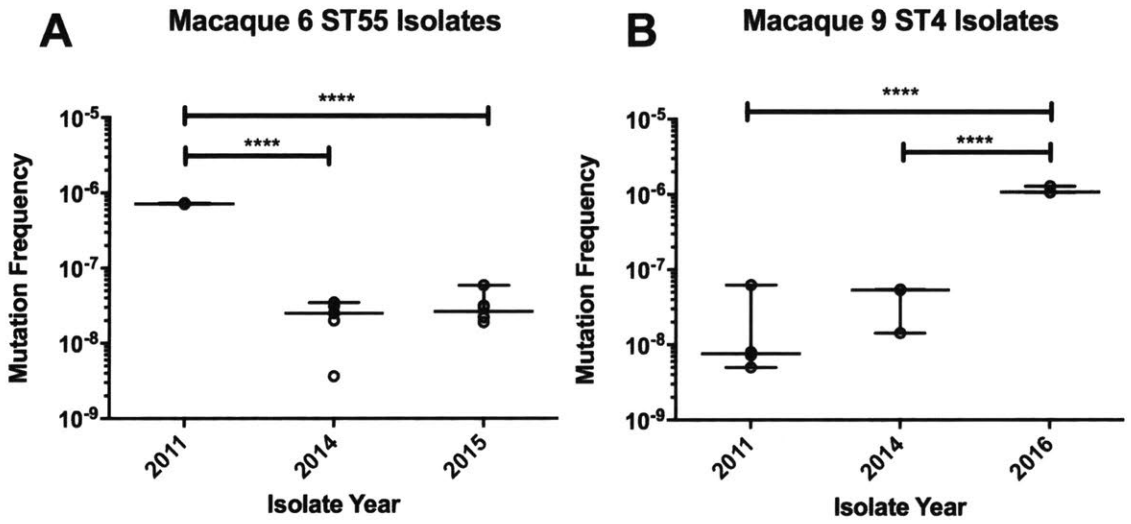

Figure 3-12: Rifampicin mutagenicity assay for ST55 and ST4 isolates over time. A. ST 55 isolates from 2011-2015 from macaque #6. B. ST4 isolates from 2011-2016 from macaque #9. Data from a representative experiment shown; bar represents sample mean. **** P<0.0001, 1-way ANOVA with Holm-Sidak's multiple comparisons test.

3.7.9 Dessication resistance

To evaluate whether ST48 success in the colony was related to increased environmental survival we performed dessication experiments to compare selected ST55, ST4 and ST48 isolates. The ST4 2016 isolate showed the

best percent recovery as compared to all other isolates tested; representative data is shown in Figure 3-13.

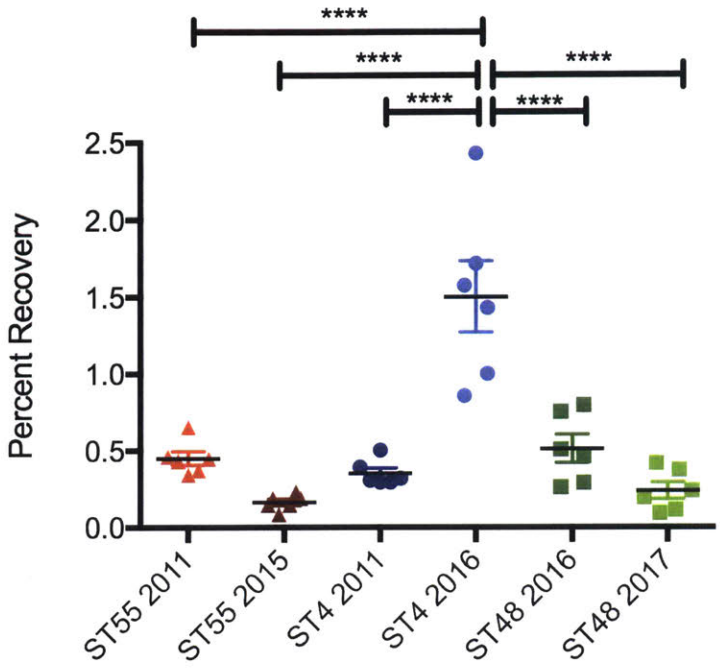

Figure 3-13: Percent recovery from dessication for selected ST4, ST55 and ST48 isolates. **** P<0.0001. One-way ANOVA with Tukey's multiple comparison test.

3.7.10 Growth kinetics and ST4-ST48 co-culture

To further evaluate competition between ST48 and ST4 isolates we evaluated growth kinetics of selected isolates. We hypothesized that ST48 success in CRCs might be related to faster growth kinetics vs. ST4 isolates. We measured growth kinetics of selected ST48 and ST4 isolates over a 6-hour period and found that ST48 isolates began the exponential growth phase more rapidly than the 2011 and 2016 ST4 isolates as measured by changes in OD_{600} (Figure 3-14). On both OD_{600} and CFU/ml curves the 2016 ST4 isolate showed delayed growth kinetics (with a right-shifted curve) as compared to all other tested isolates. When comparing CFU/ml counts for the 3 isolates from macaque #9 (2011 ST4, 2016 ST4 and 2016 ST48) we noted that the 2011 ST4 and 2016 ST48 isolates had similar concentrations at 5 hours.

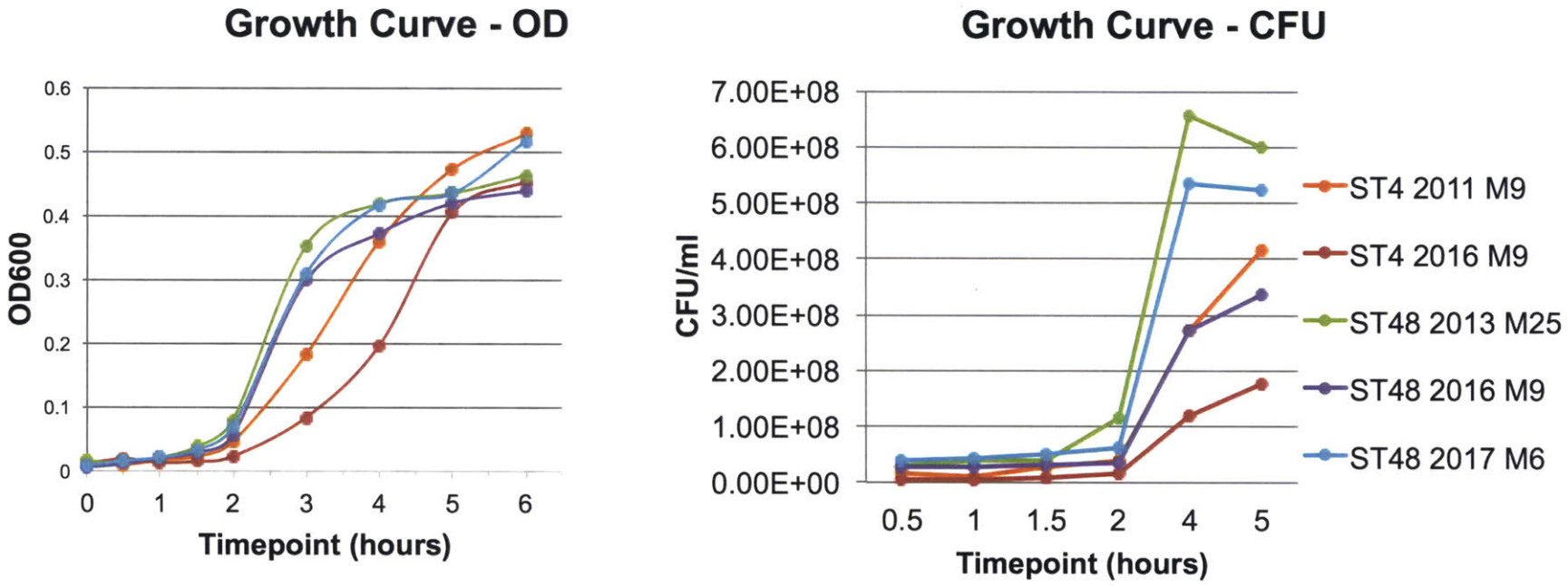

Figure 3-14: Growth curves as measured by OD_{600} and colony counts over a 6-hour period for selected ST4 and ST48 isolates

To examine competition over a longer timescale, we designed a co-culture experiment to measure relative differences in ST4 and ST48 over a 5-day period based on differential gene expression between ST using quantitative PCR. This experiment revealed that growth differences exist, but these differences varied within ST (Figure 3-15). First we compared co-cultured ST48 from macaque #9 with ST 4 isolates from 2011 and 2016. On day 5, we found a decreased amount of ST48 with a static amount of 2011 ST4, but a static amount of ST48 with a decreased amount of 2016 ST4. These findings were not replicated when co-culturing ST4 isolates from macaque #9 with an ST 48 isolate collected from macaque #27. Both the 2011 ST4 and the ST48 isolate maintained static levels at day 5 vs. day 1. When comparing the 2016 ST4 from macaque #9 with the ST48 isolate from macaque #27 we found that the initial amount of ST4 was lower on day 1, but increased by day 5, while ST48 remained stable.

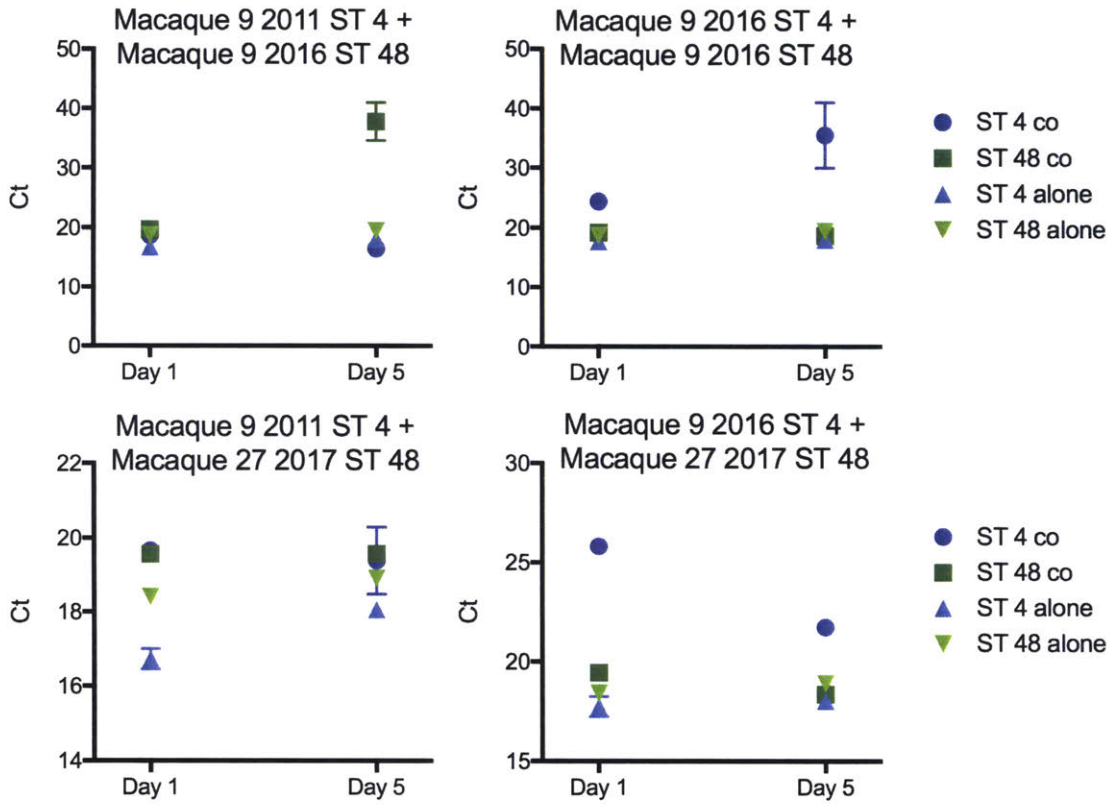

ST 4 isolate	ST 48 isolate	Relative amount ST4 Day 5 vs. Day 1	Relative amount ST48 Day 5 vs. Day 1
2011 Macaque #9	2016 - Macaque #9	Static	Decreased
2016 Macaque #9	2016 - Macaque #9	Decreased	Static
2011 Macaque #9	2017 - Macaque #6	Static	Static
2016 Macaque #9	2017 - Macaque #6	Increased	Static

Figure 3-15: Relative amounts of ST4 and ST48 at days 1 and 5 following inoculation of mono and co-cultures. Relative amounts were determined based on Ct threshold, with lower Ct values indicating larger numbers of bacteria.

3.8 Discussion

Sequential sampling of ten macaques over a seven-year time span allowed a unique opportunity to observe how *E. faecalis* persists within a polymicrobial community associated with a chronic implant. This has high relevance to human infections, where *E. faecalis* often persists on implanted medical devices such as intravascular catheters, ureteral stents, and intraocular lens materials [88, 135, 136]. Genome sequencing and phenotypic characterization uncovered two surprising findings. First, minimizing antimicrobial pressure appears to have driven the displacement of more drug-resistant strains by a less resistant, stronger biofilm-forming lineage. Second, transient hypermutator strains arose in two different ST in two different animals that were persistently colonized by the same strain.

3.8.1 Colonization patterns

Analysis of CRC cultures collected in 2011 identified 15 *E. faecalis* isolates from 11 macaques, with ST4 and ST55 as the predominant sequence types (n=7 each) (Figure 3.3). Both ST4 and ST55 have been identified among human clinical isolates [65]. Interestingly, the majority of recorded ST4 isolates were identified in samples from Asia, while ST55 strains are more commonly isolated from patients in Europe and the United States [137]. The native habitat of rhesus macaques includes a wide territory, ranging from Afghanistan to China and India [138]. While the majority of our research colony originates from primate centers located in the United States, these colonies originated from primates imported from Asia. Due to the length of time animals are present in our vivarium, it is difficult to determine whether strains colonizing macaque CRCs originated as commensal strains arriving with the macaques, or if strains were acquired after arriving at our vivarium. The relatively low diversity of strains detected and the presence of the same strain in multiple animals suggests that at least some animals became colonized at our facility.

Analysis of *E. faecalis* isolates collected since initial sampling in 2011 revealed different colonization patterns in individual animals. Macaque #6 remained colonized by the ST55 lineage from 2011 to 2015, while macaque #9 remained colonized by ST4 from 2011 to 2016, then gained ST48 prior

to August 2016 sampling. Both animals appear to have been colonized by the same strain over a 4-5 year time span, since fewer than 50 variants were observed between strains from the same animal (Figure 3.13. Strains of the same ST isolated from different animals also were very closely related to one another, suggesting that animals either transmitted strains to one another or acquired them from a common source. Macaque #8 was colonized by a ST55 strain in 2011, but subsequent sampling identified only ST16 isolates in 2014, with the addition of a ST48 strain in 2016. While a ST48 strain was first isolated in 2013 from macaque #25, our data indicate an increased prevalence of ST48 in samples collected in the 2016-2017 timeframe, coincident with the decrease of ST4 and ST55 strains in more recently implanted macaques. In the MLST database, only a single isolate of ST48 has been reported, and was identified from a fecal surveillance sample in a hospitalized patient in Spain [65].

3.8.2 Antimicrobial resistance patterns

Antimicrobial resistance within STs remained stable overall, in both genotype and phenotype, with the exception of increased neomycin resistance in ST4 over time. While we did not identify differences in antimicrobial resistance gene content within ST4, we detected a 16 bp deletion upstream of a MATE family efflux pump in the 2016 isolate that had a higher neomycin MIC. This efflux pump shows similarity to the NorM pump, which has been shown to efflux aminoglycosides [139]. We hypothesize that the observed deletion causes increased expression of the efflux pump, and thereby increases neomycin resistance. In co-colonization situations, we did not observe increases in MIC for the ST48 strain isolated from macaque #9 (co-colonized with ST4) or identify additional resistance genes in the genome of the ST48 strain isolated from macaque #8 (co-colonized with ST16).

In September 2014, CRC sanitization procedures were updated to prohibit antimicrobial use within CRCs. Removal of this selective pressure for antibiotic-resistant strains corresponded with the appearance of comparatively antibiotic susceptible ST48 isolates. Despite the standardized use of 1-2% povidone-iodine as part of routine cleaning procedures, *E. faecalis* has clearly persisted within CRCs and around the skin-implant margin of CRCs. This persistence likely arises from the inability of the disinfectant to

penetrate biofilms within the time duration of application, as the MIC and MBC for ST4, ST48 and ST55 strains are less than the current povidone-iodine concentration used (0.3125% and 0.625%, respectively). Additionally, the polymethylmethacrylate acrylic used for anchoring CRCs to the skin margin represents a likely reservoir for strains. This area is difficult to effectively sanitize with topical disinfectants, and polymethylmethacrylate has previously been demonstrated to permit *E. faecalis* biofilm formation [135].

Virulence factor genotypes remained stable over time within sequence types; however, crystal violet assays suggested an increase in biofilm production noted over time in ST4 and ST55 isolates. The 2016 ST4 isolate, in particular was found to produce significantly more biofilm than the 2011 or 2014 strains from the same animal. While no differences in virulence factor genes were observed in this strain, the increased biofilm formation in the 2016 strain could be due to one or more of the variants identified in the strain, or to a recombination event detected within the enterococcal surface protein (*esp*), a gene that has been previously shown to play a role in biofilm formation in *E. faecalis* [71]. Additionally, we determined that seven of nine tested ST48 strains were robust biofilm formers. Genome sequencing confirmed the presence of multiple biofilm-associated genes in select ST48 isolates, including the quorum-sensing operon *fsrABDC* which was not present in ST4 and ST55 isolates. The *fsrABDC* operon controls expression of the secreted proteases gelatinase (*gelE*) and serine protease (*sprE*) [103, 140, 141]. Gelatinase contributes to virulence and biofilm production via cleavage of host cell proteins to aid in surface attachment and dissemination based on bacterial density [103]. An additional difference in virulence factor gene content between strains is that ST4 isolates possessed the hemolysin-bacteriocin operon encoding the cytolysin within their pathogenicity island, which was not identified in ST48 or ST55 isolates [130]. While the presence of the cytolysin toxin has previously been established as a marker for increased virulence, morbidity, and mortality in both human enterococcal infections and animal models [142, 143, 109, 144, 145], no additional signs of disease were observed in the animal colonized with this ST4 strain.

3.8.3 Variant analysis

Analysis of single nucleotide variants (SNVs) within STs over time revealed three gene families with variants in common between ST4 and ST55 isolates: a transcriptional regulator containing a diacylglycerol (DAG) kinase domain, the phosphate transport ATP binding protein *pstB*, and DNA mismatch repair genes *mutL* and *mutS*. We first evaluated affected isolates for phenotypic effects of the identified DAG kinase mutations. DAG kinases are highly conserved enzymes among eukaryotes and prokaryotes and function in phospholipid membrane turnover processes. Specifically, DAG kinases catalyze the conversion of DAG to phosphatidic acid and prevent the lethal accumulation of DAG within the bacterial membrane [134]. Daptomycin is a cyclic lipopetide antibiotic proposed to exert its bactericidal activity via insertion and disruption of the bacterial cell membrane [146]. We hypothesized that disruption of DAG kinase functionality by the identified mutations would result in decreased DAG turnover, and increased DAG accumulation in the membrane, with a subsequent increase in membrane fragility, and thus increased susceptibility to killing by daptomycin. Analysis of time-kill curves revealed that isolates with DAG kinase mutations did not have increased susceptibility to daptomycin. In fact, we noted that mutated isolates were slightly more resistant to killing by daptomycin at 8μg/ml at 4, 6, and 8 hours as compared to their wild-type counterparts (Figure 3-11). Despite the appearance of decreased susceptibility, at 24 hours, all isolates exposed to 8μg/ml were dead. Given that there were no changes in kill-curves observed for lower daptomycin concentrations, we hypothesize that the identified DAG kinase mutations are likely insignificant in affecting functionality. Protein structural alignment of the ST4 mutated DAG kinase protein with the wild-type *S. aureus* DgkB revealed that the A168S mutation was quite distant from the ADP-nucleotide binding pocket and unlikely to cause significant functional disruption (Figure 3-7 A). Protein structural alignment of the ST55 mutated DAG kinase with the wild-type *S. aureus* DgkB predicted the T40I mutation to be approximately 4 angstroms from ADP, which is farther away then typical hydrogen bond distances of 2.7-3.3 angstroms [147] (Figure 3-7 B.)

Because hypermutator phenotypes have been observed before in infection contexts [148], we were interested in determining whether the iden-

tified *mutL* and *mutS* mutations affected strain mutagenicity. The 2016 ST4 isolate from macaque #9 was identified to have a C1999T transition in *mutL*, resulting in a Q667* nonsense mutation in the protein (Figure 3-9). The ST55 2011 isolate from macaque #6 was found to have a 10 bp deletion causing a frameshift in the *mutS* protein, resulting in mutations at protein positions 437-439 (QWL to RS*) and premature truncation of the protein (Figure 3-10). To evaluate the effects of these identified mutations, we performed rifampicin mutagenicity assays, and confirmed that the 2011 ST55 and 2016 ST4 isolates displayed a hypermutator phenotype (Figure 3-12). Previous work has evaluated the effects of mutated *mutS* and *mutL* genes in emerging antimicrobial resistance in *Enterococcus faecium* with mixed conclusions [148, 149]. While one study did not identify a hypermutator phenotype in *E. faecium* with *mutL* and *mutS* mutations in two strains that developed linezolid resistance during therapy, another case presentation described *recJ* and *mutL* mutations in a daptomycin-nonsusceptible *E. faecium* blood culture isolate from an endocarditis patient [148, 149].

We would expect that isolates with a hypermutator phenotype would be more likely to accumulate nucleotide polymorphisms. When comparing the number of variants between isolates from the same macaque, we did identify more variants when comparing the 2016 ST4 to 2011 ST4 isolate from macaque #9 (44 variants total), than between ST55 isolates from macaque #6 (21 and 19 SNVs for 2014 and 2015 isolates, respectively) (Figure 3.13). We also noticed that 90% of the variants detected in the 2016 ST4 isolate were single nucleotide polymorphisms, compared to 75-80% of variants in other comparisons. While the ST55 hypermutator phenotype did not persist, future antimicrobial therapy for macaque #9 could be complicated by the presence of the ST4 hypermutator isolate. To our knowledge, this is the first description of an *E. faecalis* isolate with a *mutL* mutation that arose *in vivo*. While limited studies have examined hypermutator *E. faecalis* strains, hypermutator phenotypes in chronic *Pseudomonas aeruginosa* infections contribute to the development of antimicrobial resistance in cystic fibrosis patients [150, 151].

3.8.4 Strain succession in *E. faecalis* within CRCs of implanted macaques

We performed several experiments to evaluate hypotheses for the success of ST48 and loss of ST4 and ST55 strains in macaques implanted with CRCs since 2014. First we evaluated the potential for strain succession caused by emergence of a lysogenic bacteriophage. Despite the presence of multiple phage elements in ST48 genomes, we were unsuccessful at inducing lytic bacteriophage from ST48 that would form plaques on ST4 and ST55 isolates. Next, we evaluated the ability of different strains to survive dessication. This hypothesis was also rejected as ST48 isolates did not demonstrate increased survival vs. other strains, and the ST4 2016 isolate demonstrated significantly more resistance to dessication (Figure 3-13). Finally, we evaluated growth kinetics of ST48 and ST4 isolates and their relative amounts at 1 and 5 days following co-inoculation in a tissue culture plate. ST48 isolates did require a shorter time to reach exponential growth in acute growth experiments than ST4 isolates; however, success over a 5-day period varied depending on the isolate. Specifically, conflicting results were observed when evaluating ST4 and ST48 isolates from macaque #9, the 2016 ST4 isolate was outcompeted by ST48 at day 5, but the relative amount of the ST48 isolate had decreased vs. the 2011 ST4 isolate at day 5. Thus, we cannot draw definitive conclusions about the success of ST48 based on growth kinetics alone. The effects of potential synergy or antagonism between *E. faecalis* strains and other members of the polymicrobial CRC community are another possible factor in strain succession and are challenging to evaluate experimentally.

3.9 Conclusions

This chapter has provided insights into how different *E. faecalis* lineages have both persisted and been displaced by other ST within polymicrobially-contaminated CRCs in research macaques over a seven-year period. Overall, our data suggest that improved antimicrobial stewardship has allowed less-resistant, more robust biofilm-forming ST48 *E. faecalis* strains to predominate in newly implanted macaques, over the previously identified more-resistant *E. faecalis* strains characterized from 2011 CRC cultures. In two

macaques monitored sequentially since 2011, ST48 strains were able to colonize in a polymicrobial milieu of CRCs that were previously colonized with strains belonging to other, more drug-resistant STs. We have also demonstrated that *E. faecalis* strains can persistently colonize CRCs, with little change in antimicrobial resistance, and that the ability to form biofilms likely contributes to this persistence. Because of the importance of biofilm formation in *E. faecalis* pathogenicity, the remaining chapter will evaluate alternative techniques for treating *E. faecalis* biofilms.

Chapter 4

Evaluation of alternative strategies to treat *E. faecalis* biofilm

4.1 Introduction

In Chapter 3 we discussed the extensive antimicrobial resistance noted in ST4 and ST55 *E. faecalis* strains isolated from macaque CRCs. As previously discussed in section 3.8, the ability to form biofilm contributes to the pathogenicity of *E. faecalis* by allowing strains to coat medical devices, and withstand 10-1000x antimicrobial concentrations compared to planktonic cultures [99, 152, 153]. Biofilms are composed of cells encased in a matrix of secreted polysaccharides, proteins, extracellular nucleic acids and lipids, sometimes collectively termed "extracellular polymeric substance" [152]. Because biofilm is hypothesized to be an essential factor for the persistence of *E. faecalis* inside and around macaque CRCs, we wished to evaluate alternative strategies for treating biofilm. Specifically, we were especially interested in evaluating strategies to target biofilm formed by multi-drug resistant *E. faecalis* isolates, as this has particular relevance for human hospital-acquired isolates.

4.2 Trends in antimicrobial development and the current antimicrobial crisis

The 2013 Antibiotic Resistance Threats report by the Centers for Disease Control and Prevention estimated that there were over 2 million illnesses and 23,000 deaths caused by antibiotic resistance [154]. Despite the growing trend of antimicrobial resistance, only two new antimicrobial classes (linezolid and daptomycin) have been released since the year 2000 (Figure 4-1). Additionally, the appearance of resistant strains has closely followed the release of new antimicrobial agents, which further complicates the effectiveness of new agents (Figure 4-1). Recently, infections with bacterial strains resistant to all known antimicrobial agents have been reported [155], necessitating the urgent need for alternative treatment strategies, such as the use of lytic bacteriophage and antimicrobial peptides.

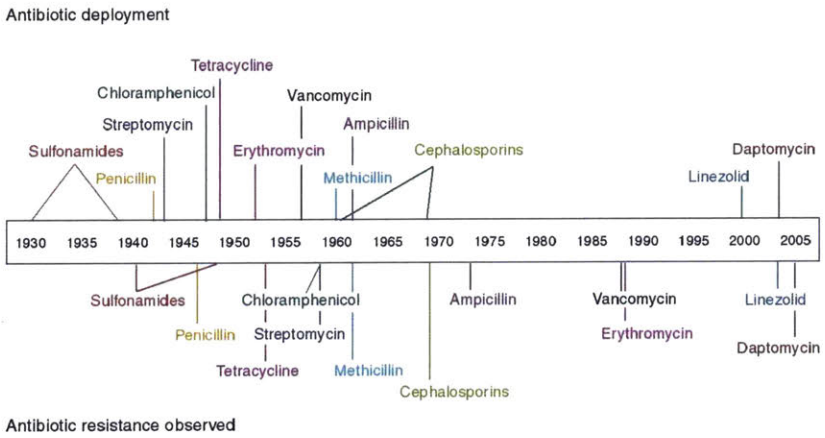

Figure 4-1: Timeline of antibiotic deployment and the evolution of antibiotic resistance. The year each antibiotic was deployed is depicted above the timeline, and the year resistance to each antibiotic was observed is depicted below the timeline. Reprinted with permission from [156].

4.3 History of lytic bacteriophage therapy

4.3.1 Discovery of bacteriophages

Bacteriophages (phages) are small viruses that naturally infect and kill bacteria, but not eukaryotic cells. Phages were first discovered independently

in 1915 and 1917 by Frederick Twort and Felix d'Herelle, noted as clearings on bacterial agar plate cultures ("plaques") [157, 158]. It was d'Herelle who first coined the term "bacteriophage", from the combination of "bacteria" and the Greek "phaegin" to imply that the phages were eating the bacteria [159].

4.3.2 Therapeutic use of lytic bacteriophages

Phages were first used therapeutically by d'Herelle in 1919 to successfully treat four *Shigella* dysentery patients; however the first published use of phage therapy in humans was described for treatment of *Staphylococcus* skin carbunculosis [160, 159]. Staphylococcal phage was injected at the at the base of the carbuncle and clinical improvement was noted with 48 hours of treatment [160]. D'Herelle devoted his career to studying phage for therapeutic use. He reported successful treatment of dysentery patients in Sudan and India, bubonic plague in Egypt, and advised other physicians on use of phage to successfully treat septicemic and pneumonic plague in Senegal, intravenous phage to cure staphylococcal and streptococcal septicemia, typhoid fever and infantile diarrhea [159]. While at the Pasteur Institute, d'Herelle met a Georgian scientist named George Eliava and the two eventually collaborated to transform Eliava's Microbiology Institute in Tbilisi into a world center for bacteriophage research. Unfortunately, communist politics complicated matters; Eliava was arrested by the secret police and executed in 1937. D'Herelle was visiting Paris and never returned to Tbilisi, however the George Eliava Institue of Bacteriophages, Microbiology and Virology exists to this day as a major center for phage research [161].

4.3.3 Bacteriophage production

While in Paris, d'Herelle produced different commercially-available phage cocktails which were marketed by the French company that later became L'Oreal. In the United States, large pharmaceutical companies, including Eli Lilly, Swan-Myers of Abbot Laboratories, E. R. Squibb and Sons (now Bristol-Myers Squibb), and Park, Davis and Company (now part of Pfizer) all produced bacteriophage preparations in the 1930s [162]. Unfortunately, the Western world lost interest with bacteriophages for several reasons.

Three reports published by the American Medical Association questioned the efficacy of phage based on lack of standardized phage preparations and poorly controlled studies additionally confounded by personal biases from the authors [163]. While the first electron micrographs of phages were obtained in 1939 in Germany, the first published images of phage in the US were not widely disseminated until 1942 [164, 162, 163, 165]. Some researchers questioned whether phages were even viruses, attributing their effects to a "lytic principle".

The beginning of the modern antibiotic era began with the discovery of penicillin in 1928 by Sir Alexander Fleming [166]. US pharmaceutical manufacturers soon abandoned phage production in favor of penicillin, which gained immediate popularity with widespread success for treating World War II soldiers, and later the general public [167, 168]. Phage therapy also became controversial from a political standpoint as it was used by enemies of the West: German and Japanese WWII armies as well as the former Soviet Union. Finally, many older publications evaluating the use of phage therapy were never translated into English, and studies were often not properly controlled, leading to further Western skepticism. While active bacteriophage use and research has continued in Georgia, Poland, and other Eastern European countries to this day, it is only recently with the emergence of serious multi-drug resistant pathogens, that interest in phage therapy has been revitalized in the United States.

4.3.4 Current use of lytic bacteriophage therapy

In 2006, the US Food and Drug Administration first approved bacteriophages for use in food safety; specifically, a preparation of 6 individual phages with activity against *Listeria monocytogenes* for application to ready-to-eat meat and poultry products [169]. More recently completed clinical trials for phage therapy of human infections include the multi-center, randomized, single-blind European Phagoburn study (evaluating treatment for burn wounds infected with *E. coli* and *Pseudomonas aeruginosa*, and a phase I clinical trial evaluating the topical safety of phage targeting *S. aureus* at Walter Reed Army Institute of Research [170, 171]. In the United States, use of phage to treat humans is currently restricted to patients that have exhausted other antimicrobial options. Recently, phages were

successfully used to treat an aortic graft chronically infected with resistant *P. aeruginosa* in a 76-year old patient living in Connecticut [172].

4.3.5 Advantages and challenges of lytic bacteriophage therapy

Bacteriophages have several potential advantages over traditional antimicrobial therapy. Because bacteriophages have a different mechanism of action than traditional antibiotics (namely, lysis of bacterial cells by phage lysin proteins), they can be effective against multi-drug resistant bacterial strains. The phage life cycle encompasses two primary strategies for survival and replication (Figure 4-2) [173]. The lytic phage cycle involves injection of phage DNA into the bacterial cell, hijacking of the bacterial host processes to replicate new phage DNA and synthesize capsid proteins, assembly of phages, and release of new phages by lysis of the bacterial cell (Figure 4-2A). The second replication strategy is lysogeny, where phage DNA is integrated into the bacterial chromosome (Figure 4-2B). Lysogenic phages can remain dormant within the bacterial chromosome for many generations of bacterial replication, or revert to a lytic phenotype, either spontaneously, or under cellular stress (i.e. radiation, exposure to antimicrobials or carcinogens). One challenge for use of bacteriophages therapeutically is making sure to select only phages utilizing the lytic replication cycle. Besides the unpredictable lysis kinetics for a lysogenic phage, the process of lysogeny can facilitate horizontal gene transfer in bacteria (transduction) and spread antimicrobial resistance genes as a result of mispackaging bacterial DNA within the phage capsid [174]. This limitation can be overcome by sequencing phages to identify genes associated with lysogeny (i.e. integrase) [175, 176].

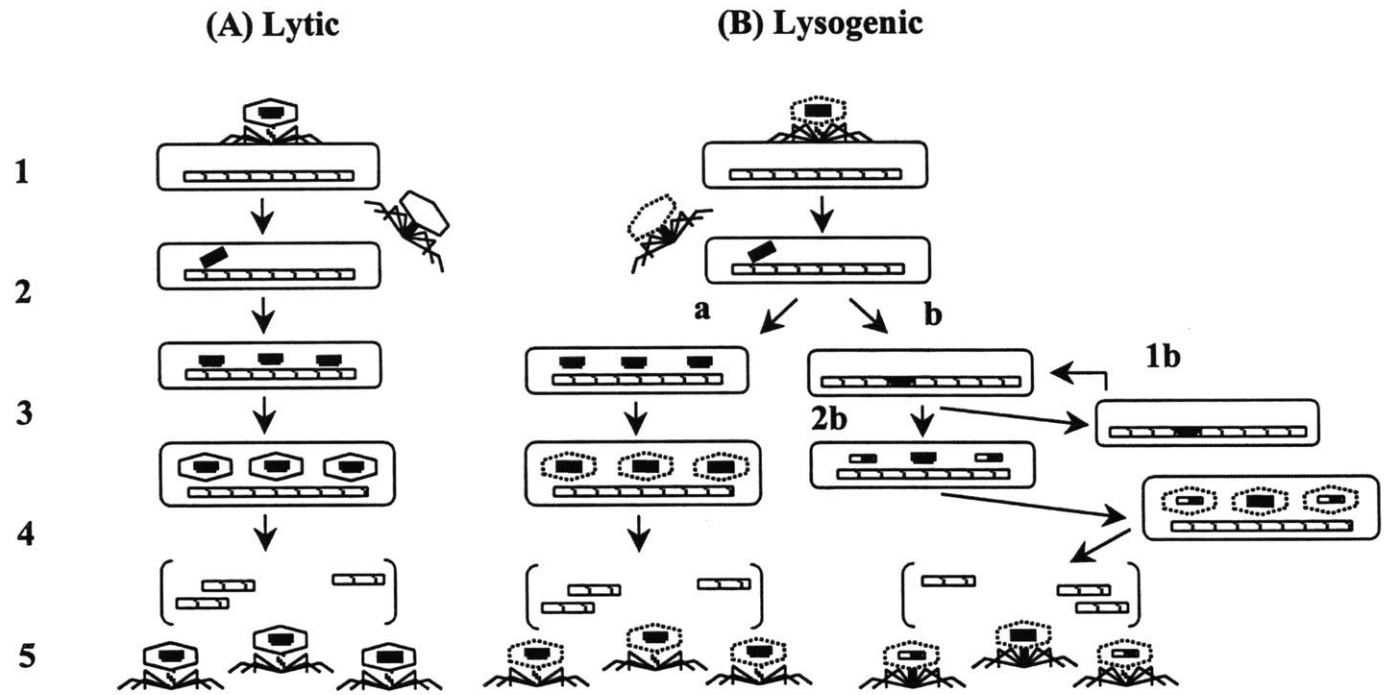

Figure 4-2: (A) Lytic phages: (1), attachment; (2), injection of phage DNA into the bacterial host; (3), replication of phage DNA, and production of new capsids; (4), phage assembly; (5), release of mature phages (lysis). (B) Lysogenic phages: (1 and 2) attachment and injection of phage DNA; (3a), lysogenic phages can initiate a lytic cycle (b) or integrate their DNA into the host bacterium's chromosome (lysogeny). Lysogenized cells can replicate normally for many generations (1b) or undergo lysogenic induction (2b) spontaneously or because of inducing agents such as radiation or carcinogens, during which time the integrated phage DNA is excised from the bacterial chromosome and may pick up fragments of bacterial DNA. Reprinted with permission [173]

Phages are highly specific in infecting their intended bacterial species, and can even be specific in targeting certain strains within a species. This narrow spectrum of activity allows the potential to precisely target only pathogens of interest, sparing widespread disruption of the microbiota. Disruption of the gut microbiota with broad-spectrum antimicrobials can lead to overgrowth of secondary pathogens, such as *Clostridium difficile*, a major cause of morbidity and mortality [177]. Additionally, multiple bacteriophages targeting the same bacterial species can be combined together without increased risk for systemic side effects, whereas administration of more than one or two antimicrobials simultaneously can lead to organotoxicity. Combination of multiple bacteriophages targeting the same bacterial species can also decrease the likelihood of the bacteria becoming resistant to the phage.

Bacteriophages are self-replicating, which offers the potential advantage for a decreased dosing frequency. This was demonstrated with early treatment of *Shigella* patients by d'Herelle, where patients recovered within 4-20 hours after a 2cc dose of a high-titer phage culture, and patients with staphylococcal septecemia improved the following day [159]. Decreased dosing frequencies are advantageous, as previous research has demonstrated that patient compliance decreases with antibiotics dosed multiple times per day vs. once daily [178]. Additionally, missed antibiotic doses or noncompliance with completing the full course can contribute to the development of antibiotic resistance [179].

Another advantage of bacteriophages over conventional antimicrobials is their ability to distribute widely through the body, including passage through privileged sites such as the blood brain barrier. Early studies found that intraperitoneal injection of phage into mice could prevent death following intracerebral inoculation of *Shigella dysenteriae* [180]. Phages were isolated from the brains of mice (both infected and uninfected with *S. dystenteriae*) within 2 hours following intraperitoneal inoculation, with infected mice demonstrating much higher titers of phages in their brain tissue than uninfected mice [180]. D'Herelle utilized multiple routes of phage administration when treating patients, including oral, intravenous, intramuscular, and direct injection in buboes for patients with bubonic plague [159]. Because phages do not infect eukaryotic cells, the only potential side effects are related to endotoxic shock accompanying rapid bacterial ly-

sis; this can also potentially occur with the administration of conventional antimicrobial agents [181].

Bacteriophage therapy shows advantages over traditional antimicrobials when considering time and cost of development. From pre-clinical testing to FDA approval, development of a new pharmaceutical is estimated to take 10-15 years and cost above 1.3 billion dollars [182, 183]. New bacteriophages can be isolated rapidly from the environment, and quickly evaluated for therapeutic potential against pathogens of interest, prior to sequencing and purification steps.

A final advantage of bacteriophage therapy is their potential efficacy against bacterial biofilms. Recent publications have evaluated phages in treating biofilms from multiple species, including *E. faecalis*, *S. aureus*, *Klebsiella pneumonia*, and *Pseudomonas aeruginosa* among others [184, 185, 186, 187]. It is hypothesized that bacteriophages show efficacy against biofilms via multiple mechanisms. Phages secrete depolymerases which are capable of degrading extracellular polymeric substance (EPS), a major component of biofilm [188, 189]. As well as lysing bacterial cells from within, adsorption of multiple phages to the bacterial membrane can weaken the bacterial membrane in selected bacterial species [190]. Because of these previous findings, we hypothesized that we could isolate lytic phages with activity against *E. faecalis* and that they would be successful at treating biofilm.

4.4 Introduction to antimicrobial peptides

Antimicrobial peptides (AMPs) are a class of naturally occurring, evolutionarily conserved small peptides, typically 10-50 amino acids in length [153, 191]. AMPs have been isolated from a variety of species across the animal kingdom including mammals (humans, cows, pigs, macaques), invertebrates (silk moths, honeybees, scorpions), amphibians (frogs) and plants [192, 193]. Typically, AMPs are isolated from blood cells, haemolymph and/or epithelial tissues and function as part of the innate immune system through both direct killing of bacteria and immune modulation [192, 191]. AMPs commonly feature clusters of cationic and hydrophobic residues ($\geq$ 30%), an overall positive charge of +2 to +9, and the ability to fold into amphipathic structures (Figure 4-3) [192, 191]. The amphipathic structures

interact with the negatively charged bacterial membrane (lipopolysaccharide in Gram-negative bacteria and wall-associated teichoic acids in Gram-positive bacteria) 4-4 [191]. Bactericidal mechanisms of AMPs include both insertion and disruption of the bilayer and translocation across the membrane to affect internal targets 4-4[191]. Acquisition of resistance to AMPs is not well described, with exceptions for bacterial species with a decreased density of acidic lipids (*Morganella*, *Serratia*) or species able to secrete proteases (*Porphyromonas*) [192]. AMPs have previously demonstrated efficacy in treating bacterial biofilms from multiple species, including *S. aureus*, *P. aeruginosa*, *Listeria monocytogenes*, and *E. coli* [194, 73, 195], thus we were interested in evaluating whether they could be used to treat *E. faecalis* biofilms.

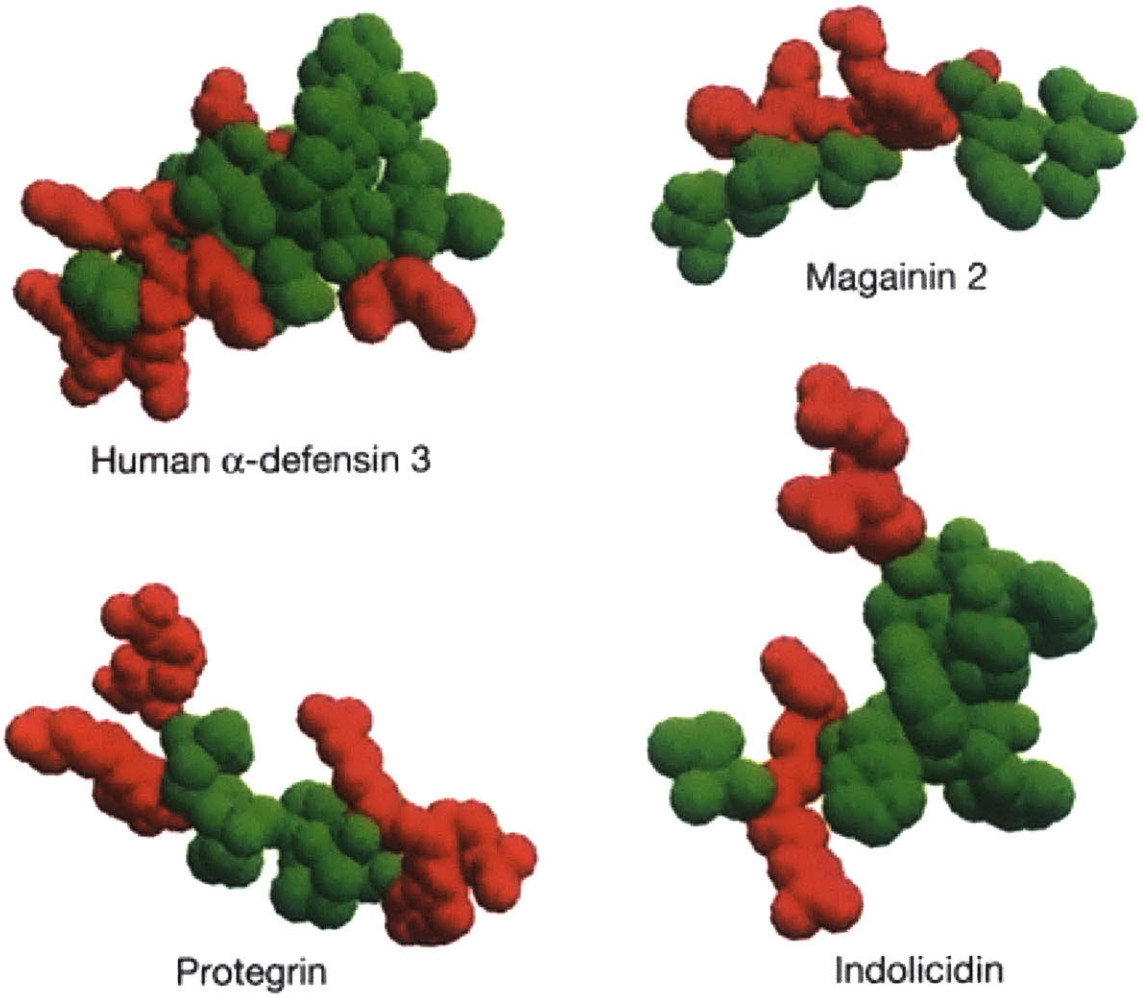

Figure 4-3: AMP structures. Clustering of cationic and hydrophobic amino acids into distinct domains in selected AMPs. Red colorations designates basic (positively-charged) amino acids; green coloration designates hydrophobic amino acids; other amino acids not shown. Reprinted with permission from [192].

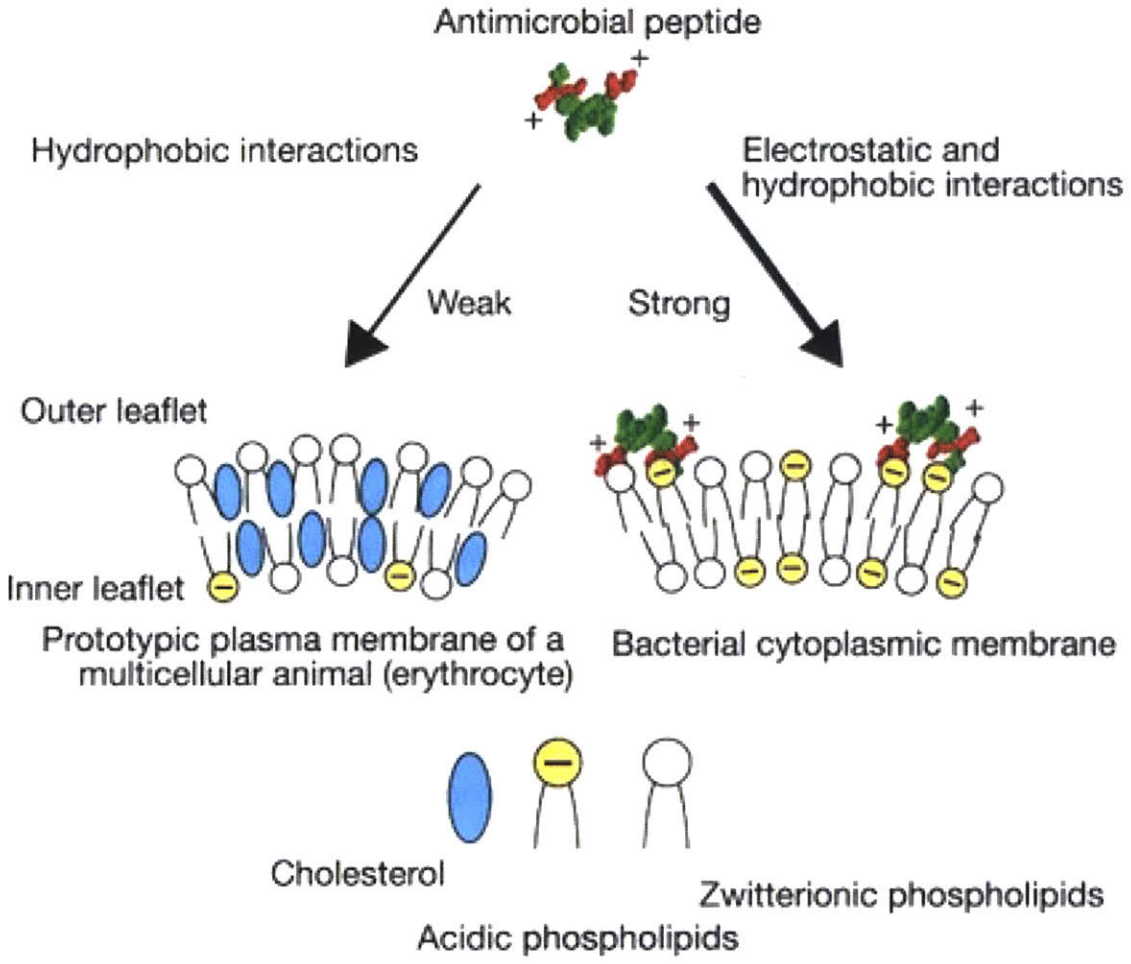

Figure 4-4: The membrane target of AMPs of multicellular organisms and the basis of specificity. Reprinted with permission from [192].

4.5 Isolation and characterization of lytic bacteriophages with activity against multi-drug resistant *E. faecalis*

4.5.1 Isolation of lytic bacteriophages

Initial isolation methods

200 ml of raw sewage was collected from a municipal sewage throughway at the intersection of Portland St and Main St in Cambridge, MA into a ster-

ilized glass bottle. Sewage was vacuum-filtered through a 0.4μm asymmetrical polyethersulfone (aPES) (ThermoFisher) bottle-top filter followed by a 0.2μm aPES bottle-top filter to obtain sewage filtrate. 15 aliquots of 9ml of sewage filtrate was combined with 9ml of double-strength tryptic soy broth (TSB) supplemented with 2mM $CaCl_2$ in 50ml conical tubes. Phage enrichment was performed by inoculating filtrate-broth mixtures with 250μl of overnight 2011 ST4 and ST55 *E. faecalis* cultures and incubating overnight, shaking at 37°C, 150rpm. The following day, phage enrichment tubes were centrifuged at 4000 x *g* for 10 min to pellet cells and debris. Phage enrichments were assayed for plaque-forming units using the double-agar overlay technique [196]. Briefly, molten 0.5-0.6% TSA with 10mM $CaCl_2$ was inoculated with 200μl of log phase test *E. faecalis* strains and poured onto 1.5% TSA bottom agar with 10mM $CaCl_2$. Plates were allowed to solidify in the hood, then 5μl of each enrichment supernatant was spotted onto the surface of the solidified top agar. Spots were allowed to dry for 10-20 minutes, then plates were incubated at 37°C overnight. Plates were examined for plaques the following day. Chloroform was added to initial enrichment tubes at a 5% vol/vol concentration; enrichment tubes were stored at 4°C.

Plaque purification and titer methods

Individual plaques were picked with a sterile pipet tip into a 1.5ml microcentrifuge tube containing 100μl of TSB with 2mM $CaCl_2$ and incubated at 37°C for 10 minutes. The pipet tip was removed and the microcentrifuged tube was briefly vortexed. Serial 10-fold dilutions were made in TSB with 2mM $CaCl_2$. 5μl of the serial dilutions were spotted onto solidified double agar overlay plates inoculated with *E. faecalis* , as described above. Plates were allowed to dry, incubated at 37°C overnight and examined for plaques the following day. Plaques were enumerated to determine the phage titer as plaque-forming-units (PFU)/ml. Plaque picking, serial dilution and spot testing was repeated a minimum of 3-4 times to ensure purity of individual phages.

Phage propagation, PEG precipitation and imaging

Overnight broth cultures of *E. faecalis* strains in brain heart infusion (BHI) broth were diluted 1:100 in fresh BHI in a 250ml Erlenmeyer flask and incubated for 1.75 hours at 37°C at 250rpm, until reaching an OD_{600} of approximately 0.15. Phages were resuspended from plaques into 400μl of SM buffer and filtered through a 0.2μm filter. 75μl of filtered phage was added to the log-phase *E. faecalis* cultures and incubated at 37°C. Cultures were monitored for lysis by periodic measurements of OD_{600}. Once OD_{600} had stabilized and visible lysis was observed, phage lysates were centrifuged at 5000 x *g* for 10 minutes and filtered through a 0.2μm bottle top filter. Following centrifugation, 10g of PEG-8000 and 5.8g of sodium chloride were added for final concentrations of 10% (w/v) PEG-8000 and 1M NaCl and lysates were split into two 50-ml aliquots in 50ml conical tubes. Tubes were incubated overnight at 4°C to facilitate precipitation. The following day, tubes were centrifuged at 10,000 x *g* for 1 hour and the pellets were re-suspended in 2ml of SM buffer and sterile-filtered using a 0.2μm syringe filter. 200μl of re-suspended phage preparations were applied to a square mesh transmission electron microscopy (TEM) grid (FCF200-Ni, Electron Microscopy Sciences, Hatfield, PA) for 90 seconds, blotted, washed with 20μl sterile water for 30 seconds and stained with 4μl 2% uranyl acetate for 30 seconds. Grids were blotted, dried for 1-2 hours and imaged using an FEI Technai Spirit transmission electron microscope at the W. M. Keck Microscopy Facility, Whitehead Institute.

4.5.2 Phage lysis kinetics and host range

Overnight cultures of 2011, 2014 and 2015 *E. faecalis* ST55 isolates from macaque #6 and ATCC *E. faecalis* strain 29212 were inoculated into 5ml of TSB and incubated at 37°C, shaking at 150rpm. After isolates reached a McFarland standard of 0.5, 0.1ml were added to flasks containing 10ml fresh Mueller Hinton broth with no phage (control), phage 1 or phage 3 at a multiplicity of infection of approximately 80. Aliquots for OD_{600} were collected at 0, 0.1, 0.5, 1, 1.5, 2, 2.5, 3, 4 and 5 hours after inoculation. Aliquots for serial spot dilutions were collected at 0, 1, 2 and 3 hours after inoculation. Following overnight incubation at 37°C, colonies were enumerated and kill curves plotted. 5μl of phages 1 and 3 were spotted onto

double agar overlay plates inoculated with ST4 2016 and ST48 2017 from macaques #9 and #27, respectively.

4.5.3 Phage precipitation, DNA extraction, sequencing and analysis

20 ml aliquots of Phage 1 and Phage 3 were each treated with DNase I and RNase at final concentrations of 20μg/ml and 10μg/ml, respectively, for 75 minutes at 37°C. After incubation, 5ml of 5M NaCl/50% polyethylene glycol was added and tubes were stored at 4°C overnight. The following day, tubes were centrifuged for 60 min at 4,000 x *g* at 4°C. The supernatant was decanted and the pellet was resuspended in 1ml of 10mM Tris/1mM EDTA/100mM NaCl. The resuspended pellets were transferred to 1.5ml microcentrifuge tubes and centrifuged for 10 minutes at 14,000 x *g* 1ml of supernatant was used for DNA extraction and transferred to a clean 1.5ml microcentrifuge tube. 100μl of 0.5M EDTA and 100μl of 10% sodium dodecyl sulfate was added and tubes were inverted to mix. 250μl of phenol-chloroform-isoamyl alcohol (25:24:1) was added to each tube, vortexed, and centrifuged at 10,000 x *g* for 4 minutes. 700μl of supernatant was carefully transferred to a clean tube before the addition of 630μl isopropanol and 70μl of 5M NaCl. Tubes were gently inverted and centrifuged at 10,000 x *g* for 10 minutes. After decanting the supernatant, 500μl of 70% ethanol was added and tubes were centrifuged for 5 minutes at 10,000 x *g*. The supernatant was decanted and tubes were left open under the blower of a class II biofsafety cabinet to air dry the pellet. DNA pellets were resuspended in 50μl of DNase-free water and DNA was quantified using a NanoDrop spectrophotometer (ThermoFisher Scientific). Phage DNA libraries were prepared using the QIAseqFX DNA library kit (Qiagen) with 765 ng of DNA per manufacturer's instructions. Fragmentation of DNA was performed at 32°C for 5 minutes. AMPure XP beads were used to perform library purification as indicated in the QIAseq FX DNA library kit manual. Barcoded and adapter-ligated DNA libraries were pooled with other DNA libraries. Quality control prior to sample loading included sizing Illumina libraries with the Advanced Analytic Fragment Analyzer and qPCR using KAPA SYBR FAST qPCR Master Mix (KM4114) on a Roche LightCycler 480II. 2x300 base paired end reads were generated on an Illumina MiSeq using

a MiSeq Reagent Kit v3 (Illumina). Phage genomes were assembled using the SPAdes assembler on PATRIC. Assembled contigs were queried using BLASTn and BLASTx `https://blast.ncbi.nlm.nih.gov/Blast.cgi` [197] to identify similar phage genomes and to search for integrase genes that might identify lysogenic potential. Assembled contigs >700 base pairs were annotated on RAST [198, 199, 200].

4.5.4 AMP MICs

Minimum inhibitory concentration testing was performed for five antimicrobial peptides against the 15 2011 *E. faecalis* isolates using the broth microdilution technique in LB medium with an initial inoculum of approximately $5x10^5$ cells (obtained by diluting an overnight culture 1/100) in polystyrene microtiter plates. The five AMPS evaluated were isolated from a variety of species (human LL-37, porcine PR-39, honeybee apidaecin Ia, toad buforin II and flounder pleurocidin) in order to evaluate different AMP classes and mechanisms of action (alpha-helical/cathelicidins, proline-rich, DNA-binding agents). The MIC was interpreted as the lowest concentration of peptide or antibiotic at which complete inhibition of visible bacterial growth was observed after 24h of incubation at 37°C. Plates were grown under the same conditions for an additional 24h to confirm growth inhibition. Each agent was tested with 6 replicates. MIC testing for LL-37 and PR-39 was also performed on the 2015 ST55 isolate from macaque #6, the 2016 ST4 isolate form macaque #9 and the 2017 ST48 isolate from macaque #27 using LB broth. Briefly, overnight cultures were inoculated into 5ml Mueller-Hinton broth and grown at 37°C, shaking at 150rpm until a McFarland standard turbidity of 0.5 was reached. 1.5μl was then inoculated into a round-bottom polystyrene plate containing test concentrations of LL-37 and PR-39 of 40 μg/ml down to 1.25μg/ml in duplicate. Plates were incubated for 24h at 37°C and the MIC was interpreted as the lowest concentration of peptide at which complete inhibition of visible bacterial growth was observed.

4.6 Results

4.6.1 Initial isolation, plaque purification and titers

Plaques were identified on ST55 double-agar overlay plates from sewage filtrate enriched with 2011 ST55 *E. faecalis* isolates #2, #3, and #7 and designated as phages 3, 1, and 2, respectively. No plaques were identified from spots of ST4 enrichments and repeated isolation attempts were unsuccessful. After plaque purification, phage 1 demonstrated a large, clear plaque morphology, while phages 2 and 3 demonstrated small, clear, plaque morphologies (Figure 4-5). Approximate phage titers following the purification steps were $6x10^7$ PFU/ml for phage 1, $3.4x10^4$ PFU/ml for phage 2 and $1x10^6$ for phage 3.

4.6.2 Phage morphology

Transmission electron microscopy identified all three phages to be likely Siphoviruses based on their non-enveloped head, capsid morphology and flexible, noncontractile tails [201]. Phage 1 displayed an icosahedral capsid morphology, approximately 65nm in diameter (Figure 4-6A). Phages 2 and 3 displayed prolate capside morphologies, approximately 99x36nm and 109x44nm, respectively (Figure 4-6B and C).

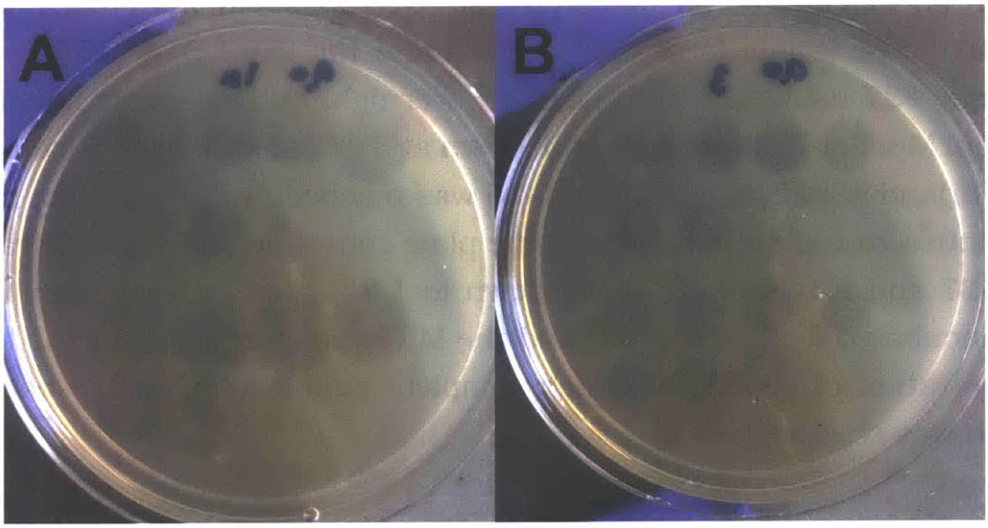

Figure 4-5: Photographs of plaques formed by Phages 1 (A) and 3 (B) on top agar impregnated with the 2015 ST55 *E. faecalis* isolate from macaque #6.

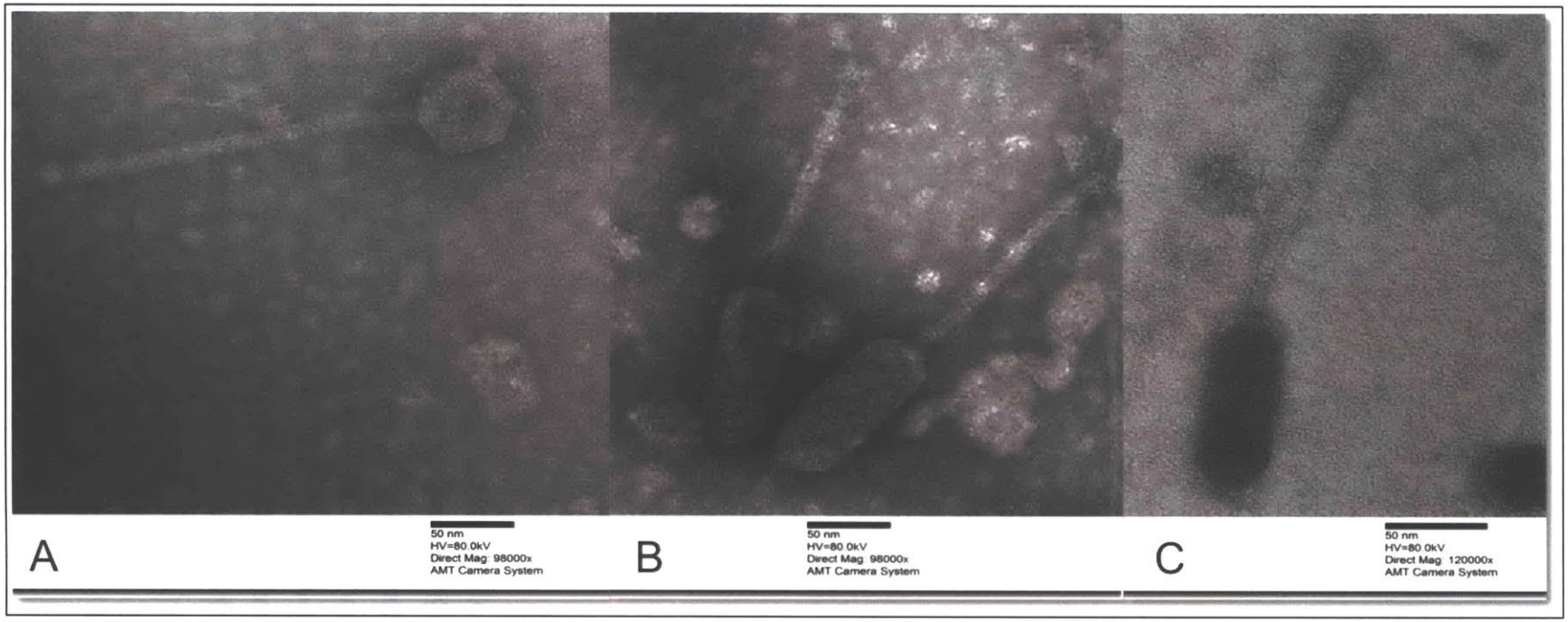

Figure 4-6: Transmission electron micrographs of three lytic bacteriophages with activity against ST55. A. Phage 1 (icosahedral capsid), B. Phage 2 (prolate capsid), C. Phage 3 (prolate capsid)

4.6.3 Phage lysis kinetics

Due to inconsistent phage lysis following propagation of phage 2, phages 1 and 3 were selected for use in further experiments. Phage lysis kinetic graphs for phages 1 and 3 are displayed in Figure 4-7. Both phages failed to infect ATCC *E. faecalis* 29212, but showed efficacy against ST55 isolates from macaque #6. 2014 and 2015 ST55 isolates showed complete killing by both phages at 2 hours; the 2011 ST55 isolates showed decreased titers but were not killed entirely. This result may be attributed to propagation of the phage using the 2011 ST55 isolate and development of some level of resistance. No plaques were identified on spot testing against ST48 isolates; large plaques were identified inconsistently from phage 3 at low dilutions (1:10, 1:100), against the 2016 ST4 isolate.

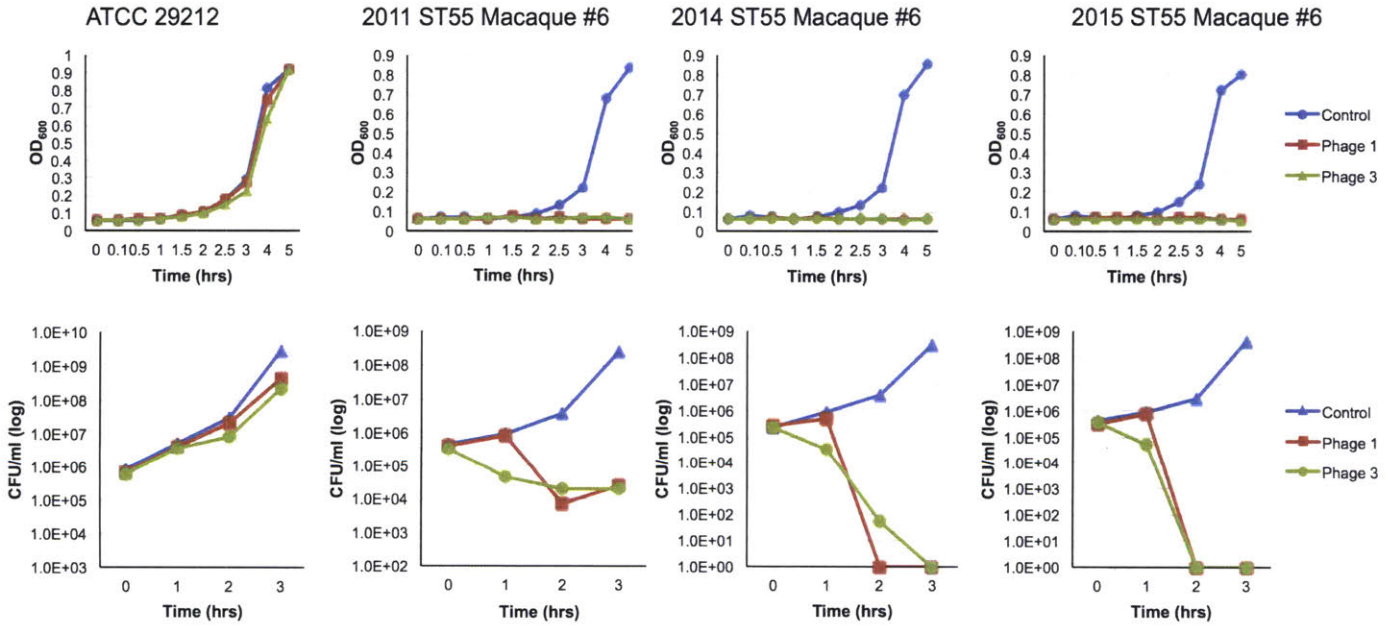

Figure 4-7: Phage 1 and 3 kill curves against ATCC 29212 and ST55 *E. faecalis* isolates from macaque #6. Top curves show OD_{600} values over time and bottom curves show CFU/ml counts over time.

Following assembly, phage 1 had a total length of 558,919 bp with 5 contigs >700bp, an N50 of 533 bp and a GC content of 40.58%. Phage 3 had a total length of 185,840 bp with 35 contigs >700bp, an N50 of 534 bp and a GC content of 40.30%. Submission of phage 1 to BLASTn identified the closest sequenced phage genomes as *Enterococcus* phages PMBT2 (99% identity, accession number MG708276.1), EfaCPT1 (97% identity, accession number JX193904.1) and IME-EF4 (90% identity, accession number KF733017.1). Submission of phage 3 to BLASTn identified the closest sequenced phage genomes as *Enterococcus* phages IME-EF1 (99% identity, accession number KF192053.1), vBEfaSIME198 (99% identity, accession number KT932699.1), EF-P29 (98%, accession number KY303907.1), and EF-P10 (97% identity, accession number KY472224.1). Annotation on RAST identified 69 coding sequences for phage 1 (with 20 non-hypothetical protein annotations) and 79 coding sequences for phage 3 (with 15 non-hypothetical protein annotations). Gene annotation lists are archived at `https://figshare.com/s/ccfcd9994c95a294049b`. No genes for either phage 1 or 3 were annotated as integrase genes by RAST, or identified following BLASTx query for integrase genes, supporting that both phages are unable to initiate lysogeny.

4.6.4 MIC results for AMPs

On initial screening of the 15 2011 *E. faecalis* isolates, we identified that MICs against apidaecin Ia, buforin II and pleruocidin were mostly $\geq$20μg/ml for all isolates tested (Table 4.1). The majority of ST55 strains displayed MICs for PR-39 and LL-37 at $\geq$20μg/ml and 10-20μg/ml, respectively. ST4 strains displayed MICs for PR-39 and LL-37 at 5μg/ml and 5-10μg/ml, respectively. Because LL-37 and PR-39 seemed to be the MICs with the most promising antimicrobial activity, they were chosen for use in further experiments. Later screening of MICs for LL-37 and PR-39 against 2015 ST55, 2016 ST4 and 2017 ST48 isolates found that ST4, ST55 and ST48 were resistant to both AMPs (MIC >40μg/ml).

E. faecalis isolate	ST	Animal ID	LL-37 (µg/mL) -human-	Cecropin PR-39 (µg/mL) -pig-	Apidaecin Ia (µg/mL) -honey-bee-	Buforin II (µg/mL) -toad-	Pleurocidin (µg/mL) -winter flounder-
2011 EF1	**4**	**1**	10	5	>20	>20	10
2011 EF2	**55**	**4**	10-20	>20	>20	>20	>20
2011 EF3	**55**	**5**	>20	>20	>20	>20	>20
2011 EF4	**4**	**5**	5	5	>20	>20	>20
2011 EF5	**330**	**5**	>20	>20	>20	>20	>20
2011 EF6	**55**	**11**	Reduced at 5, but MIC >20	Reduced at 5, but MIC >20	>20	>20	>20
2011 EF7	**55**	**16**	10	>20	>20	>20	>20
2011 EF8	**55**	**16**	10	>20	>20	>20	>20
2011 EF9	**4**	**18**	5	5	>20	>20	20
2011 EF10	**4**	**19**	5	5	>20	>20	20
2011 EF11	**55**	**6**	20	>20	>20	>20	>20
2011 EF12	**55**	**8**	20	5	>20	>20	>20
2011 EF13	**4**	**9**	5	5	>20	>20	20
2011 EF14	**4**	**11**	5	5	>20	>20	20
2011 EF15	**4**	**11**	5	5	>20	>20	20
2015	**55**	**6**	>40	>40	NA	NA	NA
2016	**4**	**9**	>40	>40	NA	NA	NA
2017	**48**	**27**	>40	>40	NA	NA	NA

Table 4.1: MICs of selected AMPs against 2011 *E. faecalis* strains and 2015-2017 ST55, ST4 and ST48 strains.

4.7 Evaluation of different methods to treat *E. faecalis* biofilm

4.7.1 General methods for biofilm treatment experimental setup

E. faecalis isolates were inoculated onto TSA with 5% sheep blood and incubated overnight at 37°C with 5% CO_2. The following day, cultures were inoculated into 5ml of TSB with 1% glucose and incubated at 37°C, shaking at 150rpm between 5 hours and overnight. To inoculate biofilm plates, 5μl of the TSB broth culture was added to 195μl of fresh TSB with 1% glucose in replicates of 3-12 per isolate, depending on the experiment. Plates were incubated overnight, statically at 37°C. The following day, the OD_{600} was recorded and wells were emptied by inversion. Wells were washed 2-3x with 200μl PBS prior to addition of tested anti-biofilm treatments. After addition of anti-biofilm treatments, plates were incubated overnight, statically at 37°C. The following day, well contents were emptied by inversion, wells were washed 3x with 200μl PBS and stained with crystal violet according to the protocol described in section 3.3.5. Biofilm production was normalized to bacterial growth by dividing OD_{570} by the OD_{600}, and the normalized OD_{570} values were used for statistical analysis. Due to the noisiness of crystal violet assays, single outliers were removed using the Grubbs outlier test. Non-parametric data was analyzed using Kruskal-Wallis with Dunn's multiple comparison test, parametric data was analyzed with one-way ANOVA with Dunnett's multiple comparison or Holm-Sidak's multiple comparison testing with $P<0.05$ considered significant. For combination biofilm treatments, two-way ANOVA testing was performed with post-hoc Tukey's multiple comparison testing.

Tested antimicrobial agents were purchased from Sigma in powdered form, weighed, and dissolved in sterile water at concentrations of either 5mg/ml or 1mg/ml. Norfloxacin was dissolved in a solution of 0.1M HCl and then diluted with water.

Sodium dodecyl sulfate, sodium bicarbonate and sodium periodate were weighed out and dissolved in sterile water at a concentration of 0.4% w/v for each and serially diluted in PBS for testing anti-biofilm efficacy.

Antimicrobial peptides were synthesized using the Fmoc strategy by Dr. César de la Fuente-Núñez. Peptides were purified by reverse-phase HPLC using analytical C18 columns (Phenomenex, USA). Molecular mass and purity of the synthesized peptides were confirmed by MALDI-ToF mass spectrometry. Analytical HPLC was also used to confirm the purity of the peptides.

Phages were added at a concentration of approximately 5-50 x10^7 PFU per well. Final volumes of treatments were either in 100μl or 200μl of PBS or SM buffer.

4.7.2 Efficacy of antimicrobials against *E. faecalis* biofilm

We first evaluated the efficacy of multiple antimicrobial agents by themselves in treating *E. faecalis* biofilms. Low-concentration antimicrobials tested included tetracycline (16-32μg/ml), bacitracin (32-128μg/ml), erythromycin (16-64μg/ml), gentamicin (16-64μg/ml) as well as ampicillin (64μg/ml), norfloxacin (64μg/ml) and vancomycin (64μg/ml). We also tested high concentrations of tetracycline (80-320μg/ml), bacitracin (160-640μg/ml), erythromycin (80-320μg/ml) and gentamicin (80-320μg/ml) against 2011 ST55 and ST4 isolates from macaques #6 and #9 respectively.

At lower antimicrobial concentrations, no significant decrease in biofilm was noted for tetracycline, bacitracin, erythromycin or gentamicin as compared to PBS for the 2015 ST55 or 2016 ST4 isolates from macaques #6 and #9, respectively (Figure 4-8). 2016 and 2017 ST48 isolates from macaques #9 and #27, respectively, showed minor but inconsistent decreases in biofilm when exposed to bacitracin (Figure 4-8). Because ST55 and ST4 isolates had strain-dependent resistance to tetracycline, bacitracin, erythromycin and gentamicin, we also tested much higher concentrations for these antimicrobials (Figure 4-9). Treatment with high concentrations of tetracycline actually resulted in increased biofilm, most likely due to decreased solubility and precipitation at the higher concentrations, thus results were excluded from statistical comparisons. We observed that bacitracin at high concentrations (160-320μg/ml) significantly decreased biofilm production for both the 2011 ST55 isolate from macaque #6 and the 2011 ST4 isolate form macaque #9. The highest concentration of bacitracin tested

(640μg/ml) decreased biofilm for the 2011 ST55 isolate from macaque #6, but no difference was observed for the 2011 ST4 isolate from macaque #9. We are unsure of the reason for this discrepancy, especially since the ST4 isolate showed a much lower bacitracin MIC (8-16μg/ml) than the ST55 isolate (>128μg/ml). We also evaluated biofilm treated with ampicillin, norfloxacin and vancomycin at 64μg/ml. We did not identify any decreases in biofilm for ST55, ST4 and ST48 isolates (Figure 4-10), and treatment with norfloxacin actually appeared to increase biofilm production in all three strains. Sub-inhibitory concentrations of ciprofloxacin have been reported to up-regulate biofilm production in *P. aeruginosa* through altering cell-cell signaling pathways [202]; however we would have expected to only see this phenotype in the fluoroquinolone-resistant ST4 isolate, and not the fluoroquinolone-sensitive ST55 and ST48 isolates (MIC 1-2μg/ml).

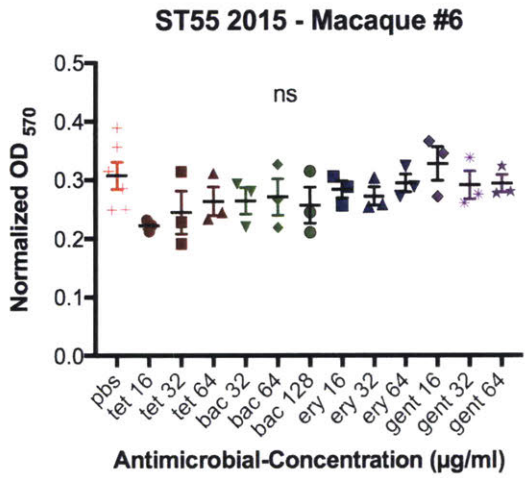

One way ANOVA with Holm-Sidak's multiple comparison test
P=0.2752, Mean with SEM

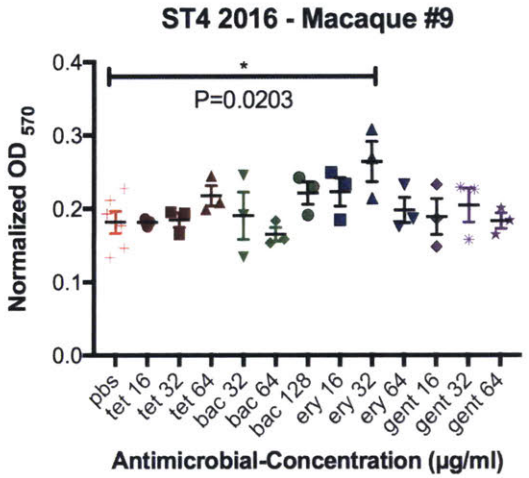

One way ANOVA with Holm-Sidak's multiple comparison test
P=0.0874, Mean with SEM

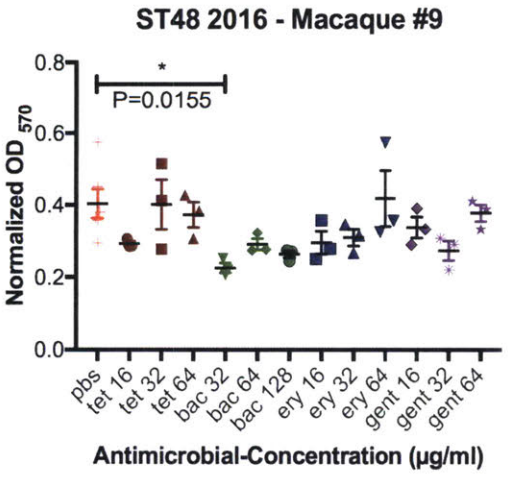

One way ANOVA with Holm-Sidak's multiple comparison test
P=0.7103, Mean with SEM

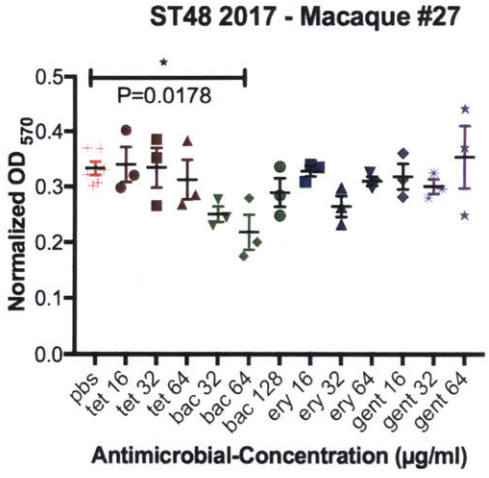

One way ANOVA with Holm-Sidak multiple comparison test
P=0.0386, Mean with SEM

Figure 4-8: Evaluation of tetracycline, bacitracin, erythromycin and gentamicin against *E. faecalis* biofilms

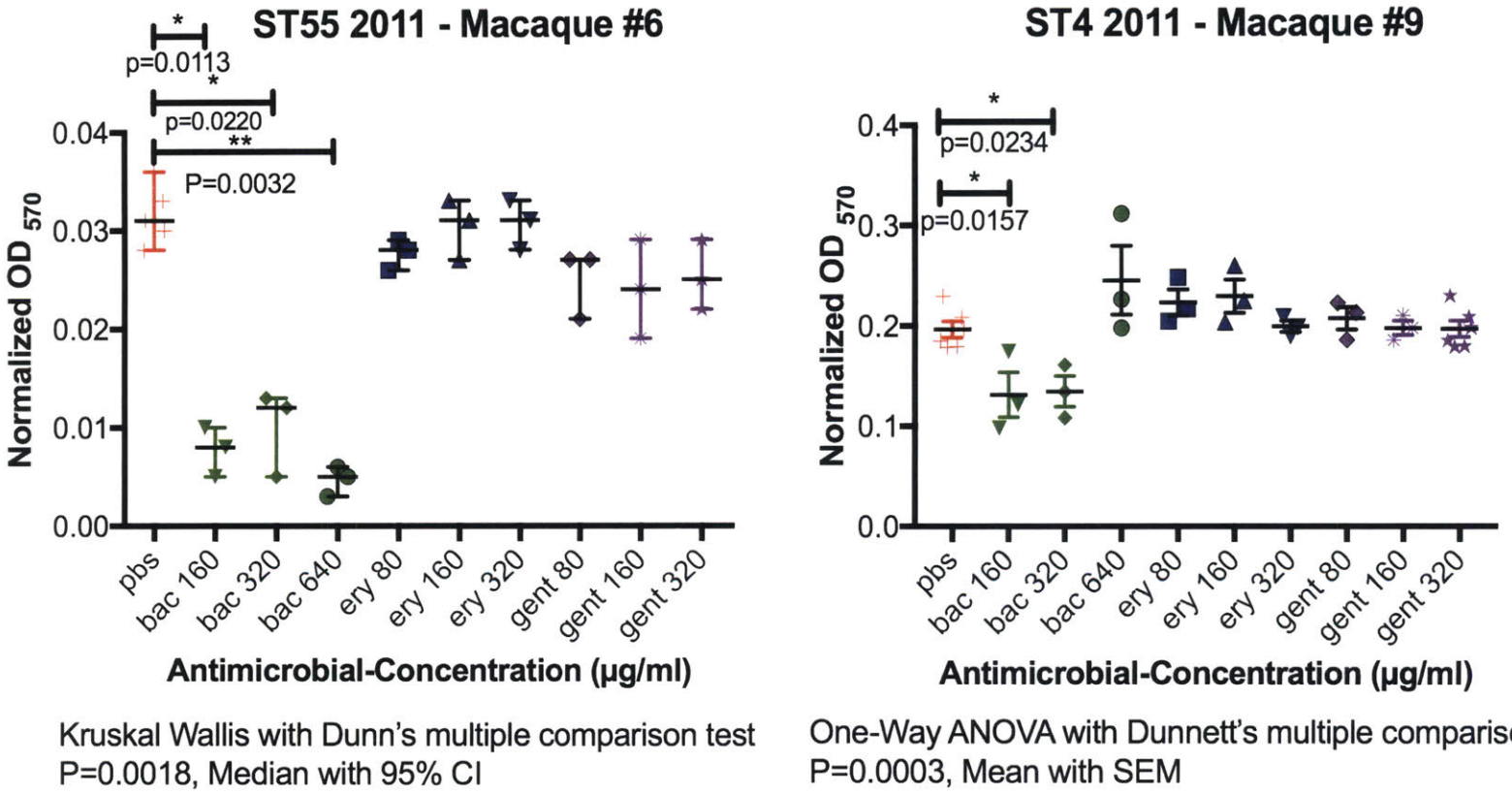

Figure 4-9: Evaluation of high concentrations of bacitracin, erythromycin and gentamicin against 2011 *E. faecalis* biofilms. Tetracycline was also evaluated but excluded from statistical analysis because biofilm increased; likely due to precipitation of tetracyline at higher concentrations

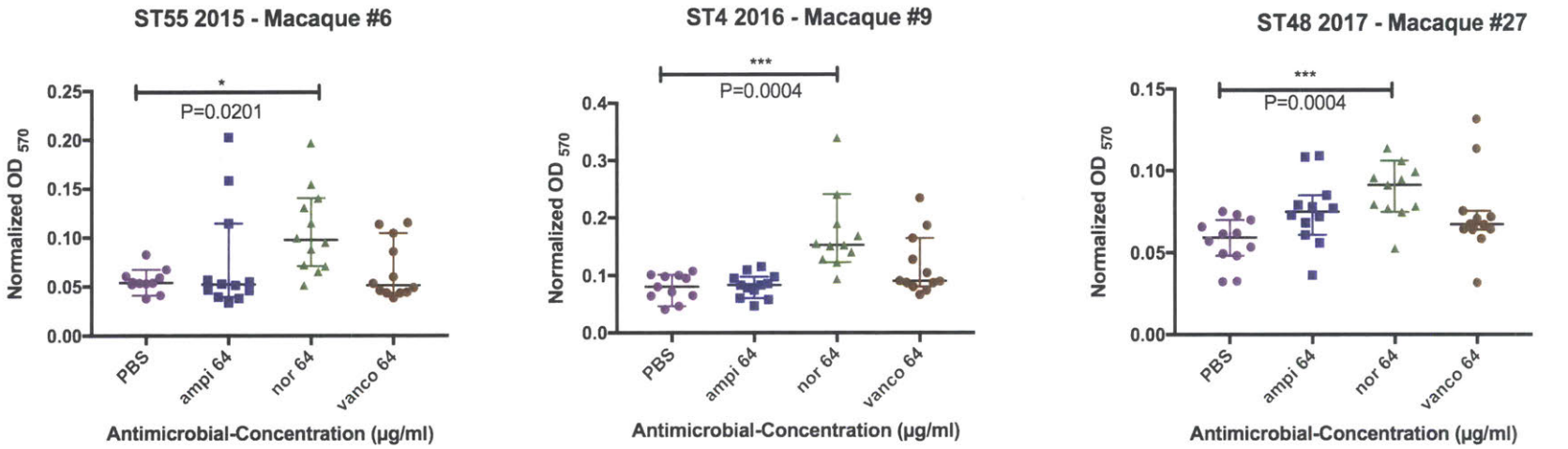

Figure 4-10: Evaluation of ampicillin, norfloxacin and vancomycin against *E. faecalis* biofilms

4.7.3 Efficacy of sodium dodecyl sulfate, sodium bicarbonate and sodium metaperiodate mixture against *E. faecalis* biofilm

Based on a previous study evaluating a 0.1% weight-volume mixture of sodium dodecyl sulfate (SDS), sodium bicarbonate and sodium periodate, we evaluated varying concentrations of this mixture against *E. faecalis* biofilms [203]. We observed that concentrations greater than 0.1% reliably decreased biofilm as compared to the PBS control for ST55, ST4 and ST48 *E. faecalis* strains (Figure 4-11).

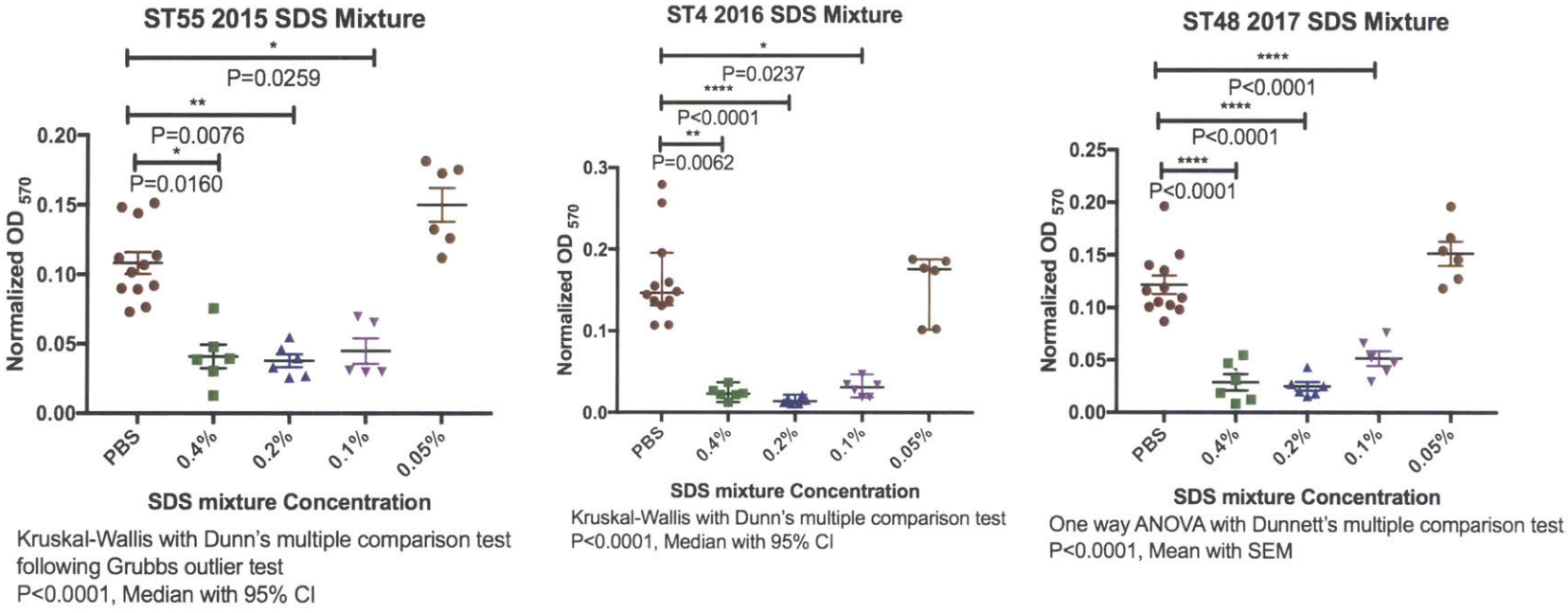

Figure 4-11: Evaluation of SDS-bicarbonate-periodate against *E. faecalis* biofilms

4.7.4 Efficacy of antimicrobial peptides LL-37 and PR-39 against *E. faecalis* biofilm

Next we evaluated the ability of LL-37 and PR-39 to decrease biofilm. We evaluated LL-37 against all three ST and PR-39 against ST4 strains. Our results did not find antimicrobial peptides to be consistently effective at decreasing biofilm for any strain (Figure 4-12).

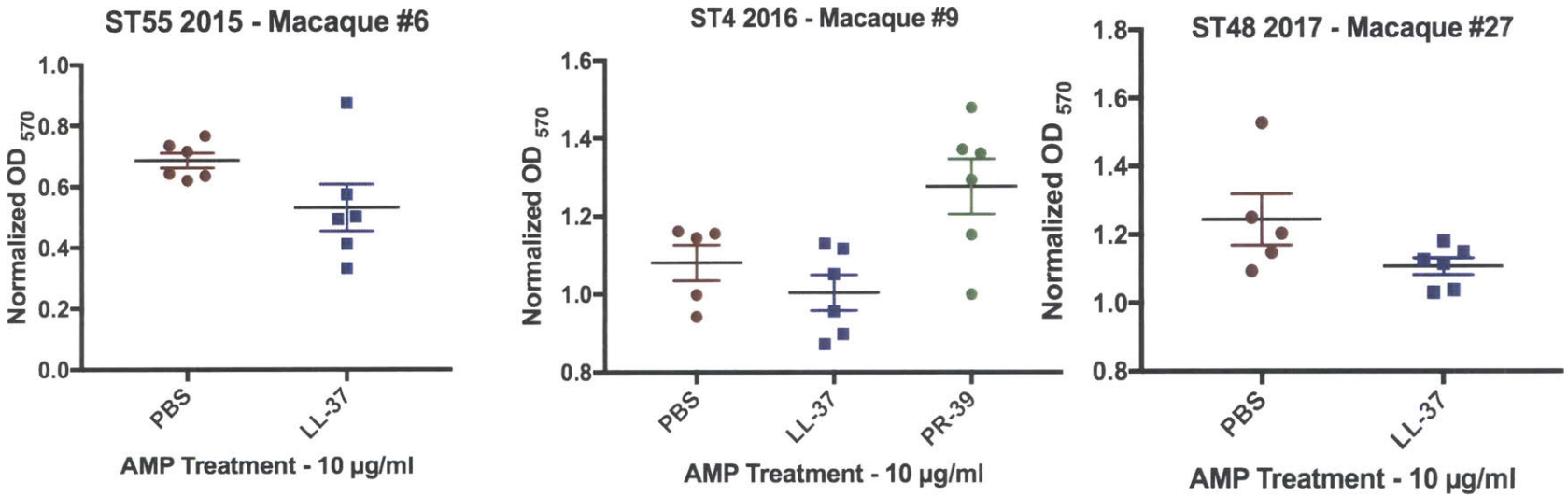

Figure 4-12: Evaluation of the AMPs against *E. faecalis* biofilm

4.7.5 Efficacy of lytic bacteriophage against *E. faecalis* biofilm

We next evaluated the ability of lytic bacteriophages 1 and 3 to decrease *E. faecalis* biofilm, at a dose of $5x10^7$ PFU/well for phage 1, $5x10^8$ for phage 3 and in combination. For ST55 (which was susceptible to plaque formation upon exposure to phages 1 and 3), biofilm was significantly decreased as compared to the control, for both phages individually, as well as in combination (Figure 4-13. Biofilm from the 2016 ST4 was also significantly reduced by treatment with phage 3, even though this isolate only intermittently forms plaques with exposure to phage 3. Neither phage 1 or 3 was effective at decreasing ST48 biofilm.

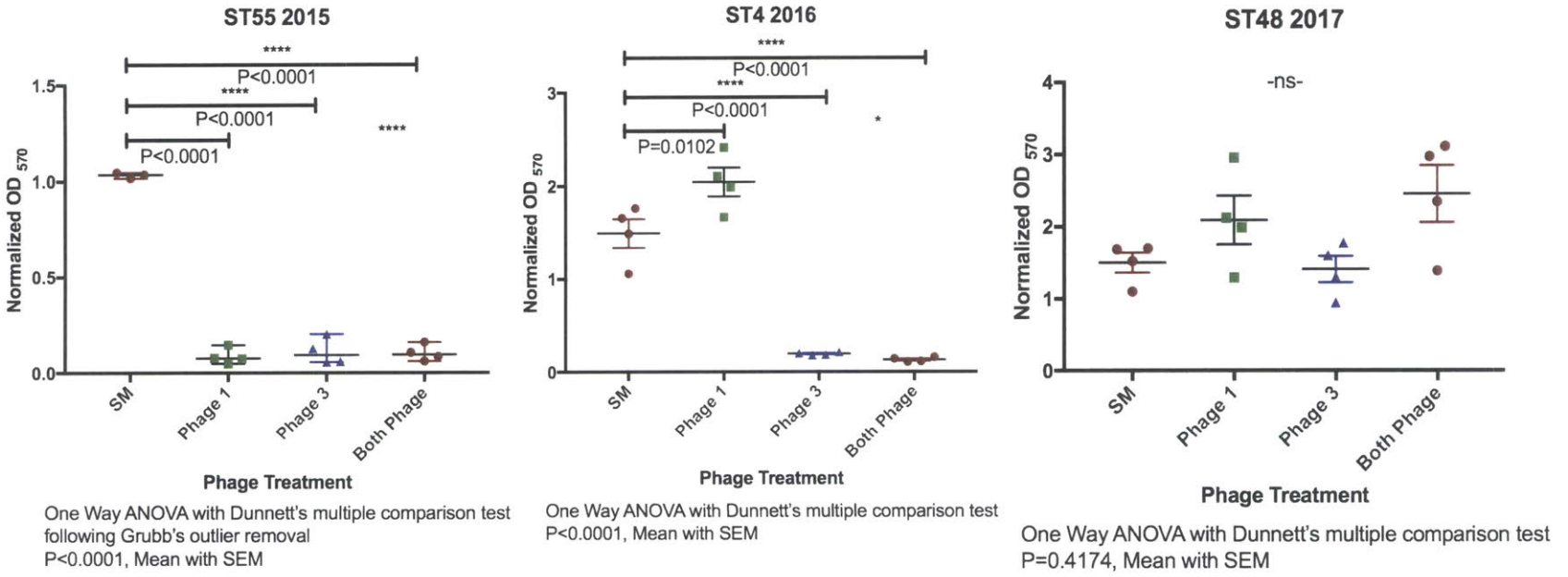

Figure 4-13: Evaluation of lytic bacteriophages 1 and 3 against *E. faecalis* biofilm. Phages were tested at a dose of $5x10^7$ PFU/well for phage 1 and $5x10^8$ PFU/well for phage 3

4.7.6 Efficacy of combination antimicrobial and phage treatment against *E. faecalis* biofilm

We next evaluated whether phage in combination with antimicrobials would be synergistic against *E. faecalis* biofilm. We evaluated combinations of phages at a dose of $5x10^7$ PFU/well with bacitracin, erythromycin, gentamicin at concentrations of 64μg/ml (Figures 4-14, 4-15, 4-16). From two-way ANOVA results, no interaction was observed between phages and antimicrobials for any strain. Post-hoc testing confirmed that phages 1, 3 and both phages in combination were more effective as compared to the control for ST55, and phage 3 and both phages in combination were effective for ST4. For ST48, post-hoc testing identified bacitracin treatment as providing some efficacy against biofilm, consistent with previous results (Figure 4-8).

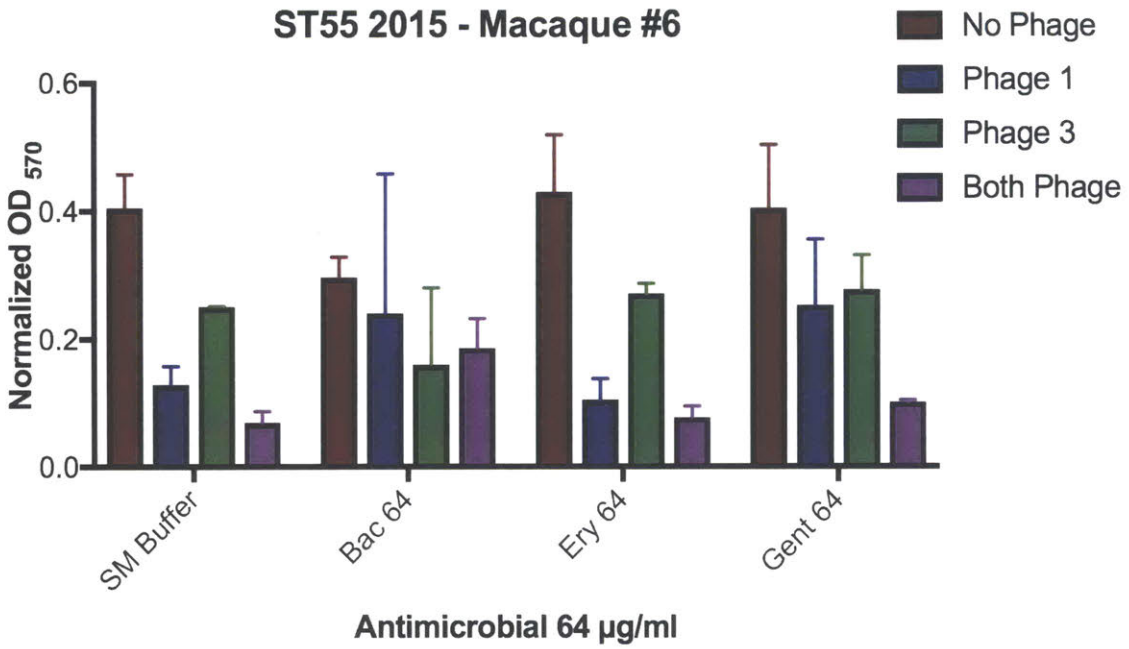

Source of Variation	% of total variation	P value	P value summary	Significant?
Interaction	14.51	0.0587	ns	No
Antimicrobial	1.805	0.5102	ns	No
Phage	59.21	<0.0001	****	Yes

Dunnett's multiple comparisons test	Mean Diff.	95.00% CI of diff.	Significant?	Summary	Adjusted P Value
No Phage vs. Phage 1	0.2024	0.1222 to 0.2827	Yes	****	<0.0001
No Phage vs. Phage 3	0.1444	0.06411 to 0.2246	Yes	***	0.0003
No Phage vs. Both Phage	0.2759	0.1957 to 0.3562	Yes	****	<0.0001

Figure 4-14: Evaluation of combination antimicrobials and lytic phage against the 2015 ST55 *E. faecalis* isolate. All antimicrobials were tested at a concentration of 64μg/ml and phages were tested at $5x10^7$ PFU/well

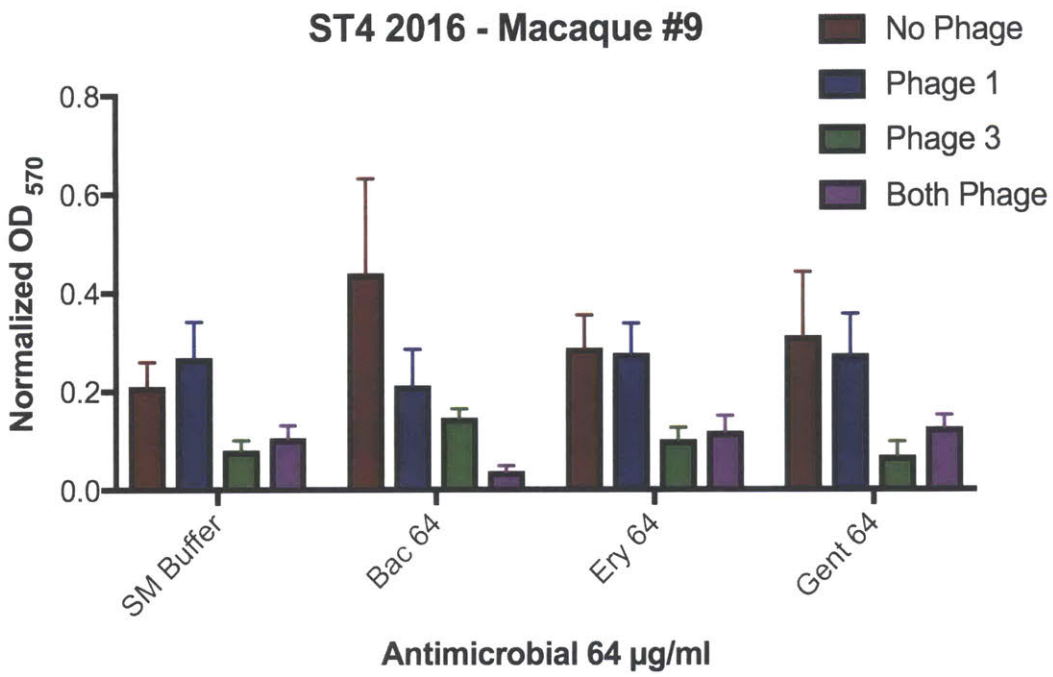

Source of Variation	% of total variation	P value	P value summary	Significant?
Interaction	14.24	0.0541	ns	No
Antimicrobial	1.581	0.5499	ns	No
Phage	60.62	<0.0001	****	Yes

Dunnett's multiple comparisons test	Mean Diff.	95.00% CI of diff.	Significant?	Summary	Adjusted P Value
No Phage vs. Phage 1	0.0541	-0.0194 to 0.1276	No	ns	0.1882
No Phage vs. Phage 3	0.2131	0.1396 to 0.2866	Yes	****	<0.0001
No Phage vs. Both Phage	0.2158	0.1423 to 0.2893	Yes	****	<0.0001

Figure 4-15: Evaluation of combination antimicrobials and lytic phage against the 2015 ST55 *E. faecalis* isolate. All antimicrobials were tested at a concentration of 64μg/ml and phages were tested at $5x10^7$ PFU/well

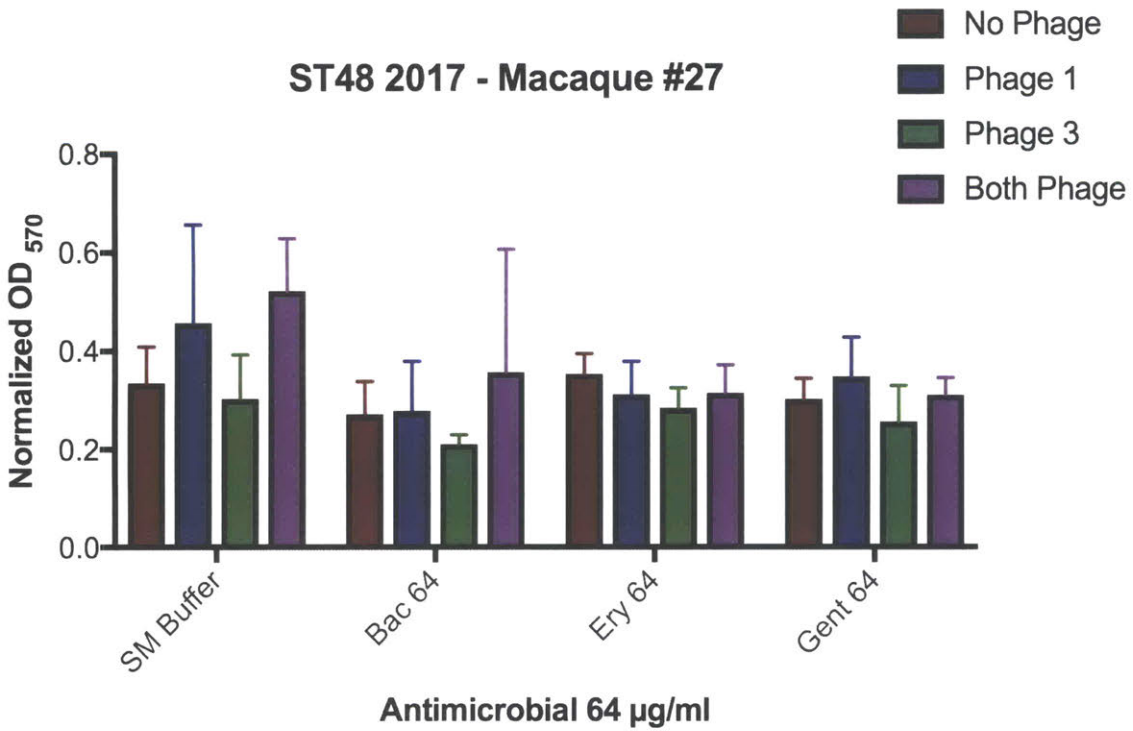

Source of Variation	% of total variation	P value	P value summary	Significant?
Interaction	10.68	0.7319	ns	No
Antimicrobial	18.17	0.0293	*	Yes
Phage	14.26	0.0640	ns	No

Dunnett's multiple comparisons test	Mean Diff.	95.00% CI of diff.	Significant?	Summary	Adjusted P Value
SM Buffer vs. Bac 64	0.1251	0.022 to 0.2282	Yes	*	0.0144
SM Buffer vs. Ery 64	0.08864	-0.01448 to 0.1918	No	ns	0.1046
SM Buffer vs. Gent 64	0.1008	-0.002368 to 0.2039	No	ns	0.0567

Figure 4-16: Evaluation of combination antimicrobials and lytic phage against the 2016 ST4 *E. faecalis* isolate. All antimicrobials were tested at a concentration of 64μg/ml and phages were tested at 5x10^7 PFU/well

4.7.7 Efficacy of combination antimicrobial and antimicrobial peptide treatment against *E. faecalis* biofilm

Because previous work has identified synergy between antimicrobials and antimicrobial peptides [73], we wanted to evaluate if combination therapy would be effective against *E. faecalis* biofilms. Specifically, we were interested in the abilities of AMPs to work with antimicrobials targeting bacterial cell wall integrity. We evaluated ampicillin, bacitracin and vancomycin at concentrations of 64μg/ml with LL-37 (all strains) and PR-39 for the ST4 strain at a concentration of 10μg/ml. We did not identify synergistic interactions or efficacy with any combinations of antimicrobials and peptides based results of two-way ANOVAs (Figures 4-17, 4-18, 4-19).

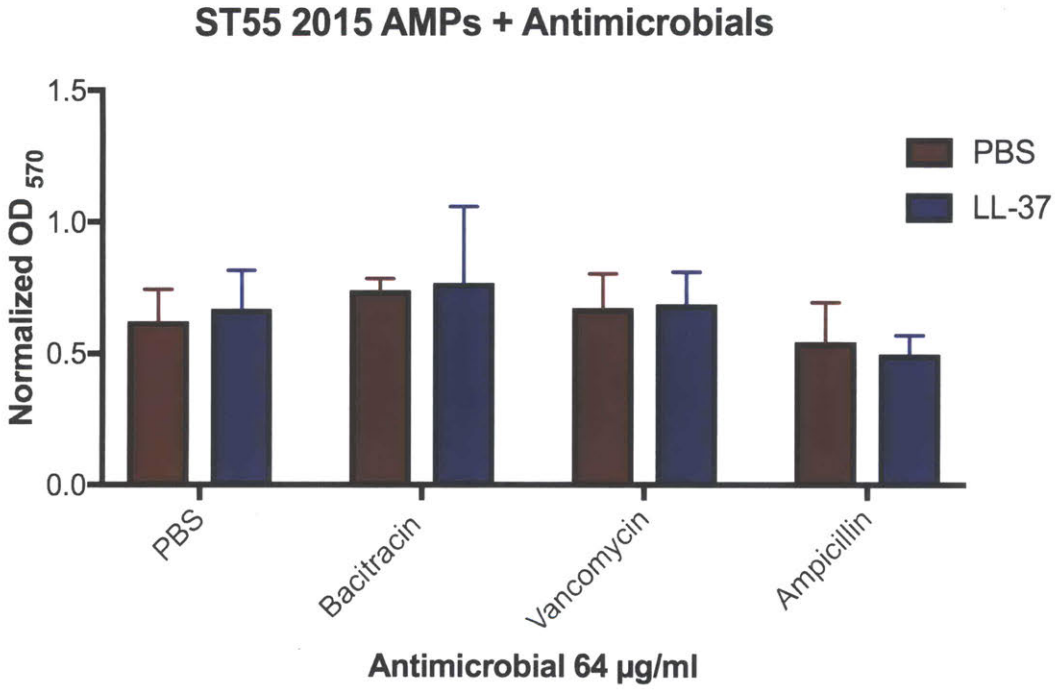

Source of Variation	% of total variation	P value	P value summary	Significant?
Interaction	1.338	0.9548	ns	No
Antimicrobial	31.76	0.0933	ns	No
AMP	0.1275	0.8634	ns	No

Figure 4-17: Evaluation of combination antimicrobials and antimicrobial peptides against the 2015 ST55 *E. faecalis* isolate. All antimicrobials were tested at a concentration of 64μg/ml and LL-37 was tested at a concentration of 10μg/ml

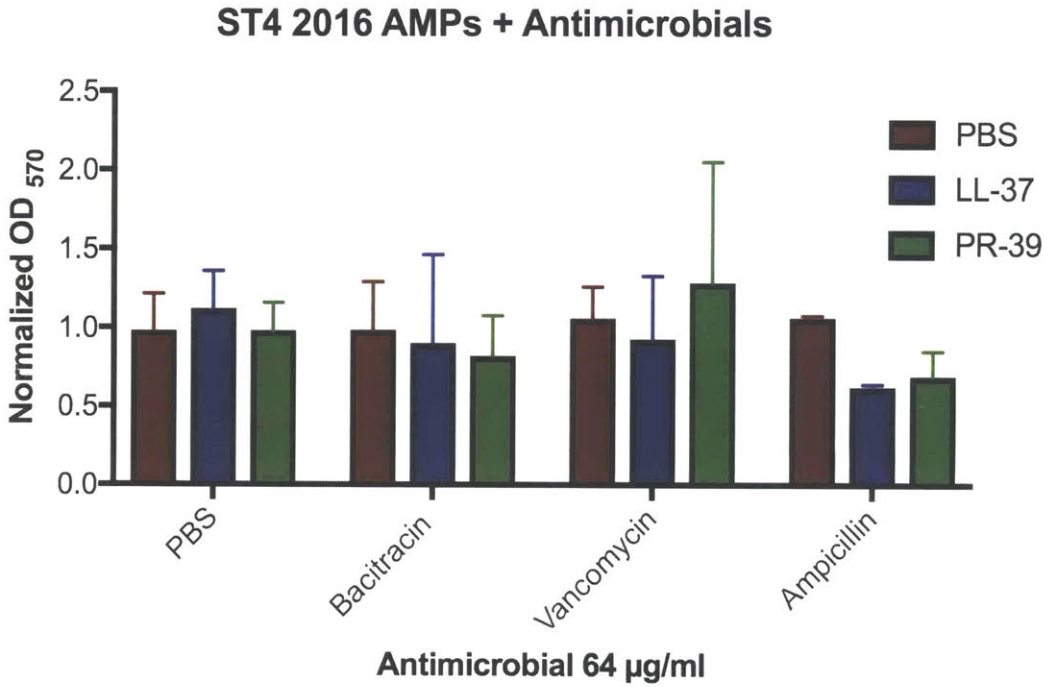

Source of Variation	% of total variation	P value	P value summary	Significant?
Interaction	13.01	0.6390	ns	No
Antimicrobial	11.94	0.2916	ns	No
AMP	2.565	0.6588	ns	No

Figure 4-18: Evaluation of combination antimicrobials and antimicrobial peptides against the 2016 ST4 *E. faecalis* isolate. All antimicrobials were tested at a concentration of 64μg/ml and LL-37 and PR-39 were tested at a concentration of 10μg/ml

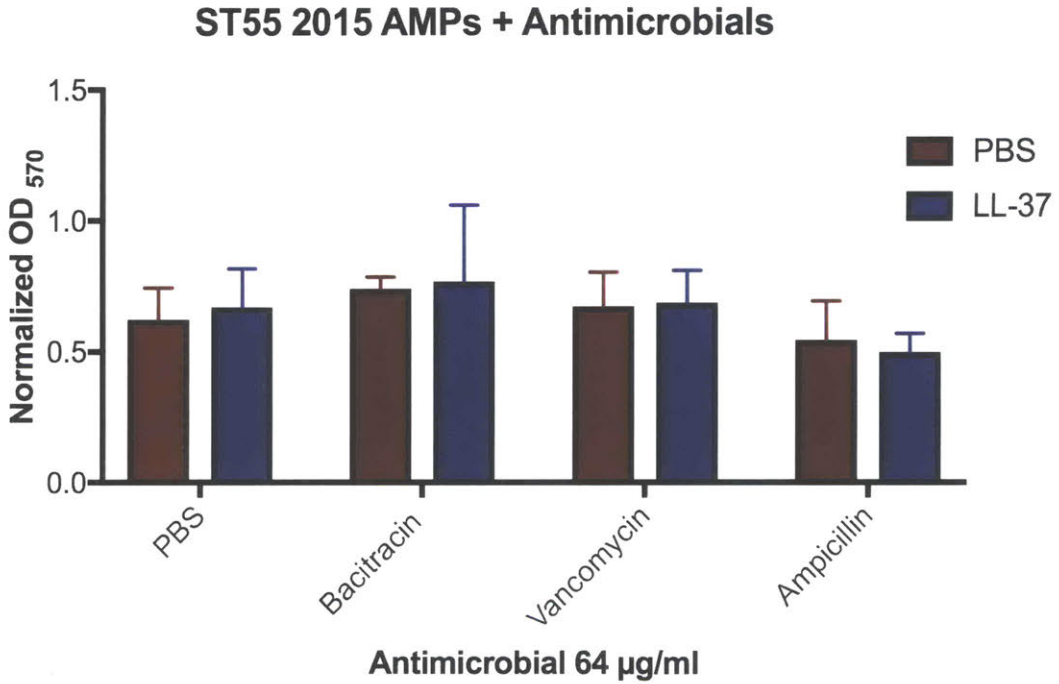

Source of Variation	% of total variation	P value	P value summary	Significant?
Interaction	1.338	0.9548	ns	No
Antimicrobial	31.76	0.0933	ns	No
AMP	0.1275	0.8634	ns	No

Figure 4-19: Evaluation of combination antimicrobials and antimicrobial peptides against the 2017 ST48 *E. faecalis* isolate. All antimicrobials were tested at a concentration of 64μg/ml and LL-37 was tested at a concentration of 10μg/ml

4.7.8 Efficacy of combination phage and AMP treatment against *E. faecalis* biofilm

Finally, we wanted to evaluate if phages and AMPs would work synergistically against *E. faecalis* biofilms. We evaluated combinations of phages 1, 3 and both phages with LL-37 for the 2015 ST55 isolate, combinations of phage 3 with LL-37 and PR-39 against the 2016 ST4 isolate and phage 3 with LL-37 for the ST48 isolate. Phages were tested at a concentration of $5x10^7$ PFU/well and peptides were tested at a concentration of 10μg/ml. No synergy was identified between phages and AMPs with any combination therapy (Figures 4-20. 4-21, 4-22).

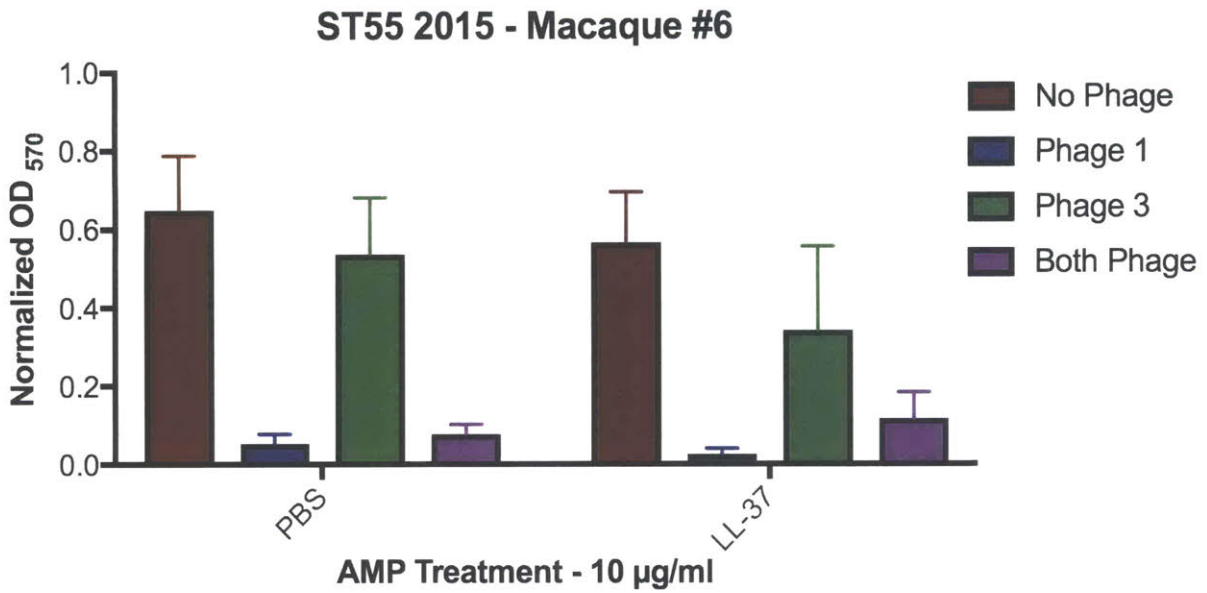

Source of Variation	% of total variation	P value	P value summary	Significant?
Interaction	2.629	0.1072	ns	No
AMP	1.592	0.0543	ns	No
Phage	79.59	<0.0001	****	Yes

Dunnett's multiple comparisons test	Mean Diff.	95.00% CI of diff.	Significant?	Summary	Adjusted P Value
No Phage vs. Phage 1	0.5682	0.4519 to 0.6845	Yes	****	<0.0001
No Phage vs. Phage 3	0.1689	0.05261 to 0.2852	Yes	**	0.0029
No Phage vs. Both Phage	0.511	0.3947 to 0.6273	Yes	****	<0.0001

Figure 4-20: Evaluation of combination lytic phage and antimicrobial peptides against the 2015 ST55 *E. faecalis* isolate. Phages were tested at a concentration of 10^7 PFU/well and LL-37 was tested at a concentration of 10μg/ml. Experiments performed with replicates of 6.

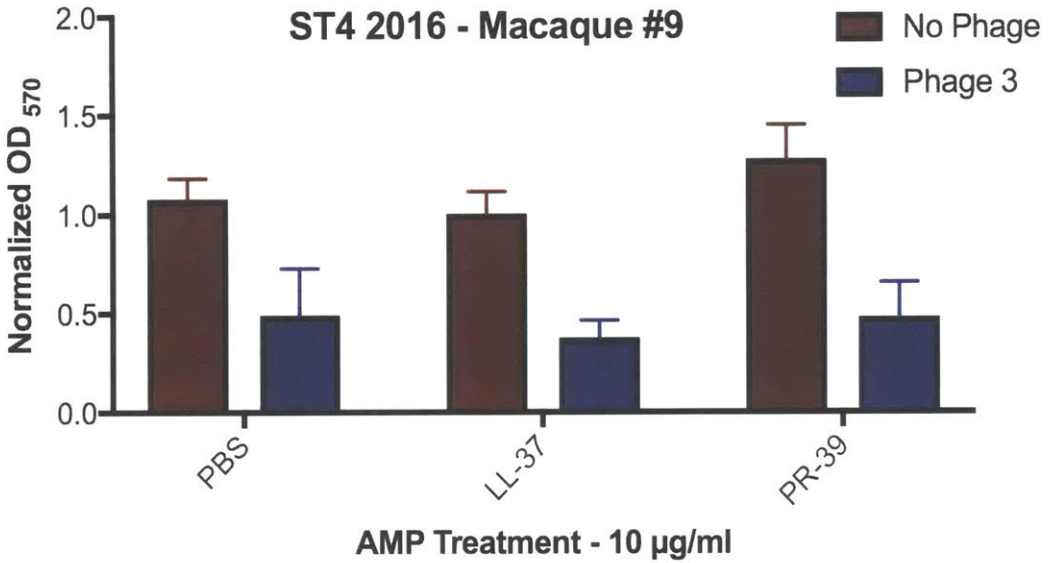

Source of Variation	% of total variation	P value	P value summary	Significant?
Interaction	1.41	0.2617	ns	No
AMP	4.26	0.0242	*	Yes
Phage	78.92	<0.0001	****	Yes

Dunnett's multiple comparisons test	Mean Diff.	95.00% CI of diff.	Significant?	Summary	Adjusted P Value
PBS vs. LL-37	0.06903	-0.08429 to 0.2224	No	ns	0.4808
PBS vs. PR-39	-0.1189	-0.2722 to 0.03445	No	ns	0.1440

Figure 4-21: Evaluation of combination lytic phage and antimicrobial peptides against the 2016 ST4 *E. faecalis* isolate. Phage 3 was tested at a concentration of 10^7 PFU/well and LL-37 and PR-39 were tested at a concentration of 10μg/ml. Experiments performed with replicates of 6.

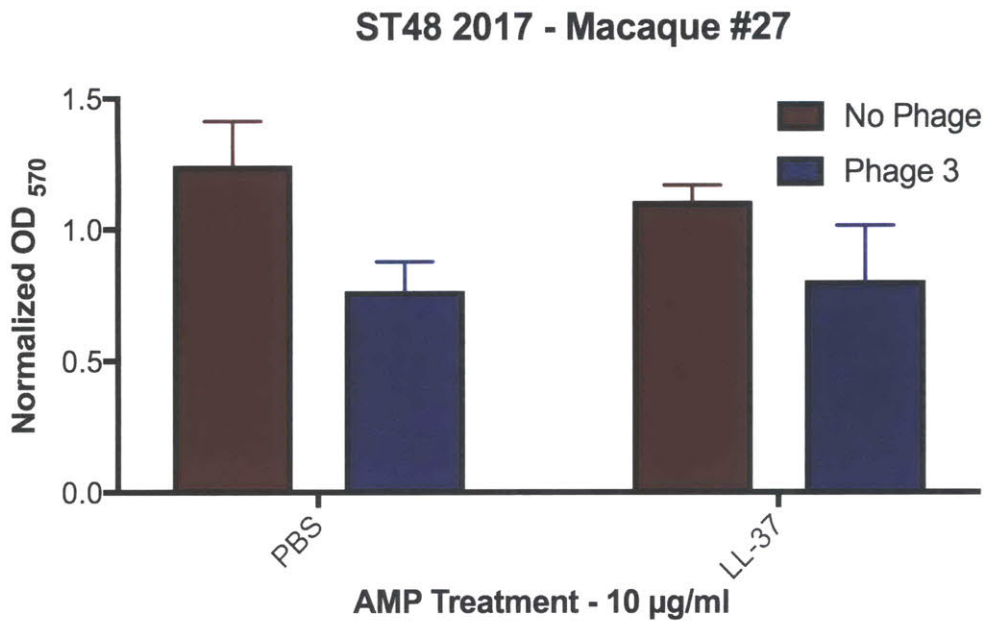

Source of Variation	% of total variation	P value	P value summary	Significant?
Interaction	3.388	0.1682	ns	No
AMP	1.103	0.4237	ns	No
Phage	66.17	<0.0001	****	Yes

Dunnett's multiple comparisons test	Mean Diff.	95.00% CI of diff.	Significant?	Summary	Adjusted P Value
PBS:No Phage vs. PBS:Phage 3	0.4774	0.2503 to 0.7045	Yes	***	0.0001
PBS:No Phage vs. LL-37:No Phage	0.1384	-0.08872 to 0.3654	No	ns	0.3052
PBS:No Phage vs. LL-37:Phage 3	0.4396	0.2125 to 0.6667	Yes	***	0.0003

Figure 4-22: Evaluation of combination lytic phage and antimicrobial peptides against the 2017 ST48 *E. faecalis* isolate. Phage 3 was tested at a concentration of 10^7 PFU/well and LL-37 was tested at a concentration of 10μg/ml. Experiments performed with replicates of 6.

4.8 Discussion

We evaluated the efficacy of traditional antimicrobials, antimicrobial peptides and lytic bacteriophages, alone, and in combination, against biofilm produced by *E. faecalis* strains isolated from CRCs of research macaques. Our results revealed that antimicrobial treatment of biofilm was generally ineffective, regardless of MIC, as demonstrated by evaluating ST48 biofilms treated with antimicrobials at concentrations ranging from 2-4x to 256x the MIC. The only antimicrobial showing efficacy at decreasing biofilm was bacitracin, which showed efficacy at 1.25x the MIC for ST55, 10x the MIC for ST4 and 2-4x the MIC for ST48. Previous studies evaluating treatment for *S. aureus* biofilms have noted efficacy of bacitracin for both *in vitro* and murine skin wound models, with the former evaluating bacitracin as a component of triple antibiotic ointment [204, 205].

Next, we evaluated two antimicrobial peptides; human LL-37 and porcine PR-39. Both peptides are members of the cathelicidin family of peptides, characterized by intracellular storage in an unprocessed form, and activated after cleavage from an approximately 100-amino acid N-terminal domain [206]. LL-37 acquires an alpha-helical structure in its activated state, while PR-39 is rich in proline and adopts a more extended structure [206]. While both peptides showed MICs of 5-40μg/ml against planktonic cultures of ST4 isolates, ST48 and ST55 isolates demonstrated MICs of >40μg/ml. Previous studies have identified lack of correlation between MICs on planktonic cultures with anti-biofilm activity, with small cationic peptides displaying strong biofilm inhibition against *Listeria monocytogenes* and *Pseudomonas aeruginosa* despite significantly higher MICs [194]. When evaluating anti-biofilm activity, we did find consistent anti-biofilm activity from either LL-37 or PR-39 at 10μg/ml. Additionally, combining AMPs together did not offer any benefit vs. using either peptide alone. Limited work has examined effectiveness of AMPs against *E. faecalis* and has mostly focused on planktonic MICs rather than as antibiofilm agents. The AMPs melittin (a peptide component of bee venom) demonstrated MICs of 2-4μg/ml against ATCC *E. faecalis* 29212 and 1.25-2.5μM (3.5-7μg/ml) against *E. faecium* in previous studies [207, 208]. Melittin is less desirable for use as an AMP because of its cytotoxic and pro-apoptotic effects on eukaryotic cells [209]. Previously, pleurocidin has also been demonstrated to have MICS of 2.5-

5μM (6.7-13.5μg/ml) against *E. faecium*, however our strains demonstrated MICs of 10 to >20μg/ml. Our findings of PR-39 (aka cecropin P1) being ineffective on planktonic cultures was supported by previous work demonstrating MICs of >256μg/ml against ATCC *E. faecalis* 29212 [207, 210].

Previously, lytic bacteriophages (both naturally isolated and genetically engineered) have demonstrated remarkable efficacy at diminishing *E. faecalis* biofilms [184, 211]. We were surprised to see that lytic phage 3 demonstrated efficacy against biofilms formed by ST4 despite inconsistent plaque formation on double-agar overlay assays. We additionally identified some efficacy of phage 3 against biofilm the 2017 ST48 isolate when evaluating phage-AMP combination therapy (Figure 4-22), and had previously confirmed that phage 3 does not form plaques on ST48. Phage 3 efficacy against ST48 was not consistent between different experiments (Figure 4-16), thus this finding needs further evaluation before definitive conclusions can be drawn. Mechanisms of biofilm disruption by phages include both penetration and infection of biofilm-forming bacteria as well as secretion of enzymes (polysaccharidases, polysaccharide lyases and hydrolases) which are able to degrade the EPS layer [212, 188, 213]. It is the latter mechanism that we hypothesize as the source of efficacy of phage 3 against ST4 (and potentially ST48) biofilms. Phage enzymes have been described against Gram-negative bacteria, including *P. aeruginosa*, *Enterobacter agglomerans*, and *Serratia marcescens*, as well as Gram-positive *Staphylococcus epidermidis* [214, 215, 216]. Similarly to our findings, evaluation of phage efficacy against *S. epidermidis* strains identified a statistically significantly decrease in biofilm production after 24 hours of treatment, in strains both highly and poorly susceptible to lysis on agar plates [216].

Combinations of the antimicrobial agents ceftazidime, ciprofloxacin, imipenem and tobramycin with D-enantiomeric cationic peptides were previously shown to decrease the minimum biofilm inhibitory concentrations of antimicrobials from 2-16 fold for several Gram negative bacterial species including *P. aeruginosa*, *E. coli*, *Acinetobacter baumannii*, *Klebsiella pneumoniae* and *Salmonella enterica* [74, 73]. The hypothesized mechanism of synergistic action is related to peptide-mediated dispersal of biofilms allowing antimicrobial penetration [74, 217]. We hypothesized that LL-37 would promote synergy for ST4 strains in combination with various antimicrobials at concentrations significantly higher than the MICS; i.e. ampicillin

was tested at 64x MIC, bacitracin was tested at 8x the MIC, and vancomycin was tested at 32-64x MIC. We unfortunately did not observe any synergy, as assessed by 2-way ANOVA, for any of the strains or antimicrobials tested (Figure 4-18). Possible reasons for failure to observe synergy is that antimicrobials and peptides interacted antagonistically, or the mechanism of peptide-antibiotic synergy is unrelated to biofilm dispersal in *E. faecalis* vs. Gram-negative bacteria.

We did not identify synergy between antimicrobials and lytic phages for ST55, ST4 or ST48 *E. faecalis* isolates tested; the observed decreases in biofilm for ST55 and ST4 were strongly related to phage treatment based on post-hoc testing and results observed for phage treatment alone. We also failed to identify synergy between peptides and bacteriophage treatment. Combination of phages and antimicrobial peptides has not previously been evaluated; future work should aim to understand the mechanisms of anti-biofilm properties to improve predictions for whether combinatorial therapies are more efficacious than bacteriophages alone.

Finally, chemical biofilm treatments consisting of sodium dodecyl sulfate, sodium bicarbonate and sodium periodate were efficacious in reducing biofilm for all three *E. faecalis* ST tested. Because sodium periodate is a skin irritant, chemical treatment of biofilm should be limited to abiotic implant surfaces, or for treating external surfaces (such as PMMA). The toxicity levels of sodium periodate are not well-described; the LD50 in mice is reported to be 58 mg/kg [218], but the contact time required for skin irritation has not been evaluated.

4.9 Conclusions

In this chapter we have described isolation and characterization of lytic bacteriophages with efficacy against multi-drug resistant *E. faecalis.* We evaluated the treatment efficacy of bacteriophages, two antimicrobial peptides and a chemical mixture against *E. faecalis* biofilms using *in vitro* models. Our results suggest that lytic bacteriophages are highly efficacious in decreasing *E. faecalis* biofilms for susceptible strains, while neither antimicrobials nor the antimicrobial peptides LL-37 or PR-39 showed consistent anti-biofilm properties. Finally, chemical treatment offers another potential tool for treating biofilms on abiotic implant surfaces. Future studies should

evaluate safety, efficacy and optimal dosing strategies for these alternative therapies, using cell culture and animal models of infection. Further characterization of bacterial binding targets for lytic phage may offer insight into genetic manipulation for expanding *E. faecalis* susceptible strain range.

Chapter 5

Summary, Conclusions and Future Directions

In this dissertation, we have probed the complex bacterial ecosystem colonizing CRCs in macaques under study for cognitive neuroscience research. Our goals were to better understand which bacterial species were most prevalent inside CRCs, and to characterize antimicrobial resistance for an improved ability to treat infectious complications of implants when they arise.

In Chapter 1 we introduced the use of CRCs in research macaques and the more common types of acute and chronic complications observed with surgical implantation. While uncommon, infectious complications can have devastating outcomes for affected macaques, necessitating understanding of the bacterial species potentially contributing to infections. CRC sanitization protocols were updated in September, 2014 and we wished to understand how improved CRC sanitization techniques and prohibition of topical antimicrobials affected bacterial species commonly colonizing CRCs (and their antimicrobial resistance profiles).

In Chapter 2 we compared traditional culture-dependent techniques for characterizing bacterial communities with state-of-the-art, culture-independent, next-generation sequencing techniques. Use of 16S community analysis on purulent polymicrobial samples is a novel use of this technique as compared to the previously described literature. As well as identifying aerobes and anaerobes living within CRCs, we compared communities between CRCs, the implant-skin margin, the oral cavity and feces to

determine that CRC communities vary between macaques, and in most cases, have greater similarities to skin margin and oral communities than fecal communities. While skin, oral and fecal bacterial communities in macaques have been previously evaluated individually, this is the first time communities have been compared together. Our data lays a preliminary foundation for a "macaque microbiome project" and can serve as a non-human primate reference point for comparison with future macaque and human studies.

Future work should evaluate skin and oral samples before and sequentially after CRC implantation to identify shifts in bacterial communities over time. Because CRC colonization is hypothesized to arise from skin and oral communities, the use of different skin margin sanitization protocols and the role of a regular dental hygiene program could be evaluated to see if overall bacterial burden can be decreased. As utilization of custom, PMMA-free CRC implants increases, more definitive conclusions can be made regarding the role of PMMA on the composition of CRC bacterial communities.

We determined that the vast majority of species living within CRCs are obligate anaerobes and are under-represented by traditional cultures, even when using anaerobic culture techniques. We also identified that the most prevalent aerobic species cultured from CRCs is *S. aureus*, and that isolates have maintained an antimicrobial-sensitive phenotype between 2011 and 2018. We determined that *E. faecalis* was the second most prevalent aerobic species isolated from CRCs in 2011 and displayed a multi-drug resistant phenotype, necessitating further understanding of this opportunistic pathogen. We were encouraged by noting decreases in the prevalence of both *E. faecalis* and *Proteus* spp. cultured from CRC samples between 2011 and 2018; because these species showed marked antimicrobial resistance, we hope that improved antimicrobial stewardship will continue to minimize selection for potential resistant pathogens.

In Chapter 3 we discussed characterization and long-term colonization dynamics of *E. faecalis* isolated from macaque CRCs between 2011 and 2017. We performed antimicrobial susceptibility testing to confirm resistant phenotypes, evaluated biofilm production and analyzed whole genome sequences to identify resistance and virulence factor genes, and to analyze variants. We determined that ST4 and ST55 lineages isolated from the

same macaques remained relatively stable over time for resistance and virulence factor genotypes, but noted subtle increases in biofilm production phenotype over time. Variant analysis identified mutations in the DNA repair genes *mut*S and *mutL*, and we confirmed that isolates with mutations in these genes displayed a hypermutator phenotype. This phenotype is important to identify as future antimicrobial treatment, if warranted, can be complicated by increased development of resistance.

We identified a shift in *E. faecalis* lineages from ST4 and ST55 strains displaying marked antimicrobial resistance, to ST48 strains displaying a strong biofilm phenotype, but minimal antimicrobial resistance. The majority of this shift occurred following updates to our CRC sanitization protocol. We hypothesize that the loss of selective pressure from prohibition of antimicrobial use within CRCs, and more judicious use of antimicrobials overall, allowed the less resistant ST48 lineage to predominate over more resistant strains. Future work should continue to monitor *E. faecalis* ST and resistance patterns, as implanted macaques can serve as a model for evolution and *E. faecalis* strain succession within a hospital environment.

In Chapter 4 we evaluated different techniques for treating *E. faecalis* and decreasing *E. faecalis* biofilm. We isolated lytic bacteriophages from sewage and demonstrated their efficacy in killing multi-drug resistant ST55 *E. faecalis* isolates, as well as treating *E. faecalis* biofilms. Transmission electron microscopy identified these phages as likely Siphoviruses based on their morphology, which was also confirmed by comparison of phage genomes to previously sequenced phages. Future work should aim to identify the receptors necessary for phage efficacy and fully characterize optimal lysis kinetics.

Finally, we investigated multiple techniques for treating *E. faecalis* biofilm. We demonstrated that traditional antimicrobials, even at concentrations well above MICs, were ineffective at decreasing *E. faecalis* biofilm. We confirmed that a detergent solution of sodium dodecyl sulfate, sodium bicarbonate and sodium periodate at 0.1% w/v each was effective at decreasing biofilm for all strains tested. Because sodium periodate has potential local toxicity effects, use of this solution should be reserved for non-biologic surfaces (dental acrylic, implant hardware) until safety can be evaluated in an *in vivo* model.

We evaluated two cathelicidin antimicrobial peptides; human LL-37 and

porcine PR-39. While both peptides showed potential anti-bacterial activity against ST4 *E. faecalis* isolates based on MICs, neither were able to show consistent anti-biofilm activity. Future work should evaluate other antimicrobial peptides of different classes for efficacy against *E. faecalis* biofilm, as these types of therapies appear to show promise for Gram-negative, biofilm-forming bacterial species.

We demonstrated that lytic bacteriophages are effective at decreasing biofilm in both ST55 and ST4 strains. As well as the ability to pass through the biofilm and infect cells, phages can secrete enzymes able to degrade extrapolymeric substance. We tested varying combinations of antimicrobials, antimicrobial peptides and lytic bacteriophages to evaluate synergistic interactions, but only recognized reliable decreases in biofilm associated with bacteriophage treatment combinations. Future work should evaluate the safety, efficacy and optimal dosing regimen of lytic bacteriophages against biofilm using an *in vivo* mouse skin wound model.

Overall, this work has provided a better understanding of CRC bacterial communities; exploring at both the population level as well as an in-depth examination of how an individual species persists and evolves over time. Macaques are a popular research model for understanding cognitive neuroscience, and our work has implications for improving animal health at both our institution and other institutions. We have demonstrated that CRC communities are complex bacterial ecosystems and can vary between and within individual macaques. We have also shown that increased antimicrobial stewardship has decreased the prevalence of mutli-drug resistant *E. faecalis* in newly implanted macaques, increasing the probability of successful antimicrobial treatment for infectious sequelae in the future. Our results emphasize the importance of biofilm production in facilitating the persistence of *E. faecalis* in implanted macaques, and highlight the need for evaluating novel strategies when treating biofilm-associated infections. We have identified promising results associated with lytic bacteriophages and further *in vivo* studies should be undertaken to evaluate efficacy of phages for future treatment of both veterinary and human multi-drug resistant *E. faecalis* infections.

Appendix A

2011 Macaque CRC Sanitization Survey

CRC Sanitization Survey Part 1

Animal ID	Sex	Age	Lab	Study ID	Episode(s) of Suspected Meningits?	Date of Sample Collection	Recording?	Gross Appearance of Discharge	Date of Last Cleaning	Cleaning Frequency	Days (Cleaning - Collection)	Recent Use of antimicrobials?	Antimicrobial used
1	F	15	A	A1	0	8/16/11	No response	Purulent, thick, copious (1/2 full)	8/15/11?	No response	1?	No?	NA
2	F	14	A	A2	0	8/16/11	No response	Serous, minimal (1/6 full)	8/12/11?	No response	4?	No?	NA
3	F	12	A	A3	0	8/16/11	No response	Not available	8/15/11?	No response	1?	No?	NA
4	M	11	B	B1	0	8/19/11	Yes	Purulent, slightly hemorrhagic (right well), copious (1/2 full)	8/18/11	SID to 1-2 x/week	1	No	NA
5	M	10	B	B2	0	8/19/11	No	Purulent, foul odor, copious (overflowing with packing)	8/15/11	1 x/week to 1 x/2 weeks	4	Yes	T-PB
6	M	13	B	B3	0	8/24/11	No	*Serous	8/22/11	2 x/week	2	Yes	T-PB
7	M	12	B	B4	0	8/23/11	No	Purulent, hemorrhagic, crusting, foul odor, minimal (1/6 full)	8/9/11	1 x/2 weeks	14	No	NA
8	M	13	B	B5	0	8/24/11	No	Serous to purulent, crusting, hemorrhage (front well), minimal	8/16/11?	1 x/week	8	Yes	T-PB
9	M	13	B	B6	0	8/24/11	No	*Serous	8/22/11	2 x/week	2	Yes	T-PB
10	M	10	B	B7	0	8/24/11	Yes?	*Purulent, minimal (1/4 full after gauze removal)	8/19/11	1 x/week	5	No	NA
11	M	10	B	B8	0	8/26/11	No response	*Serous, gray tissue along well margins (center well), slight	No response	No response	No response	No response	No response
12	M	12	C	C1	0	8/17/11	No	Serosanguinous to purulent, minimal (1/4 full)	8/15/11	3 x/week	2	Yes	G
13	M	12	C	C2	0	8/17/11	No	Serous, minimal (1/4 full)	8/15/11	3 x/week	2	Yes	BNP
14	M	11	C	C3	5/2009	8/17/11	No	Serous, minimal (1/4 full)	8/15/11	2 x/week	2	No	NA
15	M	8	C	C4	0	8/17/11	No	Serosanguinous, minimally purulent, minimal (1/4 full)	8/15/11	2 x/week	2	No	NA
16	F	10	C	C5	0	8/17/11	No	Serous, minimal (1/4 full)	8/15/11	1 x/week	2	No	NA
17	F	11	C	C6	0	8/17/11	No	Serous, purulent (center), minimal (1/4 full)	8/15/11	3 x/week	2	Yes	BNP
18	M	10	C	C7	0	8/17/11	No	Serous, minimal (1/6 full)	8/15/11	3 x/week	2	Yes	G
19	M	10	C	C8	11/2011	8/19/11	Yes	Serosanguinous, moderate (1/3 full)	8/17/11	3 x/week	2	No	NA
20	F	11	D	D1	0	8/18/11	No response	Not available	No response	No response	No response	No response	No response
21	M	8	D	D2	0	8/23/11	No	*Hemorrhagic	8/16/11	1 x/week	7	No	NA
22	M	7	D	D3	12/2011, 10/2011, (3/2011), 1/2011, 5/2010, 3/2010?, 1/2010, (12/2009)	8/23/11	No	Serosanguinous, moderate (1/3 full)	8/18/11	3 x/week	5	No	NA
23	M	7	D	D4	0	8/23/11	Yes	Serous, slightly hemorrhagic, slight	8/22/11	1-2 x/week	1	No	NA
24	M	11	D	D5	0	8/23/11	No	Purulent, slightly hemorrhagic, foul odor, copious (1/2 full)	8/17/11	1 x/week	6	No	NA
25	M	6	D	D6	5/2010	8/23/11	No response	Not available	No response	No response	No response	No response	No response

CRC Sanitization Survey Part 2

					# CRCs		CRC #1		CRC #2		CRC #3			
Animal ID	Sex	Age	Lab	Study ID	With Craniotomies	Without Craniotomies	Location	Time Since Surgery (years)	Location	Time Since Surgery (years)	Location	Time Since Surgery (years)	CRC Material	Additional Comments
1	F	15	A	A1	1	0	Expanded craniotomy-frontal cortices (w/ dura scrape)	1-3					Delrin plastic	3 x 4 cm rectangular chamber
2	F	14	A	A2	1	0	Frontal cortex and striatum	1-3					Delrin plastic	Designed to be large enough to accommodate multiple recording sites within a single well
3	F	12	A	A3	1	0	Frontal cortex	2					Delrin plastic	3 cm x 4 cm square chamber
4	M	11	B	B1	0; (previously had 2)	0	IT	?	PFC	?			Standard Crist Well (Cilux Plastic)	20 mm
5	M	10	B	B2	3	0	V4	3-5	Frontal	3-5	Parietal	1-3	Acrylic	19 mm diameter
6	M	13	B	B3	2	0	V4/pulvinar chamber over lateral occipital/parietal cortex	3-5	IT, frontal cortex	3-5			Metal/Standard Crist Well	IT chamber is metal, V4/Pulv chamber is plastic
7	M	12	B	B4	3	0	Occipital lobe	3-5	Occipital lobe	3-5	Occipital lobe	3-5	Standard Crist Well (Cilux Plastic)	Attached to skull with screws and dental acrylic; 1.0 cm ID (?), craniotomies are 1/4 - 1/3 the diameter (0.5-0.6 cm ID)
8	M	13	B	B5	3	0	Frontal eye field	1-3	V4	1-3	Hippocampus	1-3	Acrylic cylinder	19 mm diameter
9	M	13	B	B6	3	0	IT (through frontal lobe)	<1	V4	<1	Pulvinar (through parietal)	<1	Standard Crist Well (Cilux Plastic)	IT chamber leaks
10	M	10	B	B7	0 (?)	1							Standard Ultem Chamber	20 mm
11	M	10	B	B8	2	0	V4, right	1	Parietal, right	1			Acrylic-less chamber	Base is machined to very closely match the contour of the skull
12	M	12	C	C1	0?	2? (both are probably closed)	Straight over prefrontal cortex	1-3	Slightly angled over parietal cortex	1-3			Standard titanium well	19 mm wells
13	M	12	C	C2	3	0	Parietal	1-3	Frontal	1-3	Temporal	1-3	Titanium and/or stainless steel	Approximately 1 inch cylindrical wells (1.5 cm diameter) with cilux caps
14	M	11	C	C3	2	0	Prefrontal cortex (straight well)	3-5	Angled-bottom well, sensorimotor cortex	3-5			Standard titanium well	19 mm diameter
15	M	8	C	C4	1 (no longer present)	0	Prefrontal cortex	1-3					N/A	
16	F	10	C	C5	2	0	Prefrontal cortex (straight well)	1-3	Angled-bottom well, sensorimotor cortex	1-3			Standard titanium well	19 mm diameter
17	F	11	C	C6	3	0	Parietal	1-3	Frontal	1-3	Temporal	1-3	Titanium and/or stainless steel	Approximately 1 inch cylindrical wells (1.5 cm diameter) with cilux caps
18	M	10	C	C7	0?	2? (both are probably closed)	Straight over prefrontal cortex	1-3	Slightly angled over parietal cortex	1-3			Standard titanium well	19 mm wells
19	M	10	C	C8	0?	2? (both are probably closed)	Straight over prefrontal cortex	<1	Slightly angled over parietal cortex	<1			Standard titanium well	19 mm wells
20	F	11	D	D1	1	0	Left hemisphere, dorsal surface (AP=15)	3-5					Standard Crist Well (Cilux Plastic)	18 mm inner diameter
21	M	8	D	D2	1	0	Right hemisphere, IT cortex	3-5					Stainless steel	19 mm inner diameter, 22 mm outer diameter
22	M	7	D	D3	1	0	Right parietal lobe	1-3					Standard Crist Well (Cilux Plastic)	Circular
23	M	7	D	D4	1	0	?	<1					Stainless steel	50 degrees bevel
24	M	11	D	D5	2 (in one well)	0	Left Hemisphere, IT cortex	3-5					Stainless steel	19 mm inner diameter, 22 mm outer diameter
25	M	6	D	D6	1	0	?	1.5					Standard Crist Well (Cilux Plastic)	18 mm inner diameter

CRC Sanitization Survey Part 3.1

Animal ID	Sex	Age	Lab	Study ID	Description of Discharge	Cleaning Frequency during Recording	Cleaning Frequency When Not Recording	Description of CRC Cleaning	CRC Cleaning Prior to Recording	Electrode Sterilization	Antimicrobial Used	Criteria for Topical Antimicrobial Use	Systemic Antimicrobials Used?	Packing materials used in CRC
1	F	15	A	A1	Small amount of green discharge with a foul odor	Daily	Three times a week	Wash out the discharge in the well with 250 ml of sterile saline, with the suction tube; soak the inside of the chamber with 10% betadine solution for 3-5 minutes; wash out the remaining betadine solution and rinse well with 250 ml of sterile water	Same	*Not yet done; Electrodes are chronically implanted (sterilized before implant)	G	Occasionally- during recording when monkey has chronic electrode implants, and when there is green pus in the well	Yes; Baytril, Ceftriaxone, or Cefazolin- occasional--same as for topical antibiotics	None
2	F	14	A	A2	Yellow, occasionally green, milky, odorless	Daily	Twice a week	Initial rinse with 20 ml sterile saline, followed by betadine solution (5 ml betadine + 15 ml sterile saline) soak for 2 minutes; during soak, wipe inside and outside edge of well, including tissue margin, with same betadine solution; after soak, flush well and surrounding area with sterile saline; use new sterile pipettes and 20 ml syringe for each cleaning session	Same, except only the inside is cleaned before each recording (outside of well and tissue margins cleaned twice a week)	Hydrogen peroxide (sterrad)	NA	NA	No	None
3	F	12	A	A3	Transparent, odorless	Daily	Twice a week	Wash the inside of the chamber using one saline bottle (250 ml), syringe, needle, and suction; all instruments are sterilized and disposable	Same	Electrodes are chronically implanted (sterilized before implant)	1:20 Diluted enrofloxacin 22.7mg/ml	Daily	No	None
4	M	11	B	B1	Thick, white to yellow, foul odor	Daily	Twice a week	Glass pipets soaked in Nolvasan used for aspiration, chambers flushed with Nolvasan	Same with the addition that betadine swabs are used; a film of betadine is left on the tissue for 5-10 minutes before inserting electrodes	Soaked in Nolvasan for 15 minutes; after use, electrodes require a special enzymatic cleaning solution (rinsed with water)	NA	Occasionally the day of surgery	No	Sterile non-woven sponge balls
5	M	10	B	B2	White, small to moderate amount, foul odor	Daily	2 weeks	Discharge is removed by suction; hydrogen peroxide is put into well, and then removed (3x); saline used to clean inside of the well, and then removed; antibiotic ointment applied; caps replaced	Same	unknown	T-PB	Every cleaning	No	None
6	M	13	B	B3	IT chamber- foul odor, white discharge (few mm between cleanings); V4 chamber OK	Daily	Twice a week	Often use peroxide first (gets film/soft tissue out); diluted betadine; then Nolvasan; suction with metal aspirator tube soaked in Nolvasan; apply antibiotic ointment with a sterile swab; then place super stopper; replace cap (while cleaning, if chamber is left open for more than several seconds, alcohol pad placed of the top to prevent debris from entering)	Same	Soaked in Nolvasan	T-PB	Every cleaning	No	Sterile non-woven sponge balls
7	M	12	B	B4	Off white to brown, foul odor, 5 ml; appearance, odor, and amount seems unrelated to time between cleanings	Daily	Biweekly (?)	Med vac suction used with metal suction tube disinfected with Nolvasan for 24 hours; fluid suctioned out; dental acrylic wiped over bone; walls of chamber wiped using sterile q-tip (remove all visible debris); new metal suction tube used to fill chambers with Nolvasan solution, suctioned, and repeated until Nolvasan solution in chamber is clear; chambers filled with Nolvasan (sit for 10 minutes); walls wiped with new sterile q-tip (when wet/dirty, discarded); solution suctioned out; pre-disinfected caps put on	Same with the addition that chambers are rinsed with saline	Nolvasan solution (24 hours) or UV rays 10 minutes x 2 with rotation in between	NA	NA	No	None
8	M	13	B	B5	Foul odor, cream colored in 2/3 chambers, not very thick; 1 well produces little to no discharge	Daily	Weekly	Caps are removed and placed in H2O2, then into Nolvasan super stoppers are removed and discarded; chambers are suctioned and flushed with Nolvasan 3 betadine swabs are used to wipe the inside of the chamber, starting in the center of the craniotomy, and spiraling upward and out of the chamber; chamber thoroughly rinsed with Nolvasan Terramycin is spread over the granulation tissue with a sterile q-tip; sterile super stopper is placed in the chamber; cap is dried with sterile gauze and placed back on the chamber	Same	Nolvasan solution, overnight	T-PB	Every cleaning	No	Sterile non-woven sponge balls
9	M	13	B	B6	Very little discharge and odorless	Daily	Twice a week	Often use peroxide first (gets film/soft tissue out); diluted betadine; then Nolvasan; suction with metal aspirator tube soaked in Nolvasan; apply antibiotic ointment with a sterile swab; then place super stopper; replace cap (while cleaning, if chamber is left open for more than several seconds, alcohol pad placed of the top to prevent debris from entering)	Same	Soaked in Nolvasan	T-PB	Every cleaning	No	Sterile non-woven sponge balls
10	M	10	B	B7	None; was white, milky discharge post-op	Daily	1-2 weeks if craniotomy present; as needed if no craniotomy	Remove cap, place in 3% H2O2 for 1-2 minutes, place cap in Nolvasan for 15-20 minutes; rinse chamber with sterile saline while suctioning (glass suctions stored in Nolvasan, changed 2-3 times during cleaning, replaced as needed, always rinsed with Nolvasan); clean chamber and well with betadine swab (inside to up to rim of well to outside); rinse with generous amounts of Nolvasan and suction; repeat betadine and Nolvasan rinse; fill chamber with Nolvasan for 10-15 minutes; suction betadine (?); dry chamber with sterile swab, replace cap (dried with sterile swab)	Same	15-20 minute soak in Nolvasan	NA	Only post-op	No; only post-op or with signs of illness (lethargy, poor eating, foul-smelling chamber discharge with other signs)	Sterile non-woven sponge balls, only post-operatively
11	M	10	B	B8	Clear and odorless if cleaned every 1-3 days; if left for a week, yellow puss can form (50% of the time) and can produce an odor	Daily	Weekly	Chamber lid placed in hydrogen peroxide; silicone plug removed with tweezers; rinsed with Nolvasan with suction using a new Nolvasan-sterilized glass pipette (chamber filled and suctioned 5-10 times), chamber walls also cleaned of debris; betadine applied using large single-use q-tip, lightly coating the tissue and walls of chamber (circularly on tissue, then rotated around wall of chamber in upward fashion-- contact time of 5 minutes); rinsed and sutioned with saline solution (5x), then dried with sterile q-tips; sterile silicon placed in each chamber (to seal and prevent granulation tissue growth); new pipettes are used for each chamber	Same	Soaked in alcohol for 15 minutes	NA	NA	No	Silicone elastomer

CRC Sanitization Survey Part 3.2

Animal ID	Sex	Age	Lab	Study ID	Description of Discharge	Cleaning Frequency during Recording	Cleaning Frequency When Not Recording	Description of CRC Cleaning	CRC Cleaning Prior to Recording	Electrode Sterilization	Antimicrobial Used	Criteria for Topical Antimicrobial Use	Systemic Antimicrobials Used?	Packing materials used in CRC
12	M	12	C	C1	Clear or yellow/gray/green opaque or pale pink opaque, usually odorless, odor after 4 days without cleaning	Twice a day	Immediately after recording, and 2-3 times a week	Lab Protocol- pipettes are autoclaved in bulk every 6 months and well-cleaning packs are autoclaved continuously in 2 week cycles; vacuum canisters and tubing are cleaned after each well-cleaning session; deviations- for non-recording cleanings, suction out any fluid and any loose/puffy/potentially infected looking granulation tissue; for recording cleanings, clean inside of the well with Nolvasan solution diluted in sterile water (1 bottle); while cleaning, scratch walls of well with a cotton tip; also scratch the dura and granulation tissue on the edges of the craniotomy with a pipette; clean the outside wall of the well with an alcohol pad; rinse with a bottle of sterile saline; thin layer of TAO if infection detected; replace with clean cap sterilized with cidex	Yes	Cidex OPA, then rinsed 3x with sterile water	G	Discharge is very discolored and odorous	No	None
13	M	12	C	C2	Water-like consistency, clear to opaque pink-red, occasionally white/yellowish discharge	Daily	Three times a week		Same except less tissue removal to avoid aggravation	Cidex OPA	BNP	When thicker buildup between cleanings (yellow/white)	No	None
14	M	11	C	C3	1-2 ml of light yellow fluid in prefrontal well, slightly more mixed with blood in medial temporal well, occasional infection with 1 ml of pus and a foul odor	Twice a day	1-2 times a week		No; light, minimal cleaning (suction fluid and loose tissue, rinse), to not put any pressure/stress on the brain before recording; after recording will do an extensive cleaning as previously described	Soak for 20-30 minutes in Cidex OPA or Cetylcide	BNP or G	Occasional; 1-2 week course of local antibiotics in the well when there are signs of infection-- brings wells back down to basal non-/minimally-infected state; sometimes use Gentak prophylactically for 1-2 weeks when I open up a new (or newly dura-scraped) craniotomy	No; unless showing signs of meningitis; consultation with DCM vet	None
15	M	8	C	C4	N/A	Twice a day	Twice weekly		Same	10 minutes in cetylcide	BNP	Only when well is infected- once a day	No; unless chronic or severe infection in the well	Sterile petroleum jelly, occasionally with granulation tissue
16	F	10	C	C5	1-2 ml of light yellow fluid in prefrontal well, slightly more mixed with blood in medial temporal well, often a foul, fishy odor	Twice a day	1-2 times a week		No; light, minimal cleaning (suction fluid and loose tissue, rinse), to not put any pressure/stress on the brain before recording; after recording will do an extensive cleaning as previously described	Soak for 20-30 minutes in Cidex OPA or Cetylcide	BNP or G	Occasional; 1-2 week course of local antibiotics in the well when there are signs of infection-- brings wells back down to basal non-/minimally-infected state; sometimes use Gentak prophylactically for 1-2 weeks when I open up a new (or newly dura-scraped) craniotomy	No; unless showing signs of meningitis; consultation with DCM vet	None
17	F	11	C	C6	Moderate thickness, yellowish, occasionally pink, 1/2-1 mm accumulation of yellowish discharge on granulation tissue, often foul odor	Daily	5 times weekly (prior to November, 3 times weekly)		Same except less tissue removal to avoid aggravation	Cidex OPA	BNP	When thicker buildup between cleanings	No	None
18	M	10	C	C7	Clear or yellow/gray/green opaque or pale pink opaque, usually odorless, odor after 4 days without cleaning	Twice a day	Immediately after recording, and 2-3 times a week		Yes	Cidex OPA, then rinsed 3x with sterile water	G	Discharge is very discolored and odorous	No	None
19	M	10	C	C8	Clear or yellow/gray/green opaque or pale pink opaque, usually odorless, odor after 4 days without cleaning	Twice a day	Immediately after recording, and 2-3 times a week		Yes	Cidex OPA, then rinsed 3x with sterile water	G	Discharge is very discolored and odorous	No	None

CRC Sanitization Survey Part 3.3

Animal ID	Sex	Age	Lab	Study ID	Description of Discharge	Cleaning Frequency during Recording	Cleaning Frequency When Not Recording	Description of CRC Cleaning	CRC Cleaning Prior to Recording	Electrode Sterilization	Antimicrobial Used	Criteria for Topical Antimicrobial Use	Systemic Antimicrobials Used?	Packing materials used in CRC
20	F	11	D	D1	White, moderate thickness, some odor, minimal accumulation	1-2 days	Every 3-4 weeks	Remove cap and leave soaking in Nolvasan; remove Vaseline plug and clean chamber wells using q-tips soaked in Nolvasan; rinse wel with 40 ml sterile saline; reapply Vaseline and seal with cap	Same	Dipped in alcohol for 10 seconds	NA	NA	No	Sterile petroleum jelly
21	M	8	D	D2	varies; white to red, medium thickness, small amount to 1/2 inch (dependent on whether sterile Vaseline was used-less with Vaseline), occasional foul odor	Inactive	Weekly	Remove cap and wipe with alcohol and leave soaking in Nolvasan; remove Vaseline; suction fluids (bleach suction pipette and replace with new one); clean sides and rim of well with sterile alcohol prep pad and sterile swabs soaked in Nolvasan; scrape dura if necessary; flush with saline and suction (2 flushes minimum, 4-5+ if bleeding); fill chamber with sterile Vaseline; place clean cap (scrubbed with brush and Nolvasan and soaked in Nolvasan from previous cleaning)	Same	N/A	NA	NA	No	Sterile petroleum jelly
22	M	7	D	D3	Regular cleaning- small amount, clear, odorless; w/o regular cleaning- copious fluid, pus-like color, yellow/green/brown (?), foul odor	Daily	Three times a week	Clean outside of well with alcohol cloth; remove cap; clean rim of well with alcohol wipe; remove and visible debris; flush with saline (2x); lightly scrape granulation tissue with sterile pipet, removing loose material; replace with clean cap soaked in Nolvalsan	Same	Alcohol wipe	NA	NA	No; unless displaying clinical signs (star gazing, weight loss)	None
23	M	7	D	D4	1 cc of discharge, watery, yellowish-milky in color when weekly cleaning (clearer, less when on study)	Daily	Weekly	Use sterilized glass pipettes to suction the exudative discharge; clean inner walls of the well with Nolvasan; at least 6 flushes of sterilized saline applied; well filled with sterilized Vaseline	Same with more saline flushes (at least 10)	Front 7/10 of the electrode are kept in Nolvasan for 30 minutes	NA	NA	No	Sterile petroleum jelly (when not on study)
24	M	11	D	D5	varies; white to red, medium thickness, small amount to 1/2 inch (dependent on whether sterile Vaseline was used-less with Vaseline), foul odor	Inactive	Weekly	Remove cap and wipe with alcohol and leave soaking in Nolvasan; remove Vaseline; suction fluids (bleach suction pipette and replace with new one); clean sides and rim of well with sterile alcohol prep pad and sterile swabs soaked in Nolvasan; scrape dura if necessary; flush with saline and suction (2 flushes minimum, 4-5+ if bleeding); fill chamber with sterile Vaseline; place clean cap (scrubbed with brush and Nolvasan and soaked in Nolvasan from previous cleaning)	Same	N/A	NA	NA	No	Sterile petroleum jelly
25	M	6	D	D6	Minimal, clear to white	1-2 days	3-4 weeks	Remove cap and leave soaking in Nolvasan; remove Vaseline plug and clean well using q-tips soaked in Nolvasan; rinse well with 40 ml sterile saline; reapply Vaseline and seal with cap	Same	Dipped in alcohol for 10 seconds	NA	NA	No	Sterile petroleum jelly

Appendix B

Primers

Table B.1: PCR primers

Target Gene	Sequence (5'-3')	Amplicon Size (bp)	Reference
16S V4 - F515/R806	GTGCCAGCMGCCGCGGTAA GGACTACHVGGGTWTCTAAT	291	Caporaso, J. et al. 2011
16S V4-V5 - F515/R926	GTGYCAGCMGCCGCGGTAA CCGYCAATTYMTTTRAGTTT	411	Caporaso, J. et al. 2011
E. faecalis ddl gene	CAGAAGTGAAGAGCACGATG AGGTAAAGTCGTACGGACAT	647	Lieberman, M.T., et al., 2018 *In press*
16S universal primer	AGAGTTTGATCCTGGCTGAG AAGGAGGTGATCCAGCCGCA	1550	Coenye, T., et al., 1999
pstS - MLST	CGGAACAGGACTTTCGC ATTTACATCACGTTCTACTTGC	583	Ruiz-Garbajosa, P., et al., 2006
aroE - MLST	TGGAAAACTTTACGGAGACAGC GTCCTGTCCATTGTTCAAAAGC	459	Ruiz-Garbajosa, P., et al., 2006
gdh - MLST	GGCGCACTAAAAGATATGGT CCAAGATTGGGCAACTTCGTCCCA	530	Ruiz-Garbajosa, P., et al., 2006
gyd - MLST	CAAACTGCTTAGCTCCAATGGC CATTTCGTTGTCATACCAAGC	395	Ruiz-Garbajosa, P., et al., 2006
gki - MLST	GATTTTGTGGGAATTGGTATGG ACCATTAAAGCAAAATGATCGC	438	Ruiz-Garbajosa, P., et al., 2006
xpt - MLST	AAAATGATGGCCGTGTATTAGG AACGTCACCGTTCCTTCACTTA	456	Ruiz-Garbajosa, P., et al., 2006
yiqL - MLST	CAGCTTAAGTCAAGTAAGTGCCG GAATATCCCTTCTGCTTGTGCT	436	Ruiz-Garbajosa, P., et al., 2006
mutL	TCGGTCAAATGCACGGAACT TTAATGGGGGTCTTGAATGCGT	569	Lieberman, M.T., et al., 2018 *In press*
aac(6')-aph(2")	CCAAGAGCAATAAGGGCATA CACTATCATAACCACTACCG	222	Khani M., et al.
aph(3')-IIIa	GGCTAAAATGAGAATATCACCGG CTTTAAAAAATCATACAGCTCGCG	523	Emaneini, M. et al.
str	ATTGCTCTCGAGGGTTCAAG CGTTGAGACACTCCAAAACTCA	423	Lieberman, M.T., et al., 2018, *In press*
tetM	GTTAAATAGTGTTCTTGGAG CTAAGATATGGCTCTAACAA	657	Choi J.M., et al.
tetS	TGGAACGCCAGAGAGGTATT ACATAGACAAGCCGTTGACC	660	Emaneini, M. et al.
FsrB	AATCAGATGGCTGAACAGGTTCA ACTAAATGGCTCTGTCGTCTAGA	181	In-house design
RhamK	CTAGTTTAGTCCATGAGTTACTGC TCCAGATTGATCCAGCAGACA	119	In-house design

Bibliography

[1] Woods SE, Lieberman MT, Lebreton F, Trowel E, de la Fuente-Núñez C, Dzink-Fox J, et al. Characterization of Multi-Drug Resistant *Enterococcus faecalis* Isolated from Cephalic Recording Chambers in Research Macaques (*Macaca* spp.). PLoS One. 2017 January;12(1):e0169293.

[2] Aditya A. File:Rhesus Macaque with kid.jpg, 2015; Creative Commons 4.0; [cited June 8, 2018]. Available from: https://commons.wikimedia.org/wiki/File:Rhesus_Macaque_with_kid.jpg.

[3] Commons W. File:Brains-fr.svg, 2008; [cited June 8, 2018]. Available from: https://commons.wikimedia.org/wiki/File:Brains-fr.svg, PublicDomainImage.

[4] Mashour GA, Alkire MT. Evolution of consciousness: Phylogeny, ontogeny, and emergence from general anesthesia. Proceedings of the National Academy of Sciences. 2013 June;110(Supplement 2):10357–10364. Available from: http://www.pnas.org/content/110/Supplement_2/10357.

[5] Perretta G. Non-human primate models in neuroscience research. Scandinavian Journal of Laboratory Animal Sciences. 2009;36(1):77–85.

[6] Newsome WT, Stein-Aviles JA. Nonhuman Primate Models of Visually Based Cognition. ILAR J. 1999 January;39(2):78–91.

[7] Moody DB, Stebbins WC, Miller JM. A primate restraint and handling system for auditory research. Behavior Research Methods & Instrumentation. 1970 July;2(4):180–182.

[8] Davis TS, Torab K, House P, Greger B. A minimally invasive approach to long-term head fixation in behaving nonhuman primates. Journal of Neuroscience Methods. 2009 Jun;181(1):106–110.

[9] Overton JA, Cooke DF, Goldring AB, Lucero SA, Weatherford C, Recanzone GH. Improved methods for acrylic-free implants in nonhuman primates for neuroscience research. J Neurophysiol. 2017 Dec;118(6):3252–3270.

[10] Mulliken GH, Bichot NP, Ghadooshahy A, Sharma J, Kornblith S, Philcock M, et al. Custom-fit radiolucent cranial implants for neurophysiological recording and stimulation. Journal of Neuroscience Methods. 2015 February;241:146–154.

[11] Blonde JD, Roussy M, Luna R, Mahmoudian B, Gulli RA, Barker KC, et al. Customizable cap implants for neurophysiological experimentation. Journal of Neuroscience Methods. 2018 Jul;304:103–117.

[12] Feingold J, Desrochers TM, Fujii N, Harlan R, Tierney PL, Shimazu H, et al. A system for recording neural activity chronically and simultaneously from multiple cortical and subcortical regions in nonhuman primates. J Neurophysiol. 2012 Apr;107(7):1979–1995.

[13] Leggat PA, Smith DR. Surgical applications of methyl methacrylate: A review of toxicity. . Archives of Environmental and Occupational Health. 2009 Fall;64(3):207–212.

[14] Dahl OE, Garvik LJ, Lyberg T. Toxic effects of methylmethacrylate monomer on leukocytes and endothelial cells in vitro. Acta Orthopaedica Scandinavica. 1994 April;65(2):147–153.

[15] Spinks RL, Baker SN, Jackson A, Khaw PT, Lemon RN. Problem of Dural Scarring in Recording From Awake, Behaving Monkeys: A Solution Using 5-Fluorouracil. Journal of Neurophysiology. 2003 August;90(2):1324–1332.

[16] Spitler KM, Gothard KM. A removable silicone elastomer seal reduces granulation tissue growth and maintains the sterility of recording chambers for primate neurophysiology. Journal of Neuroscience Methods. 2008 Mar;169(1):23–26.

[17] van de Beek D, de Gans J, Spanjaard L, Weisfelt M, Reitsma JB, Vermeulen M. Clinical Features and Prognostic Factors in Adults with Bacterial Meningitis. New England Journal of Medicine. 2004;351(18):1849–1859. PMID: 15509818. Available from: https://doi.org/10.1056/NEJMoa040845.

[18] Brouwer MC, Tunkel AR, McKhann GM, van de Beek D. Brain Abscess. New England Journal of Medicine. 2014;371(5):447–456. PMID: 25075836. Available from: https://doi.org/10.1056/NEJMra1301635.

[19] Council NR. Guide for the Care and Use of Laboratory Animals: Eighth Edition. Washington, DC: The National Academies Press; 2011. Available from: https://www.nap.edu/catalog/12910/guide-for-the-care-and-use-of-laboratory-animals-eighth.

[20] Performance standards for antimicrobial disk susceptibility tests; Approved Standard, M02-A10. Wayne, PA; 2009.

[21] Martiny D, Dediste A, Debruyne L, Vlaes L, Haddou NB, Vandamme P, et al. Accuracy of the API Campy system, the Vitek 2 *Neisseria-Haemophilus* card and matrix-assisted laser desorption ionization time-of-flight mass spectrometry for the identification of *Campylobacter* and related organisms. Clin Microbiol Infect. 2011 Jul;17(7):1001–1006.

[22] Sampimon OC, Zadoks RN, De Vliegher S, Supre K, Haesebrouck F, Barkema HW, et al. Performance of API Staph ID 32 and Staph-Zym for identification of coagulase-negative staphylococci isolated from bovine milk samples. Vet Microbiol. 2009 May;136(3-4):300–305.

[23] Jayarao BM, Oliver SP, Matthews KR, King SH. Comparative evaluation of Vitek gram-positive identification system and API Rapid Strep system for identification of *Streptococcus* species of bovine origin. Vet Microbiol. 1991 Feb;26(3):301–308.

[24] Turnbaugh PJ, Ley RE, Hamady M, Fraser-Liggett CM, Knight R, Gordon JI. The human microbiome project. Nature. 2007 Oct;449(7164):804–810.

[25] Inagaki F, Hinrichs KU, Kubo Y, Bowles MW, Heuer VB, Hong WL, et al. DEEP BIOSPHERE. Exploring deep microbial life in coal-bearing sediment down to 2.5 km below the ocean floor. Science. 2015 Jul;349(6246):420–424.

[26] Morgan XC, Huttenhower C. Chapter 12: Human microbiome analysis. PLoS Comput Biol. 2012;8(12):e1002808.

[27] Chakravorty S, Helb D, Burday M, Connell N, Alland D. A detailed analysis of 16S ribosomal RNA gene segments for the diagnosis of pathogenic bacteria. J Microbiol Methods. 2007 May;69(2):330–339.

[28] Yarza P, Yilmaz P, Pruesse E, Glockner FO, Ludwig W, Schleifer KH, et al. Uniting the classification of cultured and uncultured bacteria and archaea using 16S rRNA gene sequences. Nat Rev Microbiol. 2014 Sep;12(9):635–645.

[29] Rintala A, Pietila S, Munukka E, Eerola E, Pursiheimo JP, Laiho A, et al. Gut Microbiota Analysis Results Are Highly Dependent on the 16S rRNA Gene Target Region, Whereas the Impact of DNA Extraction Is Minor. J Biomol Tech. 2017 Apr;28(1):19–30.

[30] Lozupone CA, Stombaugh J, Gonzalez A, Ackermann G, Wendel D, Vazquez-Baeza Y, et al. Meta-analyses of studies of the human microbiota. Genome Res. 2013 Oct;23(10):1704–1714.

[31] Lozupone C, Knight R. UniFrac: a new phylogenetic method for comparing microbial communities. Appl Environ Microbiol. 2005 Dec;71(12):8228–8235.

[32] Lozupone C, Lladser ME, Knights D, Stombaugh J, Knight R. UniFrac: an effective distance metric for microbial community comparison. ISME J. 2011 Feb;5(2):169–172.

[33] Comeau AM, Douglas GM, Langille MGI. Microbiome Helper: a Custom and Streamlined Workflow for Microbiome Research. mSystems. 2017;2(1). Available from: http://msystems.asm.org/content/2/1/e00127-16.

[34] Caporaso JG, Kuczynski J, Stombaugh J, Bittinger K, Bushman FD, Costello EK, et al. QIIME allows analysis of high-throughput community sequencing data. Nature Methods. 2010 04;7:335 EP –. Available from: http://dx.doi.org/10.1038/nmeth.f.303.

[35] Dewhirst FE, Chien CC, Paster BJ, Ericson RL, Orcutt RP, Schauer DB, et al. Phylogeny of the Defined Murine Microbiota: Altered Schaedler Flora. Applied and Environmental Microbiology. 1999 08;65(8):3287–3292. Available from: http://www.ncbi.nlm.nih.gov/pmc/articles/PMC91493/.

[36] Lawson PA, Foster G, Falsen E, Ohlen M, Collins MD. *Atopobacter phocae* gen. nov., sp. nov., a novel bacterium isolated from common seals. Int J Syst Evol Microbiol. 2000 Sep;50 Pt 5:1755–1760.

[37] Togo A, Khelaifia S, Valero R, Cadoret F, Raoult D, Million M. 'Negativicoccus massiliensis', a new species identified from human stool from an obese patient after bariatric surgery. New Microbes and New Infections. 2016 09;13:43–44. Available from: http://www.ncbi.nlm.nih.gov/pmc/articles/PMC4930332/.

[38] Zhang J, Kobert K, Flouri T, Stamatakis A. PEAR: a fast and accurate Illumina Paired-End reAd mergeR. Bioinformatics. 2014 03;30(5):614–620. Available from: http://dx.doi.org/10.1093/bioinformatics/btt593.

[39] McDonald D, Birmingham A, Knight R. Context and the human microbiome. Microbiome. 2015 Nov;3:52.

[40] McKenna P, Hoffmann C, Minkah N, Aye PP, Lackner A, Liu Z, et al. The Macaque Gut Microbiome in Health, Lentiviral Infection, and Chronic Enterocolitis. PLoS Pathogens. 2008 02;4(2):e20. Available from: http://www.ncbi.nlm.nih.gov/pmc/articles/PMC2222957/.

[41] Morris A, Paulson JN, Talukder H, Tipton L, Kling H, Cui L, et al. Longitudinal analysis of the lung microbiota of cynomolgous macaques during long-term SHIV infection. Microbiome. 2016;4:38. Available from: http://www.ncbi.nlm.nih.gov/pmc/articles/PMC4939015/.

[42] Seekatz AM, Panda A, Rasko DA, Toapanta FR, Eloe-Fadrosh EA, Khan AQ, et al. Differential response of the cynomolgus macaque gut microbiota to *Shigella infection*. PLoS One. 2013;8(6):e64212.

[43] Yasuda K, Oh K, Ren B, Tickle TL, Franzosa EA, Wachtman LM, et al. Biogeography of the intestinal mucosal and lumenal microbiome in the rhesus macaque. Cell Host Microbe. 2015 Mar;17(3):385–391.

[44] Fox JG, Handt L, Xu S, Shen Z, Dewhirst FE, Paster BJ, et al. Novel Helicobacter species isolated from rhesus monkeys with chronic idiopathic colitis. J Med Microbiol. 2001 May;50(5):421–429.

[45] Fox JG, Boutin SR, Handt LK, Taylor NS, Xu S, Rickman B, et al. Isolation and Characterization of a Novel *Helicobacter* Species, "Helicobacter macacae", from Rhesus Monkeys with and without Chronic Idiopathic Colitis. Journal of Clinical Microbiology. 2007 12;45(12):4061–4063. Available from: http://www.ncbi.nlm.nih.gov/pmc/articles/PMC2168584/.

[46] Lertpiriyapong K, Handt L, Feng Y, Mitchell TW, Lodge KE, Shen Z, et al. Pathogenic properties of enterohepatic Helicobacter spp. isolated from rhesus macaques with intestinal adenocarcinoma. Journal of Medical Microbiology. 2014 07;63(Pt 7):1004–1016. Available from: http://www.ncbi.nlm.nih.gov/pmc/articles/PMC4064350/.

[47] Marini RP, Muthupalani S, Shen Z, Buckley EM, Alvarado C, Taylor NS, et al. Persistent infection of rhesus monkeys with 'Helicobacter macacae' and its isolation from an animal with intestinal adenocarcinoma. Journal of Medical Microbiology. 2010 08;59(Pt 8):961–969. Available from: http://www.ncbi.nlm.nih.gov/pmc/articles/PMC3052472/.

[48] Ocon S, Murphy C, Dang AT, Sankaran-Walters S, Li CS, Tarara R, et al. Transcription Profiling Reveals Potential Mechanisms of Dysbiosis in the Oral Microbiome of Rhesus Macaques with Chronic Untreated SIV Infection. PLoS ONE. 2013;8(11):e80863. Available from: http://www.ncbi.nlm.nih.gov/pmc/articles/PMC3843670/.

[49] Colombo APV, Paster BJ, Grimaldi G, Lourenço TGB, Teva A, Campos-Neto A, et al. Clinical and microbiological parameters of naturally occurring periodontitis in the non-human primate *Macaca mulatta*. Journal of Oral Microbiology. 2017;9(1):1403843. Available from: http://www.ncbi.nlm.nih.gov/pmc/articles/PMC5963701/.

[50] Council SE, Savage AM, Urban JM, Ehlers ME, Skene JHP, Platt ML, et al. Diversity and evolution of the primate skin microbiome. Proc Biol Sci. 2016 Jan;283(1822).

[51] Bergin IL, Chien CC, Marini RP, Fox JG. Isolation and characterization of *Corynebacterium ulcerans* from cephalic implants in macaques. Comp Med. 2000 Oct;50(5):530–535.

[52] Oliveira A, Oliveira LC, Aburjaile F, Benevides L, Tiwari S, Jamal SB, et al. Insight of Genus Corynebacterium: Ascertaining the Role of Pathogenic and Non-pathogenic Species. Frontiers in Microbiology. 2017;8:1937. Available from: https://www.frontiersin.org/article/10.3389/fmicb.2017.01937.

[53] Kozlov A, Bean L, Hill EV, Zhao L, Li E, Wang GP. Molecular Identification of Bacteria in Intra-abdominal Abscesses Using Deep Sequencing. Open Forum Infect Dis. 2018 Feb;5(2):ofy025.

[54] de Groof EJ, Carbonnel F, Buskens CJ, Bemelman WA. Abdominal abscess in Crohn's disease: multidisciplinary management. Dig Dis. 2014;32 Suppl 1:103–109.

[55] Sohn M, Hoffmann M, Hochrein A, Buhr HJ, Lehmann KS. Laparoscopic Appendectomy Is Safe: Influence of Appendectomy Technique on Surgical-site Infections and Intra-abdominal Abscesses. Surg Laparosc Endosc Percutan Tech. 2015 Jun;25(3):e90–4.

[56] Lardiere-Deguelte S, Ragot E, Amroun K, Piardi T, Dokmak S, Bruno O, et al. Hepatic abscess: Diagnosis and management. J Visc Surg. 2015 Sep;152(4):231–243.

[57] Singh S, Khardori NM. Intra-abdominal and pelvic emergencies. Med Clin North Am. 2012 Nov;96(6):1171–1191.

[58] Lieberman MT, Van Tyne D, Dzink-Fox J, Ma EJ, Gilmore MS, Fox JG. Long-term colonization dynamics of *Enterococcus faecalis* in implanted devices in research macaques. Applied and Environmental Microbiology. 2018;84(18):*In Press*.

[59] Sievert DM, Ricks P, Edwards JR, Schneider A, Patel J, Srinivasan A, et al. Antimicrobial-resistant pathogens associated with healthcare-associated infections: summary of data reported to the National Healthcare Safety Network at the Centers for Disease Control and Prevention, 2009-2010. Infect Control Hosp Epidemiol. 2013 Jan;34(1):1–14.

[60] Kafil HS, Mobarez AM. Spread of Enterococcal Surface Protein in Antibiotic Resistant *Enterococcus faecium* and *Enterococcus faecalis*

isolates from Urinary Tract Infections. Open Microbiol J. 2015;9:14–17.

[61] Paganelli FL, Willems RJ, Leavis HL. Optimizing future treatment of enterococcal infections: attacking the biofilm? Trends Microbiol. 2012 Jan;20(1):40–49.

[62] Methods for dilution antimicrobial susceptibility tests of bacteria that grow aerobically; Approved Standard, M07-A9. Wayne, PA; 2012.

[63] Coenye T, Falsen E, Vancanneyt M, Hoste B, Govan JRW, Kersters K, et al. Classification of *Alcaligenes faecalis*-like isolates from the environment and human clinical samples as *Ralstonia gilardii* sp. nov. International Journal of Systematic and Evolutionary Microbiology. 1999;49(2):405–413. Available from: http://ijs.microbiologyresearch.org/content/journal/ijsem/10.1099/00207713-49-2-405.

[64] Ruiz-Garbajosa P, Bonten MJM, Robinson DA, Top J, Nallapareddy SR, Torres C, et al. Multilocus sequence typing scheme for *Enterococcus faecalis* reveals hospital-adapted genetic complexes in a background of high rates of recombination. J Clin Microbiol. 2006 Jun;44(6):2220–2228.

[65] Jolley KA, Maiden MCJ. BIGSdb: Scalable analysis of bacterial genome variation at the population level. BMC Bioinformatics. 2010 Dec;11:595.

[66] Chin CS, Alexander DH, Marks P, Klammer AA, Drake J, Heiner C, et al. Nonhybrid, finished microbial genome assemblies from long-read SMRT sequencing data. Nat Methods. 2013 Jun;10(6):563–569.

[67] Wattam AR, Abraham D, Dalay O, Disz TL, Driscoll T, Gabbard JL, et al. PATRIC, the bacterial bioinformatics database and analysis resource. Nucleic Acids Res. 2014 Jan;42(Database issue):D581–91.

[68] Zankari E, Hasman H, Cosentino S, Vestergaard M, Rasmussen S, Lund O, et al. Identification of acquired antimicrobial resistance genes. J Antimicrob Chemother. 2012 Nov;67(11):2640–2644.

[69] Joensen KG, Scheutz F, Lund O, Hasman H, Kaas RS, Nielsen EM, et al. Real-time whole-genome sequencing for routine typing, surveillance, and outbreak detection of verotoxigenic *Escherichia coli*. J Clin Microbiol. 2014 May;52(5):1501–1510.

[70] Minogue TD, Daligault HE, Davenport KW, Broomall SM, Bruce DC, Chain PS, et al. Complete Genome Assembly of *Enterococcus faecalis* 29212, a Laboratory Reference Strain. Genome Announc. 2014 Sep;2(5).

[71] Tendolkar PM, Baghdayan AS, Gilmore MS, Shankar N. Enterococcal surface protein, Esp, enhances biofilm formation by *Enterococcus faecalis*. Infect Immun. 2004 Oct;72(10):6032–6039.

[72] Stepanovic S, Vukovic D, Hola V, Di Bonaventura G, Djukic S, Cirkovic I, et al. Quantification of biofilm in microtiter plates: overview of testing conditions and practical recommendations for assessment of biofilm production by staphylococci. APMIS. 2007 Aug;115(8):891–899.

[73] de la Fuente-Núñez C, Reffuveille F, Mansour SC, Reckseidler-Zenteno SL, Hernandez D, Brackman G, et al. D-enantiomeric peptides that eradicate wild-type and multidrug-resistant biofilms and protect against lethal *Pseudomonas aeruginosa* infections. Chem Biol. 2015 Feb;22(2):196–205.

[74] Reffuveille F, de la Fuente-Núñez C, Mansour S, Hancock REW. A broad-spectrum antibiofilm peptide enhances antibiotic action against bacterial biofilms. Antimicrob Agents Chemother. 2014 Sep;58(9):5363–5371.

[75] King A, Boothman C, Phillips I. Comparative in-vitro activity of meropenem on clinical isolates from the United Kingdom. J Antimicrob Chemother. 1989 Sep;24 Suppl A:31–45.

[76] Schouten MA, Voss A, Hoogkamp-Korstanje JA. Antimicrobial susceptibility patterns of enterococci causing infections in Europe. The European VRE Study Group. Antimicrob Agents Chemother. 1999 Oct;43(10):2542–2546.

[77] Gemmell CG. Susceptibility of a variety of clinical isolates to linezolid: a European inter-country comparison. J Antimicrob Chemother. 2001 Jul;48(1):47–52.

[78] Yu Zj, Chen Z, Cheng H, Zheng Jx, Pan Wg, Yang Wz, et al. Recurrent linezolid-resistant *Enterococcus faecalis* infection in a patient with pneumonia. Int J Infect Dis. 2015 Jan;30:49–51.

[79] Chylinski K, Makarova KS, Charpentier E, Koonin EV. Classification and evolution of type II CRISPR-*cas* systems. Nucleic Acids Res. 2014 Jun;42(10):6091–6105.

[80] An FY, Clewell DB. Identification of the *cAD1* sex pheromone precursor in *Enterococcus faecalis*. J Bacteriol. 2002 Apr;184(7):1880–1887.

[81] Antiporta MH, Dunny GM. *ccfA*, the genetic determinant for the cCF10 peptide pheromone in *Enterococcus faecalis* OG1RF. J Bacteriol. 2002 Feb;184(4):1155–1162.

[82] Clewell DB, An FY, White BA, Gawron-Burke C. *Streptococcus faecalis* sex pheromone (cAM373) also produced by *Staphylococcus aureus* and identification of a conjugative transposon (Tn918). J Bacteriol. 1985 Jun;162(3):1212–1220.

[83] Nakayama J, Abe Y, Ono Y, Isogai A, Suzuki A. Isolation and structure of the *Enterococcus faecalis* sex pheromone, cOB1, that induces conjugal transfer of the hemolysin/bacteriocin plasmids, pOB1 and pYI1. Biosci Biotechnol Biochem. 1995 Apr;59(4):703–705.

[84] Brinster S, Posteraro B, Bierne H, Alberti A, Makhzami S, Sanguinetti M, et al. Enterococcal leucine-rich repeat-containing protein involved in virulence and host inflammatory response. Infect Immun. 2007 Sep;75(9):4463–4471.

[85] Fisher K, Phillips C. The ecology, epidemiology and virulence of Enterococcus. Microbiology. 2009 Jun;155(Pt 6):1749–1757.

[86] Nielsen HV, Flores-Mireles AL, Kau AL, Kline KA, Pinkner JS, Neiers F, et al. Pilin and sortase residues critical for endocarditis- and biofilm-associated pilus biogenesis in *Enterococcus faecalis*. J Bacteriol. 2013 Oct;195(19):4484–4495.

[87] La Carbona S, Sauvageot N, Giard JC, Benachour A, Posteraro B, Auffray Y, et al. Comparative study of the physiological roles of three peroxidases (NADH peroxidase, Alkyl hydroperoxide reductase and Thiol peroxidase) in oxidative stress response, survival inside macrophages and virulence of *Enterococcus faecalis*. Mol Microbiol. 2007 Dec;66(5):1148–1163.

[88] Sandoe JAT, Witherden IR, Cove JH, Heritage J, Wilcox MH. Correlation between enterococcal biofilm formation in vitro and medical-device-related infection potential in vivo. J Med Microbiol. 2003 Jul;52(Pt 7):547–550.

[89] Kart D, Kustimur AS, Sağıroğlu M, Kalkancı A. Evaluation of Antimicrobial Durability and Anti-Biofilm Effects in Urinary Catheters Against *Enterococcus faecalis* Clinical Isolates and Reference Strains. Balkan Medical Journal. 2017 12;34(6):546–552. Available from: http://www.ncbi.nlm.nih.gov/pmc/articles/PMC5785660/.

[90] Di Rosa R, Basoli A, Donelli G, Penni A, Salvatori FM, Fiocca F, et al. A microbiological and morphological study of blocked biliary stents. Microbial Ecology in Health and Disease. 1999;11(2):84–88. Available from: https://doi.org/10.1080/089106099435817.

[91] Lins RX, de Oliveira Andrade A, Junior RH, Wilson MJ, Lewis MAO, Williams DW, et al. Antimicrobial resistance and virulence traits

of Enterococcus faecalis from primary endodontic infections. Journal of Dentistry. 2013;41(9):779 - 786. Available from: http://www.sciencedirect.com/science/article/pii/S0300571213001735.

[92] Chow JW. Aminoglycoside resistance in enterococci. Clin Infect Dis. 2000 Aug;31(2):586–589.

[93] Palmer KL, Gilmore MS. Multidrug-resistant enterococci lack CRISPR-*cas*. MBio. 2010 Oct;1(4).

[94] Bantar CE, Micucci M, Fernandez Canigia L, Smayevsky J, Bianchini HM. Synergy characterization for *Enterococcus faecalis* strains displaying moderately high-level gentamicin and streptomycin resistance. J Clin Microbiol. 1993 Jul;31(7):1921–1923.

[95] Manson JM, Keis S, Smith JMB, Cook GM. Acquired bacitracin resistance in *Enterococcus faecalis* is mediated by an ABC transporter and a novel regulatory protein, BcrR. Antimicrob Agents Chemother. 2004 Oct;48(10):3743–3748.

[96] Miller WR, Munita JM, Arias CA. Mechanisms of antibiotic resistance in enterococci. Expert Rev Anti Infect Ther. 2014 Oct;12(10):1221–1236.

[97] Petersen A, Jensen LB. Analysis of *gyrA* and *parC* mutations in enterococci from environmental samples with reduced susceptibility to ciprofloxacin. FEMS Microbiol Lett. 2004 Feb;231(1):73–76.

[98] Onodera Y, Okuda J, Tanaka M, Sato K. Inhibitory activities of quinolones against DNA gyrase and topoisomerase IV of *Enterococcus faecalis*. Antimicrob Agents Chemother. 2002 Jun;46(6):1800–1804.

[99] Mohamed JA, Huang DB. Biofilm formation by enterococci. J Med Microbiol. 2007 Dec;56(Pt 12):1581–1588.

[100] Sussmuth SD, Muscholl-Silberhorn A, Wirth R, Susa M, Marre R, Rozdzinski E. Aggregation substance promotes adherence, phagocytosis, and intracellular survival of *Enterococcus faecalis* within human macrophages and suppresses respiratory burst. Infect Immun. 2000 Sep;68(9):4900–4906.

[101] Shankar V, Baghdayan AS, Huycke MM, Lindahl G, Gilmore MS. Infection-derived *Enterococcus faecalis* strains are enriched in *esp*, a gene encoding a novel surface protein. Infect Immun. 1999 Jan;67(1):193–200.

[102] Nallapareddy SR, Singh KV, Sillanpaa J, Zhao M, Murray BE. Relative contributions of Ebp Pili and the collagen adhesin ace to host

extracellular matrix protein adherence and experimental urinary tract infection by *Enterococcus faecalis* OG1RF. Infect Immun. 2011 Jul;79(7):2901–2910.

[103] Hancock LE, Perego M. The *Enterococcus faecalis fsr* two-component system controls biofilm development through production of gelatinase. J Bacteriol. 2004 Sep;186(17):5629–5639.

[104] Toledo-Arana A, Valle J, Solano C, Arrizubieta MJ, Cucarella C, Lamata M, et al. The enterococcal surface protein, Esp, is involved in *Enterococcus faecalis* biofilm formation. Appl Environ Microbiol. 2001 Oct;67(10):4538–4545.

[105] Chuang-Smith ON, Wells CL, Henry-Stanley MJ, Dunny GM. Acceleration of *Enterococcus faecalis* biofilm formation by aggregation substance expression in an ex vivo model of cardiac valve colonization. PLoS One. 2010 Dec;5(12):e15798.

[106] Kristich CJ, Li YH, Cvitkovitch DG, Dunny GM. *Esp*-independent biofilm formation by *Enterococcus faecalis*. J Bacteriol. 2004 Jan;186(1):154–163.

[107] Guiton PS, Hung CS, Kline KA, Roth R, Kau AL, Hayes E, et al. Contribution of autolysin and Sortase a during *Enterococcus faecalis* DNA-dependent biofilm development. Infect Immun. 2009 Sep;77(9):3626–3638.

[108] Van Tyne D, Martin MJ, Gilmore MS. Structure, function, and biology of the *Enterococcus faecalis* cytolysin. Toxins (Basel). 2013 Apr;5(5):895–911.

[109] Chow JW, Thal LA, Perri MB, Vazquez JA, Donabedian SM, Clewell DB, et al. Plasmid-associated hemolysin and aggregation substance production contribute to virulence in experimental enterococcal endocarditis. Antimicrob Agents Chemother. 1993 Nov;37(11):2474–2477.

[110] Costa DK, Barg FK, Asch DA, Kahn JM. Facilitators of an interprofessional approach to care in medical and mixed medical/surgical ICUs: a multicenter qualitative study. Res Nurs Health. 2014 Aug;37(4):326–335.

[111] Hyzy RC, Flanders SA, Pronovost PJ, Berenholtz SM, Watson S, George C, et al. Characteristics of intensive care units in Michigan: not an open and closed case. J Hosp Med. 2010 Jan;5(1):4–9.

[112] Vollaard EJ, Clasener HA. Colonization resistance. Antimicrob Agents Chemother. 1994 Mar;38(3):409–414.

[113] Lee G, Danneman P, Rufo R, Kalesnykas R, Eng V. Use of Chlorine Dioxide for Antimicrobial Prophylactic Maintenance of Cephalic Recording Devices in Rhesus Macaques (*Macaca mulatta*). Contemp Top Lab Anim Sci. 1998 Mar;37(2):59–63.

[114] Watanabe S, Kobayashi N, Quinones D, Nagashima S, Uehara N, Watanabe N. Genetic diversity of enterococci harboring the high-level gentamicin resistance gene *aac(6')-Ie-aph(2")-Ia* or *aph(2")-Ie* in a Japanese hospital. Microb Drug Resist. 2009 Sep;15(3):185–194.

[115] Freitas AR, Novais C, Ruiz-Garbajosa P, Coque TM, Peixe L. Clonal expansion within clonal complex 2 and spread of vancomycin-resistant plasmids among different genetic lineages of *Enterococcus faecalis* from Portugal. J Antimicrob Chemother. 2009 Jun;63(6):1104–1111.

[116] Yang Jx, Li T, Ning Yz, Shao Dh, Liu J, Wang Sq, et al. Molecular characterization of resistance, virulence and clonality in vancomycin-resistant *Enterococcus faecium* and *Enterococcus faecalis*: A hospital-based study in Beijing, China. Infect Genet Evol. 2015 Jul;33:253–260.

[117] Sun H, Wang H, Xu Y, Jones RN, Costello AJ, Liu Y, et al. Molecular characterization of vancomycin-resistant *Enterococcus* spp. clinical isolates recovered from hospitalized patients among several medical institutions in China. Diagn Microbiol Infect Dis. 2012 Dec;74(4):399–403.

[118] Khani M, Fatollahzade M, Pajavand H, Bakhtiari S, Abiri R. Increasing Prevalence of Aminoglycoside-Resistant *Enterococcus faecalis* Isolates Due to the *aac(6')-aph(2")* Gene: A Therapeutic Problem in Kermanshah, Iran. Jundishapur J Microbiol. 2016 Mar;9(3):e28923.

[119] Emaneini M, Aligholi M, Aminshahi M. Characterization of glycopeptides, aminoglycosides and macrolide resistance among *Enterococcus faecalis* and *Enterococcus faecium* isolates from hospitals in Tehran. Pol J Microbiol. 2008;57(2):173–178.

[120] Choi JM, Woo GJ. Transfer of tetracycline resistance genes with aggregation substance in food-borne *Enterococcus faecalis*. Curr Microbiol. 2015 Apr;70(4):476–484.

[121] Performance Standards for Antimicrobial Susceptibility Testing; Approved Standard, M07-A9. Wayne, PA; 2018.

[122] Methods for Dilution Antimicrobial Susceptibility Tests for Bacteria That Grow Aerobically; Approved Standard M100-2D. Wayne, PA; 2018.

[123] Methods for determining bactericidal activity of antimicrobial agents; Approved Guideline, M26-A. Wayne, PA; 1999.

[124] Kelley LA, Mezulis S, Yates CM, Wass MN, Sternberg MJE. The Phyre2 web portal for protein modeling, prediction and analysis. Nature Protocols. 2015 05;10:845 EP –. Available from: http://dx.doi.org/10.1038/nprot.2015.053.

[125] Schrödinger, LLC. The PyMOL Molecular Graphics System, Version 2.0.7; 2015. Accessed 6-25-18.

[126] Du X, Hua X, Qu T, Jiang Y, Zhou Z, Yu Y. Molecular characterization of Rifr mutations in *Enterococcus faecalis* and *Enterococcus faecium*. J Chemother. 2014 Aug;26(4):217–221.

[127] Hollenbeck BL, Rice LB. Intrinsic and acquired resistance mechanisms in *Enterococcus*. Virulence. 2012 Aug;3(5):421–433.

[128] Shaw KJ, Rather PN, Hare RS, Miller GH. Molecular genetics of aminoglycoside resistance genes and familial relationships of the aminoglycoside-modifying enzymes. Microbiol Rev. 1993 Mar;57(1):138–163.

[129] Shankar N, Baghdayan AS, Gilmore MS. Modulation of virulence within a pathogenicity island in vancomycin-resistant *Enterococcus faecalis*. Nature. 2002 Jun;417(6890):746–750.

[130] Coburn PS, Gilmore MS. The *Enterococcus faecalis* cytolysin: a novel toxin active against eukaryotic and prokaryotic cells. Cell Microbiol. 2003 Oct;5(10):661–669.

[131] Tendolkar PM, Baghdayan AS, Shankar N. Putative surface proteins encoded within a novel transferable locus confer a high-biofilm phenotype to *Enterococcus faecalis*. J Bacteriol. 2006 Mar;188(6):2063–2072.

[132] McBride SM, Fischetti VA, Leblanc DJ, Moellering RCJ, Gilmore MS. Genetic diversity among *Enterococcus faecalis*. PLoS One. 2007 Jul;2(7):e582. NLM: Original DateCompleted: 20070806.

[133] Sullivan MJ, Petty NK, Beatson SA. Easyfig: a genome comparison visualizer. Bioinformatics. 2011 Apr;27(7):1009–1010.

[134] Miller DJ, Jerga A, Rock CO, White SW. Analysis of the *Staphylococcus aureus* DgkB structure reveals a common catalytic mechanism for the soluble diacylglycerol kinases. Structure. 2008 Jul;16(7):1036–1046.

[135] Kobayakawa S, Jett BD, Gilmore MS. Biofilm formation by *Enterococcus faecalis* on intraocular lens material. Curr Eye Res. 2005 Sep;30(9):741–745.

[136] Keane PF, Bonner MC, Johnston SR, Zafar A, Gorman SP. Characterization of biofilm and encrustation on ureteric stents in vivo. Br J Urol. 1994 Jun;73(6):687–691.

[137] Kawalec M, Pietras Z, Danilowicz E, Jakubczak A, Gniadkowski M, Hryniewicz W, et al. Clonal structure of *Enterococcus faecalis* isolated from Polish hospitals: characterization of epidemic clones. J Clin Microbiol. 2007 Jan;45(1):147–153.

[138] Magden E, Mansfield K, Simmons J, Abee C. Laboratory Animal Medicine. In: Fox J, Anderson L, Otto G, Pritchett-Corning K, Whary M, editors. Laboratory Animal Medicine. Elsevier; 2015. .

[139] Morita Y, Kodama K, Shiota S, Mine T, Kataoka A, Mizushima T, et al. NorM, a Putative Multidrug Efflux Protein, of *Vibrio parahaemolyticus* and Its Homolog in *Escherichia coli*. Antimicrobial Agents and Chemotherapy. 1998 07;42(7):1778–1782. Available from: http://www.ncbi.nlm.nih.gov/pmc/articles/PMC105682/.

[140] Qin X, Singh KV, Weinstock GM, Murray BE. Characterization of *fsr*, a Regulator Controlling Expression of Gelatinase and Serine Protease in *Enterococcus faecalis* OG1RF. Journal of Bacteriology. 2001 06;183(11):3372–3382. Available from: http://www.ncbi.nlm.nih.gov/pmc/articles/PMC99635/.

[141] Del Papa MF, Perego M. *Enterococcus faecalis* Virulence Regulator *FsrA* Binding to Target Promoters. Journal of Bacteriology. 2011 04;193(7):1527–1532. Available from: http://www.ncbi.nlm.nih.gov/pmc/articles/PMC3067650/.

[142] Huycke MM, Spiegel CA, Gilmore MS. Bacteremia caused by hemolytic, high-level gentamicin-resistant *Enterococcus faecalis*. Antimicrobial Agents and Chemotherapy. 1991 08;35(8):1626–1634. Available from: http://www.ncbi.nlm.nih.gov/pmc/articles/PMC245231/.

[143] Miyazaki S, Ohno A, Kobayashi I, Uji T, Yamaguchi K, Goto S. Cytotoxic effect of hemolytic culture supernatant from *Enterococcus faecalis* on mouse polymorphonuclear neutrophils and macrophages. Microbiol Immunol. 1993;37(4):265–270.

[144] Jett BD, Jensen HG, Nordquist RE, Gilmore MS. Contribution of the *pAD1*-encoded cytolysin to the severity of experimental *Enterococcus faecalis* endophthalmitis. Infect Immun. 1992 Jun;60(6):2445–2452.

[145] Stevens SX, Jensen HG, Jett BD, Gilmore MS. A hemolysin-encoding plasmid contributes to bacterial virulence in experimental *Enterococcus faecalis* endophthalmitis. Invest Ophthalmol Vis Sci. 1992 Apr;33(5):1650–1656.

[146] Steenbergen JN, Alder J, Thorne GM, Tally FP. Daptomycin: a lipopeptide antibiotic for the treatment of serious Gram-positive infections. Journal of Antimicrobial Chemotherapy. 2005;55(3):283–288. Available from: http://dx.doi.org/10.1093/jac/dkh546.

[147] McRee DE. 3. In: Computational Techniques. 2nd ed. San Diego: Academic Press; 1999. p. 91–cp1. Available from: https://www.sciencedirect.com/science/article/pii/B9780124860520500051.

[148] Matono T, Hayakawa K, Hirai R, Tanimura A, Yamamoto K, Fujiya Y, et al. Emergence of a daptomycin-non-susceptible *Enterococcus faecium* strain that encodes mutations in DNA repair genes after high-dose daptomycin therapy. BMC Research Notes. 2016;9:197. Available from: http://www.ncbi.nlm.nih.gov/pmc/articles/PMC4818489/.

[149] Willems RJ, Top J, Smith DJ, Roper DI, North SE, Woodford N. Mutations in the DNA Mismatch Repair Proteins MutS and MutL of Oxazolidinone-Resistant or -Susceptible *Enterococcus faecium*. Antimicrobial Agents and Chemotherapy. 2003 10;47(10):3061–3066. Available from: http://www.ncbi.nlm.nih.gov/pmc/articles/PMC201155/.

[150] Ciofu O, Riis B, Pressler T, Poulsen HE, Høiby N. Occurrence of Hypermutable *Pseudomonas aeruginosa* in Cystic Fibrosis Patients Is Associated with the Oxidative Stress Caused by Chronic Lung Inflammation. Antimicrobial Agents and Chemotherapy. 2005 06;49(6):2276–2282. Available from: http://www.ncbi.nlm.nih.gov/pmc/articles/PMC1140492/.

[151] Maciá MD, Blanquer D, Togores B, Sauleda J, Pérez J, Oliver A. Hypermutation Is a Key Factor in Development of Multiple-Antimicrobial Resistance in *Pseudomonas aeruginosa* Strains Causing Chronic Lung Infections. Antimicrobial Agents and Chemotherapy. 2005 08;49(8):3382–3386. Available from: http://www.ncbi.nlm.nih.gov/pmc/articles/PMC1196247/.

[152] Donlan RM, Costerton JW. Biofilms: survival mechanisms of clinically relevant microorganisms. Clin Microbiol Rev. 2002 Apr;15(2):167–193.

[153] de la Fuente-Núñez C, Cardoso MH, de Souza Cândido E, Franco OL, Hancock RE. Synthetic Antibiofilm Peptides. Biochimica et bio-

physica acta. 2016 05;1858(5):1061–1069. Available from: http://www.ncbi.nlm.nih.gov/pmc/articles/PMC4809770/.

[154] for Disease Control C, Prevention OoID. Antibiotic resistance threats in the United States, 2013.; 2013 [cited June 27, 2018]. Available from: https://www.cdc.gov/drugresistance/threat-report-2013/.

[155] Chen L, Todd R, Kiehlbauch J, Walters M, Kallen A. Notes from the Field: Pan-Resistant New Delhi Metallo-Beta-Lactamase-Producing *Klebsiella pneumoniae* - Washoe County, Nevada, 2016. MMWR Morb Mortal Wkly Rep. 2017 Jan;66(1):33.

[156] Clatworthy AE, Pierson E, Hung DT. Targeting virulence: a new paradigm for antimicrobial therapy. Nat Chem Biol. 2007 Sep;3(9):541–548.

[157] Twort FW. AN INVESTIGATION ON THE NATURE OF ULTRA-MICROSCOPIC VIRUSES. The Lancet. 1915;186(4814):1241 – 1243. Originally published as Volume 2, Issue 4814. Available from: http://www.sciencedirect.com/science/article/pii/S0140673601203833.

[158] d'Herelle F. On an invisible microbe antagonistic to dysentery bacilli. Note by M. F. d'Herelle, presented by M. Roux. Comptes Rendus Academie des Sciences 1917; 165:373–5. Bacteriophage. 2011;1(1):3–5. Available from: https://doi.org/10.4161/bact.1.1.14941.

[159] d'Herelle F. Bacteriophage as a Treatment in Acute Medical and Surgical Infections. Bulletin of the New York Academy of Medicine. 1931 05;7(5):329–348. Available from: http://www.ncbi.nlm.nih.gov/pmc/articles/PMC2095997/.

[160] Bruynoghe R, Maisin J. Essais de thérapeutique au moyen du bacteriophage du Staphylocoque. Compt Rend Soc Biol. 1921;85(1120-1121).

[161] Institute E. George Eliava Institue of Bacteirophages, Microbiology and Virology; [cited June 28, 2018]. Available from: http://www.eliava-institute.org/?rid=1.

[162] Häusler T. Viruses vs. Superbugs, A Solution to the Antibiotics Crisis? New York, NY: Macmillan; 2006.

[163] Summers WC. The strange history of phage therapy. Bacteriophage. 2012 Apr;2(2):130–133.

[164] Ruska H. Visualization of bacteriophage lysis in the hypermicroscope. Naturwissenschaften. 1940;28:45–46. Available from: http://www.ncbi.nlm.nih.gov/pmc/articles/PMC3626388/.

[165] Luria SE, Anderson TF. The Identification and Characterization of Bacteriophages with the Electron Microscope. Proc Natl Acad Sci U S A. 1942 Apr;28(4):127–130.

[166] Fleming A. On the Antibacterial Action of Cultures of a Penicillium, with Special Reference to their Use in the Isolation of *B. influenzæ*. British journal of experimental pathology. 1929 06;10(3):226–236. Available from: http://www.ncbi.nlm.nih.gov/pmc/articles/PMC2048009/.

[167] Shama G. The role of the media in influencing public attitudes to penicillin during World War II. Dynamis. 2015;35(1):131–152.

[168] Quinn R. Rethinking Antibiotic Research and Development: World War II and the Penicillin Collaborative. American Journal of Public Health. 2013 03;103(3):426–434. Available from: http://www.ncbi.nlm.nih.gov/pmc/articles/PMC3673487/.

[169] Lang LH. FDA Approves Use of Bacteriophages to be Added to Meat and Poultry Products. Gastroenterology. 2006 2018/06/28;131(5):1370. Available from: http://dx.doi.org/10.1053/j.gastro.2006.10.012.

[170] PhagoBurn. PhagoBurn; 2018 [cited 28]. Available from: http://www.phagoburn.eu/.

[171] of Health US National Libary of Medicine NI. Ascending Dose Study of the Safety of AB-SA01 When Topically Applied to Intact Skin of Healthy Adults; 2018 [cited 28]. Available from: https://clinicaltrials.gov/ct2/show/NCT02757755.

[172] Chan BK, Turner PE, Kim S, Mojibian HR, Elefteriades JA, Narayan D. Phage treatment of an aortic graft infected with *Pseudomonas aeruginosa*. Evol Med Public Health. 2018;2018(1):60–66.

[173] Sulakvelidze A, Alavidze Z, Morris JGJ. Bacteriophage therapy. Antimicrob Agents Chemother. 2001 Mar;45(3):649–659.

[174] Colavecchio A, Cadieux B, Lo A, Goodridge LD. Bacteriophages Contribute to the Spread of Antibiotic Resistance Genes among Foodborne Pathogens of the Enterobacteriaceae Family –A Review. Frontiers in Microbiology. 2017;8:1108. Available from: http://www.ncbi.nlm.nih.gov/pmc/articles/PMC5476706/.

[175] Zhou Y, Liang Y, Lynch KH, Dennis JJ, Wishart DS. PHAST: A Fast Phage Search Tool. Nucleic Acids Research. 2011 07;39(Web Server issue):W347–W352. Available from: http://www.ncbi.nlm.nih.gov/pmc/articles/PMC3125810/.

[176] Skaar K, Claesson M, Odegrip R, Hogbom M, Haggard-Ljungquist E, Stenmark P. Crystal structure of the bacteriophage P2 integrase catalytic domain. FEBS Lett. 2015 Nov;589(23):3556–3563.

[177] Britton RA, Young VB. Role of the intestinal microbiota in resistance to colonization by *Clostridium difficile*. Gastroenterology. 2014 May;146(6):1547–1553.

[178] Falagas ME, Karagiannis AKA, Nakouti T, Tansarli GS. Compliance with Once-Daily versus Twice or Thrice-Daily Administration of Antibiotic Regimens: A Meta-Analysis of Randomized Controlled Trials. PLoS ONE. 2015;10(1):e0116207. Available from: http://www.ncbi.nlm.nih.gov/pmc/articles/PMC4283966/.

[179] Niederman MS. Principles of appropriate antibiotic use. International Journal of Antimicrobial Agents. 2005 2018/06/28;26:S170–S175. Available from: http://dx.doi.org/10.1016/S0924-8579(05)80324-3.

[180] Dubos RJ, Straus JH, Pierce C. The multiplication of bacteriophage in vivo and its protective effect against an experimetnal infection with *Shigella dystenteriae*. J Exp Med. 1943 Sep;78(3):161–168.

[181] Prins JM, van Deventer SJ, Kuijper EJ, Speelman P. Clinical relevance of antibiotic-induced endotoxin release. Antimicrobial Agents and Chemotherapy. 1994 06;38(6):1211–1218. Available from: http://www.ncbi.nlm.nih.gov/pmc/articles/PMC188188/.

[182] Norman GAV. Drugs, Devices, and the FDA: Part 1: An Overview of Approval Processes for Drugs. JACC: Basic to Translational Science. 2016;1(3):170 – 179. Available from: http://www.sciencedirect.com/science/article/pii/S2452302X1600036X.

[183] DiMasi JA, Grabowski HG, Hansen RW. Innovation in the pharmaceutical industry: New estimates of R&D costs. Journal of Health Economics. 2016;47:20 – 33. Available from: http://www.sciencedirect.com/science/article/pii/S0167629616000291.

[184] Khalifa L, Brosh Y, Gelman D, Coppenhagen-Glazer S, Beyth S, Poradosu-Cohen R, et al. Targeting *Enterococcus faecalis* biofilms with phage therapy. Appl Environ Microbiol. 2015 Apr;81(8):2696–2705.

[185] Jamal M, Hussain T, Das CR, Andleeb S. Characterization of *Siphoviridae* phage Z and studying its efficacy against multidrug-resistant *Klebsiella pneumoniae* planktonic cells and

biofilm. Journal of Medical Microbiology. 2015;64(4):454–462. Available from: http://jmm.microbiologyresearch.org/content/journal/jmm/10.1099/jmm.0.000040.

[186] Alves DR, Gaudion A, Bean JE, Perez Esteban P, Arnot TC, Harper DR, et al. Combined use of bacteriophage K and a novel bacteriophage to reduce *Staphylococcus aureus* biofilm formation. Appl Environ Microbiol. 2014 Nov;80(21):6694–6703.

[187] Alves DR, Perez-Esteban P, Kot W, Bean JE, Arnot T, Hansen LH, et al. A novel bacteriophage cocktail reduces and disperses *Pseudomonas aeruginosa* biofilms under static and flow conditions. Microb Biotechnol. 2016 Jan;9(1):61–74.

[188] Parasion S, Kwiatek M, Gryko R, Mizak L, Malm A. Bacteriophages as an alternative strategy for fighting biofilm development. Pol J Microbiol. 2014;63(2):137–145.

[189] Chan BK, Abedon ST. Bacteriophages and their enzymes in biofilm control. Current Pharmaceutical Design. 2015;21(1):85–99.

[190] Abedon ST. Lysis from without. Bacteriophage. 2011 Jan-Feb;1(1):46–49. Available from: http://www.ncbi.nlm.nih.gov/pmc/articles/PMC3109453/.

[191] Hancock REW, Sahl HG. Antimicrobial and host-defense peptides as new anti-infective therapeutic strategies. Nat Biotechnol. 2006 Dec;24(12):1551–1557.

[192] Zasloff M. Antimicrobial peptides of multicellular organisms. Nature. 2002 Jan;415(6870):389–395.

[193] Zhao C, Nguyen T, Boo LM, Hong T, Espiritu C, Orlov D, et al. RL-37, an Alpha-Helical Antimicrobial Peptide of the Rhesus Monkey. Antimicrobial Agents and Chemotherapy. 2001 10;45(10):2695–2702. Available from: http://www.ncbi.nlm.nih.gov/pmc/articles/PMC90719/.

[194] de la Fuente-Núñez C, Korolik V, Bains M, Nguyen U, Breidenstein EBM, Horsman S, et al. Inhibition of Bacterial Biofilm Formation and Swarming Motility by a Small Synthetic Cationic Peptide. Antimicrobial Agents and Chemotherapy. 2012 05;56(5):2696–2704. Available from: http://www.ncbi.nlm.nih.gov/pmc/articles/PMC3346644/.

[195] Dosler S, Mataraci E. In vitro pharmacokinetics of antimicrobial cationic peptides alone and in combination with antibiotics against methicillin resistant *Staphylococcus aureus* biofilms. Peptides. 2013 Nov;49:53–58.

[196] Kropinksi AM, Mazzocco A, Waddell TE, Lingohr E, Johnson RP. 7. In: Clokie MRJ, Kropinksi AM, editors. Enumeration of Bacteriophages by Double Agar Overlay Plaque Assay. vol. 501 of Methods in Molecular Biology. Humana Press; 2009. p. 69–76.

[197] Zhang Z, Schwartz S, Wagner L, Miller W. A greedy algorithm for aligning DNA sequences. J Comput Biol. 2000 Feb-Apr;7(1-2):203–214.

[198] Aziz RK, Bartels D, Best AA, DeJongh M, Disz T, Edwards RA, et al. The RAST Server: rapid annotations using subsystems technology. BMC Genomics. 2008 Feb;9:75.

[199] Overbeek R, Olson R, Pusch GD, Olsen GJ, Davis JJ, Disz T, et al. The SEED and the Rapid Annotation of microbial genomes using Subsystems Technology (RAST). Nucleic Acids Res. 2014 Jan;42(Database issue):D206–14.

[200] Brettin T, Davis JJ, Disz T, Edwards RA, Gerdes S, Olsen GJ, et al. RASTtk: a modular and extensible implementation of the RAST algorithm for building custom annotation pipelines and annotating batches of genomes. Sci Rep. 2015 Feb;5:8365.

[201] Family - Siphoviridae. In: King AMQ, Adams MJ, Carstens EB, Lefkowitz EJ, editors. Virus Taxonomy. San Diego: Elsevier; 2012. p. 86 – 98. Available from: http://www.sciencedirect.com/science/article/pii/B9780123846846000045.

[202] Linares JF, Gustafsson I, Baquero F, Martinez JL. Antibiotics as intermicrobial signaling agents instead of weapons. Proceedings of the National Academy of Sciences of the United States of America. 2006 12;103(51):19484–19489. Available from: http://www.ncbi.nlm.nih.gov/pmc/articles/PMC1682013/.

[203] Gawande PV, LoVetri K, Yakandawala N, Romeo T, Zhanel GG, Cvitkovitch DG, et al. Antibiofilm activity of sodium bicarbonate, sodium metaperiodate and SDS combination against dental unit waterline-associated bacteria and yeast. Journal of Applied Microbiology. 2008;105(4):986–992.

[204] Hammond AA, Miller KG, Kruczek CJ, Dertien J, Colmer-Hamood JA, Griswold JA, et al. An in vitro biofilm model to examine the effect of antibiotic ointments on biofilms produced by burn wound bacterial isolates. Burns : journal of the International Society for Burn Injuries. 2011 03;37(2):312–321. Available from: http://www.ncbi.nlm.nih.gov/pmc/articles/PMC3034806/.

[205] Roche ED, Renick PJ, Tetens SP, Carson DL. A Model for Evaluating Topical Antimicrobial Efficacy against Methicillin-Resistant *Staphylococcus aureus* Biofilms in Superficial Murine Wounds. Antimicrobial Agents and Chemotherapy. 2012 08;56(8):4508–4510. Available from: http://www.ncbi.nlm.nih.gov/pmc/articles/PMC3421576/.

[206] Zanetti M. Cathelicidins, multifunctional peptides of the innate immunity. J Leukoc Biol. 2004 Jan;75(1):39–48.

[207] Ebbensgaard A, Mordhorst H, Overgaard MT, Nielsen CG, Aarestrup FM, Hansen EB. Comparative Evaluation of the Antimicrobial Activity of Different Antimicrobial Peptides against a Range of Pathogenic Bacteria. PLoS One. 2015;10(12):e0144611.

[208] Cho J, Choi H, Lee DG. Influence of the N- and C-terminal regions of antimicrobial peptide pleurocidin on antibacterial activity. J Microbiol Biotechnol. 2012 Oct;22(10):1367–1374.

[209] Rady I, Siddiqui IA, Rady M, Mukhtar H. Melittin, a major peptide component of bee venom, and its conjugates in cancer therapy. Cancer letters. 2017 08;402:16–31. Available from: http://www.ncbi.nlm.nih.gov/pmc/articles/PMC5682937/.

[210] Agerberth B, Lee JY, Bergman T, Carlquist M, Boman HG, Mutt V, et al. Amino acid sequence of PR-39. Isolation from pig intestine of a new member of the family of proline-arginine-rich antibacterial peptides. Eur J Biochem. 1991 Dec;202(3):849–854.

[211] Tinoco JM, Buttaro B, Zhang H, Liss N, Sassone L, Stevens R. Effect of a genetically engineered bacteriophage on *Enterococcus faecalis* biofilms. Arch Oral Biol. 2016 Nov;71:80–86.

[212] Motlagh AM, Bhattacharjee AS, Goel R. Biofilm control with natural and genetically-modified phages. World J Microbiol Biotechnol. 2016 Apr;32(4):67.

[213] W SI, A HK, C SL, Karen T. The interaction of phage and biofilms. FEMS Microbiology Letters. 2006 2018/07/08;232(1):1–6. Available from: https://doi.org/10.1016/S0378-1097(04)00041-2.

[214] Glonti T, Chanishvili N, Taylor PW. Bacteriophage-derived enzyme that depolymerizes the alginic acid capsule associated with cystic fibrosis isolates of *Pseudomonas aeruginosa*. Journal of Applied Microbiology. 2010;108(2):695–702. Available from: http:https://doi.org/10.1111/j.1365-2672.2009.04469.x.

[215] Hughes KA, Sutherland IW, Jones MV. Biofilm susceptibility to bacteriophage attack: the role of phage-borne polysaccharide depolymerase. Microbiology. 1998 Nov;144 (Pt 11):3039–3047.

[216] Cerca N, Oliveira R, Azeredo J. Susceptibility of *Staphylococcus epidermidis* planktonic cells and biofilms to the lytic action of staphylococcus bacteriophage K. Letters in Applied Microbiology. 2007 2018/07/08;45(3):313–317. Available from: https://doi.org/10.1111/j.1472-765X.2007.02190.x.

[217] de la Fuente-Núñez C, Reffuveille F, Haney EF, Straus SK, Hancock REW. Broad-Spectrum Anti-biofilm Peptide That Targets a Cellular Stress Response. PLOS Pathogens. 2014 05;10(5):1–12. Available from: https://doi.org/10.1371/journal.ppat.1004152.

[218] Sodium metaperiodate SDS; 2018 [cited July 20]. Available from: https://noahtech.com/data/safety.13459.pdf.